Characterising and modelling time-varying rainfall extremes and their climatic drivers

Mari Jones

A Thesis Submitted for the Degree of Doctor of Philosophy

Newcastle University

Faculty of Science Agriculture and Engineering
School of Civil Engineering and Geosciences

April 2012

Abstract

Extreme climate responses such as floods or droughts pose multi-dimensional hazards to critical infrastructure and the most vulnerable sectors of society; these hazards may increase under climate change. The extreme rainfall events driving these responses may arrive non-uniformly in time, clustering on intra- and inter-annual scales; yet the dependent relationship between events is often ignored.

This thesis examines extreme daily rainfall within year clustering to determine whether changes in their temporal pattern are apparent in observational records. It then identifies the key atmospheric variables which drive event frequency and intensity, before testing hypotheses related to clustering.

Extreme rainfall regions were developed from the station maxima of a comprehensive new set of 223 daily rainfall observations, spanning the period 1856-2009. The observations are contained within 14 regions which represent the distinctive seasonal clustering, orographic and atmospheric variations in UK extreme rainfall.

Significant increases in annual maxima and associated return frequencies over the period 1961-2009 were observed from a Generalized Extreme Value (GEV) analysis. Increases in spring, autumn and winter maxima and their estimated return frequencies were also found. Estimates from summer maxima were variable across the country but indicated an increase in the highest intensity events.

Extreme rainfall seasonal clustering and the dependence on sea surface temperatures (SST), air temperature range and the North Atlantic Oscillation (NAO) were represented in flexible GEV and Poisson parameter estimates using Vector Generalized Additive Models. There is a strong negative correlation with air temperature range, reflecting heightened event intensity and probability when the diurnal temperature range is at its lowest. Event frequency is positively correlated with SST for all regions; event magnitude is dependent on either SST or NAO with a north-south divide. While the timing of events has not changed substantially, event probability has increased - resulting in greater within-year clustering. Climate projections indicate increasing SST and decreasing temperature range; this extreme rainfall model corroborates projected increases in event intensity and frequency.

Acknowledgements

I would like to thank my supervisors Hayley Fowler, Christopher Kilsby and Stephen Blenkinsop for their guidance, support, humour and critical insight. I particularly appreciated their encouragement to pursue numerous opportunities which arose and their assistance with the necessary applications.

I am grateful to NERC and the School of Civil Engineering and Geosciences who funded this research, and made it possible for me to attend numerous conferences and summer schools. Also to the Willis Research Network who facilitated several timely networking opportunities.

Thanks are due to NERC for funding a placement with the Scottish Government, and to my supervisors in the Climate Change Adaptation team, James Simpson and Jody Fletcher. For their invaluable advice and statistical guidance with respect to event clustering, thanks to David Stephenson and Renato Vitolo of Exeter University. Thanks are also due to Stephan Sain, Eric Gilleland and Rick Katz at NCAR, for giving me the opportunity to attend the summer colloquium and then to benefit from their knowledge during subsequent weeks' secondment to the IMAGe lab.

Considerable thanks are due to my father, Peter, for persevering with proof reading this thesis; the improved clarity is due to him, while any remaining obscurity is my own. Diolch yn dwlpe to Mam, Alys and Christopher, who have encouraged and motivated me throughout and never doubted that I would achieve my goal. And finally to Aaron, who has only known me as a final stage student, but who was there in the dark hours and has faith that I am less fretful in real life!

Glossary

α	Gamma shape parameter
β	Gamma scale parameter
Γ	Gamma function
η	Linear functions of parameters of a Generalized Additive Model
θ	Extremal index, $\frac{1}{\theta}$ is the degree of clustering or dispersion coefficient
Θ	Temperature covariate
λ	GAM/VGAM smoothing parameter
Λ	Poisson rate parameter
μ	GEV location parameter; or mean of the distribution
ξ	GPD and GEV scale parameter
$\tilde{\sigma}$	GPD shape parameter
σ	GEV shape parameter
Φ	Nominal parameter or covariate
AIC	Akaike Information Criterion
AMAX	Annual Maxima
ASC	Adaptation Sub-Committee of the Committee on Climate Change (UK)
BADC	British Atmospheric Data Centre
BIC	Bayesian Information Criterion
C-C	Clausius-Clapeyron constraint on atmospheric moisture holding capacity
CEE	Central and Eastern England (HadUKP)
CET	Central England Temperature
CH	Central Highlands (Extreme regions)
DJF	December-January-February
EA	East Anglia (Extreme regions)
edf	Effective degrees of freedom
ENSO	El Niño Southern Oscillation
EOF	Empirical orthogonal functions
ES	East Scotland (HadUKP, Extreme regions)
EVD	Extreme Value Distribution
EVT	Extreme value theory
EWP	England and Wales Precipitation series
FEH	Flood Estimation Handbook

FOR	Forth (Extreme regions)
FSR	Flood Studies Report
GAM	Generalized Additive Model
GCM	Global Circulation Model
GEV	Generalized Extreme Value
GHG	Greenhouse Gases
GLM	Generalized Linear Model
GPD	Generalized Pareto Distribution
HadUKP	Hadley Centre UK Precipitation Regions
HU	Humber (Extreme regions)
ICOADS	International Comprehensive Ocean-Atmosphere Data Set
IID	Independent and identically distributed
IOD	Indian Ocean Dipole
IRLS	Iteratively reweighted least squares
IPCC	Intergovernmental Panel on Climate Change
ITCZ	Inter-Tropical Convergence Zone
JJA	June-July-August
LRD	Long-range dependence
LTP	Long term persistence
MAM	March-April-May
MIDAS	Met Office Land Observation Network
MJO	Madden-Julian Oscillation
MLE	Maximum Likelihood Estimates
MW	Mid Wales (Extreme regions)
MSLP	Mean sea level pressure
NAO	North Atlantic Oscillation
NAM	Northern Annular Mode
NEE	North East England (HadUKP)
NCAR	National Center for Atmospheric Research
NCEP	National Centers for Environmental Prediction
NI	Northern Ireland (HadUKP, Extreme regions)
NHI	North Highlands and Islands (Extreme regions)
NO	Northumbria (Extreme regions)
NOAA	National Oceanic and Atmospheric Administration

NS	North Scotland (HadUKP)
NWE	North West England (HadUKP, Extreme regions)
PCA	Principal component analysis
PDO	Pacific Decadal Oscillation
PNA	Pacific North American
POT	Peaks-over-threshold, a series of data exceeding a specific threshold
PWM	Probability weighted moments
Q95	95th Quantile of the wet day distribution (“very heavy”)
Q99	99th Quantile of the wet day distribution (“extremely heavy”)
RBAR	Mean annual maximum rainfall (Flood Studies Report, 1975)
RCM	Regional Climate Model
RFA	Regional Frequency Analysis
RMED	Median annual maximum rainfall
SAM	Southern Annular Mode
SE	Southern England (Extreme regions)
SEE	South East England (HadUKP)
SH	South Highlands (Extreme regions)
SLP	Sea level pressure
SOI	Southern Oscillation Index
SOL	Solway (Extreme regions)
SON	September-October-November
SMED	Median seasonal maximum rainfall
SS	South Scotland (HadUKP)
SST	Sea surface temperature
SW	South West (Extreme regions)
SWE	South West England (HadUKP)
UBRE	Unbiased risk estimator
VGAM	Vector Generalized Additive Model
VGLM	Vector Generalized Linear Model
WC	West Country (Extreme regions)

Table of Contents

List of Figures

List of Tables

Chapter One Introduction

"Climate Change is the Janus faced challenge of our time. It is simultaneously the significant environmental challenge of our time and future generations, and it is the issue that is leading us into sustainability."

Cynthia Rosenzweig NASA GISS (2011)

Climatic extremes such as flood, drought, windstorm and heat wave pose multi-dimensional hazards to critical infrastructure and the most vulnerable sectors of society and are expected to become worse with global warming (IPCC, 2011). The UK has been identified as most sensitive, in terms of spatial impacts, to pluvial and fluvial flooding, and hence to extreme rainfall (Stern, 2007; Krebs *et al.*, 2010; Met Office, 2011b). While other extreme climatic events also have considerable societal impacts, this thesis is focussed only on extreme rainfall. Research programmes in engineering have only recently started to address the issue of adaptation planning for these complex hazards even though it has been identified as an urgent requirement (IPCC, 2007b; Krebs *et al.*, 2010; Rosenzweig *et al.*, 2011). However, appropriate risk and hazard management strategies cannot be devised without a proper understanding of the potential impacts and vulnerability of infrastructure and society to extreme rainfall under current climatic conditions. While it is not possible to attribute any single event to climate change, there appear to be increased incidences of heat waves, droughts and floods and climate projections indicate that these will increase in the future (Murphy *et al.*, 2009). Detection and attribution of the enhanced probability of extreme events occurring as a result of climate change is rapidly gaining importance on the research agenda (Pall *et al.*, 2011; Trenberth, 2011).

Climate change is a continuous process, arising from atmospheric responses to internal perturbations and external forcing whether natural (e.g. volcanic activity (Stenchikov *et al.*, 2002; Mosley-Thompson *et al.*, 2005), solar variability (Solanki *et al.*, 2004; Usoskin *et al.*, 2004)) or anthropogenic. However, these atmospheric responses are changing more rapidly than previously experienced as a consequence of the post-industrial anthropogenic forcing (Trenberth *et al.*, 2007). The primary consequences of increased mean global temperature are well understood - such as

increased drought periods, rapid melting of icecaps and glaciers, and an enhanced hydrological cycle. However, establishing the point at which the primary responses differ from natural climate variability and display irrefutable evidence of a change in climate is a subject of much recent research (Hegerl *et al.*, 2007).

There will always be a new extreme event which breaks previous records, and which may not be foreseeable (Benestad, 2003; Taleb, 2011) and, as with any stochastic distribution, there is a tendency for extremes to cluster together (von Storch and Zwiers, 1999); thus, it is difficult to discern the difference between natural climatic variability and long term changes in behaviour (Hegerl *et al.*, 2004). While Extreme Value Analysis applied to very rare, highly damaging, events (Ghil *et al.*, 2011) is limited by the paucity of records, it does serve to "domesticate" some of the unforeseen extremes, known as "black swan" events (Taleb, 2011) and identify the likely return frequency for use in practical applications such as flood defence design (Mandelbrot and Wallis, 1968). However, in addition to the ambiguity of risk analysis in the current climate, stationarity assumptions which were appropriate for use in shorter term calculations (<50 years) no longer hold true (Milly *et al.*, 2008), and extreme events are occurring more frequently than can reasonably be expected (Trenberth, 2011).

To understand the probability of an extreme rainfall event, it is first necessary to understand the governing weather systems which generate these extremes. Heavy and extreme rainfall can arise from two different scales of rain bearing systems: synoptic, operating over 100-1000's km^2; and meso-scale in the order of 1-10km^2. Synoptic scale systems include:

- The *inter-tropical convergence zone* (ITCZ), a region of thunder and rain around the equator which shifts north and south seasonally and is driven by the coriolis force;
- *Monsoon systems*, a seasonal reversal of surface winds and rain, arising from differential heating between the ocean and land masses in tropical and subtropical regions;
- *Tropical Cyclones*, from depressions and storms to hurricanes, typhoons or cyclones (dependent on the oceanic basin of origin);

- *Mid-latitude frontal depressions*, which frequently affect the UK and are most common in winter. Frontal depressions are usually generated over the North Atlantic, are often very large and can be fast travelling. Frontal depressions which occur during the summer often contain embedded convection cells which generate intense areas of localised rainfall and exacerbate flooding.

Meso-scale systems by contrast are more frequent in the summer or where high temperature differentials occur, such as in highly mountainous areas:

- *Thunderstorms* or convective cloud systems, are the most common cause of summer storms in the UK and are often short lived and very small in area making them particularly hard to reproduce in weather prediction or climate models without parameterising the processes. These systems produce some of the highest rainfall rates in northwest Europe.
- *Lee Lows* are intense depressions formed on the downward slope of mountains.

Different air masses have particular characteristics related to stability, air pressure and humidity which drive different weather conditions. While the extremes of wind and rain do not often occur at the same time, extreme rainfall events are governed by storm scale circulations, where the cyclonic winds draw additional precipitation into the water column from a radius of 3 to 5 times greater than the precipitating region (Trenberth, 2011). Extreme rainfall is, therefore, often associated with strong winds. A simple process diagram relating atmospheric drivers to the consequences of extreme rainfall is shown in Figure 1-1.

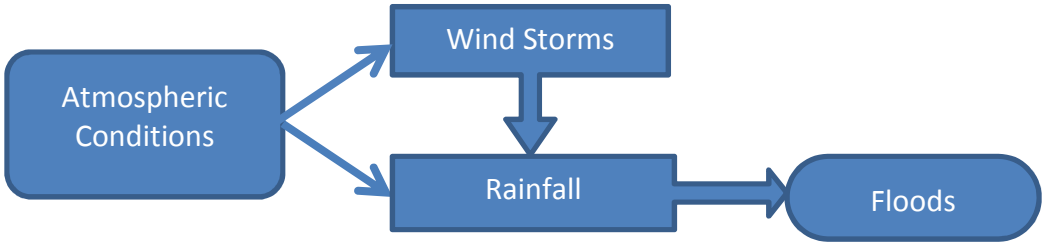

Figure 1-1 : Consequences of atmospheric instability

There is a widely held perception that flooding incidents have increased over the last decade; anthropogenic influence on catchments may be in part responsible for this perception, through increased development on flood plains. However, recent

studies of flood events in the UK (Wilby *et al.*, 2008) and Europe (Blöschl and Montanari, 2010) do point towards an increase in flooding (refer to Figure 1-2) compared with a similar event count for the previous decades. Similarly, many flood "hot spots" around the world have experienced several devastating floods in the most recent decade (Figure 1-3), more than would be expected from natural variability alone (Min *et al.*, 2011). Each of the events had enormous social and financial consequences (Maynard, 2006); projections of future climate responses indicate that this is likely to become worse (Zhang *et al.*, 2011).

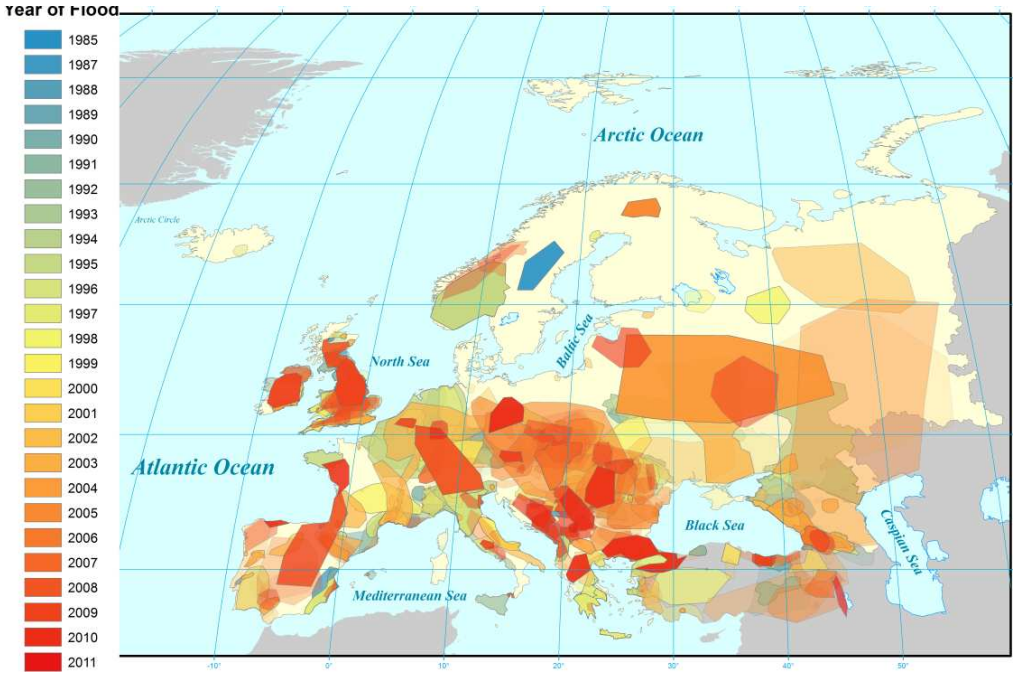

Figure 1-2 : Extent of annual flood events in Europe between 1985 and 2011 (based on data from Dartmouth Flood Observatory)

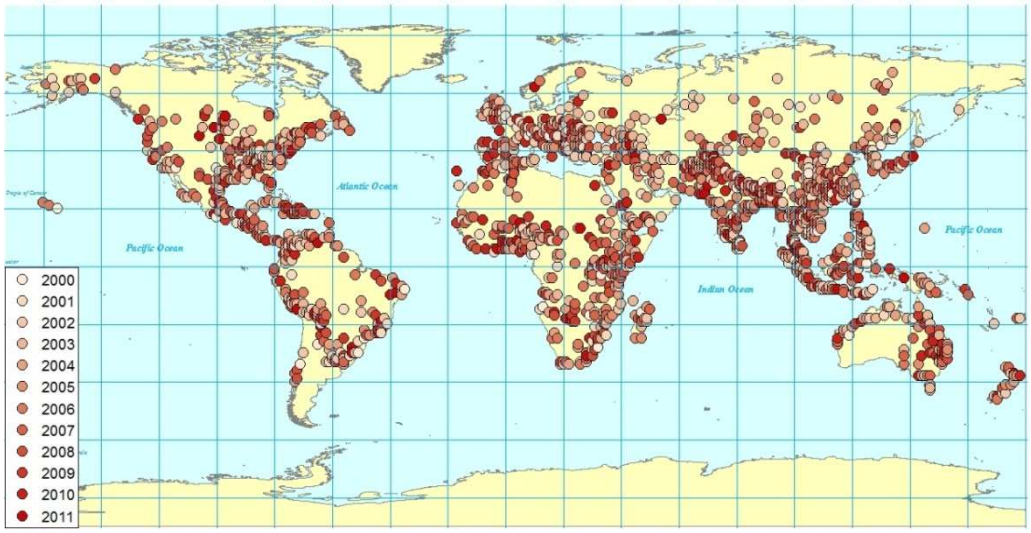

Figure 1-3 : Recurrence of Global large flood events 2000- 2011 identifiable from news, government, instrument, and remote sensing sources (Brackenridge, 2011)

Many organisations and governments worldwide are endeavouring to understand the true impacts, both current and future, of climate change. The UK Committee on Climate Change is one such organisation aiming to identify the observable impacts in different sectors (e.g. health, agriculture), their secondary impacts on other sectors, and their likely future evolution, using the UK Climate Change Projections (Murphy *et al.*, 2009). The first phase of a similar exercise has recently been completed in New York, addressing the specific concerns of their urban environment (Rosenzweig *et al.*, 2011), and similar risk assessments are taking place in many other countries (Moncel *et al.*, 2011 and references therein). The difficulty with implementing these assessments is that changes in mean climate behaviour are better understood than changes in the extremes, yet the damage caused by the latter will have the greatest impact on society (Tebaldi *et al.*, 2006). Furthermore, it is likely that climate change will enhance natural climate variability, exacerbating the magnitude of extreme events and the resultant collective risk (IPCC, 2011).

Recent years are notable for exceptionally strong La Niña and El Niño conditions, (refer to Section 2.1.2) which are associated with extreme weather conditions in different parts of the world (World Meteorological Organization, 2011), as well as particularly strong North Atlantic sea level pressure differentials described by the North Atlantic Oscillation index (NAO; refer to Section 2.1.2). These atmospheric-ocean coupling dynamics, known collectively as teleconnections, are often held to be the cause of severe and extreme storm conditions (Della-Marta *et al.*, 2007); although they are one of several explanatory variables in a highly complex system. The UK Adaptation Sub-Committee recently identified a lack of acknowledgement of climate related risks in major strategic decisions in the UK (Krebs *et al.*, 2011), even though flexible adaptation actions which are implemented now will limit future potential damages and may also bring short term benefits. In order to understand the likely risks from extreme rainfall and their future evolution, it is necessary to understand the dependence of these extreme events on atmospheric processes and their relationship with other meteorological conditions and teleconnections.

Given the non-stationarity of the climate, including diurnal heating and cooling or seasonal variations, it is important to use observations which are long enough to distinguish natural trends and variability from other divergent behaviour. Furthermore, the quality of the data used is of paramount importance to support the conclusions (Alexander *et al.*, 2009). While the observational records provide fundamental atmospheric knowledge which will assist in assessing the likely future behaviour of extreme rainfall, the complexity of the climate system means that a simple extrapolation of observed trends into the future is not judicious. However, these observations can validate the output from physically based models, such as global circulation or regional climate models (GCM, RCM), which have been subjected to different forcing scenarios to project future behaviour. Improved characterisation of the driving mechanisms for extreme rainfall may also improve the composition of these models.

GCMs are effective at reproducing the large scale atmosphere-ocean responses for the recent and past climate, giving confidence in probabilistic future projections (Meehl *et al.*, 2007; Murphy *et al.*, 2009). Computational costs limit GCMs to a grid resolution of around 1000km^2, resulting in powerful representation of global scale circulation responses and continental precipitation or temperature patterns, but less effective regional descriptors (Rummukainen, 2010). Figure 1-4 illustrates the differences in representation of regional mean precipitation between different model scales and gridded observations.

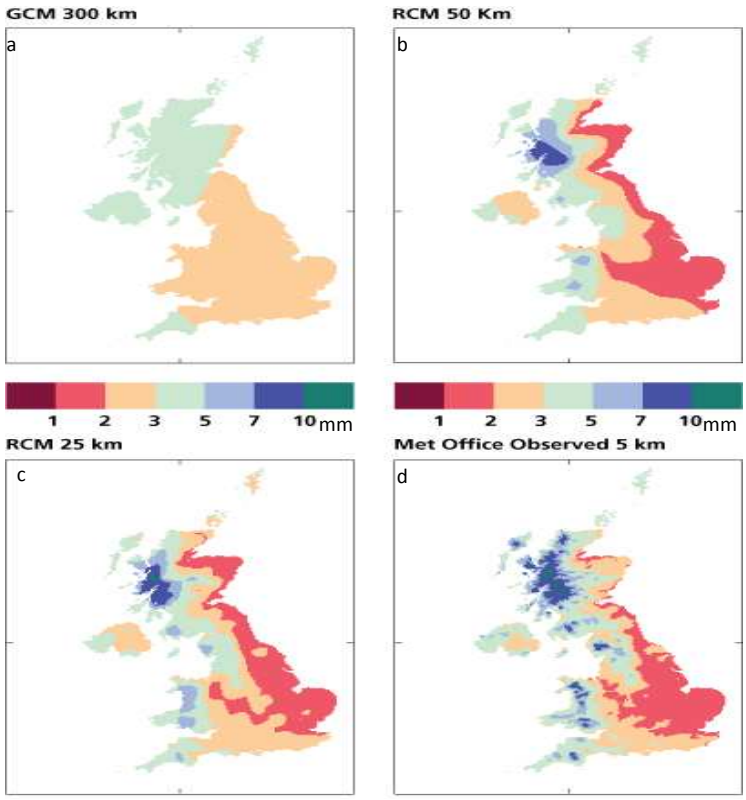

Figure 1-4 : Comparison of Mean Wet Day Precipitation Patterns (mm) outputs from (a) GCM with 300km^2 grid; (b) RCM with 50km^2 grid; (c) RCM with 25km^2 grid and (d) observations at 5km^2 grids (Courtesy Met Office)

RCMs employ boundary conditions derived from the downscaled outputs of GCMs to run atmospheric responses on a smaller scale. However, the resultant models cannot always reproduce the different scaled atmospheric processes within the model layers, due to interactions between large-scale flow and the topographical features which are not included in GCMs. Furthermore, meso-scale weather features such as extreme convective rainfall, occur over much smaller areas than the resolution of most RCMs.

The influence of higher temporal and spatial resolution to improve the outputs from RCMs, as employed for numerical weather predictions, is being investigated at present with some success in reproducing observed extreme rainfall patterns (Kendon *et al.*, 2012). Information on these extreme events is urgently required by those planning for climate change adaptation, but is not currently available. Enhancing climate projections for use in planning and decision making requires a combination of higher resolution climate models, together with greater understanding of the processes driving extreme weather events. By characterising

the drivers, it will be possible to improve their physical representation within the models and consequently, it is hoped, the projections of future extreme weather.

A commonly cited reason for not planning adaptive actions to contend with a changing climate, and particularly enhanced extreme events, is the level of uncertainty in future estimates based on climate projections (Overpeck, 2000), and imbalance between the outlay costs and potential benefits of the actions (Wilby and Dessai, 2010). Detection of real changes in climate responses is therefore essential to facilitate appropriate adaptation action to be taken by decision makers; however, detection of changes in the extremes may not be possible in the desired timescale for action (Fowler *et al.*, 2010). Similarly, those involved with implementing adaptation plans often require well defined design parameters rather than large uncertainty envelopes. It is hoped that by understanding current mechanisms and risks the uncertainty surrounding future projections can be reduced (Tebaldi *et al.*, 2006), providing a realistic decision framework for designers and planners.

This thesis aims to identify several key target variables which try to "explain" the behaviour of extreme rainfall. This will be achieved by examining different metrics of extreme rainfall to discover those most sensitive to changes in the climate system, before analysing the large scale atmospheric and oceanic drivers and correlated responses (temporal and spatial). By understanding more fully which extreme events interact, and how they in turn respond to larger atmospheric circulation patterns, it should be possible to comprehend the current behaviour and permit the insurance industry and policy planners *inter alia* to respond more effectively in planning adaptive actions. Improvements in characterising the drivers of extreme rainfall, should also lead to better identification of the likely frequency and intensity of future extremes, through use as a statistical downscaling tool from regional or global climate models.

1.1 Aim and Objectives

This thesis aims to identify several key target variables which, collectively, will contribute to an extreme rainfall model with which to identify and quantify climatic changes which have occurred to date, and having particular utility in hydrology, climatology and related industries.

1.1.1 Objectives

1. To develop a comprehensive data set of UK daily rainfall records to the present day, from existing data sets, with which to explore the frequency and magnitude of extreme and very heavy rainfall.
2. To explore metrics of extreme daily rainfall and identify the most appropriate for use in examining changes in the frequency and magnitude of extreme events.
3. To update existing analyses of trends in UK annual and seasonal daily rainfall maxima to the present day.
4. To develop a new set of rainfall regions for the UK which are more appropriate for use with extreme rainfall than the existing Hadley UK Precipitation regions.
5. To identify key atmospheric and oceanic drivers, with long historic records which may influence the frequency or magnitude of extreme and very heavy daily rainfall.
6. To use statistical models, premised on the dependence of extreme daily rainfall on atmospheric and oceanic drivers, to characterise the spatial and temporal differences in extreme rainfall behaviour.
7. To explore the sources of non-stationarity in observed extreme and very heavy daily rainfall and better characterise the physical processes governing event frequency and magnitude.

1.2 Project limitations

To keep the project to a manageable size, it has been necessary to consider only extreme and very heavy daily rainfall and their corresponding driving mechanisms, such as temperature or atmospheric oscillations; the behaviour and evolution of the drivers over time will not be explored in detail. Responses to extreme rainfall – both direct such as flooding, or indirect such as agricultural responses – will also not be examined.

1.3 Thesis outline

The remainder of this thesis will adopt the following structure: Chapter 2 synthesises the current understanding of observed changes in the global climate system, the inter-relationships and drivers of hydrometeorology, and extant research on extreme rainfall. Chapter 3 describes the statistical tools and methods

which will be employed throughout the project, Chapter 4 summarises the data sets, while Chapter 5 provides a comprehensive over view of the exploratory data analyses. Examination of the selected metrics of extreme rainfall, the relationship with driving atmospheric and oceanic processes, and temporal evolutions in extreme rainfall frequency (such as clustering) are covered in Chapters 6 to 8. The results are then summarised and conclusions drawn in Chapter 9, together with a brief exploration of possible future directions.

Chapter Two Climate Variability and Change Relating to Extremes

"But what is the difference between literature and journalism? ...Journalism is unreadable and literature is not read. That is all."

Oscar Wilde, The Critic As Artist

This chapter reviews the current state of research on extreme events, with particular emphasis on extreme rainfall. It focusses on the potential sources of climate variability, prior to exploring the oceanic-atmospheric interactions which cause extremes, concluding with the observed and projected changes in extreme rainfall. The methods used by others, and those selected for use in this project will be summarised in Chapter 3.

Detection of climate change is "the process of demonstrating that climate has changed in some defined statistical sense, without providing a reason for that change" (Baede, 2007). To detect climate change within a particular measure or variable, it is essential to demonstrate that the change is greater than that expected from natural variability alone (Koutsoyiannis, 2003). In the context of this project, it is important to discern which patterns represent some form of climate variability from those which constitute a longer term change in behaviour. Within this thesis, it is not intended to attribute the causes of the long term variations in extreme and very heavy rainfall, rather to characterise the responses relating to atmospheric patterns and thence to assess anticipated future climatic extremes.

Trend detection has a high demand for long duration spatially distributed climate observations to characterise fully the short and long term fluctuations against which to test the reliability of any possible trends (Kundzewicz and Robson, 2000). This demand is further enhanced when examining extreme events which, by definition, are rare (Allamano *et al.*, 2011). Furthermore, even discounting increasingly unusual extremes anticipated as a result of climate change, the probability of such events does not remain constant as a direct consequence of natural variability (Cohn and Lins, 2005).

2.1 Sources of Climate Variability

The climate system is complex and interactive, with stochastic responses to a

variety of influences. 'Internal' responses are those arising from the dynamic relationship between the atmosphere and ocean; external forcing such as solar radiation, volcanic eruptions or anthropogenic pollution all affect the atmospheric responses (Le Treut *et al.*, 2007). Atmospheric observations taken to understand these processes are also subject to human error and, hence, further sources of uncertainty. The focus of this project is on the response of very heavy and extreme rainfall to atmospheric processes, rather than external forcing, while making suitable allowance for abrupt and gradual changes.

2.1.1 Abrupt and gradually varying changes

The presence of abrupt or gradually varying changes in the data, arising from anthropogenic influences or gauge drift, can be suggestive of a significant trend or autocorrelation where none exists (Villarini *et al.*, 2009). Changes may include gauge station relocation or alterations to the hydrological cycle through upstream housing development or dam construction. Many tests to determine change points in the distribution focus solely on the mean of the data in question (e.g. occurrence frequency of extreme events) and are less reliable when examining the variance of the data (Pettitt, 1979; Perreault *et al.*, 2000b; Villarini *et al.*, 2009). However, it is equally important to understand the changes in the variance of the distribution, which is more sensitive to increases in global mean temperature (Katz, 1999; Trenberth and Shea, 2005; Zolina *et al.*, 2010).

Many studies assess whether any trends are present in the data prior to establishing whether change points occur. However, this directly contradicts the aim of detecting a true trend within the data; particularly given the sensitivity of trend detection within short time series (Frei and Schar, 2001), fluctuating data (Kundzewicz and Robson, 2000; Kottegoda *et al.*, 2008), or comparisons against different base periods (Zhang *et al.*, 2005). It is more robust to assess the presence of abrupt changes prior to establishing whether other variability is present in the data, then testing for trends (Villarini *et al.*, 2009).

Trends may be observed in many metrics of a data series, from mean occurrences to the variability in frequency and magnitude of the extremes; determining whether a data series is non-stationary requires the assessor to account

for diurnal and annual cycles (Robson, 2002), as well as identifying sudden changes in the distribution which may show up as trends (Serinaldi, 2009). Pezzulli *et al.* (2005) suggest that while normalising monthly data may remove non-stationarity introduced by annual cycles, these techniques introduce greater sensitivity and may result in false trend detection. Furthermore, the inherent noisiness in hydrological data means that it may not be possible to distinguish non-stationarity from long-term persistence, as a stationary process with long term persistence may appear to be very similar to a non-stationary process with a trend (Lins and Cohn, 2011). Paleo-hydrological records indicate that small changes in the mean result in far larger changes in the extremes (Knox, 2000). As argued by Matalas (1997), in the absence of physical proof, caution should be exercised with trend analysis that variability is greater than that expected from a stochastic process. Similarly, Cohn and Lins (2005) considered that the assumption of stationarity is important in order to assess effectively whether long term departures in observed data can be attributed to ordinary process dynamics or whether they are symptomatic of a greater change.

The more recent focus on trend analyses within a changing climate has revived interest in distinguishing climatic variability from “real” changes (Koutsoyiannis, 2003; Sakalauskiene, 2003; Ammann *et al.*, 2007). Scientists critical of a tendency to exaggerate the impacts of climate change have also reiterated the need to account for persistence (Alexander *et al.*, 2006). As Cohn and Lins (2005) observed “It is easy to imagine that long term persistence could be mistaken for trend”, as fractional noises often display multiple ‘features’ including trends and cycles (Mandelbrot and Wallis, 1968). Similarly, different forms of non-stationarity are not always evident as climatic variability may account for apparent trends in ordinarily “long duration” series (Beran, 2002; Robson, 2002; Koutsoyiannis, 2003). Long established hydrological practice assumes that for the purposes of design, observational series are stationary (Matalas, 1997; Lins and Cohn, 2011); however this may no longer be appropriate for extreme hydrology if stationarity cannot be assumed over the engineering design life (Milly *et al.*, 2008).

All hydrological series exhibit variability on at least a seasonal scale; effective trend detection requires quantification of the scale of the variability and removal of

the seasonal signal, e.g. Allamano *et al.* (2011). Cyclic variability on a multi-annual to decadal scale has been the subject of observation since the Egyptians' control of Nile flood waters, as reviewed by Hurst (1951) in relation to modern flows in the River Nile. Hurst identified that hydrologic series tend to cluster such that high flow and low flow years tend to occur together; also known as the 'Noah and Joseph effect' of operational hydrology (Mandelbrot and Wallis, 1968). Recent analyses of historical stream flow observations, circa 150 years, indicate that the UK experiences sequences of greater or fewer floods and is entering a "flood rich" period of the record (Yates, 2008). The question is how much can be determined from a stationary historic record where the most extreme events under current climate conditions may not have occurred (Taleb, 2011).

Hurst (1951) formally identified that severe hydrological events follow a decaying power law relationship. The Hurst exponent, H, describes the decaying power law between severe hydrological events and may take a value between 0 and 1, where $H>0.5$ signifies a data series with long range dependence (LRD). The greater the value of H, the greater the degree of persistence within the data series. As the length of the series tends to infinity, H tends to a value of 0.5 and independence. For most real-world applications, H tends to adopt a value of around 0.7 with a standard deviation of 0.09, and therefore demonstrates some natural degree of event clustering (Hurst, 1951).

Klemes (1974) summarised previous attempts to quantify the Hurst Exponent, identifying the potential use of fractional Gaussian noise processes for simulation and prediction. However, he cautioned that "an ability to simulate, and even successfully predict a specific phenomenon does not necessarily imply an ability to explain it correctly". The aim of this project is not to determine the controls on the phenomenon (here, extreme and very heavy rainfall), whether infinite memory, non-stationarity of the mean, long-term dependence or persistence, but to distinguish any trends from these fluctuations. The importance of LRD can be reduced through the use of regional pooling (Fowler and Kilsby, 2003b), which both improves trend detectability (Westra and Sisson, 2011) and improves convergence to the GEV distribution in the presence of LRD (Rust, 2009); or through using a spatial smoother to analyse spatially correlated data (Maraun *et al.*, 2008). Following other analyses

to identify changes in individual gauged records, regional pooling will be used in this thesis for all analyses to minimise the importance of any single event or trend (Hosking and Wallis, 1988).

2.1.2 Atmospheric influences

Internal climatic variability responds to interactive processes on several different timescales. Shorter, daily, cycles include water vapour and temperature fluctuations; medium-term reactions relate to seasonal and annual fluctuations and troposphere-stratosphere exchanges; while the oceanic thermohaline currents drive variability on scales of several decades to hundreds of years. The interactions between these responses introduces a degree of complexity to the climatic response system, which is further enhanced by coupled interactions between the atmosphere and ocean (Goosse *et al.*, 2009).

Teleconnections refer to the connectivity between climatic variations across a large spatial scale (often ≥1000km), which arise from large-scale wave motions and energy transfers (Baede, 2007). Atmospheric circulation patterns are zonally averaged motions which follow multi-annual cycles. The most influential of these patterns are described as "spatial patterns with varying amplitude" (Trenberth *et al.*, 2007), quantified by a set of linear transformations derived from station or gridded measurements of mean sea level pressure (MSLP), temperature, or geostrophic pressure. The climatic responses of different regions to the atmospheric circulation patterns are often diametrically opposed as storm track and strength are modulated by the atmospheric oscillation (Goosse *et al.*, 2009). Table 2-1 describes the teleconnection patterns which have the most global influence; they are also represented diagrammatically, indicating the approximate region of measurement, in Figure 2-1. The teleconnections which are most relevant to UK climatology are the North Atlantic Oscillation (Hurrell *et al.*, 2001; Jones *et al.*, 2003), which is the only teleconnection prominent throughout the year in the Northern Hemisphere (Barnston and Livezey, 1987), and the El Niño Southern Oscillation (Zanchettin *et al.*, 2008). These are each discussed in more detail below.

Teleconnection	Measured / Zone of Operation	Approximate Periodicity	Series Developer
Southern Oscillation Index (SOI)	MSLP difference between Tahiti and Darwin, normalised by the long-term mean and standard deviation	~ monthly, with annual phases	Troup (1965); Können *et al.* (1998)
North Atlantic Oscillation Index (NAO)	Difference of normalised MSLP between Lisbon and Stykkishólmur or Gibraltar and Reykjavík	3-4 days with annual to multiannual persistence	Hurrell (1995); Jones *et al.* (1997)
Northern Annular Mode (NAM) or Arctic Oscillation (AO)	Leading Empirical Orthogonal Function (EOF) pattern of winter monthly mean Northern Hemisphere MSLP anomalies pole-ward of 20°N	~10 days	Thompson and Wallace (1998); (2000); Thompson *et al.* (2000)
Southern Annular Mode (SAM) or Antarctic Oscillation (AAO) or High Latitude Mode	Leading EOF pattern of winter monthly mean Southern Hemisphere MSLP anomalies pole-ward of 20°S Or the difference in long term mean MSLP between 45°S and 65°S	~10 days	Thompson and Wallace (2000); Thompson *et al.* (2000) Gong and Wang (1999); Marshall (2003)
Pacific North American (PNA)	The mean of normalised 500hPa height anomalies at 20°N, 160°W and 55°N, 115°W minus 45°N, 165°W and 30°N and 85°W	daily with monthly phases	Wallace and Gutzler (1981)
Pacific Decadal Oscillation (PDO)	The first EOF of SST over the North Pacific north of 20°N; known as Inter-decadal Pacific Oscillation when covering the whole Pacific basin	Multi-annual	Mantua *et al.* (1997)
Madden Julian Oscillation (MJO)	Coupled ocean-atmosphere continuous wave like motion measured at 200mb and 850mb affecting region between 30°N-30°S and 60°-180°E	30-60 days	Madden and Julian (1971, 1972, 1994)
El Niño – Southern Oscillation (ENSO)	The coupled ocean-atmosphere process measured via the SOI and SST in the central and eastern equatorial Pacific (150°-90°W, 5°N-5°S)	3-4 days with strong seasonal component	Trenberth (1976; 1997)
Indian Ocean Dipole (IOD)	Normalised difference of SST anomalies between 50°-70°E, 10°N-10°S and 90°-110°, 0°-10°S	~10 days	Saji *et al.* (1999)

Table 2-1 : Principal Teleconnection Patterns and related indices (from IPCC AR4 Box 3.4; Trenberth *et al.*, 2007)

Each oscillation pattern induces complementary wind motions in conjunction with the pattern of sea level pressures, generating global temperature and precipitation responses. The most notable are situated around the equator and are particularly related to El Niño and the Madden Julian Oscillation (Madden and Julian, 1994).

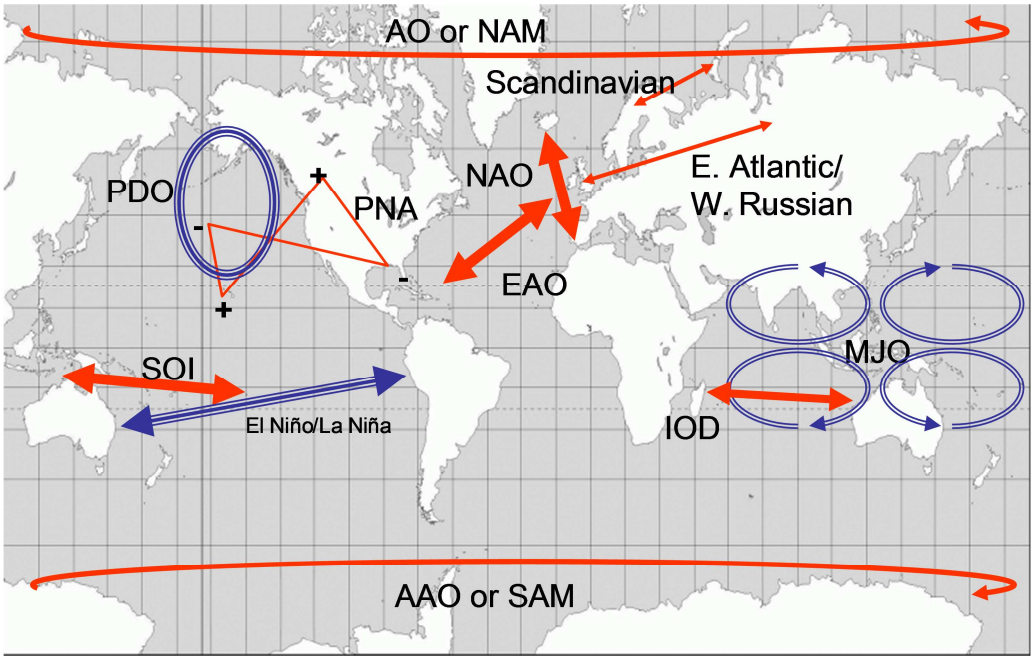

Figure 2-1 : Location of Principal Teleconnection Patterns. Red arrows indicate normalised Sea Level Pressures; Blue arrows indicate a composite analysis of one or more measurements.

The North Atlantic Oscillation and Northern Annular Mode

The principal actor in the Northern Hemisphere, and in particular European, weather patterns throughout the year, is the North Atlantic Oscillation. This is a dipole of sea level pressures between Iceland and the southern tip of the Iberian Peninsula, measured either between Stykkishólmur and the Azores (Hurrell and Deser, 2009, and references therein) or Reykjavík and Gibraltar (Jones *et al.*, 1997). Positive (negative) phases represent enhanced (diminished) Icelandic Low and Iberian High pressure fields. Although not a major influence on global precipitations, the NAO explains ~8% of the annual variability in Northern Hemisphere precipitation (New *et al.*, 2001).

The most profound effects of the NAO are displayed through winter time surface temperatures, storminess and precipitation across much of the Northern Hemisphere. In its positive phase, warm moist air from enhanced westerly flows

move across Europe to generate dry conditions over southern Europe and North Africa and influence drought persistence (Della-Marta *et al.*, 2007). In contrast, reduced North Atlantic temperatures and enhanced northerly winds over Greenland and north-eastern Canada create wet conditions in northern Europe. Positive phase winters are associated with a north-eastward motion of the storm track (path from storm genesis to its completion point), with enhanced activity in north Europe and decreased activity in the south (Mailier *et al.*, 2006). Considerable research has established the influence of the NAO on UK (Fowler and Kilsby, 2003b; Allan *et al.*, 2009), and European (Moberg and Jones, 2005; Bartolini *et al.*, 2009) weather systems. When the NAO is negative, westerly winds tend to be weaker leading to lower rainfall totals in northern Europe. Research has also determined a significant correlation between flora and fauna responses and the preceding winter NAO phase (Kettlewell *et al.*, 2006; Atkinson *et al.*, 2008; Gouveia *et al.*, 2008). While less strongly correlated to precipitation and temperature anomalies, summertime (JJA) NAO indices also have an impact on European weather (Linderholm *et al.*, 2009). Seasonal correlation between the NAO phase and precipitation anomalies over Europe are illustrated in Figure 2-2.

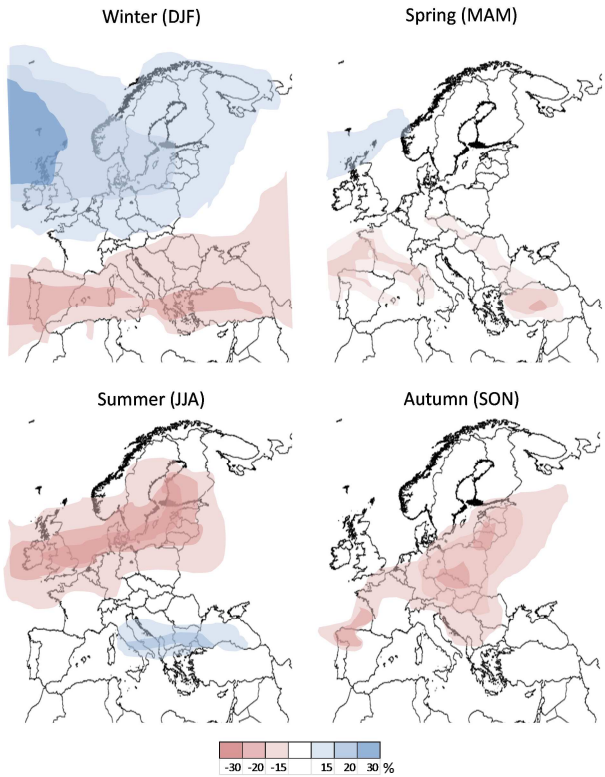

Figure 2-2 : Percentage degree of correlation between NAO index and European precipitation seasonal departures from the 1961-1990 mean conditions between 1950-2000 (NOAA, 2005)

Recent work has correlated inter-decadal variability in storm patterns with fluctuations in large scale teleconnection patterns, finding the NAO to have a strong influence on UK storm activity (Allan *et al.*, 2009). The winter NAO index for the period from 1961-1990 was positive for several consecutive years interspersed with solitary negative winters, with few years experiencing particularly high or low index values. In contrast, the most recent two decades have experienced several exceptionally high and several exceptionally low NAO years. While the impact of increasing global temperatures on the NAO signal is not fully understood, the most negative winter NAO indices on record for both 2009 and 2010, accompanied by record high global mean temperatures, also appear to have led to exceptionally heavy UK rainfall in the summer and autumn.

Wilby *et al.* (2002) examined several drivers of rainfall around the UK, confirming that different variables have influence at different locations or times of the year on the probability of wet days. The research confirmed a strong positive correlation between winter and spring NAO indices and the corresponding probability of rain in Atlantic bordering stations; with negative correlations during the summer for southeast stations. Negative correlations between area averaged SST anomalies over the Atlantic region and wet day probability were also apparent, strongest during the autumn and in central England and the southeast.

The NAO index is highly variable, demonstrating sustained periods of positive or negative values over past centuries (Jones *et al.*, 2003). During the late 1960s the NAO index values were negative, reversing toward the mid-1990s to a strongly positive index. Following the peak of the mid-1990s, the NAO index fluctuated throughout the early 2000s before falling to the most negative indices recorded since 1823 during the winters of 2009 and 2010. The IPCC Fourth Assessment Report IPCC (2007a) found evidence to suggest that inter-decadal NAO variability, which is influenced by tropical ocean currents and temperature forcing, is increasing (Forster *et al.*, 2007). Thermohaline circulations may influence a multi-decadal oscillation within the index (Zanchettin *et al.*, 2008) in addition to other global oscillations such as ENSO (Brönnimann, 2007). The influence of the NAO can also be detected at a considerable distance from the primary source. For example, Archer and Fowler

(1999) found that there are significant links between the Indian monsoon and both ENSO and the NAO. Similarly, Gong and Wang (1999) noted signatures of the NAO within Antarctic ice sheets and the Southern Annular Mode evolution.

El Niño-Southern Oscillation

The El Niño and Southern Oscillation teleconnection pattern is a coupled ocean-atmosphere response originating in the Eastern Pacific, leading to changes in the trade winds, precipitation patterns and global circulation. El Niño refers to the upwelling of warm water near Eastern Australia and eastwards propagation, weakening the sea surface temperature (SST) gradient across the Pacific and bringing warmer conditions to the west coast of South America. These events occur every 3 to 7 years, alternating with a counterpart (La Niña) or neutral conditions (Trenberth *et al.*, 2007), although weather patterns continue to be influenced by the preceding El Niño conditions for up to around three months after the end of an event (Trenberth, 1997). El Niño events are classified as occurring when the continuous five month running SST anomaly in the central Pacific remains above 0.4°C over a period of six months (Trenberth, 1976).

The combined effect of the El Niño-Southern Oscillation (ENSO) has global impacts, particularly manifest during the period from November to March. El Niño/La Niña events enhance the general global hydrological response, such as the Australian drought of 2003 (Trenberth *et al.*, 2007), or the 2011 floods in North America (World Meteorological Organization, 2011) and Australia. The extreme global mean temperatures and SST anomalies of 1998 and 2005 were both associated with very strong El Niños (Hansen *et al.*, 2002; Bindoff *et al.*, 2007).

Recent research has identified that the ENSO signature can have a considerable influence on extreme European weather patterns (Trenberth *et al.*, 2002; Sapiano *et al.*, 2006; Seierstad *et al.*, 2007; Zanchettin *et al.*, 2008; Vitolo *et al.*, 2009), although modulated by very positive NAO winters. Van Oldenborgh *et al.* (2000) identified a strong correlation between spring precipitation in Europe and the phase of El Niño. The impacts are indirect as they arise from the effects of a strong ENSO signal elsewhere, however El Niños appear to be accompanied by negative phase NAO as a result of the pole-ward shift in MSLP anomalies (Brönnimann *et al.*,

2007; Zanchettin *et al.*, 2008). While Allan *et al.* (2009) and Zanchettin *et al.* (2008) found that ENSO has a modulating influence on severe storms in the British Isles during particularly warm years; in contrast, particularly strong NAO years can mask the ENSO response in mainland Europe (Zanchettin *et al.*, 2008).

2.2 Observed Responses and Projected Changes

2.2.1 Ocean-atmosphere

Circulation at the ocean surface is driven by the trade winds at mid-latitudes and atmospheric westerly winds at higher latitudes, with the strongest atmospheric-ocean coupling driven by the Ekmann transport along the equator and the surrounding Inter-tropical convergence zone (ITCZ). The atmospheric winds control moisture convergence zones and storm genesis as enhanced sea surface temperatures lead to increased baroclinic instability enhancing tropical storm magnitude (Bengtsson *et al.*, 2009). Deeper ocean responses are dependent on the relative density and salinity of the water, these processes respond over decades to centuries, exacerbating the difficulty in discerning changes (Held, 1993; Goosse *et al.*, 2009).

The most significant and probable atmospheric-ocean responses to increased global temperature will be changes to thermohaline circulation patterns and deep water formation, increased sea level caused by melting ice bodies and thermal expansion, and resultant changes in sea level pressure (Lenton *et al.*, 2008). The primary source of future changes in thermohaline circulation will arise from a freshening of the Atlantic Ocean, resulting from ice melt and increased storm genesis (Held, 1993). In the long term, significant dilution would lead to a shutoff of the Deep Water formation and eventual halting of the cross global thermohaline circulation (Lenton *et al.*, 2008); it is likely that existing oceanic circulation patterns would remain, although within reduced extents. Current projections show that this is unlikely to occur within the next 100 years, even under the most aggressive emissions scenario (Lowe *et al.*, 2009). The consequences of changes in atmospheric-oceanic interactions would be devastating on the global hydrological cycle as an increased temperature differential between the north and south hemisphere would displace monsoonal rains and cause expansion of the Sahel region (Held, 1993).

Research suggests that sea surface temperatures (SST) are a strong driver of southwest England mean daily rainfall (Phillips and McGregor, 2002); however, the dominant centre of influence varies throughout the year from an area in the east Atlantic during winter to the North Sea during the spring (Van Oldenborgh *et al.*, 2000). Phillips and McGregor (2002) concluded that monthly SST measurements are more strongly correlated with mean daily rainfall characteristics, with lower SST corresponding with increased intensity, while seasonal measurements are more reflective of atmospheric circulation. In contrast, Wilby *et al.* (2004) examined this further in southeast England finding that most predictors offered only a low explanation of the variance in summer low flow anomalies. The research supported the use of several different variables, both local and equatorial, for summer rainfall predictions, although finding that all variables performed considerably better for dry conditions than wet.

2.2.2 Temperature

Increases in post-industrialisation global mean temperatures are well established, with the first decade of the new millennium featuring the 12 warmest years since 1856 (Jones, 2011). Some of the direct consequences of increasing global temperature are immediately evident such as: reduced land and sea ice; increased heat wave frequency; increases in frost-free days and increased growing season length. The potential societal and ecological impacts are of great interest to governing bodies when determining future action plans for adaptation (Dessai *et al.*, 2009), and may have enormous repercussions on the hydrological cycle through feedback mechanisms (Burt and Shahgedanova, 1998; Zaitchik *et al.*, 2006; IPCC, 2007a; Prasad *et al.*, 2008; Prudhomme and Genevier, 2011).

Alexander *et al.* (2006) built on previous studies (Karl and Knight, 1998; Peterson *et al.*, 2001; Frich *et al.*, 2002), using a series of international workshops to obtain data and to define a set of temperature and precipitation characteristics (indices) which can be monitored for signs of changes in a warming climate. Over 70% of the examined land area had experienced increased mean and maximum temperatures since 1951. The success of the initial workshops was repeated, as a reliable method of obtaining climate data from politically sensitive regions, with

similar results and higher confidence through the increased spatial coverage (Choi *et al.*, 2009; Caesar *et al.*, 2011; Vincent *et al.*, 2011). Indices which are expected to decrease with an increase in global mean temperature, such as the number of frost days, will also bring increases in parasites or vector borne diseases either through range shifts or reduced periods of dormancy (Zhou *et al.*, 2008; Logan *et al.*, 2010; Mills *et al.*, 2010). While the expected increase in other indices, e.g. growing season length, may bring some positive impacts in the short-term in very northern latitudes, most impacts are anticipated to become negative beyond 2050 (Jenkins *et al.*, 2010).

Temperature increases are expected to be greatest in the Northern Hemisphere, where the larger land mass contributes to a higher heat capacity; slower oceanic responses, as a result of mixing and heat sink, will also enhance the impacts over land (Held, 1993; Goosse *et al.*, 2009). Direct consequences, such as summer ice loss and increases in the duration of ice free passages through Arctic sea ice, retreating glaciers, and reduction in areal coverage of Antarctic, and Greenland ice-sheets, will have significant secondary impacts on the global hydrological cycle (Fowler and Archer, 2006; Lenton *et al.*, 2008).

2.2.3 Rainfall

The Clausius-Clapeyron (C-C) equation (Hess, 1959) defines the relationship between the temperature gradient and water vapour pressure as

$$\frac{de_s}{dT} = \frac{L_v e_s}{R_v T^2}$$

Equation 2-1

where:

- e_s = saturation water vapour pressure
- T = temperature (°K)
- L_v = latent heat of evaporation
- R_v = water vapour gas constant.

As atmospheric water vapour content is dependent on temperature, it follows that increases in global mean temperature (both at the surface and in the atmosphere) will lead to an increase in the amount of water vapour held in the atmosphere of approximately 7%/°K (Trenberth, 2005b). However, as the

hydrological cycle is not solely controlled by the availability of moisture, but also by the available energy budget, increases in precipitation will be smaller in mid-latitudes and nearer to the equator than in northern latitudes (Allen *et al.*, 2002). In particular, increases in extreme rainfall will vary with latitude and are unlikely to equal the rate of increase in atmospheric moisture (O'Gorman and Schneider, 2009).

Observed decreases in snow cover in many areas are attributable to reduced snowfall and decreases in cloud cover, minimising surface melt, as a result of the decreasing diurnal temperature range (DTR; Bolch *et al.*, 2008). Some regions have experienced increases in snowfall such as that experienced across many parts of the northern hemisphere during the winters of 2009 and 2010 (Met Office, 2010b), although these specific events may have arisen from natural climatic variability. At very low temperatures air conditions tend to be very dry and not conducive to precipitation; as the air temperature approaches 0°C, precipitation is more likely to lead to larger flakes and heavier snowfall (Trenberth, 2011). Similarly, some increases in glacier mass have been reported in the western Himalayas, arising from increased snowfall over a longer proportion of the cold season, in addition to an increased summer DTR which enhances cloud formation and thus decreases air temperatures and snow melt (Yadav *et al.*, 2004; Fowler and Archer, 2006).

2.3 Extreme Events

Seldom does a day go by without reports of extreme events or climate records being broken in some part of the world. The impression of an increasing frequency of "record breakers" is hard to ignore, despite oft quoted caveats regarding event attribution, and may be heightened in some small part by media availability, although it is not a new development (Chandler, 1952). It is understandable, as the potentially devastating consequences of extreme events enhance our awareness of their incidence far more than the occurrence of lower magnitude events.

There are two problems: one of assessing the probability of an extreme event occurring and the other of determining the likely future behaviour of these extreme events and their resultant impact on society. Emil Gumbel, noted that "Il est impossible que l'improbable n'arrive jamais" [it is impossible that an unlikely event will never happen]; engineering design has long made use of Gumbel's theories on

the extreme value distribution and subsequent developments to quantify the realistic probability of an event. This leads to the second problem of identifying the symptoms of the changing frequency of extreme events and whether future behaviour will continue in the same manner for which there is an increasing body of literature and software available (World Meteorological Organization, 2009; Gilleland and Katz, 2011).

Making allowance for extreme event data scarcity, it is *very likely* that daily temperature extremes are increasing, with a commensurate reduction in the frequency of very cold days and nights and an increase in heat wave frequency and duration (IPCC, 2011). While it is *likely* that extra tropical cyclone tracks have shifted pole-ward, increasing heavy precipitation in higher latitudes, there is also *low confidence* in the extent of changes. Confidence in projected changes is also low, although it is *virtually certain* that temperature extremes will continue to increase and that increases in heavy precipitation are *likely* to continue (IPCC, 2011). Refer to Appendix C for definitions of confidence and probability.

Brown *et al.* (2008) identified significant increases in extreme daily maximum and minimum temperatures since 1950, particularly in Canada and Eurasia, using extreme value analyses. Using similar techniques, increases in daily maximum and minimum temperatures have also been demonstrated in Spain (Cebrián and Abaurrea, 2006), North America and continental Europe (Gershunov and Douville, 2008; Furrer *et al.*, 2010), identifying a dependency between severity of the change and the driving atmospheric circulation patterns. Extensions to these analyses, making allowance for the annual cycle or atmospheric conditions demonstrated improvements in the trend coherence derived from extreme value models fitted to temperature maxima in Greece (Katsoulis and Hatzianastassiou, 2005).

Meteorological drought is often coupled with heat waves, as the anti-cyclonic circulation patterns which produce heat waves also preclude precipitation (Gershunov and Douville, 2008). Dry summers leading to drought conditions show evidence of year to year clustering, as well as an increase in spatial extent since 1750 (Briffa *et al.*, 2009). Burt and Horton (2007) found a sequence of periods of drought followed by heavy rainfall in the Durham observation series. Extensive drought

conditions often also correspond with enhanced rainfall occurrence in proximate regions, showing a tendency to increases in longevity and/or spatial extent in recent decades (Dai *et al.*, 1998; Groisman and Knight, 2008).

An increase in pressure gradients, arising from increases in SST, has led to an increase in frontal systems and more frequent and severe extra-tropical cyclones (Mailier *et al.*, 2006; Allan and Soden, 2008; Ulbrich *et al.*, 2009; Vitolo *et al.*, 2009) and possibly more frequent UK tornadoes. Apparent increases in UK tornado frequency may not be statistically significant, given improvements in observational capability over recent decades which artificially inflates the event record (TORRO, 2009). There is little agreement regarding the development of future wind storm activity, although most anticipate more frequent and intense extreme wind storms (Seierstad *et al.*, 2007; Ulbrich *et al.*, 2009; Vitolo *et al.*, 2009), with potentially more frequent high category storms as energy budgets constrain cyclone re-genesis (Trenberth, 2005a). As atmospheric winds, particularly storm life and intensity, are strongly correlated with sea surface temperature (SST) they are considered *highly likely* to increase in the future (IPCC, 2011).

2.4 Observed Extreme Rainfall Changes

The perception that extreme rainfall events have become both more frequent and intense in the most recent decade is reinforced by some particularly persistent events in the UK. The precipitation record for autumn-winter 2000-2001 was identified at the time as the wettest in the UK (Marsh and Dale, 2002); however, extreme events, both in terms of duration and intensity, have since surpassed this (Hanna *et al.*, 2008; Marsh, 2008). June 2007 was recorded as the wettest month for over 140 years in Yorkshire (Hanna *et al.*, 2008), September 2008 witnessed the 5th highest 3-day rainfall total since 1897 in Albemarle (Northumberland), and the UK record 24-hour total of 316.4mm was recorded in Seathwaite, Cumbria in November 2009 causing widespread devastation (Sibley, 2010).

While the probability of a new record breaker increases with the length of the record (Benestad, 2003) and the difficulty of detecting changes in precipitation behaviour, particularly extremes, are both acknowledged (Milly *et al.*, 2008), it is also apparent that rainfall patterns are changing in many regions (Trenberth *et al.*, 2007),

particularly in the extremes (Della-Marta *et al.*, 2007; Maraun *et al.*, 2008; Portmann *et al.*, 2009; Trenberth, 2011). Recent work has identified an increase in precipitation extremes, although not spatially coherent across the globe (Alexander *et al.*, 2009; Bocheva *et al.*, 2009). However, apparent differences in reported changes in extreme rainfall may also be apparent due to inconsistencies in the definition of "extreme" (Pryor *et al.*, 2009), or in the duration of events under comparison (Liu *et al.*, 2009).

While detection, as defined by the IPCC (Baede, 2007), is not a focus of this thesis, it is acknowledged that formal detection studies are required to determine whether apparent changes are part of natural climatic variability or a response to anthropogenic forcing (Hegerl *et al.*, 2004). Premised on projected increases in intensity of 7%/°K, in line with C-C constraints, and a global increase in temperature of 0.74°C, detection tests need only be sensitive to a change of 5% over 100 years of observed extreme rainfall (Westra and Sisson, 2011); however, this is also dependent on the unlikely occurrence of no changes to vertical atmospheric circulation patterns (Lenderink and van Meijgaard, 2008). A number of different studies of extreme rainfall have determined that although changes are not yet detectable at a regional level, they are likely to become more apparent during the coming decades (Frei *et al.*, 2006; Min *et al.*, 2009; Fowler *et al.*, 2010; Fowler and Wilby, 2010). For instance, increases in 10-day winter rainfall in the north of the UK could become important as early as 2030 (Fowler and Wilby, 2010).

2.4.1 Defining "extreme" rain

Different approaches have been used to assess extreme precipitation, with considerable discrepancies between the definitions of "extreme", e.g. annual maximum, upper 95% of the total annual rainfall (Burauskaite-Harju *et al.*, 2012) or wettest 5 days of the year (Liu *et al.*, 2011), and between the apparent changes (Liu *et al.*, 2009). Thus, selection of the "extreme" metric is very important as some metrics are more sensitive to changes than others, while changes in seasonal mean values are differ greatly from changes in extreme values (Hegerl *et al.*, 2004).

Approaches to identify changes in rainfall impacts have also differed between those focussed on specific event frequency (Karl and Knight, 1998) or intensity (Osborn and Hulme, 2002), to the probability of events with a specific magnitude

(Fowler and Kilsby, 2003b; Maraun *et al.*, 2009). Peak-over-threshold analyses, prior to applying an extreme value distribution, are also subject to the selection of a suitably high threshold. Different techniques include parameter stability estimates (Coles, 2001), high quantiles of the wet day distribution (Beguería, 2005) or a value exceeding a certain proportion of the mean wet day total (Fowler and Kilsby, 2003a). Although fixed thresholds of heavy and very heavy rain have been used (Villarini *et al.*, 2011b), it is not advisable where there are considerable differences in event magnitude between stations (Frei and Schar, 2001). Extreme value analysis to estimate the likely magnitude of events with a specific probability is popular as it has practical application in engineering design, policy making or water resource management (Villarini *et al.*, 2011a).

The various merits of these different approaches have been explored (Pryor *et al.*, 2009), concluding that quantile based tests are more sensitive to reporting biases arising from gauge metrification and that results from several methods should be compared. An alternative approach would be to consider "record breakers", whereby the first event in a chronological series automatically breaks the record, then each subsequent maximum is added to the series (Beran, 2002). As the time series from which maxima are extracted increases, so also does the number of record breakers and the probability that the current maximum will be exceeded (Taleb, 2011). Benestad (2003) explored chronological ('forward') and reverse chronological ('backward') record breakers and their relative influence on trend analyses. He observed that the same series analyses in both directions can reveal trends of different direction and significance, neither of which may necessarily be true.

Alexander *et al.* (2006) defined a set of ten indicators to facilitate comparison of extreme rainfall in different regions, indicated in Table 2-2. The sensitivity of a selection of these measures, and those identified above, will be explored in Chapter 5 to identify the most appropriate for use in later analyses.

Indicator	Name	Definition
RX1day	Maximum 1-day precipitation	Maximum daily total per year or season
RX5day	Maximum 5-day precipitation	Maximum 5-day total per year or season
SDII	Simple daily intensity	Mean precipitation on wet days ≥1mm
R10	Heavy precipitation days	Number of days per year ≥10mm
R20	Very heavy precipitation days	Number of days per year ≥20mm
CDD	Consecutive dry days	Longest dry spell per year
CWD	Consecutive wet days	Longest wet spell per year
PRCPTOT	Annual total precipitation	
R95p (or Q95)	Very wet days	Days ≥ 95% of 1961-90 mean wet day distribution
R99p (or Q99)	Extremely wet days	Days ≥ 99% of 1961-90 mean wet day distribution

Table 2-2 : Indicators of extreme rainfall from Alexander *et al.* (2006)

2.4.2 Changes in intensity

Regardless of the definition of extremity, however, there appears to be a consensus of an upward trend in the magnitude of extreme rainfall events in conjunction with the changing climate (Groisman *et al.*, 2001; Kunkel *et al.*, 2003; Alexander *et al.*, 2006; Gallant *et al.*, 2007; Liu *et al.*, 2011). Increases in event magnitude are particularly apparent in the longer duration events, e.g. 5- and 10-days (Fowler and Kilsby, 2003b; Bocheva *et al.*, 2009) in high northern latitudes; and in sub-daily rainfall in regions such as Eastern Australia (Westra and Sisson, 2011).

The reported increases in the frequency and vigour of extra-tropical cyclones (Ulbrich *et al.*, 2009; Vitolo *et al.*, 2009) correlate well with the observed changes in extreme rainfall, as increases in moist static energy and gross moist instability have led to changes in winds, drawing storm tracks pole-wards and enhancing moisture convergence at higher latitudes. This also corresponds with recent work demonstrating that increases in atmospheric moisture content are most likely to exacerbate extreme rather than mean rainfall (Allan and Soden, 2008; Trenberth, 2011).

Liu *et al.* (2011) concluded that extreme rainfall, estimated from the wettest days of the year, is increasing in China. Comparing their findings with a comparable study in the USA, they observed that trends estimated using a fixed number of maxima per year are sensitive to the chosen number of events; trends may be insignificant if

non-extreme wet days are included in the analyses (Michaels *et al.*, 2004) although the contrary is also true (Pryor *et al.*, 2009). Comparing trends in more extreme events (97.5^{th} and 99^{th} quantiles; Suppiah and Hennessy, 1998) with those in the mean or median established that the former are more readily detected, as imputed by observed increases in rainfall variability (Hegerl *et al.*, 2007).

Prompted by the severe flooding which occurred in the UK during 2001-2002, Fowler and Kilsby (2003b) examined multi-day annual maxima (AMAX) from 1961-2000, finding an increase in the magnitude of longer events in northern and western regions over the period of study, while equivalent events had decreased in the south. A downward trend in the estimated magnitude of summer events, particularly for 1-day events in Southeast England, and the median seasonal maximum event (SMED) was also found (Fowler and Kilsby, 2003a), in common with UK observations for southern regions (Maraun *et al.*, 2008; Jenkins *et al.*, 2010). In contrast, increases were found in summer maxima in northern England (Burt and Ferranti, 2010) and Scotland (Perry, 2006). Increasing trends in winter maxima are also apparent with the greatest increases in Scotland (Fowler and Kilsby, 2003a) and other parts of the UK, although with conflicting confidence in the estimated increases (Osborn and Hulme, 2002; Perry, 2006; Burt and Ferranti, 2010).

Assessing only the monthly England and Wales Precipitation series, between 1766 to 2002, Mills (2005) identified increasing trends in winter rainfall and decreasing trends in the summer. While the metrics under consideration differed, these findings were corroborated by Rodda *et al.* (2010)'s exploration of intense UK daily rainfall between 1911 to 2006 and Burt and Ferranti (2010)'s regional examination of intense rainfall in northwest England. The latter associated the observed decreases in extreme summer rainfall with cyclonic weather systems (Lamb, 1972), and increased extreme winter rainfall with enhanced westerly flow.

Maraun *et al.* (2009) examined UK monthly maxima between 1900 to 2006, confirming well known correlations between seasonal variability in event magnitude and orography. A statistical model premised on these results (Rust *et al.*, 2009) confirmed that improved return level estimates could be obtained for different magnitude events, by allowing for the annual cycle within estimated Generalized

Extreme Value distribution parameters. Further analysis demonstrated strong correlations between airflow strength, direction and vorticity, used as proxies for atmospheric circulation patterns, in addition to seasonality (Maraun *et al.*, 2011). Hand *et al.* (2004) compared extreme UK rainfall events between 1900 to 2000, finding similar correlations between seasonality and event classification, defined by Lamb (1972) circulation types. Similarly, using several different measures of winter rainfall extremity, Haylock *et al.* (2008) also found that the main drivers of inter-annual variability in the north of Europe are atmospheric pressure indices, such as the NAO index, temperature, humidity and sea surface temperature.

Changes in extreme UK rainfall are discussed in greater detail in relation to the analyses of seasonal and annual maxima in Chapter 6; while specific correlations found between rainfall maxima and atmospheric or meteorological drivers are outlined in Chapter 7.

2.4.3 Changes in frequency

Buishand (1977) established, from observations in the Netherlands, that there is no correlation between the rainfall total on the first day after a dry spell and the duration of the subsequent wet period; the beginning and end of any spell have the lowest mean total compared to other wet days; and there is some dependence between successive wet day totals, which is enhanced during the winter period. Again not specifically examining extreme rainfall, Cowpertwait (2001) determined that there is a distinct seasonality in the inter-arrival times of all wet spells caused by cyclonic or anti-cyclonic weather. The probability of two wet spells being generated by the same weather system was higher for summer storms than winter, while the frequency and size of clusters was larger during winter. However, these approaches have not been widely applied to extreme rainfall. Assessments of temporal variability in extreme precipitation mostly concentrate on the likely return frequency of seasonal or annual maxima (Rust *et al.*, 2009; Villarini *et al.*, 2011b), with little attention paid to the time elapsed between individual maxima (Li *et al.*, 2011). Since precipitation is a direct cause of flooding, characterising the behaviour of rainfall extremes would be a first step toward linking meteorological research to flood management.

The variability of events within a year can also be assessed through the dispersion of the annual count of events exceeding a high threshold (Villarini *et al.*, 2010). Long range dependence is particularly evidenced by 'clusters' of years (referred to as *overdispersion*) with high and low frequencies of floods or heavy rainfall (Villarini *et al.*, 2009). The count of extreme events per year is known to approximate a Poisson process (Hsing, 1988); the natural sequence of these extreme events will display some irregularity, which may appear within a reasonably short series to be overdispersion but on closer inspection the data will be found to approximate an exponential distribution (Shinohara *et al.*, 2010).

However, it is the occurrence of several periods of heavy rainfall in quick succession which may generate flood conditions. Zolina *et al.* (2010) examined trends in the longevity of wet spells over the period 1950-2008 in mainland Europe, finding an increase in wet period duration although the total number of wet days per year had not changed. As with other literature on wet spell duration (Underwood, 2009; Li *et al.*, 2011), or event frequency, the authors acknowledge the importance of several events occurring in succession but did not specifically assess whether the spells were occurring closer together in time.

As outlined above, event clustering within the literature appears to refer to three different attributes of extreme meteorological events: year to year clusters or sequences of wet years followed by dry years (Villarini *et al.*, 2011a); in-year dispersion (or clustering) of events (Mailier *et al.*, 2006; Vitolo *et al.*, 2009); and events which span a "cluster" of several days e.g. a hot spell (Ferro and Segers, 2003). For clarity, this thesis will make reference to:

1. **Long range dependence** resulting in some sequences of similar years.
2. In year event clustering.
3. **Spells** of extreme wet events (EWE).

There is strong evidence that rainfall events cluster in time, driven by a seasonal non-homogenous Poisson Process (Tramblay *et al.*, 2011); this process can also be simulated with other statistical models such as the Cox Regression model to represent randomly varying rates of occurrence (Villarini *et al.*, 2012). Although the relationship between these dependent events is often ignored in order to conform

with extreme value theory (Revfeim, 1983; Fawcett and Walshaw, 2008) by selecting only the maximum of a sequence (Furrer *et al.*, 2010) or increasing the threshold (Davison and Smith, 1990). The focus of this research project is on extreme rainfall event **clustering**, that is the annual inter-arrival times of daily rainfall maxima, addressing this omission regarding inter-arrival dependency.

2.4.4 Hydrological impacts

The hydrological impacts of changes in extreme rainfall can be observed at both ends of the spectrum through changes in drought and flood frequency. Heightened variability in the hydrological cycle (Hegerl *et al.*, 2007) coupled with changes in rainfall frequency have had an impact on both with varying impacts dependent on the location or region of study. Within the UK, drought frequency is high variable yet, despite the current drought conditions (Environment Agency, 2012), significant changes are not yet observable (Burt and Horton, 2007; Hannaford and Marsh, 2008). In contrast, droughts in southern Mediterranean regions and parts of Australia are demonstrably increasing in rigour and frequency (Pnevmatikos and Katsoulis, 2006; Gallant *et al.*, 2007; Costa and Soares, 2008; Jakob *et al.*, 2011). This largely arises from the feedback loop created by reduced evaporation potential, in the absence of rainfall, which serves to enhance temperatures and thus droughts while exacerbating heavy rainfall elsewhere (Gershunov and Douville, 2008).

Understanding the true nature of changes in flood frequency is difficult due to abrupt changes in catchments such as dam construction (Villarini *et al.*, 2011c) or more gradual impacts from urbanisation (Hannaford and Marsh, 2008; Prudhomme and Genevier, 2011) or agriculture and forestry practice (Stahl *et al.*, 2010). Results mirror those for droughts, with increases in stream flow found in the higher latitudes of Europe and North America (Bocheva *et al.*, 2009; Fowler *et al.*, 2010; Villarini *et al.*, 2011c) and decreases towards the Mediterranean (Stahl *et al.*, 2010; Hannaford *et al.*, 2011).

2.5 Projected Changes in Extreme Rain

The likely changes in precipitation patterns are less well understood than likely temperature changes, although climate models have been used (Fowler and Ekström, 2009; Portmann *et al.*, 2009) to demonstrate that the influence of increased global

mean temperature on the hydrological cycle will be an enhancement of variability affecting the extremes more than mean rainfall (Hegerl *et al.*, 2004; 2007). As wind and rain storms are strongly associated through storm-scale enhancements of moisture convergence (Trenberth, 1998; Trenberth *et al.*, 2003), increases in wind storms will lead to increased extreme rainfall (Trenberth, 2011). However, the global distribution of changes in rainfall intensity will not be uniform across the globe and is likely to mimic the changes in surface temperature, with the largest relative increases in projected extremes likely to occur in the higher latitudes, as a result of the pole-ward shift of storm tracks (Meehl *et al.*, 2005). Lenderink and van Meijgaard (2008) caution that while projected changes in rainfall intensity are likely to be dominated by thermodynamically driven processes, the future dependency on temperature may not continue in the same manner as under current climate conditions.

At higher latitudes, where the moisture-adiabatic lapse rate is less important (Pall *et al.*, 2007), changes will be governed by the C-C relationship. However, the increase in moisture holding capacity may not in itself lead to an increase in precipitation, which would require an increase in the rate of evaporation or in atmospheric water; so resultant impacts on rainfall will be location dependent (Benestad, 2006). Atmospheric moisture condensation only increases at a rate of 2.9%/°K (O'Gorman and Schneider, 2009) as a result of the rate of decrease of temperature in rising air. O'Gorman and Schneider (2009) also noted that extreme precipitation responses to warm anomalies, such as ENSO, are likely to differ considerably from the responses to more gradual increases in global mean temperature.

Increases in sub-daily extreme rainfall intensity may increase at a higher rate than the constraining C-C relationship, with no increase in frequency (Lenderink and van Meijgaard, 2008). It is more likely that extreme rainfall intensity will be governed by moisture availability, and hence seasonal moisture patterns (Berg *et al.*, 2009), with the majority of Global Circulation and Regional Climate Model simulations indicating increases in extreme events at the expense of lighter rainfall (Wilson and Toumi, 2005; Wentz *et al.*, 2007; Min *et al.*, 2009).

Anticipated responses to increasing global mean temperature can be summarised as (Allen *et al.*, 2002):

- In high-latitudes where evaporation potential is high, moisture convergence is also high and energy budgets are less important, precipitation will increase at a rate of at least 7%/°K
- In mid-latitudes and at the equator where there is a high evaporation potential, precipitation will increase with increased warming at a rate of around 3%/°K.
- In arid regions where the evaporation rate is constrained, the hydrological cycle will decrease with increased warming.

A further effect of the C-C relationship is that, where evaporation rates allow, increasing temperatures will lead to a concomitant rise in cloud formation. This may have a limiting effect as the resultant decrease in solar irradiance will in turn reduce the local temperature and atmospheric moisture capacity. Thus, areas of the UK such as North Scotland are likely to be more overcast in future climatic conditions, although not necessarily wetter (Murphy *et al.*, 2009).

Anticipated changes in hydrological responses are toward increased drought occurrence and severity (IPCC, 2011; Bladé *et al.*, 2012) as well as increased flood frequency (Christensen and Christensen, 2004; Beniston *et al.*, 2007; Fowler and Wilby, 2010; IPCC, 2011; Trenberth, 2011) as the natural variability of the hydrological cycle is enhanced. As a result of interconnections between atmospheric circulation patterns and moisture budget movements, large scale droughts in one region accompanied by severe flooding in an adjacent location are also likely to increase in severity through enhanced feedback (Trenberth, 2011). While the pole-ward transportation of atmospheric moisture via Atmospheric Rivers may also considerably enhance rainfall intensity in regions such as North America and the UK which lie in the path of these systems (Lavers *et al.*, 2011).

A responsibility lies with scientists to ensure that advances in climate change research, particularly in sensitive areas such as extremes of the hydrological cycle, are reflected properly in policy development. Some argue that we require better

predictions of these extremes in order to adapt effectively to the changing climate (Dessai *et al.*, 2009) while others believe that a better understanding of exposure risk from the *environment* to the *development* in question is required in order to adapt effectively (McEvoy *et al.*, 2010). Others still seek ways of employing complex mathematical tools to quantify the risks (Schertzer *et al.*, 2010; Taleb, 2011).

With the recent release of the Adaptation Sub-Committee (ASC) of the Committee on Climate Change's report (Krebs *et al.*, 2010) assessing the UK's state of preparedness for climate change, there has been a shift in focus from whether climate change is occurring to determining the likely consequences. The first release of the UK Climate Change Risk Assessment (DEFRA, 2012), in combination with the forthcoming Adaptation Action Plans for Scotland, Wales, Northern Ireland and many regions of England, will further enhance this focus and derive a greater need to understand extreme weather patterns. In particular, the ASC identified that in order to avoid maladaptation (that is adaptive actions which have a negative impact elsewhere, or at a later point in time), there is a need to quantify the UK's vulnerability to climate change. Nelson (2011) highlights that both individual and governance risk and decision frameworks are hampered by the lack of clarity and limited predictive power for future changes in extreme events. The authors of a recent assessment of the potential for cities to adapt to climate change concur with this, and demonstrate that those who are more capable of taking action are generally at a lower level of governance (Rosenzweig *et al.*, 2011).

2.6 Summary

This chapter synthesised the research underpinning this project, outlining the sources of variability which may arise in meteorological observations in general terms. The ocean-atmosphere relationships which govern weather systems in general, and extreme weather in particular, were summarised. Resultant changes in extremes identified within the literature, both in general and with particular attention to daily rainfall, and the consequences which are being experienced at present were summarised. Further detail on the observed changes in extreme and very heavy UK daily rainfall is included in later chapters, particularly within Chapter 6 which deals with annual and seasonal maxima. Some anticipated changes in the

hydrological cycle, again focussed on rainfall, were also explored. Methods associated with the previously cited research were not described here, rather those methods which will be used in this thesis are outlined in Chapter 3.

The overarching aim of this project is to examine within year clustering of extreme daily rainfall and the key atmospheric or meteorological variables driving event frequency and intensity. Therefore, the thesis will initially focus on the sources of variability in extreme and very heavy daily rainfall, repeating approaches used in other parts of the world specifically for the UK. Metrics of extreme rainfall which have been used to effect by others will be explored for their applicability to this project. Atmospheric relationships established from the literature will then be examined in relation to extreme rainfall. Where appropriate, such as in the exploratory data analysis in Chapter 5, results which were briefly outlined in this chapter will be explained in greater detail.

Chapter Three Statistical Tools

"He uses statistics as a drunken man uses lamp posts
- for support rather than illumination."

Andrew Lang

Rigorous statistical analysis is required to distinguish seasonal and other short term climate fluctuations from longer-term variability and external forcing affecting climate dynamics, to identify changes (von Storch and Zwiers, 1999) and to avoid drawing spurious conclusions. The objective is to demonstrate that any apparent changes are significantly different from those which would be expected given natural climate variability (Koutsoyiannis, 2003; Trenberth *et al.*, 2007). This is a notable challenge given the complexity of the climate system and natural variability, but is considerably enhanced when accounting for anthropogenic influences (Milly *et al.*, 2008).

Following the development of a comprehensive set of rainfall observations, outlined in Chapter 4, the data will need testing for homogeneity and discontinuities arising from the quality control process or external influences such as gauge relocation. Apparent trends in the data must then be distinguished from cyclic variability and randomly occurring processes. In order to identify an appropriate metric of extremity, an appreciation of the representative statistical distributions is required. Finally, as the aim of this project is to determine the relationship between extreme daily rainfall and atmospheric covariates, tools are required to incorporate this spatial and temporal information and to test the model validity in representing the data.

While Chapter 2 explored the results which have been published previously, this chapter briefly summarises the published methods and identifies those to be used in this project. The structure of this chapter is similar to the overall thesis. It examines: abrupt and gradually varying changes; statistical distributions for extremes; methods to incorporate multiple variables in the distributions; and model testing approaches.

3.1 Abrupt and Gradually Varying Change

Hydrological records are highly volatile and dominated by climate variability to a greater extent than temperature records (Zhang *et al.*, 2011), so it is more difficult to capture abrupt and gradual changes as the data may simply be exhibiting normal temporal perturbations (Lins and Cohn, 2011). While the data to be used in this research have been subjected to quality control and homogeneity checks at source, assessing gradual or abrupt changes will help to identify any remaining sources of error. These tests will also ensure that the influence of any repeated variability (e.g. seasonal oscillations) is incorporated within later statistical analyses.

3.1.1 Abrupt change points

Trends may appear to exist in data where none is truly present, arising from abrupt changes in the data (change points) or from cyclic variability (Chen and Grasby, 2009). Tests for change points in the data may focus on single or multiple points, dependent on the eventual purpose of the application (Reeves *et al.*, 2007). For instance, in producing a homogenous observation record, multiple change point detection tests such as the minimum description length or the Rodionov test (Rodionov, 2004) are recommended. However, these methods require *a priori* knowledge of likely change points and can be computationally expensive (Rodionov, 2005). Furthermore, identifying too many change points in a data series will over-fragment the data and can potentially enhance any apparent trends (Chen and Grasby, 2009).

The cumulative sums test (Page, 1957) is the simplest test for a single change point, but has been shown to be very sensitive to highly variable series (Villarini *et al.*, 2009) such as rainfall maxima. As a result, the non-parametric Pettitt test (Pettitt, 1979) will be used in this thesis. The test statistic, $U_{t,T}$, premised on the Mann-Whitney two sample test for population similarity, compares the sample mean and variance calculated from two portions of a time series, X, for increasing sequences:

$$U_{t,T} = \sum_{t=1}^{t} \sum_{j=t+1}^{T} D_{ij} \qquad \text{where} \qquad D_{ij} = (X_i - X_j)$$
$$= 2W_t - t(T+1)$$

Equation 3-1

with a critical value, P, calculated from (Gao *et al.*, 2010):

$$K_T = \max_{1 \le t \le T} |U_{t,T}| \qquad \text{and} \qquad P \simeq 2\exp\left(\frac{-6K_T^2}{T^3 + T^2}\right)$$

Equation 3-2

3.1.2 Gradual changes - long range dependence

Prior to testing for trends within the data, it is necessary to establish the influence of any other type of variability, such as seasonal or longer cycles, on apparent changes in the data. Some authors have argued that (fractional) auto-regressive moving average (ARMA, FARIMA) models are potential explanatory variables for the Hurst Phenomenon, or other long-term memory processes (e.g. Allan *et al.*, 2009). Methods to quantify the Hurst Exponent, H, include comparison with white noise series, fractional Gaussian noise or fraction Brownian motion (Serinaldi, 2010). Koutsoyiannis (2002) also developed a linear estimator from a simple scaling signal (Klemes, 1974) of the non-stationary process. However, the estimation of variance has standard errors proportional to the inverse of the data series duration; e.g. for $n=100$ years, s.e.= $\sigma/2.5$ rather than $\sigma/10$.

The aggregated variance method is the most commonly adopted method for estimation of H (Taqqu *et al.*, 1995), with the differenced variance method being more effective when significant change points or trends exist in the data (Perreault *et al.*, 2000a). In this method, the time series X_i are divided into m-sized blocks and the aggregated average calculated for successive values of m:

$$X^m(k) = \frac{1}{m} \sum_{i=(k-1)m+1}^{km} X(i) \qquad k = 1, 2, \ldots,$$

Equation 3-3

for which the sample variance can then be estimated, $Var(\bar{X^m}) \backsim \sigma^2 m^{2H-2}$. When plotted on a logarithmic scale, the gradient of the sample variance estimates form a straight line with gradient $\beta = 2H - 2, \quad 1 \le \beta \le 0$. Significance of the estimate of H is established by destroying the memory of the process through resampling.

3.1.3 Gradual changes - monotonic linear trends

The most widely used technique for examining gradually varying changes is that of ordinary least squares regression (OLS); although it is reliant on homogenous, independent and identically distributed (i.i.d.) data, and normally distributed departures from the regression line (Kundzewicz and Robson, 2000). This is not appropriate for serially dependent data (Hess, 1959; Alexander *et al.*, 2006) and represents un-transformed hydrological data trends poorly (Yue and Pilon, 2004; Pryor *et al.*, 2009), often reporting a trend where one is not present (Cohn and Lins, 2005). However, where data are independent and can be transformed to fit a normal distribution, OLS regression is a powerful tool and often more satisfactory in describing a whole data series than more complicated regression analyses (von Storch and Zwiers, 1999). Traditional linear regression models focus on the median of the data, potentially ignoring changes in other quantiles of the highly complex and variable annual maxima series. By contrast, quantile regression characterises the relationship over time by assessing OLS trends at different levels of the response variable (Cade and Noon, 2003); a combination of both techniques will be employed in the exploratory data analysis.

Testing for the significance of such trends can vary from simple data manipulation techniques to formal distribution tests. Data permutation and bootstrapping are considered effective in establishing trend realism, (Davis and Mikosch, 2008), while simplifying the data with a simple running median or more sophisticated locally weighted scatter plot smoother to remove some natural variability (Kundzewicz and Robson, 2000), or ranking data can also be powerful tools (Moberg and Jones, 2005).

Bootstrapping is an enhancement of the Jack-Knife approach making better use of the available data through resampling (Efron, 1979), outlined in Appendix 1. While less powerful than permutation approaches, it is more flexible in its application (Kundzewicz and Robson, 2000), with its success lying in its simplicity and lack of distributional dependence (von Storch and Zwiers, 1999). A simple adaptation to this process to allow for short-term dependence within a series is the moving

block bootstrap (Yue and Pilon, 2004), wherein groups of l consecutive observations, rather than individual observations, are sampled.

The most robust significance tests commonly employed with OLS are both non-parametric: the Mann-Kendall test statistic and Spearman's rank correlation test. While the latter is simple and efficient in removing the effects of seasonality, it is not considered to be as robust in trend estimates for censored, non-normal data as the Kendall correlation coefficient (τ) (Yue *et al.*, 2002). In contrast, Kendall's τ is robust to the presence of extreme values (Hamed and Ramachandra Rao, 1998), a noteworthy consideration for this application. Chen and Grasby (2009) recommend commencing the trend test at different points within a data series to obviate the Mann-Kendall sensitivity to diurnal and seasonal cycles.

The Mann-Kendall test statistic, S, which will be used in the thesis, is estimated by ranking n pairs of concordant and discordant data, then estimating the variance given the presence of tied data pairs and calculation of the test statistic with a critical value τ:

$$Z = \begin{cases} (S-1)/Var(S)^{1/2} & \text{for } S > 0 \\ 0 & \text{for } S = 0 \\ (S+1)/Var(S)^{1/2} & \text{for } S < 0 \end{cases}$$

$$\tau = \frac{2S}{n(n-1)}$$

Equation 3-4

3.1.4 Sequences of events

The distributions described later assume that extreme events are i.i.d., although this is rarely completely true (Katz *et al.*, 2002) as threshold maxima are often generated by the same weather system and so tend to occur in clusters (Smith and Weissman, 1985). Independent sequences of peak-over-threshold (POT) events can be identified using a declustering algorithm, accepting only the maximum of several clustered events. The concept of clustering at high levels was explored by Leadbetter (1983) who defined an 'extremal index' θ related to the cluster size composed from a sequence of events. If $0 < \theta \leq 1$ is a measure of the data tendency to cluster at high levels, then $\theta \to 1$ as the degree of clustering decreases.

Hsing (1988) showed that clusters of exceedances are independent at the upper limit of their distribution.

A parameter stability exercise can be used to determine the minimum duration between each cluster (Coles, 2001) or simply prior knowledge of the typical climatology (Abaurrea *et al.*, 2007). More complex models exist to assimilate all of the data relating to the maxima, conditioning subsequent excesses of a cluster on the first in a sequence (Furrer *et al.*, 2010). Alternatively, the combined properties of the extremal index and the Poisson process, with a de-cluster interval of $r \geq \frac{1}{\theta}$ is appropriate to identify independent event clusters (Ferro and Segers, 2003) and will be used here.

The theory of runs assumes that events occur randomly in sequences of similar nature, exhibiting some apparent clustering (Rubin *et al.*, 1990) and can be used to approximate the arrival times of POT events. The efficacy of the declustering algorithm can be assessed by reviewing the frequency of spells with rainfall below the threshold, or randomness of the events (Englehart and Douglas, 2006).

The Wald-Wolfowitz runs test (Wald and Wolfowitz, 1940) is a powerful tool to assess the randomness of a sequence of events (McWilliams, 1990). While enhancements have been proposed to remove the sensitivity of the data to the selected distribution and assess the confidence level (Wendy Lou, 1996), the original test will be adequate for exploratory analyses in this thesis. Consider POT events as a positive occurrence, denoted by 1, and events below the threshold denoted by 0. A run, R, is the number of successes in any sequence. Then, indicating the number of positive successes by n, and zero occurrences as m:

$$E(R) = 1 + \frac{2nm}{n+m}$$
$$\sigma^2(R) = \frac{2nm(2nm-n-m)}{(n+m)^2(n+m-1)}$$

Equation 3-5

which may then be tested at a suitable confidence level against the statistic

$$Z = \frac{R - E(R)}{\sqrt{\sigma^2(R)}}$$

Equation 3-6

3.2 Probability Distributions

Three basic forms of statistical distribution are appropriate for extreme rainfall analysis: discrete describing the frequency; continuous relating to the magnitude of less heavy rain; and extreme values governing the tail properties. These will be described briefly below, with the underlying theory included in Appendix B.

3.2.1 Discrete distributions

Consider the probability of extremely heavy rain occurring on a given day as a Bernoulli trial, with success 1 and failure 0. A number, n, of these events occurring over a fixed interval of time or space is described by the Poisson distribution with arrival rate, Λ. Events are assumed to be i.i.d. over the spatial and temporal frame with arrival rate equal to the mean and the variance of the series, that is equally dispersed with a coefficient of dispersion $\frac{1}{\theta} = 1$, equivalent to the cluster index.

Even following data declustering, strict independence is often hard to prove (Wilks, 2005), particularly with respect to extreme events derived from one synoptic scale weather system, or driven by seasonal processes. When $\frac{1}{\theta} < 1$, the sequence is under dispersed, events arrive at a rate which is more regular or uniform than expected from a Poisson process. By contrast, $\frac{1}{\theta} > 1$ relates to an over-dispersed (or clustered) sequence of events, often demonstrated by hydrological extremes through sequences of wet and dry years (Mandelbrot and Wallis, 1968). A visual representation of over-, under- and regularly dispersed series is illustrated from the frequency of rainfall maxima per year over a 30 year period in Figure 3-1.

As the stationarity assumption is invalid in the presence of substantial seasonal cycles, the negative binomial distribution is often considered more representative, describing the frequency of failures before the x^{th} success (Anselmo *et al.*, 1996). While the negative binomial can be a good approximation for wet spell durations, it over-represents their frequency (Wilks, 1999), recommending the use of an alternative representation of non-homogeneity within the Poisson distribution.

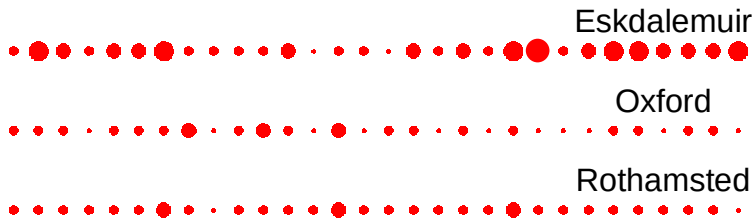

Figure 3-1 : Dispersion of number of peak-over-threshold rainfall events per year (top) over-dispersed ($\frac{1}{\theta} > 1$); (middle) regular ($\frac{1}{\theta} = 1$), (bottom) under-dispersed ($\frac{1}{\theta} < 1$) from three UK gauge stations. Point size represents the event count.

3.2.2 Gamma distribution

Atmospheric data, such as daily rainfall totals, which are distinctly skewed to the right and bounded to the left by zero, are well approximated by the gamma distribution (Thom, 1958; Groisman *et al.*, 1999; Husak *et al.*, 2007; Wang *et al.*, 2008). The distribution is controlled by the dimensionless shape parameter, α, and the scale parameter, β, which takes the dimensions of the data distribution.

3.2.3 Extreme Value distributions

Block Maxima

It is well established that a collection of maxima, M_i, over a series of n blocks, such as annual maxima follow the *Generalized Extreme Value (GEV)* distribution:

$$G(x;\mu;\sigma;\xi) = \exp\left[-\left(1+\frac{\xi(x-\mu)}{\sigma}\right)^{-1/\xi}\right] \qquad \text{where } 1+\frac{\xi(x-\mu)}{\sigma} > 0$$

Equation 3-7

with parameters location $-\infty < \mu < \infty$, scale $\sigma > 0$ and shape $-\infty < \xi < \infty$ (Coles, 2001). Three limiting forms of the GEV exist for $\xi = 0$ (Gumbel, light tail); $\xi > 0$ (Fréchet, heavy tail); and $\xi < 0$ (Weibull, bounded distribution). Quantile estimates of the distribution are often used to estimate the probable return frequency of rainfall maxima (Faulkner, 1999; Fowler and Kilsby, 2003b).

Parameters for the GEV are best estimated by the L-moments method for small samples (Hosking, 1990), while Maximum Likelihood Estimates are more appropriate in the presence of external influences such as a changing climate or covariate data (Smith, 1987; Katz *et al.*, 2002; Zhang *et al.*, 2004); refer also to Section 3.4. As parameter estimation can be affected by long range dependence,

which increases uncertainty (Rust, 2009), parameter uncertainties are best estimated with a bootstrap by replacement method (Efron, 1979).

The model can be expanded to include the *r* largest events per block by defining $M_n^{(r)} = r^{\text{th}}$ largest of $(X_1, X_2, ...X_n)$, assuming that the parameters correspond with those of the AMAX limiting GEV distribution (Smith, 1986). However, the series are no longer independent as the outcome of each subsequent event is dependent on the magnitude and occurrence of the previous value (Coles, 2001). Although parameter estimates are generally improved, compared with using the annual maxima alone, increases in the data set must be balanced against the increased bias towards less extreme rainfall (Robinson and Tawn, 1997; Coles, 2001).

Peak-over-threshold (POT) Maxima

Analysing only the annual maximum value disregards useful information during particularly wet years; the extension to the *r*-largest statistical model is an improvement but can also omit maxima within a predefined block (Coles, 2001). The alternative is to derive a partial duration series from excesses over a high threshold, u, or peaks-over-threshold. While care must be taken with the threshold selection (Zhang *et al.*, 2005; Kenyon and Hegerl, 2008), this approach offers considerable advantages by only incorporating extreme data, without limiting the analysis set. The POT maxima follow the *Generalized Pareto Distribution (GPD)*, shape ξ and scale $\tilde{\sigma}$ parameters (Coles, 2001).

$$H(y) = 1 - \left(1 + \frac{\xi y}{\tilde{\sigma}}\right)^{-1/\xi}$$

Equation 3-8

The three limiting forms are dependent on the shape parameter: $\xi = 0$ (exponential, light tail); $\xi > 0$ (Pareto, heavy tail); and $\xi < 0$ (beta, bounded distribution).

Approximating the frequency of POT events with a Poisson distribution, the frequency and magnitude of the maxima are often analysed using a *Point Process* relationship (Lana *et al.*, 2006; Abaurrea *et al.*, 2007; Furrer *et al.*, 2010). This combines the GPD with the Poisson distribution by linking the occurrence rate, scale and shape parameters through those of the GEV. The point process is convoluted to

fit, but facilitates interpretation of results and calculation of error terms (Davison and Smith, 1990). Alternatively, an *orthogonal process*, where the two models are fitted independently, is simpler to apply but introduces greater difficulty in interpretation of the model parameters.

3.3 Generalized Additive Models

While Generalized Linear Models (GLM; refer to Appendix B.3) are effective in modelling daily rainfall event occurrence, and their dependence on atmospheric circulation patterns (Sapiano *et al.*, 2006), they can over-simplify data or processes which are known to be highly random from year to year (Chavez-Demoulin and Davison, 2005). As GLMs relate the mean of a set of random response variables to a collection of explanatory variables, they are not appropriate for direct transformation to extreme value distributions (Yee and Stephenson, 2007). Yee and Wild (1996) formally introduced the concept of Vector Generalized Linear Models (VGLM), allowing statistical models to be data driven rather than model driven. Although care must be taken in the application of this approach to extreme value distributions, which by definition are model driven as the asymptotes of the distribution are extrapolated, nesting the two methods has been shown to be very powerful (Stephenson and Gilleland, 2006).

An enhancement to the GLM is that of Generalized Additive Models (GAM, Hastie and Tibshirani, 1990) where the linear predictor term is replaced by the sum of smooth non-linear functions of the covariates. The GAM has been widely adopted as an effective model for strongly seasonal or forced responses (Wood, 2006; Villarini *et al.*, 2011b), as well as examining longer term changes in behaviour in temporally variable data (Morton and Henderson, 2008; Mestre and Hallegatte, 2009; Underwood, 2009), and is considered particularly appropriate for use in this project. GAMs allow much greater flexibility in the model specification and simplify complex linear relationships through a model specification based on ‘smoothness’. Hastie and Tibshirani (1990) recommend the use of a combination of several polynomials or p-splines to model the smoother; this shifts the focus to a model driven representation, focussing on a model which is flexible without over- or under-smoothing the response. Wood (2006) concurs, emphasising that while this is not

the only approach, other solutions are theoretically over-complicated and computationally intensive.

Vector Generalized Additive Models (VGAM) are an enhancement of VGLMs and applicable to a wide range of non-exponential family models, including Extreme Value Distributions (Yee and Wild, 1996). As the focus of this project is on extreme value distributions, the R software package (R Development Core Team, 2011) which will be employed is VGAM (Yee, 2011) in which the smoothers are chosen by default. Faraway (2006) finds this approach to be advantageous, in removing the subjectivity required to choose the degree of smoothness. The software's enhanced flexibility and functionality permits direct estimation of parameters, e.g. for the GEV:

$$\mu(\mathbf{x}) = \eta_1 = \beta_{1(1)} + f_{1(2)}(x_{1(2)}) + \ldots + f_{1(n)}(x_{1(n)})$$
$$\log(\sigma(\mathbf{x}) = \eta_2 = \beta_{2(1)} + f_{2(2)}(x_{2(2)}) + \ldots + f_{2(n)}(x_{2(n)})$$
$$\log(\xi(\mathbf{x}) + \frac{1}{2}) = \eta_3 = \beta_3$$

Equation 3-9

The shape parameter, ξ, is fit by default as an intercept only term as it is numerically difficult to estimate (Katz *et al.*, 2002; Yee and Stephenson, 2007).

3.4 Multivariate Distributions in Time and Space

Extreme value distributions premised on stationarity are invalid in the presence of a strong seasonal pattern, atmospheric circulation patterns or anthropogenic changes. A pragmatic approach introduces a linear model term into the distribution parameters. For instance a monotonic trend over the observation period can be incorporated into the GEV parameters as:

$$\mu(t) = \beta_0 + \beta_1 t$$
$$\ln \sigma(t) = \beta_0 + \beta_1 t$$

Equation 3-10

More complex terms can also be built up to express change points in the data (Coles *et al.*, 1999) or dependence on different processes. Increased covariate complexity and flexibility leads the parameter terms to represent GLM and GAM definitions as explored above (Dobson, 2002; Chavez-Demoulin and Davison, 2005; Wood, 2006). Furthermore, linear temporal trends are often too specific for use with

climatic variables, necessitating the greater flexibility of GAMs or VGAMs (Ghil *et al.*, 2011).

Trends in individual station extremes do not necessarily reflect a larger spatial pattern or response to larger scale changes, and may only represent the 5% error which would be expected at any 95% test of significance (Kanji, 1999). Similarly, direct comparison of the same properties at several proximate locations may not be appropriate as the observed events will not necessarily be independent without allowance for extremal dependence (Davison and Smith, 1990).

An effective method for spatial comparison of temporal changes uses regionally pooled data, weighted in some manner to reflect differences between station longevity or elevation. Spatial weightings have been used to effect in studies of individual metrics (Perry, 2006; Maraun *et al.*, 2008), a major drawback is that only one climate signal may be compared at a time. Other techniques which have been used to assess spatial variability include kriging (Haylock *et al.*, 2008) and Principal Component Analysis (PCA, Hurrell and Deser, 2009). The former is overly complex when assessing more than one variable (Carreau *et al.*, 2009) and has no allowance for parameter uncertainty. Similarly, PCA is inappropriate for direct application to extreme value analyses as the components tend to be derived from distributional means (Cooley and Sain, 2010). Regional Frequency Analysis (RFA, Hosking and Wallis, 1997) is another well-established method which is efficient and robust in estimating hydrological return periods where data are insufficient (Robson, 1999).

While multivariate spatial extreme models, centred on the marginal relationship of two extreme distributions (Cooley *et al.*, 2007; Naveau *et al.*, 2009) could be used to assess spatial maxima, application of the theory is complex and unreliable (Carreau *et al.*, 2009). An alternative is to incorporate spatial characteristics into individual station model estimates of the extreme value parameters, achieving spatial comparison indirectly (Cooley *et al.*, 2007). This technique was also applied to effect in South Africa by Sang and Gelfand (2009) and provides a considerable improvement over RFA in regions which are heavily dominated by orographic effects (Cooley and Sain, 2010). Despite the ease of

application, and improvements in model fits, there is a dependence on suitably long and complete observations to estimate the initial model distributions which will not be achieved with the data available. As a result, preference will be given to an RFA pooling approach, in combination with atmospheric covariates to assess spatial and temporal variability within the data.

3.5 Parameter Estimation

Maximum Likelihood Estimates (MLE) are asymptotically normally distributed, the variance is asymptotically minimal and they are asymptotically unbiased (Coles, 2001). However, the asymptotic properties are a draw-back when the sample size is small or when a combination of records (e.g. pooled flood maxima) are analysed (Hosking, 1990). MLEs may also not be appropriate for establishing confidence intervals in data where the distribution is known to be changing (Benestad, 2006; Rust, 2009). Where there are no prior constraints on the estimator, the MLE will occur at a point where the first derivative of the log-likelihood function equals zero; this first differential also determines the sensitivity of the log-likelihood function to changes in its parameters.

L-moments are a special case of the method of moments for estimating parameters of a distribution, in particular those of meteorological series (Hosking, 1995a). They exist where a series has a finite mean and are considered most appropriate for parameter fitting in skewed or small sample distributions (Hosking and Wallis, 1997). L-moment ratio measures of skewness and kurtosis are particularly useful in describing distribution shape and approximating distribution parameters (Robson, 1999).

When dealing with small samples, say <50, parameter estimates are best approximated by the L-moments method (Hosking, 1990); this method is also widely adopted in the UK for parameter estimates of rainfall and river flood flow frequency applied to pooled extreme value data. However, in the presence of an external influence such as changing climate or covariate data, MLE have been shown to be more appropriate (Zhang *et al.*, 2005; White *et al.*, 2008). A further advantage of MLE is that standard error estimates are inherently calculated, whereas L-moment ratios require further manipulation to determine the confidence limits. Furthermore,

MLE are more readily adapted to include covariates such as a trend term (Wilks, 2005), which is important where the data may display non-stationarity as a result of climate change (Katz *et al.*, 2002). A comparison of the GEV parameters estimated through MLE and L-moment ratios confirmed that differences between the methods two are minor, and both will be used as appropriate.

3.6 Significance Testing

3.6.1 Null hypothesis testing

Having established hypotheses from extreme metrics, whose sensitivity to different forms of variability has been minimised, and developed appropriate models, significance testing still requires caution. It is important to recognise that rejecting the null hypothesis (H_0) is only a failure to reject the hypothesis, and not a confirmation that the alternative hypothesis (H_1) is true (Nicholls, 2001). Failing to reject H_0 can arise from an absence of evidence to the contrary; e.g. the upwards trend since 1985 in the Central England Temperature series was only recently determined to be significant when additional data became available (Jones *et al.*, 2011).

The power of a significance test lies in the probability of detecting a genuine trend, that is to reject H_0 when it is indeed false (Kanji, 1999); where the probability of a Type II error, rejecting H_0 when it is true, is given by *1 minus* the power of the test (Yue and Pilon, 2004). In addition to the tests mentioned in Section 3.1 and below, a parametric test for significance which will be used is the Student's t-test, applied to normalised data (Wilks, 2005).

3.6.2 Model fit

The one-sample Kolmogorov-Smirnov test is a distribution free test of goodness of fit tests for continuous data distributions and considered to be a robust technique in combination with MLE for establishing the goodness of fit (Ghil *et al.*, 2011). Wilks (2005) cautions that where parameters for the fitted distribution are estimated from the same sample as that used for comparative testing, the strength of the test is weakened and that the critical test values should be obtained through repeated simulation.

Statistical models derived from multiple criteria should respect the laws of parsimony and be only as complex as required to explain the variable being modelled. The simplest qualitative test of model suitability is the deviance statistic, or likelihood ratio test, which compares the ratio of the likelihood functions for each fitted model (Wilks, 2005). An enhancement is to include the number of model components, as the deviance statistic always favours higher dimension models and can lead to unnecessary complexity (AIC, Akaike, 1974). However, when used for large sample data, the AIC also favours higher dimensional models as it ignores asymptotic optionality; this can be avoided by incorporating an additional log term for the number of estimators (BIC, Schwarz, 1978). The Generalized Cross Validation score (Hastie and Tibshirani, 1990), and the unbiased risk estimator (Wood, 2006) which are flexible re-scalings of the deviance statistic and AIC, respectively, are recommended for use with GAMs.

All model testing criterion can penalise models unnecessarily, despite evident improvements in model fit with additional parameters, suggesting that several should be used in addition to subjective testing (Villarini *et al.*, 2009). These tools will be used in combination with more quantitative tests such as Quantile-Quantile plots, visual assessment of model fit or absolute model indices such as the mean errors of estimated variables.

3.7 Conclusion

Methods for exploratory data analysis, such as the Pettit test for abrupt and gradually varying changes, Wolf-Waldowitz test for data randomness, or aggregated variance test for Long Range Dependence, will be applied to daily rainfall observations in Chapter 5. The return frequencies of annual maximum rainfall magnitudes will be estimated, using maximum likelihood estimates to obtain regionally pooled GEV distributions in Chapter 6. Chapter 7 will extend the extreme value data set, examining daily excesses over a high threshold with an orthogonal Poisson and GPD model. The chapter will also make use of multivariate statistics and Principal Component Analysis to define coherent regions of UK extreme rainfall. Finally, Chapter 8 will draw these analyses together with VGAMs to identify the

principal mechanisms driving very heavy rainfall events and their influence on within-year event clustering, and to examine any changes in behaviour.

Chapter Four Data

"No good *model ever accounted for* all *the facts, since some data was bound to be misleading if not plain wrong."*

James Dewey Watson, Some Mad Pursuit

This chapter identifies the data sets which have been selected to examine the temporal and spatial behavioural characteristics of extreme rainfall. The data described here include UK daily precipitation observations, daily and monthly temperature observations, and measures of atmospheric processes such as the North Atlantic Oscillation (NAO) Index. The chapter also describes the method followed to ensure that the rainfall observations were homogenous and did not include erroneous readings.

4.1 Precipitation

This project will concentrate on the frequency and magnitude of extreme and very heavy rainfall totals and will not refine on the type of precipitation, because hail and snow form a small proportion of the observed precipitation falling on UK wet days (≥1mm) as shown in Figure 4-1 (Met Office, 2011c). Furthermore, their liquid equivalent is reported in daily observation totals (Met Office, 2011a). It will also be shown in later chapters that the heaviest daily totals tend to have a distinct seasonal pattern centred around the summer months.

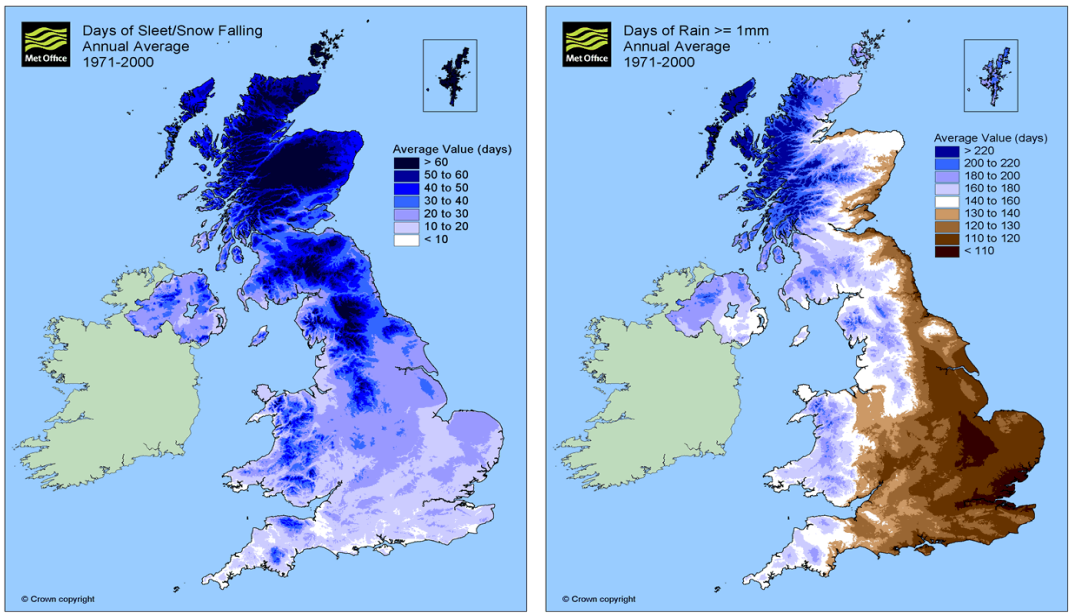

Figure 4-1 : Comparison of days of snow fall and wet days (Met Office, 2011c)

Various gridded or regionally averaged daily rainfall data sets are available, such as the Hadley Centre UK Precipitation (HadUKP) series (Alexander and Jones, 2000), the England and Wales Precipitation series (Manley, 1974) each developed from ≥7 stations per region, or a 5km gridded set covering 1961-2009 (Perry *et al.*, 2009). Gridded and pooled data series benefit from their lack of reliance on individual station data; however, the area averaged data may miss localised intense storms and underestimate specific point maxima. The underestimation can be considerable for small radius convective storms, making gridded data unsuitable for an examination of extreme events. As a result, this project will employ individual station observations for assessing extreme events.

No observation station has a continuous, homogenous, uninterrupted rainfall record. While longer observation series may appear to be preferable, to distinguish natural climatic variability from long term behavioural changes or trends, strict statistical analyses cannot be carried out if there are inhomogeneities in the data series arising from changes in instrumentation or gauge drift (Klein Tank *et al.*, 2002). There is no specific "minimum" duration record length; various studies have adopted different criteria dependent on the reliability of data used. However, Chen and Grasby (2009) recommend records of ≥60 years to remove the influence of "quasi-cycles" in the order of 40-60 years, while Kundzewicz and Robson (2004) suggest that at least 50 years of observations are required. Fowler and Kilsby (2003b) defined a minimum observation period as 40 years of records with fewer than 5 years missing; Wigley and Jones (1987) compared two portions of a 110 year rainfall record with an overlap period of 55 years to determine the homogeneity of regional pools.

Other analyses of individual daily rainfall records within the UK have been carried out using spatially extensive data sets (Osborn and Hulme, 2002; Fowler and Kilsby, 2003b; Maraun *et al.*, 2008). To avoid duplication and minimise data preparation, updating to 2010 a spatially distributed subset of the most recent data set (M2008; Maraun *et al.*, 2008) appeared to be an ideal approach. M2008's set comprises 689 stations, of varying duration from 1853 to 2006, around a third of which were previously utilised by Osborn and Hulme (2002; OH2002), shown in

Figure 4-2(a). The subset would focus on maintaining Fowler and Kilsby (2003b)'s spread of stations across each of the homogenous rainfall regions (Wigley *et al.*, 1984) to preserve independence between stations and minimise event duplication (Dales and Reed, 1989).

4.1.1 Issues with alternative data

A comprehensive review of M2008's data revealed that stations were selected on the basis of record duration with little regard for spatial representation. A disproportionate number of operational UK stations lie in central and southeast England, with the density of the network reducing further afield. In selecting stations on the basis of longevity, M2008 biased the sample toward central and southeast England, as illustrated by Figure 4-1(b). Although each record was weighted with respect to duration and de-correlation length, it could be argued that spatial analyses are unreliable as a result of the effective repetition of extreme data (Dales and Reed, 1989; Smith, 2009).

By comparison, Fowler and Kilsby (2003b; FK2003), used only 204 stations located in Figure 4-2(c), equally distributed among the nine UK rainfall regions (Wigley *et al.*, 1984) which are described in greater detail in Section 4.1.4. Although this led to a reduction in data availability and some omission of extreme events, the records used were of continuous duration with enhanced confidence in the analyses. The dependence between single day extreme rainfall totals reduces both with increasing distance between the stations and reduced event frequency (Buishand, 1984; Dales and Reed, 1989). Buishand (1984) concluded that rainfall maxima within the Netherlands can be considered to be independent at 30km separation; while orography has an influence, this distance has been largely corroborated within the UK (Salter, 1921; Dales and Reed, 1989; Smith, 2009). Separation distance was an important factor when identifying stations to replace those which no longer operate; it was also significant in determining the suitability of a station to supplement an incomplete record.

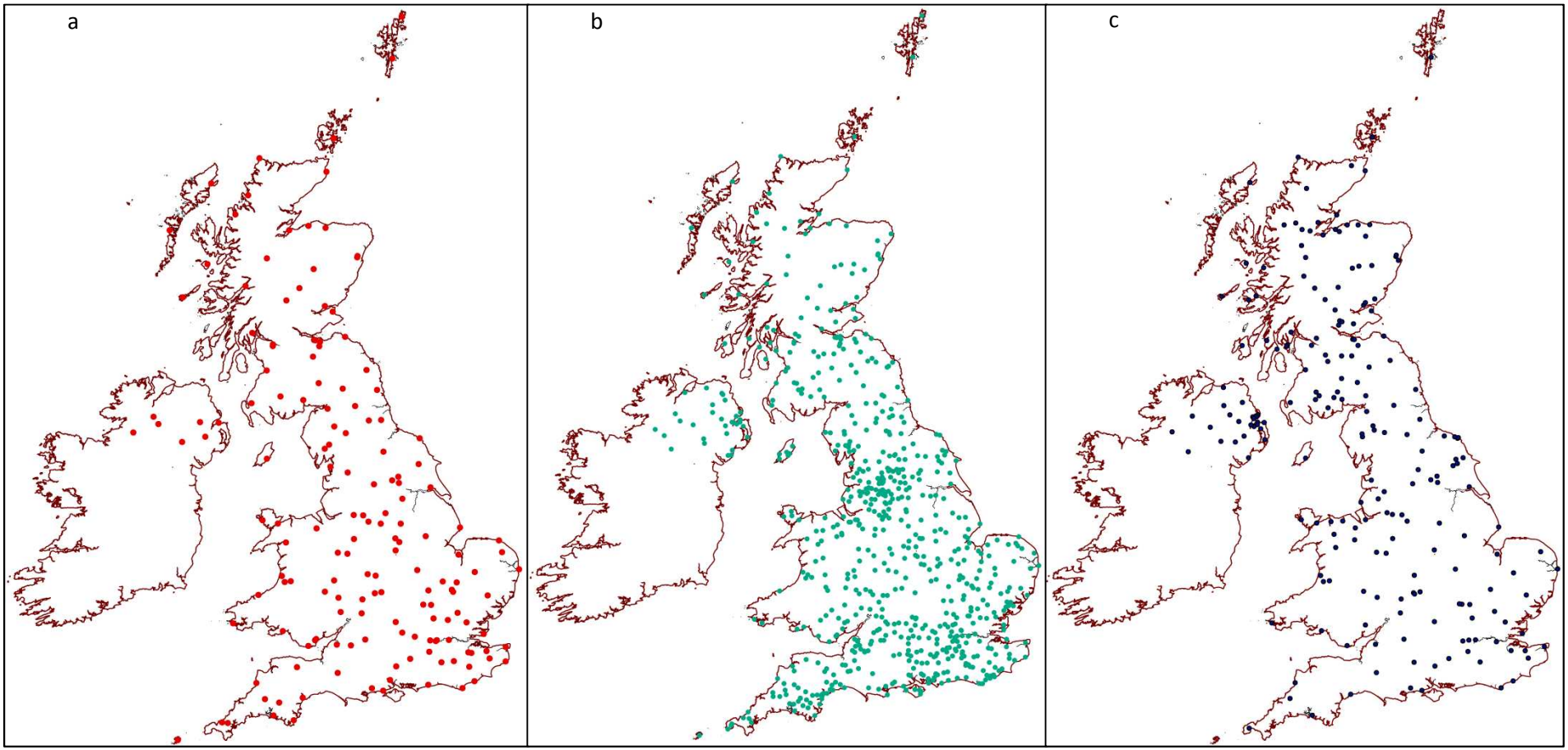

Figure 4-2 : Rainfall gauges used in studies by (a) OH2002, (b) M2008, (c) FK2003

The set of gauges analysed by M2008 were a combination of updates to the records developed by FK2003 and OH2002, both forward and backward in time, and supplementary stations to increase the spatial coverage. For the purposes of this thesis, the decision was made to maintain the coherent spatial structure established in FK2003 and to extend to 2010 only those 204 station records where data was available or a suitable replacement station could be identified. This ensured that all analyses would cover at least a period of 50 years, as well as minimising duplicate extremes.

The annexe to M2008's assessment of trends in daily rainfall illustrates trends in mean daily rainfall around the UK; the trends found at several locations, are suspiciously large. To verify these trends and to determine the homogeneity of all selected records, a random sample of the records supplied by M2008 including the suspect locations were assessed to identify major flaws or discontinuities. This process identified that many records, both for the updated period (2001-2006) and the full records of newly added stations, frequently included unreasonably large maxima with comparison to neighbouring stations and the station median annual maximum value (RMED). These observations were instead omitted within the analysis (Pers. Com. Maraun, 2009). However, records for several extremely large observations, which occurred either within or after missing data, were annotated as single day counts and so led to spurious trend calculations by M2008. Further personal communication confirmed that an allowance had not been made for these errors within the analysis program. Edinburgh Blackford Hill is a clear example, reproduced in Figure 4-3, which accounts for the highly significant positive trend in mean rainfall reported by M2008.

Daily rainfall data were obtained from the British Atmospheric Data Centre (BADC, http://www.badc.rl.ac.uk) for the period 2000-2010, for all recording stations in the UK. Further records were also obtained from Durham University, the Met Office and the Rothamsted Research Archive to supplement data which were unavailable through the BADC repository. A more rigorous analysis of the overlap periods between data from M2008, FK2003 and BADC identified that where repeated daily observations are present in the raw BADC data files, different values were selected by M2008 from those chosen using the predefined Met Office quality codes. Similarly, data cross-checked against earlier records (i.e. prior to 2000) do not always match; exact totals may differ as a result of differing selections of replacement gauges, but differences ≥10mm are concerning.

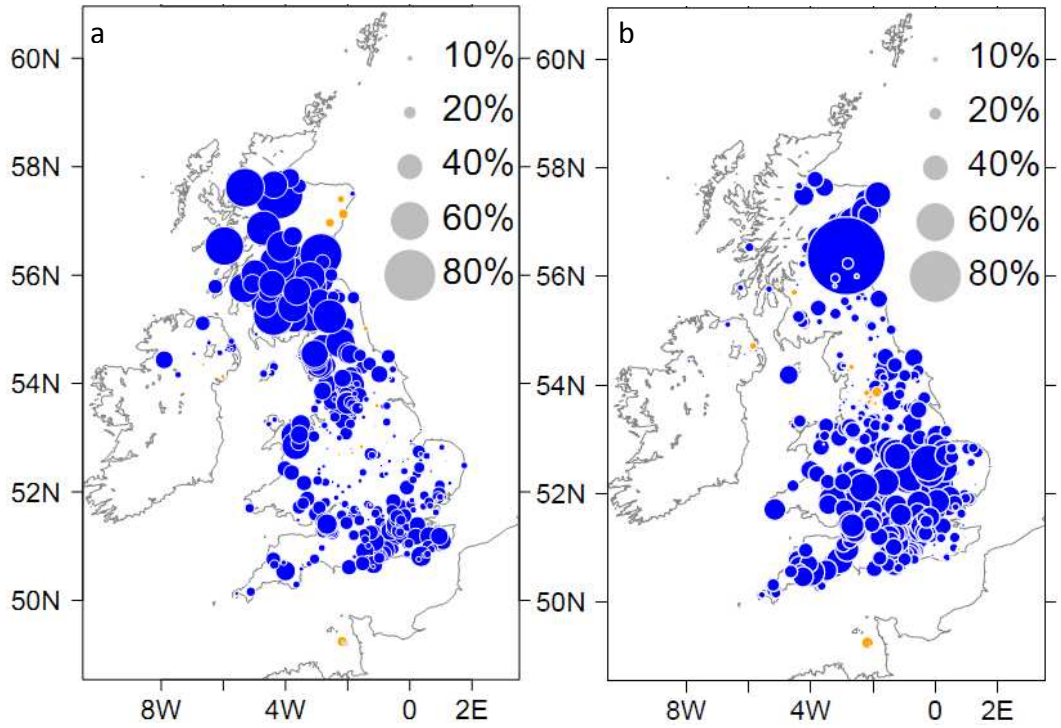

Figure 4-3 : Trend of mean rainfall relative to 1961-1990 mean, for (a) DJF; and (b) SON reproduced from Maraun *et al.* (2008) "Supplementary Details Figure 2". Blue circles denote increasing trends, yellow circles decreasing trends; the magnitude of the trend is signified by circle size.

Table 4-1 shows an extract of the record for Lerwick from 1999, indicating the difference between FK2003 and M2008, errors which been included as a result of missing observations are highlighted in bold italic. Finally, the analysis revealed large daily totals (>0.5RMED, where RMED is the median annual maximum) had not been cross-checked against others in the near vicinity of the station, leaving some questionable daily totals.

Year	Month	Day	Rainfall Total (mm) from FK2003	Rainfall Total (mm) from M2008
1999	11	14	0.4	0.3
1999	11	15	5.3	1
1999	11	16	***9.6***	***12.3***
1999	11	17	***3.4***	***NA***
1999	11	18	1.5	3.6
1999	11	19	0.1	0.8
1999	11	20	7.9	1.5
1999	11	21	3.5	8.3
1999	11	22	2	2.6
1999	11	23	5.8	6.5
1999	11	24	6.7	5.1
1999	11	25	9.3	9.8
1999	11	26	6.9	5.3
1999	11	27	***11.2***	***NA***
1999	11	28	***12.8***	***20.9***
1999	11	29	1.3	1.6

Table 4-1 : Comparison of observed daily rainfall totals for Lerwick between M2008 and FK2003

The data rejection criteria adopted by Maraun *et al.* (2008) were less strict than other studies of a similar nature (Onof and Wheater, 1994; Moberg and Jones, 2005; Overeem *et al.*, 2008), rejecting a season only if more than 50% of the seasonal observations were missing. No evidence exists in the article to confirm whether stations were removed from the final complement of 689 if an excessive portion of the record was missing. Finally, the records for some stations known to be still operating, e.g. Durham, were only included to the limit of the BADC record - 2000. Although this is not an error in itself, the records were easily obtained by direct contact with the station operatives and have been included within the new data set described below.

It was, therefore, concluded that updated daily rainfall observations from 2000 to 2010 should be obtained directly from BADC or appropriate alternative sources. The records produced by OH2002 supplement those used by FK2003 and, where possible, extend the records backwards in time.

4.1.2 The UK Rainfall Recording Network

Approximately 16600 meteorological stations, observing land surface measurements of rain, wind and temperature *inter alia*, are currently operational at locations throughout the British Isles reporting on timescales from sub-hourly to monthly. The daily rainfall records vary in duration from 1 to >150 years, as illustrated in Figure 4-4. Respecting the project minimum criteria of record length ≥45 years, ending in the present decade, further restricts the set to around 600 stations, many of which are co-located or have poor data quality. There is a balance to be achieved between the use of data records which allow the identification of recurrent patterns from long term behavioural changes, but which do not introduce further uncertainty as a result of data inhomogeneities.

There are many sources of inhomogeneity in meteorological observation series including: instrument replacement or relocation; instrument failure; changes in calculation methods or reading times; changes in the surrounding area; human error; gauge under-catch in less sheltered locations. All of which can lead to abrupt or gradual biases in observations (Peterson *et al.*, 1998). George Symons, founder of the British Rainfall publications, chastised observers for their laxity during heavy events when buckets overflowed (Pedgley, 2010) and frequently corrected readings he considered to be anomalous; a practice continued by his successors. This is now achieved through algorithms

run by the Met Office to homogenise the records, removing the influence of station relocation or changes in equipment. Operational gauges are subject to careful quality control procedures, and occasional re-estimation of readings, prior to their incorporation within the BADC database (Alexander and Jones, 2000). However, errors can remain within the records such as duplicate readings, or multiple day accumulations which have been incorrectly recorded as a single day. Considerable work was still required to validate the annual maxima for each record when compiling this set of daily rainfall records.

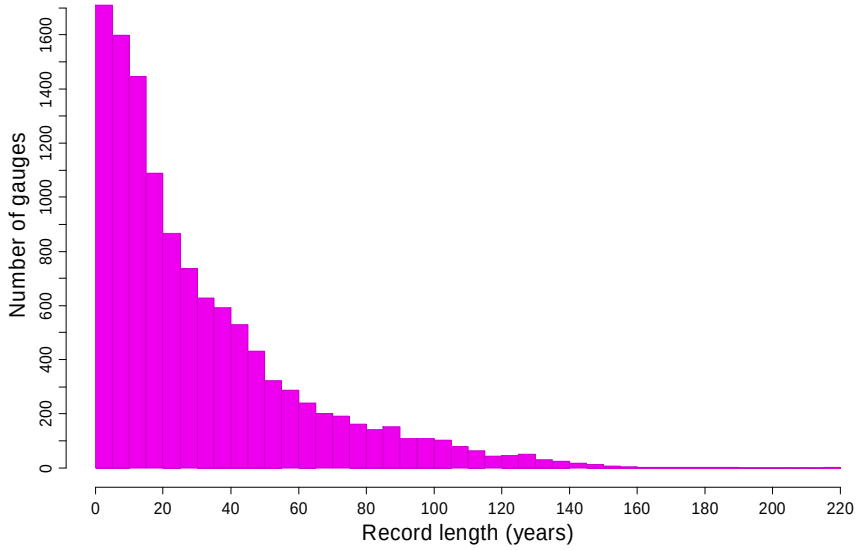

Figure 4-4 : Distribution of observation stations with respect to record length, based on BADC records

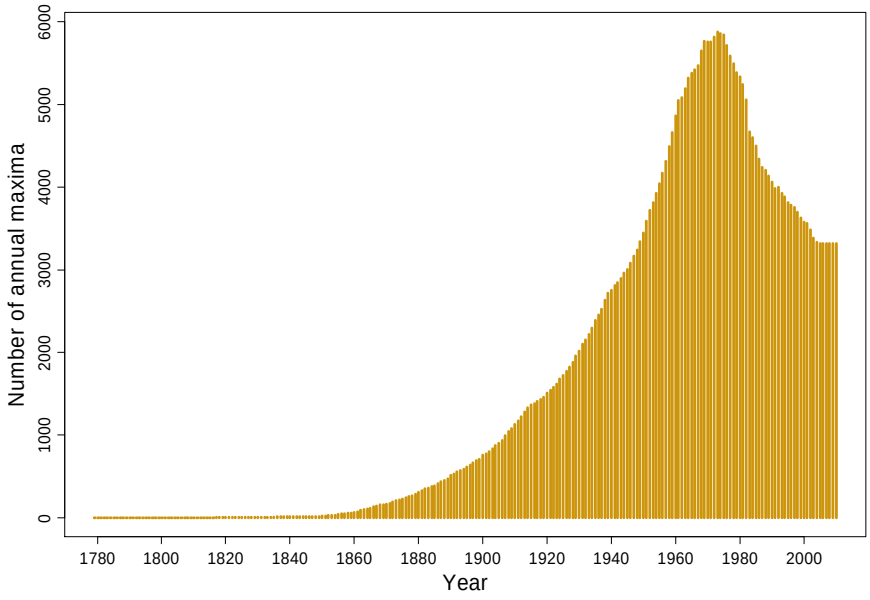

Figure 4-5 : Number of stations producing valid Annual Maxima per year, based on BADC records

4.1.3 Quality control measures

Quality control measures and rejection criteria for observation records vary considerably, dependent on the proposed application of the data. Dales and Reed (1989) found that where at least six months of daily rainfall data exist, a reasonably accurate estimate of the annual maximum value can be estimated and verified against annals such as British Rainfall. In contrast, such limited data would be very unreliable for estimates of higher frequency events; Overeem *et al.* (2008) rejected any station with >5 days missing per year, retaining only 12 stations with at least 29 complete years of data. Similarly, Moberg and Jones (2005) permitted only 2 days missing per month and fewer than three years missing in any 20 year period. However, applying such stringent criteria to the record updates (2000-2010) severely limited the analysis set because approximately 140 stations with records >40 years have ceased to operate since 2000, and a further 20 only report monthly. Faulkner (1999) reported that the daily recording rainfall gauge network peaked in the late 1970s, and since then has experienced decline as sub-daily stations were established in their stead and longer term stations either moved or discontinued, as shown in Figure 4-5. This decline appears to have continued, with the greatest losses among the most remote stations, leading to reduced coverage in the north Scotland region.

Monthly records were rejected due to the errors introduced through disaggregation to equivalent daily totals using neighbouring gauges as a proxy. Similarly, 24 hour accumulations may under-estimate the daily total due to factors such as evaporation losses or poor accuracy during high intensity storms. While a generic scaling factor to account for these losses can be used (Institute of Hydrology, 1999), this does not account for individual station characteristics and so it is preferable to avoid the problem by using only measured daily rainfall totals.

The influence of metrification is significant in early records (Smith, 2009) demonstrated by the heavy weighting of even valued observations. No data were corrected for metrification biases, as the procedures adopted by the Met Office account for both these and errors related to instrument relocation or replacement. Most extreme events were verifiable against neighbouring stations, while errors in smaller totals have a limited influence on the subset of extreme measurements.

The correlation between stations experiencing the same extreme rainfall event drops off rapidly beyond a radius of ~25km^2 (Buishand, 1984), represented by the areal reduction

factor for point rainfall in the Flood Estimation Handbook (Faulkner, 1999; Smith, 2009). A minimum of three gauges located within this radius are recommended for validation checks to avoid mistakenly identifying storm patterns (Upton, 2002). For the purposes of data validation for this thesis, it was assumed that the spatial variation of daily rainfall totals is approximately normally distributed (Upton and Rahimi, 2003), allowing for up to 25% variance between verification stations to accommodate factors such as localised storms, gauge aspect and elevation (Salter, 1921).

A less onerous set of criteria was adopted in this project to retain sufficient stations from the original analyses to facilitate comparisons, while minimising errors arising from the use of incomplete records. Daily records were deemed insufficient where >3 days were missing in a month or >10 days over the whole year; in either case the whole year was rejected. A station was rejected from the set where more than three years were missing within the decade 2000-2010. Wherever possible missing periods of record were replaced from an appropriate neighbouring source identified from the following constraints:

- No data missing for >14 days prior to, or after, the replacement period
- Replacement gauge located within 5km
- Replacement gauge elevation within 100m
- Correlation between the mean (1961-1990) daily rainfall observations ≥ 90%
- Correlation of maxima (>0.5RMED for the station) ≥ 95%

Where the neighbouring source extended a terminated gauge record, a minimum overlap duration of ten years was required to ascertain the suitability. Of the gauges used by FK2003, those which had more than three years missing within the update period (once replacement gauges had been identified) or which had terminated prior to 2008 were rejected. Unfortunately, 52 of the FK2003 gauge set were deemed inappropriate for extension.

Data for all stations were corrected for duplicate entries and multiple day accumulations prior to quality assessment of the totals exceeding the 95th wet day quantile. Where duplicate observations were available from different reporting sources, observations measured over 24 hours were selected in preference to those derived from sub-daily accumulations (Met Office, 2011a). Subsequently, the gauges were scrutinised to check the

validity of recorded maxima (values >0.5RMED$_{61\text{-}90}$). Maxima were cross checked against gauges located within a radius of 25km^2. In locations where the gauge network is sparse, such as North Scotland, the verification distance was extended to 50km and 100m elevation. Manual checks for significant outliers were carried out using data provided on the Met Office Climate Statistics page, from the *Weather Report* (e.g. Met Office, 2010b) or the Royal Meteorological Society's monthly *Weather Log*.

The final selection of gauges, extended both forward to 2010 and backward in time as appropriate, are illustrated in Figure 4-6. Additional gauges were selected from OH2002 partly to supplement data which would otherwise be lost, and partly to ensure a minimum number of stations within each of the UK precipitation regions (Wigley et al., 1984); the following section outlines in greater detail the rationale behind selecting the number of gauges per region and the relevance of the precipitation regions.

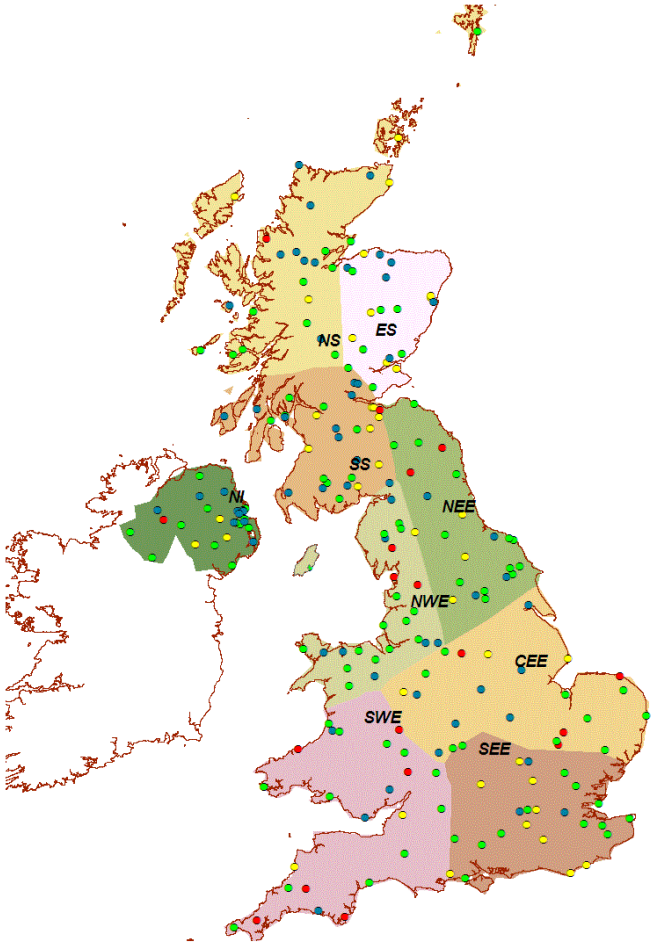

Figure 4-6 : Final selection of 223 rainfall gauging stations updated to 2010, in relation to the Hadley UK Precipitation regions. ● 52 original stations used by FK2003 covering 1961-2000; ● 116 original stations used by FK2003 covering 1961-2010; ● 36 stations used by both FK2003 and OH2002 covering at least 1961-2010; ● 19 stations used by OH2002 covering at least 1961-2010

4.1.4 Regionalisation

Gregory (1975) examined different regions of rainfall behaviour throughout England, Wales and Scotland on the basis of fluctuations in total annual rainfall volumes. Introducing their definition of 12 homogenous regions, Dales and Reed (1989) provided a useful summary of alternatives which have been applied, before adopting a selection based on generalized extreme value parameters. Wigley *et al.* (1984) defined five homogenous regions of mean rainfall in England and Wales from principal component analyses of monthly, seasonal and annual means and maxima. The regions approximately replicate orographic influences on westerly flow such as over the Scottish Highlands or Pennines in northwest England. Gregory *et al.* (1991) later extended the precipitation regions to incorporate Northern Ireland and three Scottish regions; the nine regions were digitised to produce the HadUKP series (Alexander and Jones, 2000). Hosking and Wallis (1988) also discussed methods to pool groups of similar catchments affected by the same widespread rainfall events, which can then be studied in relation to external drivers or weather types (Lamb, 1972) for the selected series of extremes.

It could be argued that the use of regions defined from mean annual characteristics is not appropriate for use in a study of extreme rainfall. However, alternative regional definitions based on water company jurisdictions, or governance regions, such as those used within the UK Climate Projections (Murphy *et al.*, 2009), do not necessarily relate directly to climatic responses. Another approach is to examine all extremes on an individual point basis, before applying spatial clustering at a later stage to identify geographical regions which display similar behaviour (Maraun *et al.*, 2008). The digitised HadUKP regions are used in this project for the purposes of comparison with FK2003, although an alternative grouping consistent with extreme behaviour will also be explored in Chapter 7 based on the regions defined by Dales and Reed (1989). The regional allocation, ensures consistency in observation station selection and reduces the concentration of observations within any particular area of the UK. Some gauges used by FK2003 have been reallocated to different regions through use of the new digitally defined boundaries.

The analyses described in Chapter 6 adopt a Regional Frequency Analysis (RFA) methodology, where return period estimates are obtained from a Generalized Extreme Value analysis of the pooled regional maxima. Regional pools are established from time

series of individual gauge maxima within each region by standardising each station by the individual station median to remove orographic or exposure effects prior to pooling. Regional mean seasonal and annual medians (SMED and RMED, respectively) are calculated from the weighted mean of all gauges in the region, where individual station weighting is based on the effective record length to reflect the reliability of the relevant set of observations (Hosking and Wallis, 1988):

$$w_i = \frac{n_i}{\sum_{i=1}^{N} n_i}$$

Equation 4-1

where w_i is the effective record length at the ith station, N the number of stations in the pooling group and n represents the number of station years.

Changes in the pooling group, as a result of gauge termination, may have an impact on the regional curve, particularly if the omitted or included station had experienced several notable storms, and hence on any comparison made with FK2003. Faulkner and Prudhomme (1997) found that for single site analysis the effect of including incomplete years on estimates of the AMAX is small as generally the abstracted maxima are correct. Those instances where AMAX were underestimated tended to draw the estimated RMED value down, with a compensatory increase in calculated growth rates and thus a neutralised estimate of return levels. Regional frequency analysis removes inhomogeneities such as repeated event records, ensuring that no individual gauge unduly influences the results, so missing extremes will not affect the global analysis. Although the return period estimate may be unaffected, confidence in the results will reduce for a smaller regional pool, thus it is important to analyse the influence of the group size on confidence estimates.

A replacement bootstrap (Efron, 1979) analysis was carried out to compute the relative levels of confidence in regionally pooled statistics for pools of different sizes, to identify the minimum target number, m, of stations to include in each region. Refer to Appendix B.2. for the method. Two regions were selected for the analysis, North Scotland (NS) and Southeast England (SEE), to represent the disparity between both regional rainfall regimes and the differing densities of stations in the observation network. Two test statistics were examined using the pool of gauges compiled by FK2003, using the maximum number of stations in the original regional pools, M=23, and AMAX from 1961-2000.

The first test statistic fitted regional generalised extreme value (GEV) growth curves; the second calculated the ten year running mean of the pooled annual maxima. The procedure entailed:

1. Estimate the test statistic for a complete regional pooling group from 1961-2000.
2. Re-sample 1000 times with replacement, and re-estimate the test statistic.
3. Repeat the process with sample sizes of m = 5, 10 or 15.

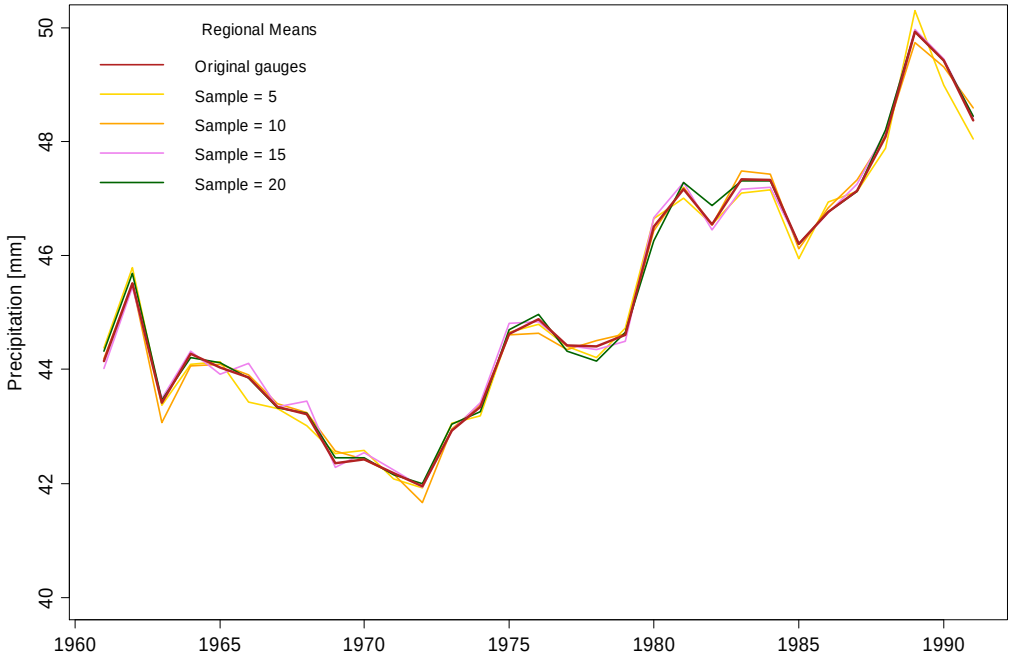

Figure 4-7 : Regional running mean calculated for North Scotland using different sample sizes

A comparison of the calculated running means from different sample sizes and the full NS regional pool demonstrates that the results all lie very close together (Figure 4-7); a similar result was obtained for SEE. Figure 4-8 represents the distribution of all bootstrapped results for the calculated ten year running mean for 1991, obtained from a sample size m=5, and indicates the breadth of the 95% confidence interval from the bootstrap analyses. The regional mean was calculated directly from the data without applying any standardisation to remove location bias such as orography or aspect. The width of the confidence bands for NS compared with SEE (Figure 4-9) reflects the greater spatial heterogeneity in NS, which is dominated by westerly flow over the mountains and so exhibits greater dissimilarities in its station maxima. The minimal decreases in the confidence regions beyond m=15 concurs with Hosking and Wallis (1988) who observed that increases in the number of gauges in a pool beyond this number yields little improvement to errors in the estimated value.

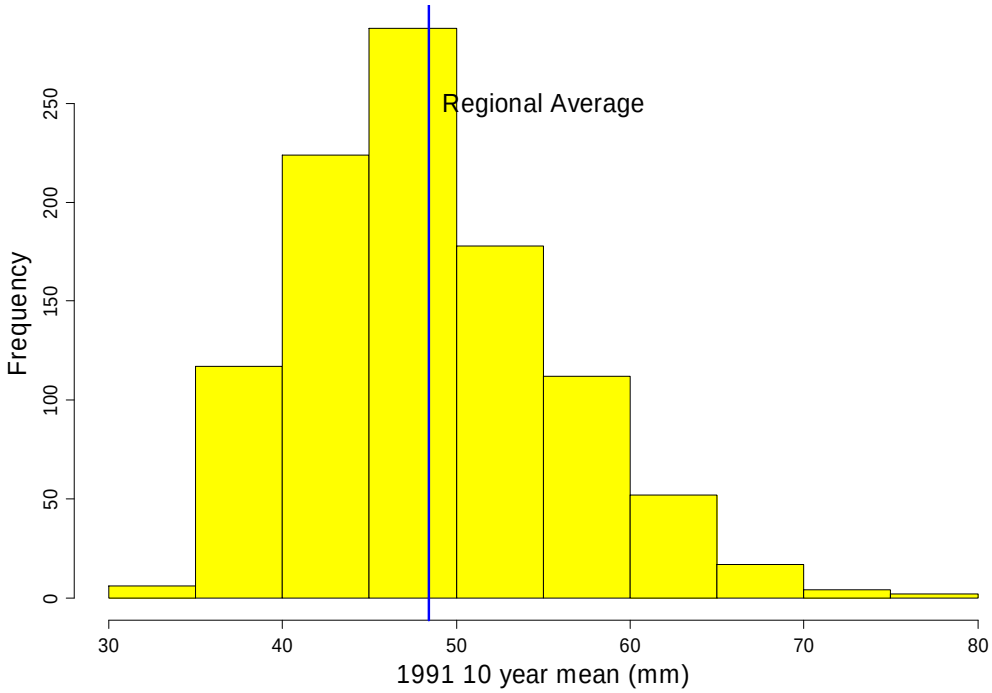

Figure 4-8 : Distribution of re-sampled estimates of running mean for 1991 for *m*=5

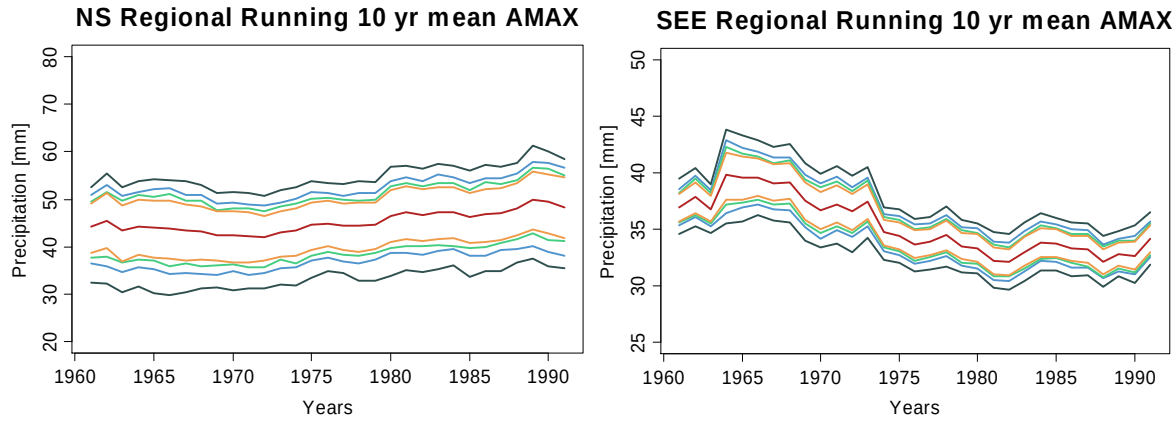

Figure 4-9 : Comparison of 10 year running mean for North Scotland and Southeast England with confidence intervals for sample size *m*. Regional mean (brown), *m*=5 (dark grey), *m*=10 (light blue), *m*=15 (aquamarine), *m*=20 (dark yellow)

A similar exercise was carried out for the regionally pooled GEV growth curves, fitted to standardised 1-day maxima for both regions (Figure 4-10) indicating a similar increase in standard error relative to decreases in n. Interestingly, the estimates of the test statistics were consistent for all sample sizes. Although it would ideally be preferable to increase the sample size to at least 20, these results indicate that, where necessary, reasonable confidence can still be obtained from a minimum regional pool size of 15 for the updated results. To ensure fair comparison of results with FK2003, all long term analyses were

carried out with a composite group of the 152 stations updated to 2010 and the 71 used by FK2003 which end in 2000.

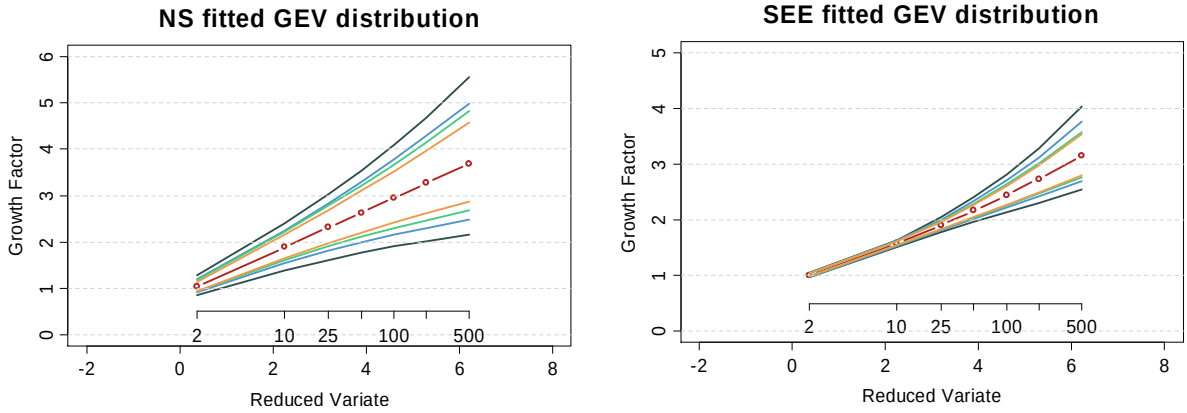

Figure 4-10 : Comparison of fitted GEV distribution for North Scotland and Southeast England with confidence intervals for sample size n. Standardised growth curve (brown), n=5 (dark grey), n=10 (light blue), n=15 (aquamarine), n=20 (dark yellow)

4.2 Temperature

This project is focussed on the response of extreme daily rainfall to atmospheric variables or other meteorological conditions which may initiate events. The research synthesised in Chapter 2 suggested that air and sea surface temperatures, mean sea level pressure and atmospheric teleconnections are the most important data to include in any correlation analyses.

As the moisture holding capacity of the atmosphere is governed by temperature, described by the Clausius-Clapeyron equation, and recent warming trends are associated with enhanced water vapour (Gershunov and Douville, 2008) it seems obvious to investigate the relationship between air temperature and extreme rainfall.

The Central England Temperature (CET) series (Parker *et al.*, 1992) comprises mean daily temperatures from 1772 and minima/maxima from 1878, for a region approximately bounded by Lancashire, London and Bristol, and has been recently corrected for urban development and early instrumentation errors (Parker, 2010). Complementary series were also produced for Scotland and Northern Ireland (Jones and Lister, 2004), but are not publicly available; no data were produced explicitly for Wales. Rather than limit the analysis of the relationship between air temperature and extreme rainfall events to those gauges located within central England, the alternative options are to use individual station data or gridded data. Temperature does not vary as rapidly over the spatial domain, so errors

associated with gridded temperature observations are far less than those for rainfall, making these an acceptable alternative to station data. Gridded observations provide a homogenous series, with fewer missing values, and publicly available data sets have been fully quality controlled and peer-reviewed; whereas individual station records may retain some errors or have longer periods missing.

Global monthly air surface temperature high resolution gridded data sets (1901-2005) for minimum, maximum and mean temperature (Mitchell and Jones, 2005) updated to 2009 (Jones and Harris, 2008) were selected for use in this project. The updated data set improves previous gridded products in its increased spatial and temporal resolution, through the incorporation of many additional observation stations. The gridded data are supplied on a resolution of either 25km or 50km up to the current month. For simplicity, and to correspond with other data sets such as sea surface temperature, grid box averaged air temperatures were extracted over 5° x 5° grid boxes. While daily temperatures may better represent atmospheric fluctuations than monthly measurements, they also introduce an unnecessary level of complexity through the enhanced noise.

Several authors have linked temperature extremes and the development of heat waves to anomalous sea surface temperatures (SST) (Della-Marta *et al.*, 2007; Gershunov *et al.*, 2009; Vincent *et al.*, 2011). Increases in the North Atlantic SST (Wang and Dong, 2010) would enhance the hydrological cycle, leading to positive moisture anomalies in the hot air masses moving over the UK and Western Europe. Colman (1997) found a positive correlation between January and February North Atlantic SST anomalies and the following summer CET, and a minor correlation with the England and Wales Precipitation (EWP) series. The lack of significance was not surprising as the averaged regional rainfall series is not fully representative of extreme events, or the smaller scale rainfall responses to SST. Hydrological responses to SST, including drought evolution (Dai, 2011; Vincent *et al.*, 2011) and extreme rainfall (Karnauskas and Busalacchi, 2009; Muza *et al.*, 2009), have been demonstrated in several different regions. Lagged North Atlantic SST is one of several strong predictors of summer flows in the River Thames (Wilby *et al.*, 2004); a positive correlation exists between the North Atlantic SST and southwest England rainfall anomalies (Phillips and McGregor, 2002) and for summer rainfall in east England (Neal and Phillips, 2009).

The sea surface temperature data set supplied by the Met Office Hadley Centre, HadSST2, is a monthly global gridded (5° x 5° boxes) set of SST values from 1850 to present. The majority of the database was constructed from the International Comprehensive Ocean-Atmosphere Data Set (ICOADS) from 1850-1997 which collated measurements taken from shipping routes; from the 1970s onwards these measurements were supplemented by moored and drifting buoys. Corrections for spurious trends caused by changes in measurement practices and uncertainties due to data scarcity (e.g. during the World Wars) are summarised by the compilers of the most up to date data set (Rayner *et al.*, 2005).

Figures of data availability for different decades (Rayner *et al.*, 2005) indicate that greatest confidence in the SST database surrounds the major shipping routes from western Europe to the eastern USA and the southern hemisphere. Similarly, regions surrounded by coastal waters, such as the UK and the Netherlands, contributed the highest proportion of data to the ICOADS and are less plagued by data scarcity during the two global conflicts.

4.3 Mean Sea Level Pressure

Connections between mean sea level pressure (MSLP) and temperature and rainfall patterns are well established, either through the use of a composite such as the North Atlantic Oscillation Index (Jones *et al.*, 2003) or through direct comparison (Della-Marta *et al.*, 2007). Meteorological correlations with both the lagged and concurrent MSLP include glacier mass balance (Nordli *et al.*, 2005), extremes of rainfall (Meehl *et al.*, 2005; Rodríguez-Puebla and Nieto, 2010) and wind storms (Allan *et al.*, 2009; Jiménez *et al.*, 2009). The concurrence of wind storms and extreme rainfall was described in Chapter 2, indicating that where a clear correlation between MSLP and wind exists (Allan *et al.*, 2009) there is likely to be a similar relationship with rainfall.

The Met Office Hadley Centre's MSLP data set, HadSLP2r, is an update from 1850 to the present day of HadSLP2 (Allan and Ansell, 2006) which is constructed from monthly NCEP/NCAR reanalysis fields for 2005 onwards. The authors suggest that this series represents one of the best available for any historical investigation of the influences of large-scale circulation patterns. The homogenous data set (HadSLP2) is a combination of land and marine pressure observations, derived from the ICOADS and blended terrestrial observations series for a 5° x 5° global grid. As for HadSST2, the oceanic observations are

less spatially extensive away from major shipping lines, and have larger measurement and sampling errors in the North Atlantic during times of global conflict.

Correlation analyses between the NCEP/NCAR reanalysis data used for updates and HadSLP2 indicate that considerable differences exist between the two series in high altitude regions of the Northern Hemisphere (Allan and Ansell, 2006); the compatibility of the two series is much more reliable in the Southern Hemisphere. The data have been adjusted to account for differences in climatological averages between the different data products, resulting in a series which is homogenous in the mean, but with a higher variance post 2005. As the errors are highest in altitudinous regions, such as the Himalaya where there are also few observation stations, the use of the extended series for the UK is considered to be acceptable.

4.4 North Atlantic Oscillation Index

Chapter 2 discussed the influence of the North Atlantic Oscillation (NAO) on northern hemisphere weather, particularly in locations abutting the North Atlantic. The two indices commonly used are the normalised MSLP difference between Iceland (Stykkishólmur or Reykjavík) and one of the southern stations (Azores or Gibraltar), starting in 1821, (Hurrell, 1995; Rogers, 1997; Jones *et al.*, 2003) or a principal component derived index from 1899, which is less sensitive to modal displacements (Hurrell, 1995; NOAA, 2011). While the individual station based indices are useful for extended analyses prior to 1899, they may not be fully representative of the most influential weather patterns (Allan and Ansell, 2006). The centre of NAO action shifts over time, with the result that the principal component analyses of the index may be more reliable (Casty *et al.*, 2005; Allan and Ansell, 2006). As only 14 of the daily rainfall observations described in Section 4.1 commenced before 1899, the longevity of the NAO series will not be a deciding factor in selecting the best index.

Traditionally the wintertime composite (December to March, or October to March) is adopted for analyses; however, the effect of the summertime NAO on European temperatures may also influence rainfall and storm tracks on a smaller scale (Hurrell, 2003). The influence of the summer NAO has also been correlated with droughts in the eastern Atlantic, Mediterranean and Sahel regions (Linderholm *et al.*, 2009).

Sub-seasonal NAO indices may be more descriptive of the coincident sea level pressure, and hence the immediate weather, rather than an atmospheric pattern describing the climate (Hurrell and Deser, 2009). In particular, monthly values are more effective in explaining the occurrence of extreme weather patterns than their seasonal counterparts (Scaife *et al.*, 2008; Hurrell and Deser, 2009; Villarini *et al.*, 2011b). While the winter NAO, calculated as the mean value between December and the following March, is well known to correlate with winter storms (Allan *et al.*, 2009) or European summer droughts (Della-Marta *et al.*, 2007), it is not well correlated with summer rainfall maxima, which have a greater correlation with the June-July index (Folland *et al.*, 2009). Anti-correlations between the summer NAO and UK summer rainfall are strong in the UK for all periods of the record, mirroring the decrease in SE England rainfall in the 60s and 70s (Baines and Folland, 2007), and therefore recommending the use of the seasonal aggregate.

The NAO index considered to be the most reliable descriptor of year to year storm tracks will be adopted in this project. The monthly time series derived from the leading EOF of monthly MSLP anomalies over the Atlantic sector (20-80N, 90W-40E) was, therefore, obtained from the Climate Analysis Section, NCAR, Boulder (Hurrell, 1995), from which seasonal aggregates can also be calculated.

4.5 El Niño-Southern Oscillation (ENSO)

The ENSO signal has been shown by several studies to have a considerable influence on extreme European weather patterns, as described in Chapter 2 (Zanchettin *et al.*, 2008). Traditionally, Nino 3.4 is used as a measure of ENSO strength, but this index alone explicitly omits atmospheric processes which are reflected through SST anomalies. The BEST index (Smith and Sardshmukh, 2000) is a combination of the atmospheric component of the ENSO (the Southern Oscillation Index) and the Niño 3.4 SST (averaged over the region 5°N-5°S, 170°W-120°W). Monthly mean climatologies were removed from all data prior to monthly standardisation and application of a 3-month running mean to the averaged SST and SOI series. The composite series covers the period from 1871 to the present day, courtesy of recent work to extend the ENSO index and remove anomalies in the data (Wolter and Timlin, 2011). Monthly data were obtained from the Earth System Research Laboratory, NOAA.

4.6 Summary

This chapter identified the daily rainfall data sets which were available for the UK, the rationale for selecting the stations to be updated, and the quality control procedures employed in their update. The HadUKP regions were summarised, together with their importance in selecting spatially distributed rainfall stations for later analyses. Other observation data, such as sea surface temperature, which will be used in later extreme rainfall models and analyses and teleconnection indices were also described.

Chapter Five Exploratory Analysis

"Far better an approximate answer to the right question, which is often vague, than the exact answer to the wrong question, which can always be made precise."

John W. Tukey (1962)

5.1 Data Homogeneity Checks

The quality control undertaken on daily rainfall observations, described in Chapter 4, was an iterative procedure. Once major errors had been removed, the exploratory trend and variability analyses outlined in this section identified remaining inhomogeneities which may have been introduced while updating stations. For instance, abrupt changes in the data where series were appended to create the updated record are identifiable with tests for change points. Apparent regularity in event dispersion may arise from excessive missing data, identified with tests for randomness. This section summarises the tests carried out both to remove these erroneous points and to identify long-term changes and variability. A summary of the relevant equations from Chapter 3 are provided in Appendix B.

5.1.1 Abrupt changes

Much attention is focussed on long-term changes in rainfall statistics, yet there may be apparent trends as a result of abrupt changes or natural variability where no true trend exists. Abrupt changes may arise from sudden changes in climatic behaviour, e.g. changes of mode in the NAO (Rodionov, 2004), or anthropogenic influence such as station relocation (Villarini *et al.*, 2009). It is unlikely that the former will be distinguishable from other sources of variability within daily rainfall data; non-homogeneity arising from anthropogenic influences will be more obvious and could impact later analyses.

Several change points may exist within the daily rainfall series as a result of instrument relocation or replacement, although the quality control algorithms applied by the Met Office minimise their influence (Met Office, 2011a). All station records were examined for abrupt changes in the mean and variance of the annual maxima using the Pettitt test (Pettitt, 1979) for a single change point to ensure that that no residual errors remained; these changes are most likely to occur where updated records were obtained from a neighbouring station and blended with the original record. A single change point test was adopted to identify the maximum change in the series and its influence on the record, rather than to decompose the series into multiple short sections. Later analyses, in Chapters 6 to 8, will incorporate

significant change points and subsequent trend information, or discard unreliable stations identified from multiple subsequent change points after rectifying any data errors.

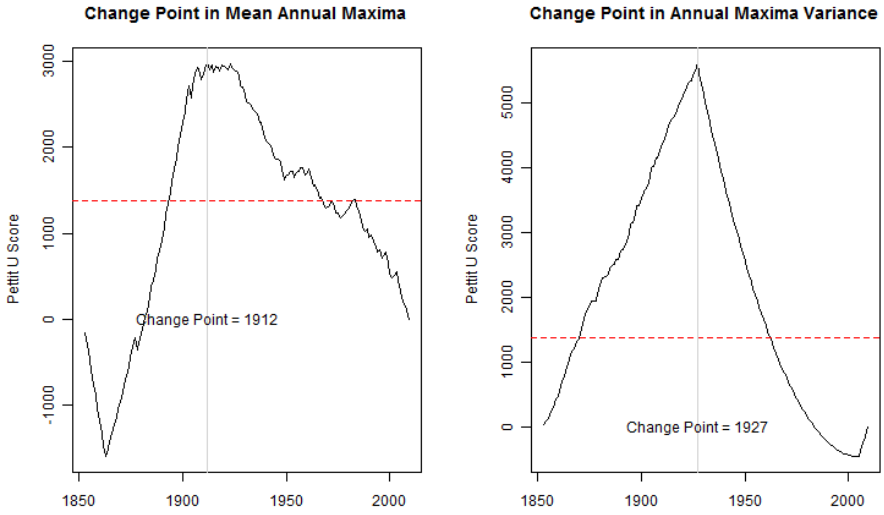

Figure 5-1 : Change point analyses using the Pettitt Test for changes in the mean and variance of daily rainfall maxima at Oxford (black line) and the critical threshold for a change point (red dashed line)

A typical example of change points found in the running mean and variance of a time series of annual maxima is shown in Figure 5-1 for Oxford (black line) with the critical test threshold (red dashed line). The variability in the running mean results indicates that several change points may have occurred over the period of record; station metadata corroborates the maximum change in the mean in 1912 which coincided with the relocation of the station. The most significant change in the variance occurs in 1927, coinciding with another, less significant, change point in the mean of the series.

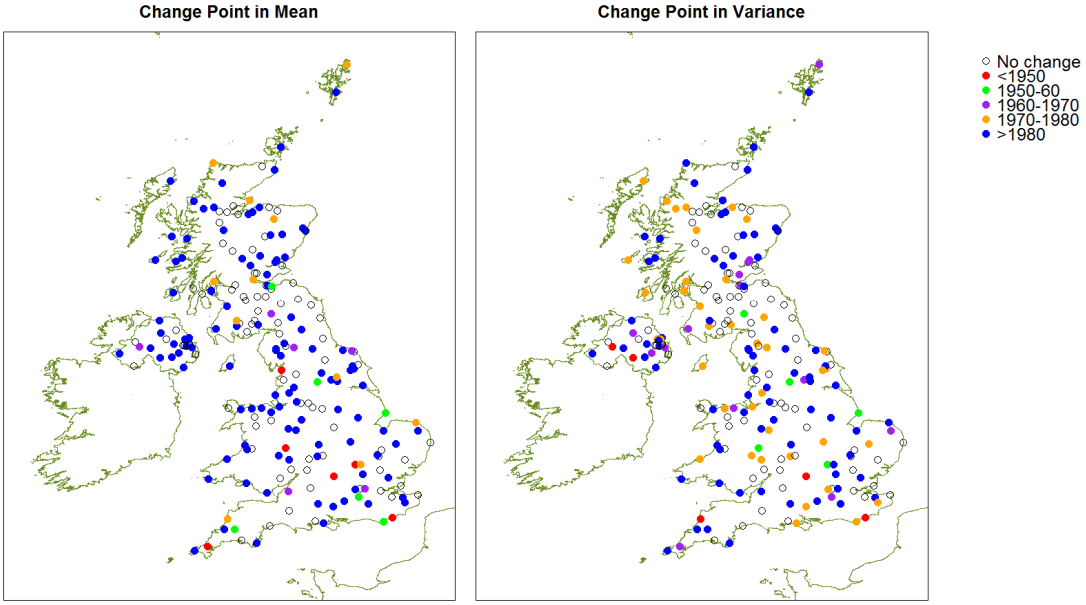

Figure 5-2 : Significance of change points in the mean and variance of daily rainfall maxima using the Pettitt test, identifying the decade where the change occurs

A two-tailed test was adopted in the absence of *a priori* knowledge about the direction of change, testing against a 5% critical value, U_k. Figure 5-2 shows the Pettitt test results for all 223 stations, indicating whether a significant change point existed in the mean or variance of the series and the relevant decade of change. Of these stations, 84 did not have a significant change point in the data; a further 6 had significant change points prior to 1950, allowing the analysis period to start after the change point. No stations updated from neighbouring records had a significant change point in the blended portion of the series.

5.1.2 Monotonic changes

Monotonic linear trends in the mean and variance were then tested at each station using the Mann-Kendall test for significance (Kendall, 1962) and permutation. Trend magnitudes and significance were compared for the whole time series as well pre- and post-change point (where a significant change point was found). While linear regression may not be the most appropriate tool for analyses of highly variable extreme data, it is adequate for exploratory analyses (Zhang *et al.*, 2004). There are some discrepancies between the significance of results found by the two tests (Figure 5-3), highlighting the importance of using several different methods (Kundzewicz and Robson, 2004). Trends, where significant, were generally ≤1mm over the period of record, or effectively null; the only significant trends >5mm were for $\lesssim$15 years of record post-change point, and so not representative of changes in the rainfall distribution (Robson, 2002). Furthermore, it is anticipated that about 5% of stations, for a 5% significance level test, will display a significant trend (Kanji, 1999).

As daily rainfall maxima are irregular, they are unlikely to demonstrate any clear signals in linear regressions based on the series median. Testing other parts of the series through quantile regression analysis (Cade and Noon, 2003) can, however, help to identify whether there is enhanced variability in the more extreme quantiles of the AMAX distribution. The only significant trends found in the quantile regression analysis had magnitudes ≤5mm over the whole period of record. The number of stations with a significant trend is not conclusive: decomposition of the data series into several quantiles results in insufficient data used for a statistically robust trend analysis. However, the results suggest that the extremes are more sensitive to changes than other quantiles of the distribution. The significance of trends and the direction of change are shown for four quantiles in Figure 5-4, while the distribution of significant trends by number of gauges and

quantile are shown in Figure 5-5. The proportion of stations indicating a significant trend is approximately equal to the significance of the trend tests, suggesting the detection of a trend where none is present (Hess *et al.*, 2001). These results also highlight that there are insufficient data to include specific trend components in later analyses (Ghil *et al.*, 2011).

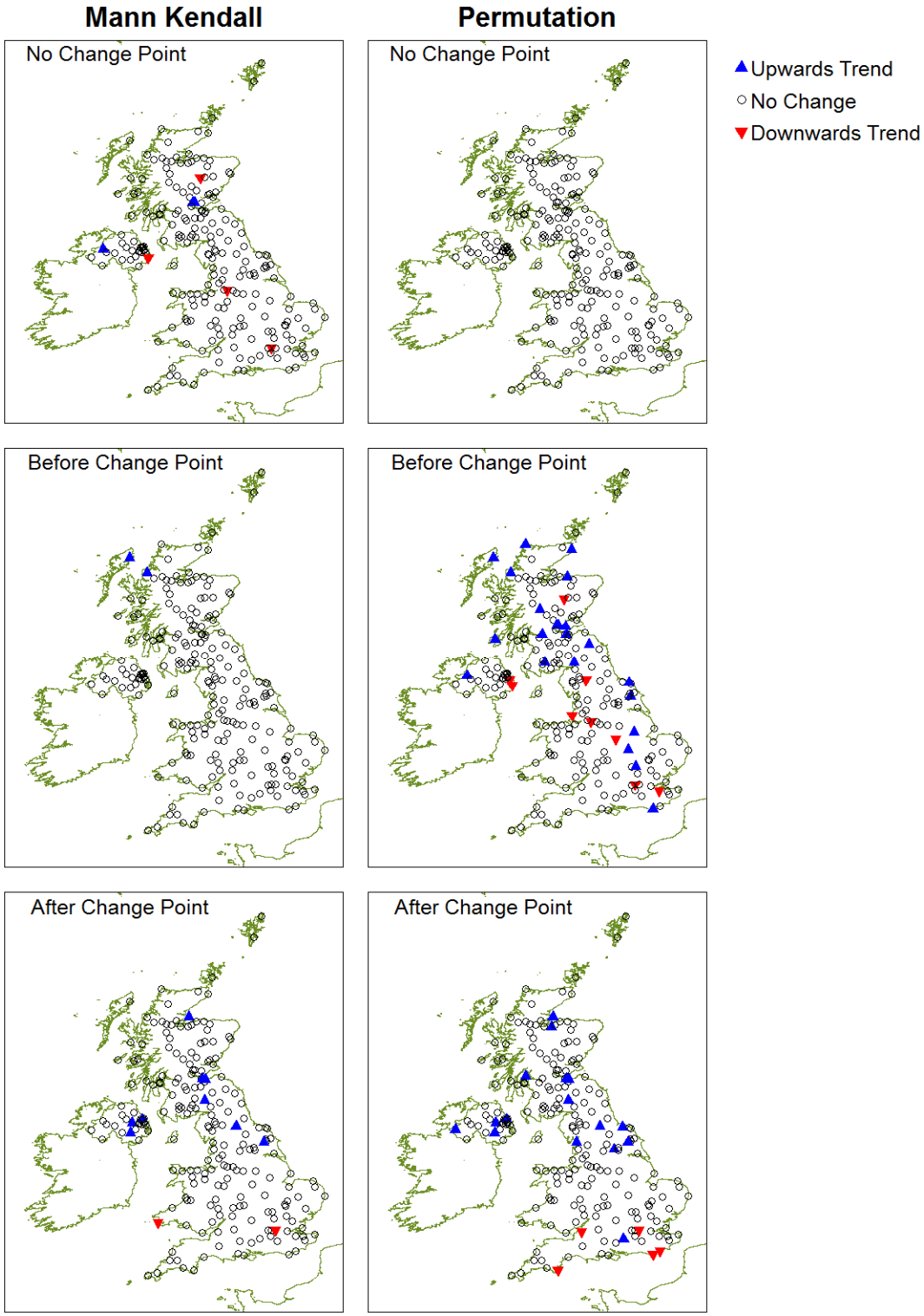

Figure 5-3 : Significant trends in the mean annual maximum series tested using Kendall's τ (left panel) and data permutation (right panel) for the whole station record with no, or assuming no, change point (upper row); before the change point (middle row); and after the change point (bottom row)

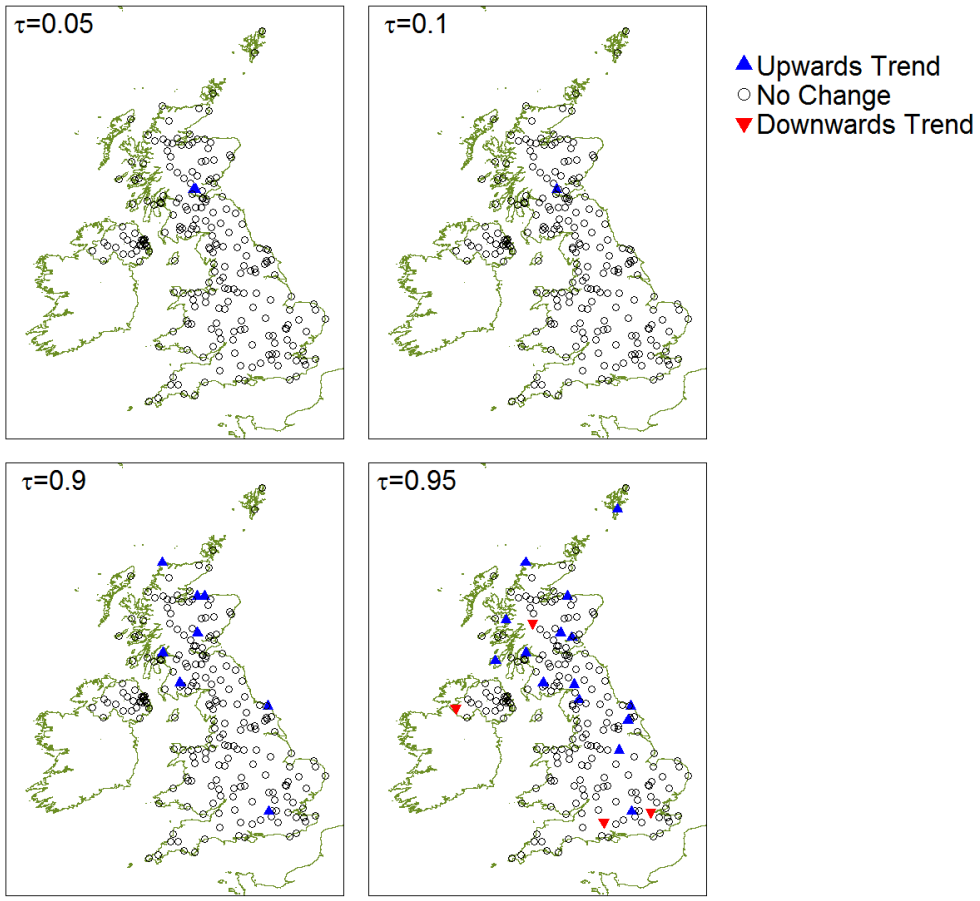

Figure 5-4 : Significant trends in four quantiles (τ=0.05, 0.1, 0.9, 0.95) of the station specific distribution of Annual Maxima rainfall calculated using linear quantile regression

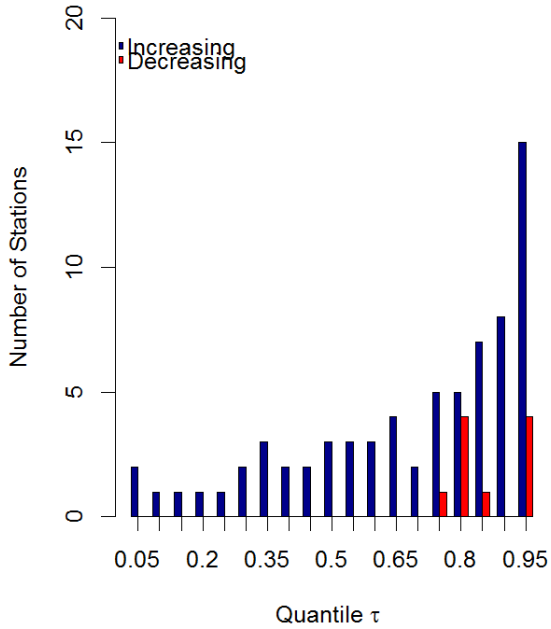

Figure 5-5 : Histogram of gauges with significant increasing and decreasing trends in Annual Maxima per quantile of the station distribution calculated using linear quantile regression

5.1.3 Long range dependence

Estimators of the Hurst exponent (H; Hurst, 1951) were also calculated to determine whether long range dependence (LRD) is an important factor in the data variability, that is

whether a cyclic pattern occurring over a period of years or decades is present in the observations. A secondary aim, if LRD was not significant in most observations, was to filter the stations used in subsequent analyses to use only those with minimal errors or missing data. H>0.5 is generally indicative of an LRD process (Koutsoyiannis, 2006), with most hydrological series exhibiting a value in the order of 0.7 (Hurst, 1951). All observations were tested for the full record duration as trend and change point analyses were only significant for very short portions of the observed record, or equated to a null trend over the whole record. Hurst exponent values were calculated by aggregated variance, tested for significance using a bootstrap of 5000 repetitions (Efron and Tibshirani, 1993), and are shown in Figure 5-6.

Of the 99 stations with H>0.5, only nine were shown to have significant LRD. Two of these comprised only 40 maxima each which is insufficient for reliable estimation (Serinaldi, 2010). The remaining 7 station records all had between one and several intermittent years missing from the record which may have affected estimates of H; all stations with missing sequences >5 years in duration were, therefore, removed from subsequent analyses. It is considered reasonable to apply statistical models which do not explicitly account for monotonic trends, change points or long range dependence to the remaining 199 stations, modelling effects such as seasonality or inter-year variability with interactive parameters.

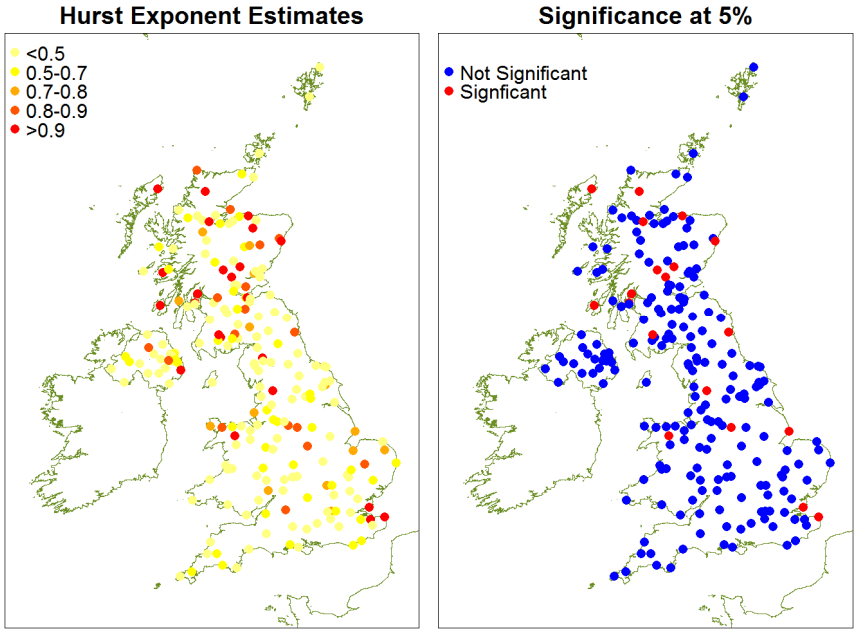

Figure 5-6 : (a) Values of Hurst Exponent calculated with aggregated variance; (b) Significance of Hurst Exponent tested with a bootstrap procedure

5.1.4 Event dispersion

It is assumed that the frequency of events above a high threshold is Poisson i.i.d. While parameter stability tests for the suitability of Poisson and extreme value distributions can be used to identify the most appropriate high threshold (Coles, 2001), the tests favour lower thresholds which increase the data used for estimation and reduce the standard error. However, events exceeding a relatively low threshold do not always conform to a Poisson distribution or may contain a mix of heavy and extreme events which are dependent on different governing variables.

A selection of different thresholds was explored to select the most appropriate thresholds for excess models: several fixed values at levels considered to be high (from Alexander *et al.*, 2006) and a station specific threshold defined by (Fowler and Kilsby, 2003a). The influence of threshold choice is explored further in Section 5.2, together with a formal selection of the thresholds to be used in this project. The thresholds are:

- 20mm, 25mm, 35mm, 40mm
- Mean wet day total + 2 x variance in wet day total ($\mu + 2\sigma^2$)

The suitability of a homogenous Poisson process to represent the data was first examined through the dispersion of event counts per year over the period of record. Figure 5-7 illustrates the mean and variance in the number of peak over threshold (POT) events per year exceeding a station specific threshold $\mu + 2\sigma^2$, and shows a clear demarcation of stations in western regions experiencing more frequent “very wet days”. By contrast, the dispersion coefficient (mean event count/variance) for these stations is <1, denoting a more regular distribution of events than expected from a Poisson process (Hsing, 1988); this suggests that the selected threshold for very wet days is too low. Event counts which are over-dispersed also do not conform to the requirements of a homogenous Poisson process, suggesting that different regimes are in operation across several years, possibly arising from an external influence such as the North Atlantic Oscillation.

A primary cause for apparent under dispersion in the POT maxima series is missing data, thus assessing the suitability of the Poisson distribution was part of the iterative procedure used to derive homogenous data series. Secondly, understanding whether the data are homogenously dispersed, or correlate with an external influence, will assist in the identification of suitable covariates for use in later statistical analyses.

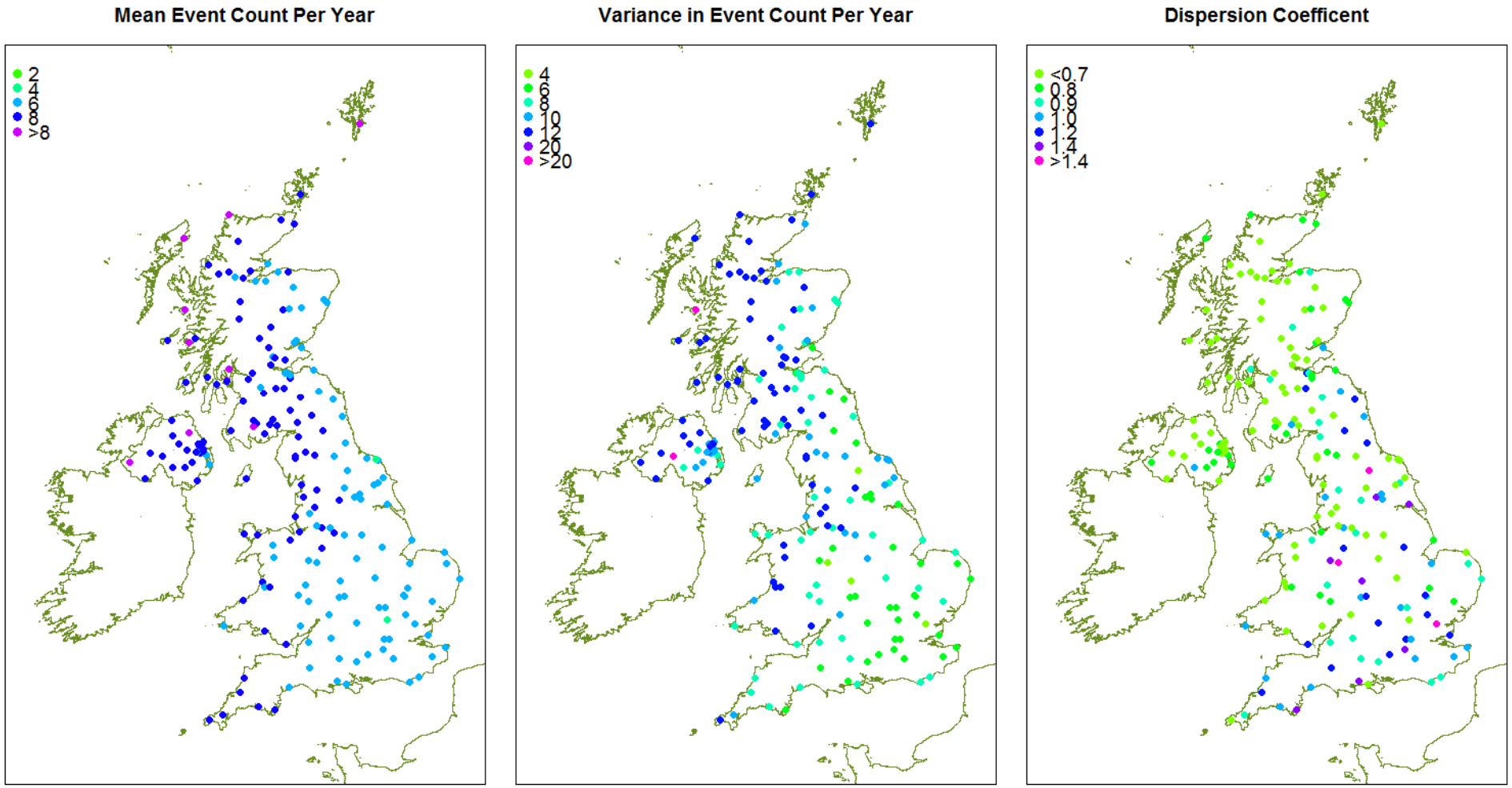

Figure 5-7 : POT Events per year exceeding a station specific threshold of *wet day mean + twice the station wet day variance* (a) Mean event count; (b) variance in event count; (c) Dispersion Coefficient

Dispersion coefficients obtained from the fixed threshold excesses are illustrated in Figure 5-8, confirming that higher selection thresholds are required to remove mean behaviour from the analysis; the lower threshold includes too many non-extreme events, artificially reducing the dispersion coefficient below 0.9 (Shinohara *et al.*, 2010). It is also clear that a fixed threshold for all stations is not appropriate and that a station specific threshold based on the wet day distribution should be used instead, as outlined in Section 5.2.2.

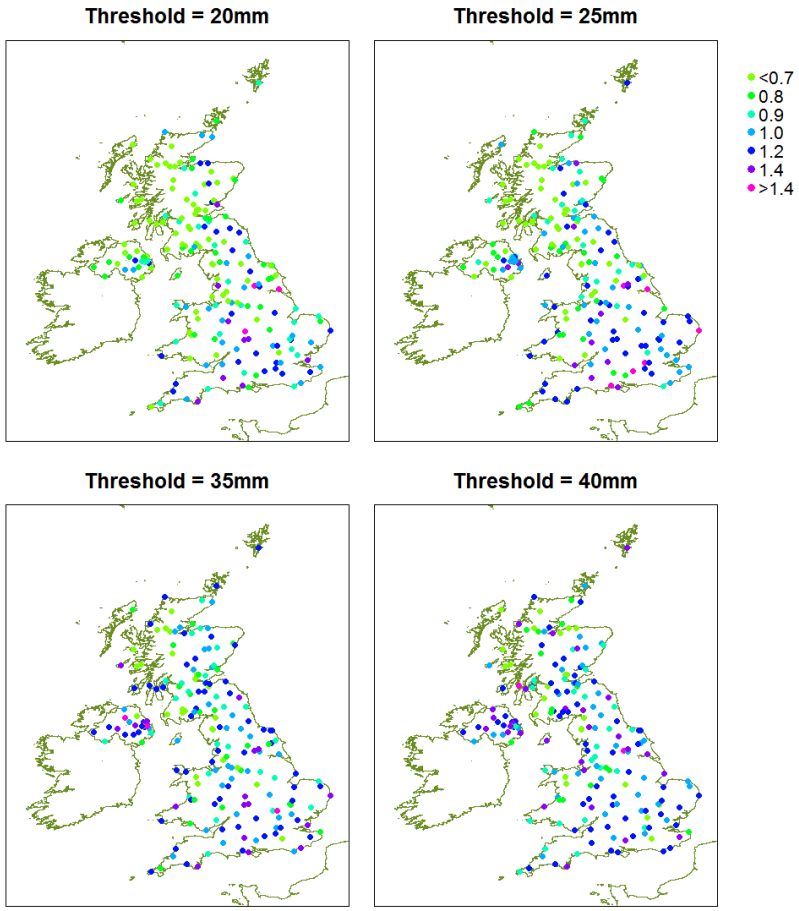

Figure 5-8 : Coefficient of dispersion calculated from all events per year exceeding thresholds of (a) 20mm; (b) 25mm; (c) 35mm; (d) 40mm

The dispersion coefficient is representative of Hurst variability giving sequences of similar years, rather than a measure of within-year event clustering. Within-year clustering is well represented by an exponential distribution with arrival rate Λ. Figure 5-9 shows the spatial distribution of stations conforming to the null hypothesis (H0) that events follow an exponential model, or alternative hypothesis (H1) that events follow a different distribution, in relation to the interval between events for the four fixed thresholds, and the progressive

improvement in distribution fit as the threshold increases and reduces the event count. Figure 5-10 depicts the same information as a histogram.

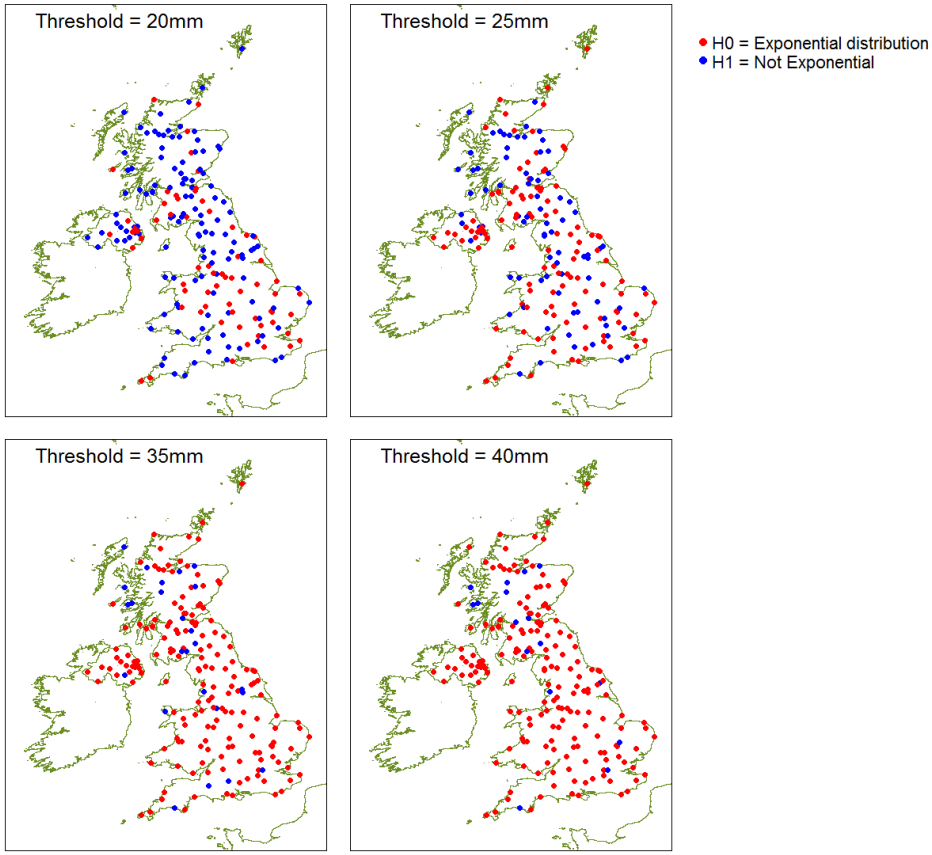

Figure 5-9 : Representation by an exponential model of interval between events exceeding thresholds of (a) 20mm; (b) 25mm; (c) 35mm; (d) 40mm

These results confirm that using a threshold which is too low in relation to the station mean wet day distribution will incorporate too many events, which are not exponentially distributed throughout the year. Similarly, adopting a threshold which is too high will severely restrict the number of events used in the analysis. A higher station specific threshold will encapsulate extreme behaviour more effectively, with events randomly distributed throughout the year and with more spatial coherence in the responses to atmospheric drivers.

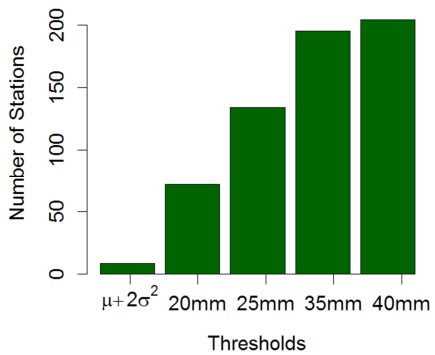

Figure 5-10 : Number of stations adequately represented by an exponential model by threshold for excesses

Runs testing was carried out using the Wald-Wolfowitz runs test (Wald and Wolfowitz, 1940) for randomness, to examine whether the interval between POT events are randomly distributed (H0), although clustered within specific seasons (Allamano *et al.*, 2011). Each event exceeding the threshold was assigned as a positive outcome and the runs statistics tested for randomness, following the method outlined in Chapter 3. The results, illustrated in Figure 5-11, demonstrate that events are only randomly distributed for all stations at extremely high thresholds, when the paucity of events per year in the south east prevents analysis of within-year clustering. In regions with low mean wet day totals, e.g. southeast England, there are insufficient events of > 40mm to test the randomness reliably. Initial runs testing also confirmed that only the 199 stations, selected from the trend analyses, are suitable for use in POT analyses, due to the missing years of missing data in the remaining stations noted earlier.

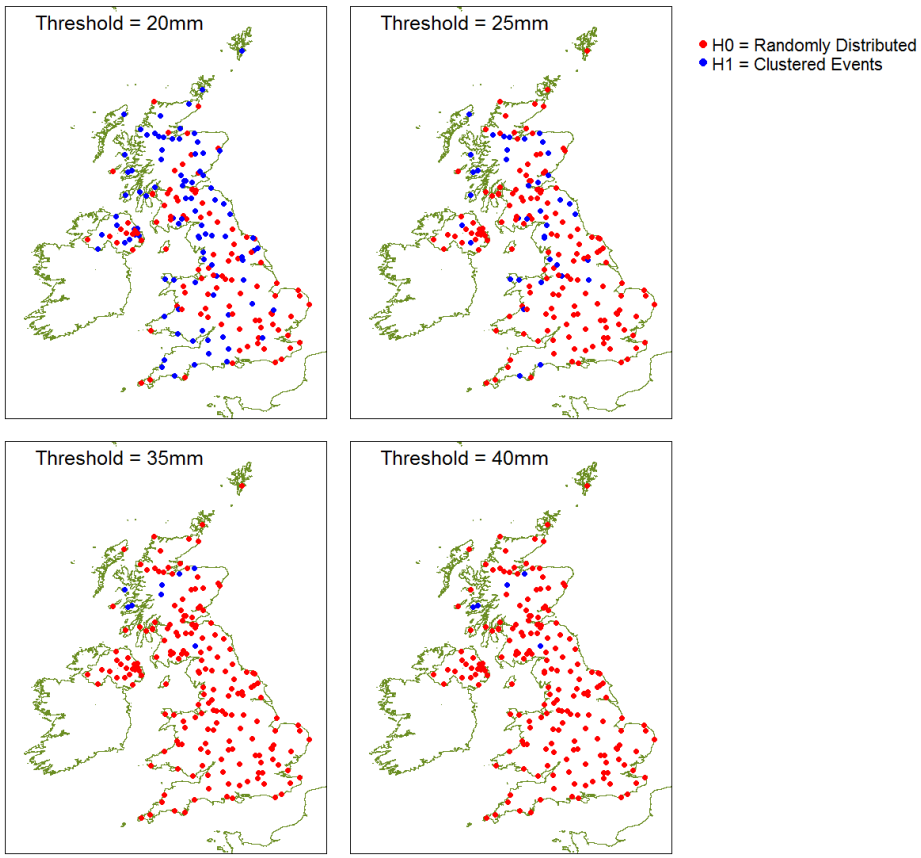

Figure 5-11 : Randomness of events exceeding fixed thresholds as for Figure 5-9 tested using the runs test

5.1.5 Dependence on atmospheric conditions

Poisson regression models, examining the dependence of event frequency on another variable were used to examine the significance of difference covariates. The simplest regression models relate the frequency of events to a linear coefficient (1 or 0); more complex

models are premised on linear regression models. Likely extreme event drivers identified in Chapter 2 were incorporated into Poisson regression models and the relationship tested for significance at the 5% level against the χ^2 distribution. The results of the most important relationships, that is with a test score of ≤0.25, are illustrated in Figure 5-12 for seasonality, sea surface temperature (SST), mean sea level pressure (MSLP), maximum monthly air temperature and two measures of the NAO. Seasonality is approximated from the calendar day, while monthly covariates such as SST were selected from the corresponding month of occurrence.

Seasonality appears to have a considerable influence on POT occurrence rate within each year, with all stations correlated at a significance level <1%; high dispersion rates from year to year suggest that variability in atmospheric conditions may govern event frequency. MSLP also has a highly significant positive correlation with POT occurrence rate; the PCA derived NAO index has a positive correlation in the high elevated Atlantic facing regions such as northwest Scotland, while other stations are negatively correlated. Both SST and air temperature are generally positively correlated with the occurrence rate, implying increased frequency with elevated temperatures, with some stations in central England and eastern Scotland correlated negatively; however, neither of these covariates were significantly correlated. The influence of aggregated indices, such as seasonal NAO, and of lagged coefficients, such as MSLP or SST, will be explored more thoroughly in Chapter 7.

A measure for ENSO was also examined in the Poisson regression model, but obtained a very low significance rating and high Akaike Information Criterion (AIC, Akaike, 1974) rating showing that this covariate is unimportant. Two monthly measures of the North Atlantic Oscillation Index were examined: normalised sea level pressure differences between Reykjavik and Gibraltar (Jones *et al.*, 1997) and an index derived from principal component analysis (PCA; Hurrell and Van Loon, 1997). The latter index places less emphasis on the centre of action (Hurrell and Deser, 2009) and in common with other research correlates better with extreme rainfall (Hurrell, 2003). While not all of the covariates included in the Poisson regression model were significant at the 5% level, the AIC scores demonstrated that each significantly improved the model fit. Given the high, but insignificant, correlation with rainfall maxima, MSLP, SST and monthly maximum air temperature will be incorporated, together with the PCA derived NAO index, into more complex models described in Chapters 7 and 8.

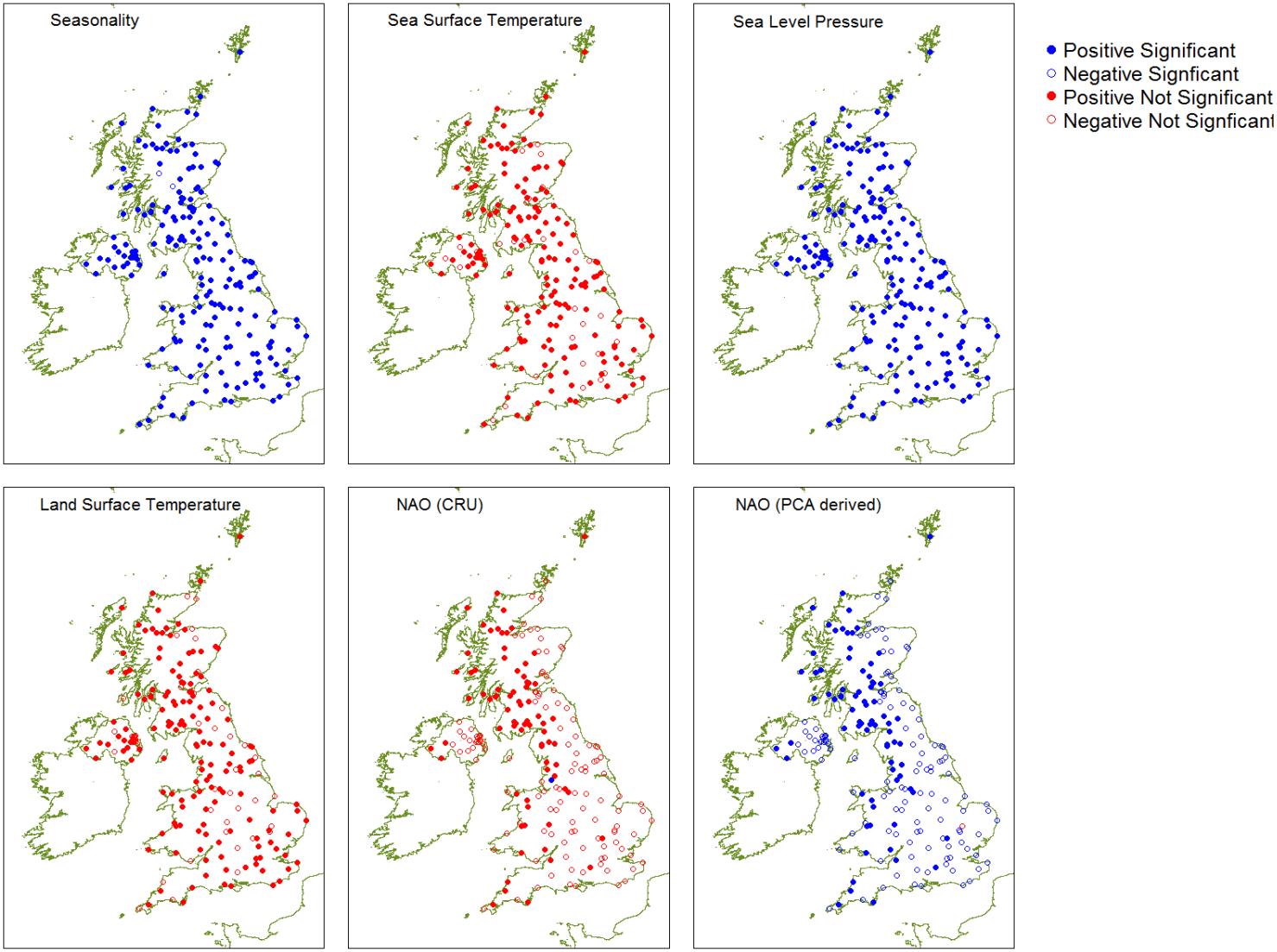

Figure 5-12 : Significance (at 90%) of external covariates on Poisson regression model for events exceeding 95% of the wet day distribution (a) Seasonality, represented by calendar day; (b) Sea Surface Temperature; (c) Sea Level Pressure; (d) Monthly maximum air temperature; (e) Monthly NAO index with respect to the event month, derived from normalised SLP difference between Reykjavik-Gibraltar (Jones *et al.*, 1997); (f) Monthly NAO index derived from PCA (Hurrell and Van Loon, 1997)

The data exploration found long runs of missing months or years in 24 stations. While these stations will be omitted from all POT analyses, their annual maxima are verifiable from alternative sources, such as British Rainfall (Pedgley, 2010), and can be used in Chapter 6 which examines annual and seasonal maxima. No allowance needs to be made for abrupt or gradually varying changes in the data as there is insufficient data to make specific trend allowances; these changes are better represented through the use of specific covariates related to seasonality or multi-annual atmospheric variability.

5.2 Thresholds for Wet and Extremely Wet Days

5.2.1 Low thresholds

The definition of a high threshold for exceedance models requires a corresponding definition of the minimum value for wet days. Salter (1921) noted that the minimum rainfall measurement unit was $\frac{1}{100}$in. until 1914 when metrication was formally adopted; given the potential errors of reading such a small volume and conversion errors, he recommended 1mm (0.04in.) to define a wet day. Lower thresholds (≥0.2mm, $\simeq \frac{1}{100}$in.) have been adopted in dry regions to avoid removing useable data (Wilks, 1990; Husak *et al.*, 2007). Others have found that although mean rainfall characteristics are well described by low thresholds, extreme value models are more reliably estimated from statistics based on a wet day threshold ≥1mm (Moberg and Jones, 2005; Alexander *et al.*, 2006) even though higher wet thresholds are more commonly used in climate models to minimise problems in representation of drizzle (Zhang *et al.*, 2011).

Two gauges, representing two very different extreme rainfall regimes and shown in Figure 5-13, were chosen to review the suitability of the gamma distribution and the impacts of different thresholds on extreme value analyses. Visual and statistical testing demonstrated that a wet day threshold of ≥0.1mm gave the best fit to the gamma distribution (illustrated in Figures 5-14 and 5-15), based on the station properties; this threshold includes trace rainfall but removes completely dry days.

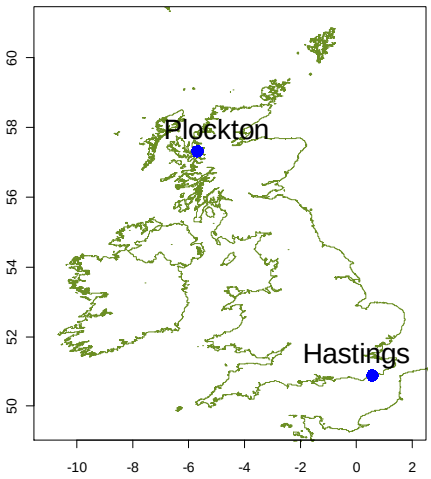

Figure 5-13 : Location of stations used to explore daily rainfall characteristics

The quantile-quantile plots in Figure 5-14 demonstrate that the gamma distribution is an appropriate choice for mean daily rainfall, but that the upper tail properties are not as well reproduced. The point of deviation from the red line (approximately 20mm for Hastings and 35mm at Plockton) coincides with the 95% quantile of the wet day distributions at both stations; Burauskaite-Harju *et al.* (2012) also found this to be the point where quantiles estimated from extreme value theory outperform "ordinary" quantiles.

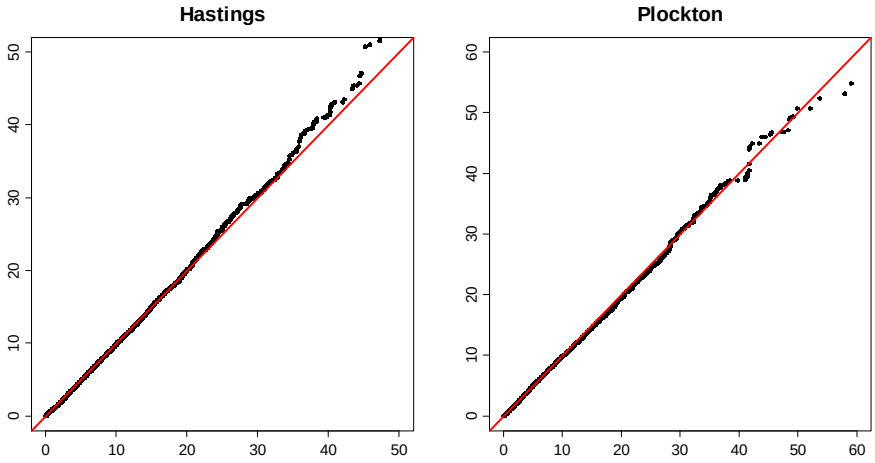

Figure 5-14 : Quantile-Quantile plots for Gamma distribution of daily rainfall with a wet day threshold ≥0.1mm based on daily rainfall records at Hastings and Plockton

Histograms in Figure 5-15 also show a good fit between the observed frequency of rainfall totals (red bars) and the fitted gamma distribution (blue curve). Statistical testing failed to accept the fit as the modified Kolmogorov-Smirnoff test (Zwiers and von Storch, 2004) is calculated from squared differences between the distributions. For the purposes of examining the sensitivity of high thresholds, the gamma distribution based on a wet day threshold ≥0.1mm provides the best fit for the whole distribution. However, for specific analysis of the upper end of the distribution a wet day threshold of ≥1mm will be adopted

as this was found to give a better fit to the extreme value distribution in common with other research (Katz *et al.*, 2002; Zhang *et al.*, 2011).

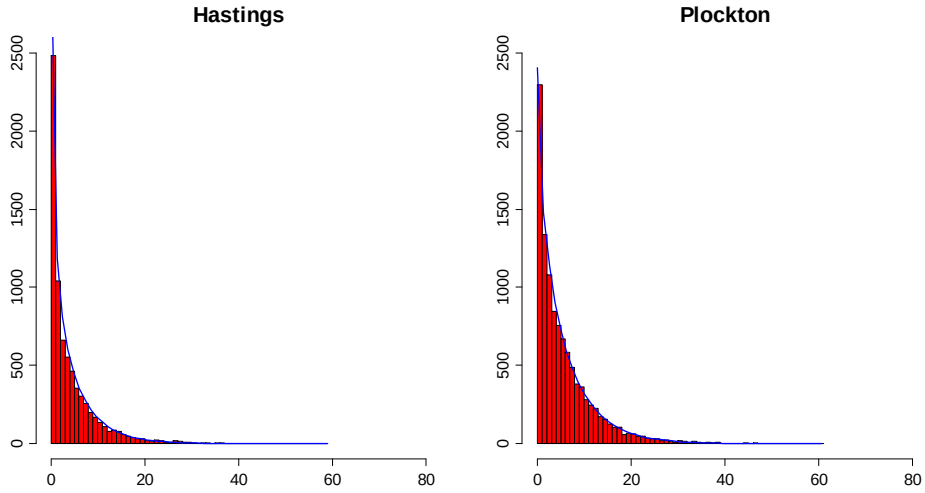

Figure 5-15 : Histograms of Gamma distribution fit for wet days ≥0.1mm estimated from observations between 1963-2006 at Hastings and Plockton demonstrating wetter characteristics in North Scotland

5.2.2 High thresholds

The duration of data used to define a threshold for exceedance models (base period) can have an influence on the threshold value and a commensurate impact on observable trends. Portmann *et al.* (2009) identified that small changes in POT frequency are insignificant when compared to the base period, but can display considerable differences when compared to other years. Zhang *et al.* (2005) found a higher probability of false trend identification or inhomogeneities in these trends when thresholds are not defined from the whole period of the record.

Base Period	Threshold of Quantile (mm)								
	10%	20%	30%	40%	50%	60%	70%	80%	90%
1961-1990	2.3	4	5.6	7.3	9.1	11.2	14.4	17.9	25.2
1971-2000	2.4	4.1	5.8	7.5	9.3	11.7	14.5	18.2	26
1961-1995	2.3	4.1	5.7	7.4	9.1	11.4	14.4	17.9	24.9
1896-2006	2.5	4.1	5.8	7.4	9.2	11.4	14.1	17.8	24.1

Table 5-1 : Comparison of quantile thresholds for different base periods. Drawn from Hastings annual daily rainfall observations

The sensitivity of trends in events exceeding a volumetric quantile (method outlined in Section 5.3) was examined for different base periods and is outlined in Table 5-1 and illustrated in Figure 5-16; the orange line is a simple linear trend and the green line shows the expected frequency of events in each year of 0.1. Although there is very little difference between the numeric value of the lower thresholds for different base periods, the 90%

threshold differs by up to 2mm with significant trends only found for the lower threshold values (i.e. calculated from the 1961-1995 or 1896-2006 base periods).

Although the above analyses have established the sensitivity threshold calculation from different base periods, the most appropriate duration is not immediately apparent. While using the whole record period may be the ideal solution, it would not be possible to compare analyses from gauge records commencing in different years. Furthermore, the focus of this project is extreme rainfall but a threshold of 90% of the wet day distribution includes too many events per year to make the use of an extreme value distribution appropriate (Katz *et al.*, 2002). As a result, the accepted definitions of very wet and extremely wet days (IPCC, 2011), calculated in relation to a base period of 1961-1990 and defined by Alexander *et al.* (2006) will be used in this project for all examination of events exceeding high thresholds.

- Very wet days Q95: RR_{wi} is the daily rainfall total on any wet day $w \geq 1$mm, in period j and $RR_{wn}95$ is the 95th quantile of rain on wet days between 1961-1990, then for W wet days:

$$Q95_j = \sum_{w=1}^{W} RR_{wj} \qquad \text{where } RR_{wj} > RR_{wn}95$$

- Extremely wet days Q99: for the same notation, $RR_{wn}99$ is the 99th quantile of rain on wet days between 1961-1990:

$$Q99_j = \sum_{w=1}^{W} RR_{wj} \qquad \text{where } RR_{wj} > RR_{wn}99$$

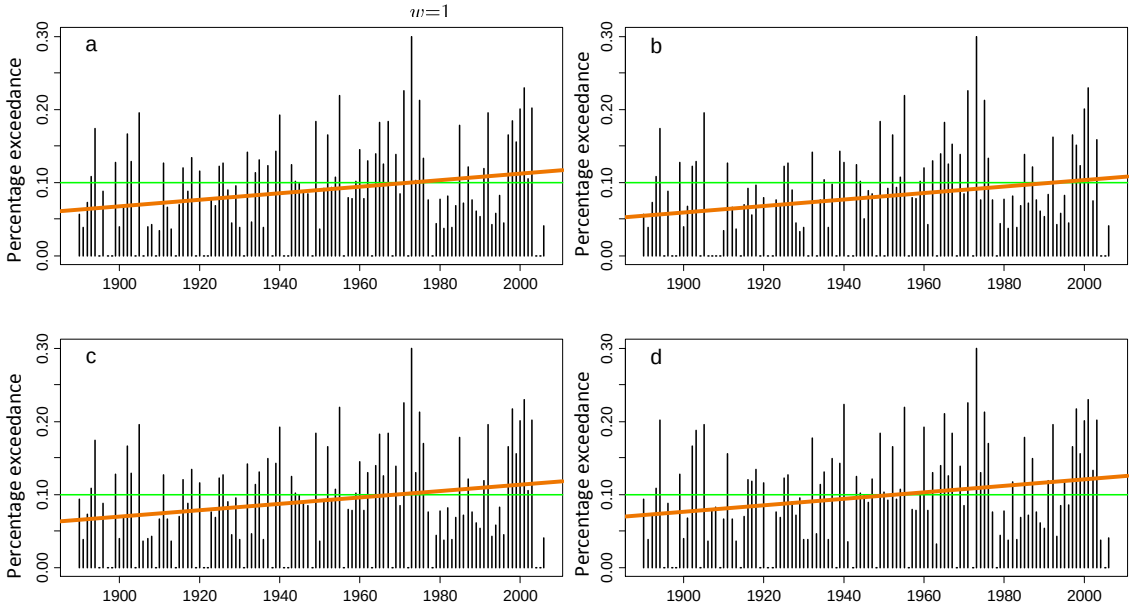

Figure 5-16 : Variation in percentage of events at Hastings exceeding 90% of the mean wet day total for base periods: a) 1961-1990 b) 1971-2000 c) 1961-1995 d) 1896-2006. The green line represents the expected frequency of events in this category in each year and orange line the apparent trend in quantile contribution.

5.3 Metrics of Extreme Rainfall: Quantiles

Quantiles of rainfall on wet days can be analysed with extreme value theory to assess the frequency and magnitude of excess events; an alternative is to examine changes in different quantiles of rainfall magnitude or wet day frequency. Using a histogram type analysis the rainfall events may be "binned" either according to the frequency of events exceeding R10p:R90p, using the notation above, (Karl and Knight, 1998; Groisman *et al.*, 2001); or according to some volumetric threshold (Maraun *et al.*, 2008). The first assesses changes in the *frequency* of different magnitude events, while the second appraises changes in event *intensity*. However both aspects are important for engineering design or strategic risk management planning and should not be isolated in this manner. Extreme value theory facilitates examination of both the frequency and magnitude of the event distribution; thus the only reason to examine quantile behaviour in this manner is if it provides greater clarity on changes in the intensity or frequency of events.

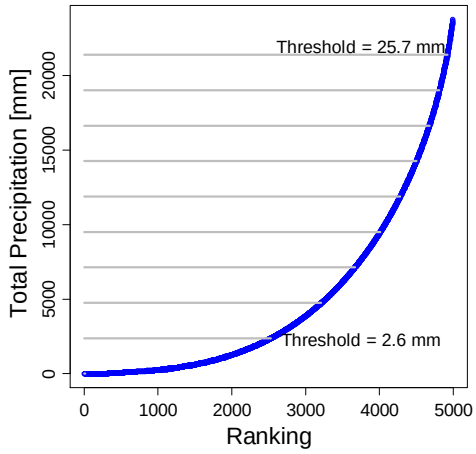

Figure 5-17 : Volumetric quantile thresholds from Hastings daily rainfall observations obtained by ranking the magnitude of all events within the base period, and selecting the upper observation of each quantile. Blue line indicates cumulative event total; grey lines the threshold of each volumetric quantile.

The aim of this exploratory analysis is to review the merits of volumetric quantiles in characterising extreme rainfall and whether the results clarify apparent changes in event intensity. Adopting the methodology outlined by Maraun *et al.* (2008), the fractional contribution of total rainfall to each volumetric quantile is estimated by:

- Ranking all wet day totals by magnitude within the base period.
- Dividing the cumulative total by 10, to obtain volumetric quantiles.
- Selecting the upper observation of each quantile as the bin threshold (Figure 5-17).
- Assigning all rainfall observations to the quantile bins for each year.

The upper quantile may contain only a few events which together total 10% of the base period rainfall, while the lower quantile will contain considerably more than 10% of the total number of wet days.

Michaels *et al.* (2004) were critical of this approach as increases in total rainfall will result in changes to the distribution parameters; uniform changes in the characteristics of the distribution may have a non-uniform manifestation in the quantiles. Further, simple examination of trends in the upper quantiles of the rainfall frequency or intensity distributions (Karl and Knight, 1998; Groisman *et al.*, 2001; Maraun *et al.*, 2008) will demonstrate changes relative to a defined period but not their significance. This requires an assessment of the changes in proportion to those in the overall rainfall distribution.

Method of moments estimators for the Gamma distribution parameter estimates can be obtained from the wet day mean and variance, facilitating a simple diagnostic to identify likely distributional changes. Trends in either the mean or the variance, as shown in Figure 5-18, will result in changes in the rainfall distribution, and hence the upper volumetric quantile. Comparison of Hastings and Plockton also highlights the sensitivity of trend analyses to the starting point, for example a regression line commencing in 1963 for Hastings would be steeper than one commencing in 1893 as shown. While considerable climate variations have occurred since the 1960's (IPCC, 2007a), care must be taken to distinguish natural climate variability from abrupt changes in behaviour.

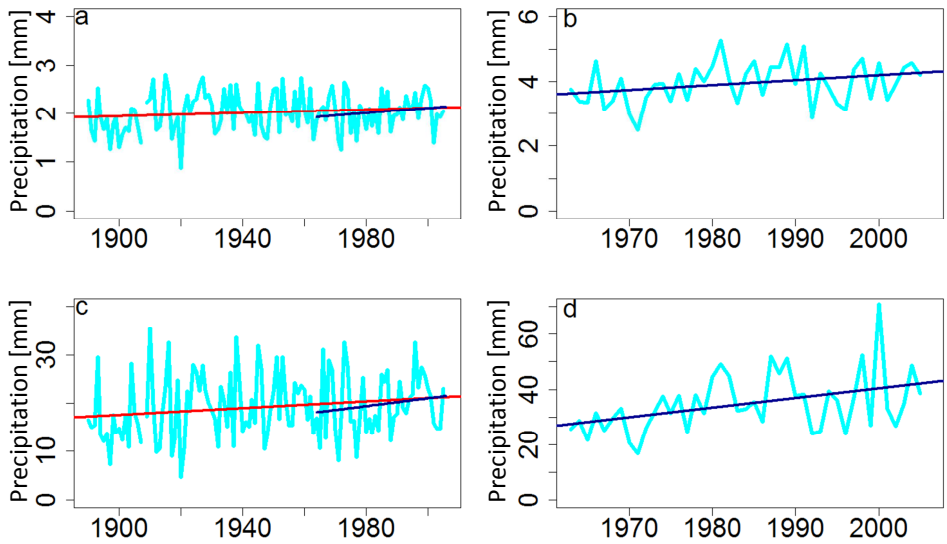

Figure 5-18 : Wet day statistics for mean wet day total for (a) Hastings and (b) Plockton; variance in wet day totals for (c) Hastings and (d) Plockton. Red lines represent linear regression in relation to Hastings record (1893:2006), dark blue lines represent linear regression in relation to Plockton record (1963:2006).

The volumetric quantile method was used to determine thresholds in relation to a base period of 1961-1990 and the resultant fractional contribution of events in each year; shown in Figure 5-16(a). The green line indicates the "expected" fractional contribution if each quantile contributed 10% of the annual total rainfall (as Maraun *et al.*, 2008); a linear trend is indicated in orange. As the regression lines in Figure 5-18 suggest that the rainfall distribution is changing in relation to the 1961-90 period, simple linear trends do not give a full picture of the significance or magnitude of changes in extreme rainfall. A more relevant test would compare observed changes in quantiles with those expected from changes in the gamma distribution. Although changes to the individual shape (α) and scale (β) parameters do not represent direct changes to the rainfall regime, manipulating the parameters can illustrate their influence on the extreme responses. This analysis is illustrative only as the exact magnitude of the extremes are not well represented by a gamma distribution (Katz *et al.*, 2002), as shown earlier. However, the method is useful to determine whether apparent trends in the upper quantiles are greater than would normally be expected from changes in the wet day distribution.

Gamma distribution parameters were estimated from Hastings wet days (≥0.1mm) using maximum likelihood estimates (MLE); thresholds were estimated for the period 1961-1990. A synthetic series representing 30 years of rainfall was then created by randomly sampling from the distribution 10,950 times, and data categorised by threshold. The influence of changes in α and β was examined by re-simulating the gamma distributions with each parameter increased in turn by 10%. The mean fractional contributions to each quantile from 100 simulations, using the three simulated series, are shown in Figure 5-19.

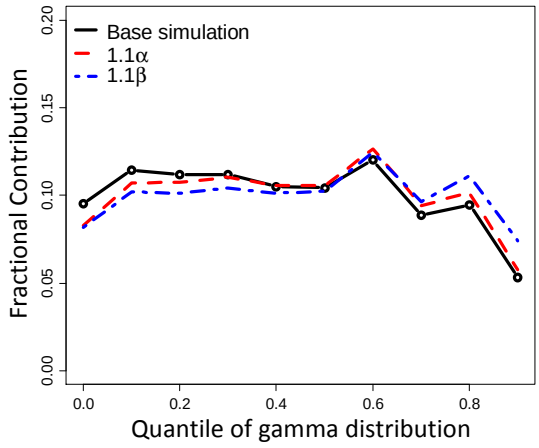

Figure 5-19 : Fractional contribution by quantile for base gamma distribution (black) fitted to Hastings daily rainfall, and with increased shape (α, red dashes) and scale (β, blue dot-dash) parameters

The results indicate the impact of each of the parameters on the distribution; by increasing α the distribution becomes more kurtotic about the mean with a smaller fractional contribution to the lower quantiles. In contrast, increasing β affects kurtosis and variance resulting in the greatest increases in the upper quantiles. These results also demonstrate that the distribution is not uniform and while thresholds were chosen according to quantiles of the cumulative total rainfall, the fractional contribution of events does not equate 10%. Furthermore, thresholds were derived empirically from finite observations rather than theoretically from an asymptotic distribution, leading to skewed estimates. Based on the method of moments variations in the scale parameter, $\beta = \mu_{\text{wet day}}/\sigma^2_{\text{wet day}}$, may be easier to identify than changes in the shape parameter, $\alpha = \mu_{\text{wet day}}/\beta$, which controls the skew of the distribution. The scale parameter has been shown to explain seasonal and spatial variations in rainfall, particularly in strongly seasonally driven regions (Wilby and Wigley, 2002), and better reflects changes to extreme rainfall patterns (Osborn and Hulme, 2002); refer also to Chapter 3.

The same base gamma distribution was then used to simulate uniform quantitative changes to the rainfall distribution arising from increased event intensity, frequency or both intensity and frequency. This analysis assumed for the sake of simplicity that changes to the rainfall distribution will be uniform, which is unlikely (Allen *et al.*, 2002; Trenberth, 2011). A base sample of 10,000 was taken from the un-modified gamma series and the number of events exceeding the original thresholds was increased by a total of 10% in:

- intensity: each of 10,000 original draws multiplied by 1.1
- frequency: 1000 additional draws from the original distribution
- intensity and frequency (general): each of 10,000 original draws multiplied by 1.05, and 475 additional draws.

The results in Figure 5-20 compare the fractional contribution of ‘events’ to each quantile from the different simulations. The curves from the base distribution and increased frequency are overlain as the additional points resulted in no net change to the fractional contribution only to the total number of ‘events’.

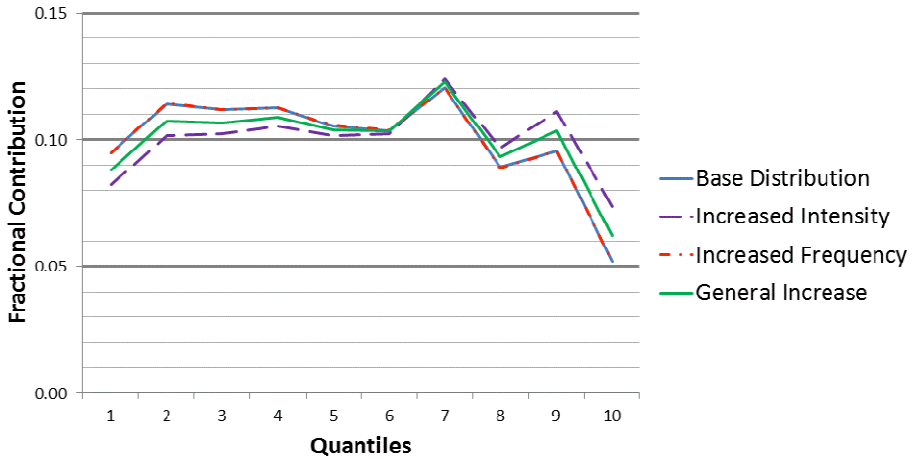

Figure 5-20 : Impact of increases to the Hastings gamma distribution on fractional contribution to volumetric quantiles manipulated to reflect uniform changes in rainfall

The greatest changes in fractional contribution occur for the largest change to the distribution parameters and are reflected in the upper quantiles. The simulated increases in rainfall intensity equate to a decrease in the scale parameter of $\simeq 0.1\%$ and commensurate increase in shape parameter $\simeq 10\%$; simulating increased frequency results in no net change to the parameters; and simulated increases in frequency and intensity gives $\Delta\alpha \simeq -0.1\%$ and $\Delta\beta \simeq 5\%$. These results emphasise that changes to the hydrological cycle are more complex than can be reflected by volumetric quantiles (Trenberth, 2011; Burauskaite-Harju *et al.*, 2012), which is found to be an unnecessarily restrictive approach. In particular, concentrating on changes in a specific quantile does not identify either the combined impacts of changes in event frequency and intensity or the individual changes in frequency even where the change is known. The volumetric quantiles approach will not be used further in this project, as a method is required which examines holistic changes in extreme rainfall patterns, considering frequency, intensity, timing and duration.

5.4 Metrics of Extreme Rainfall: *r*-largest events

Analyses of annual maxima, while potentially including Q95 events rather than just Q99 have the advantage of being insensitive to the selection of wet day or upper quantile threshold (Pryor *et al.*, 2009). Expanding the maxima series to include 'r-largest' events per year increases the analysis set, while providing a statistically unbiased measure of extremity, and may improve extreme value distributions parameter estimates (Smith, 1986). Although this expansion will also increase the number of events used in the analysis, it may improve heavy rainfall characterisation in wetter and drier years if other information such as the occurrence dates or range of magnitudes are analysed in parallel.

Extreme value applications of the *r*-largest order statistic model are used to improve return frequency estimates (Coles, 2001) where data are hard to pool, such as sea surges (Hosking and Wallis, 1997). For example, Smith (1986) analysed the 10 highest sea levels per year modelling the joint probability distribution with a multivariate GEV distribution, as have others examining wave heights (Guedes Soares and Scotto, 2004; Butler *et al.*, 2007) but the method has rarely been applied to extreme rainfall analyses (Zhang *et al.*, 2004). It is assumed that if the extreme value distribution is a reasonable fit for the annual maxima then different sample sizes r will also follow a GEV distribution with the same parameter estimates for all values of r (refer to Chapter 3). Selection of the most appropriate value of r is easily achieved using parameter stability plots (Coles, 2001), where μ, σ and ξ are depicted as functions of r, and identifying the largest value for which all three parameters appear to be stable (Butler *et al.*, 2007). The magnitude of r is critical, as too many events will introduce large variability and the limiting condition of $r/n \to 0$ will not hold true, while too few events will increase uncertainty in the GEV parameter estimates.

Table 5-2 shows the values of r at which the GEV parameters (standard errors) stabilise (minimise) for nine daily rainfall maxima series; a typical parameter stability plot is included in Figure 5-21 comparing parameter estimates and standard errors from the r-largest daily rainfall maxima at Armagh. While there is considerable variability between the stations, inspection of the standard error (s.e.) terms suggests that r =4 or r =5, the smallest value at which parameter and standard error stability is achieved, is the most appropriate value.

Gauge Reference	Name	Record Length	Region	GEV parameters for *r*-maxima		
				Location, μ (s.e.)	Scale, σ (s.e.)	Shape, ξ (s.e)
12	Baltasound No. 2	98	NS	8 (5)	13 (13)	5(4)
147	Braemar	137	ES	12(3)	14(11)	7(4)
251	Edinburgh, Blackford Hill	113	SS	7(6)	5(6)	4(4)
326	Durham	129	NEE	8(5)	9(4)	4(3)
606	Oxford	156	SEE	5(5)	5(3)	2(2)
671	Ross-on-Wye	132	SWE	4(4)	4(3)	8(5)
1530	Armagh	156	NI	14(8)	12(5)	9(2)
4436	Stretham	138	CEE	14(7)	12(8)	8(5)
12936	Appleby Castle	119	NWE	12(5)	10(8)	5(4)

Table 5-2: Number of *r*-maxima where approximate stabilisation is visually apparent for the multivariate GEV parameter estimates and standard error estimates (s.e.; in parentheses)

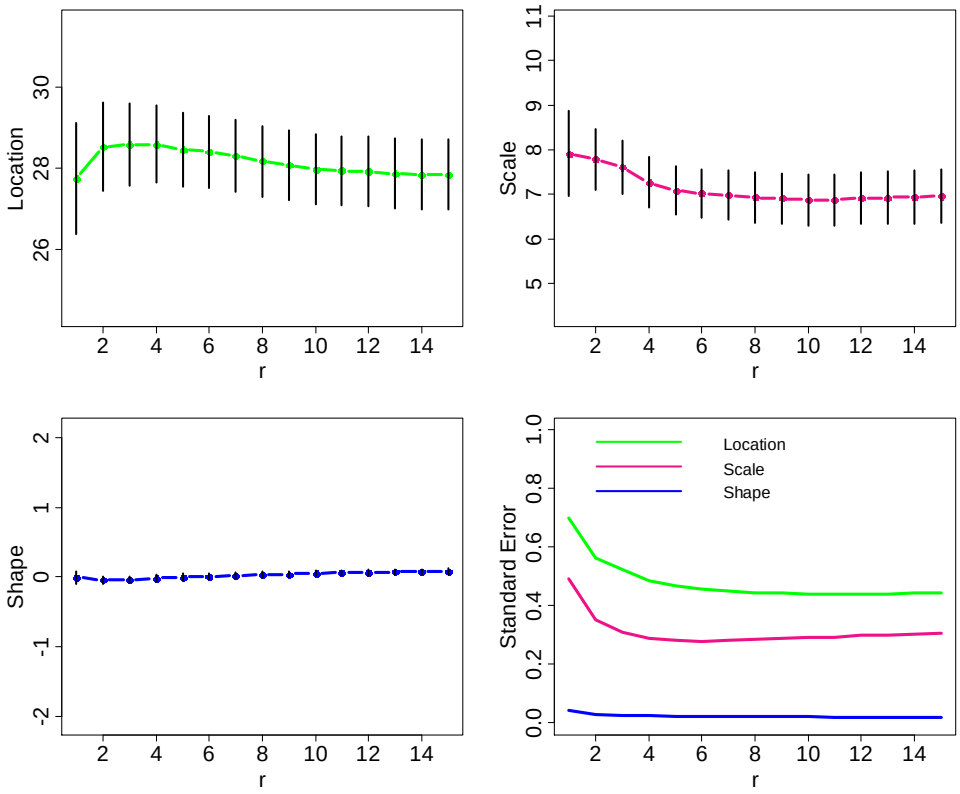

Figure 5-21 : Parameter stability plots for the multivariate GEV distribution, comparing parameter estimates (coloured lines) and standard errors (bars) from the *r*-largest daily rainfall maxima at Armagh

Quantile-quantile plots, with the empirical distribution derived from AMAX (Stephenson, 2002), and return level estimate plots were also used to examine the influence of different values of *r*. Table 5-3 contains the value of *r* at each station for which: all parameters become stable; the best quantile-quantile fit occurs; and greatest accord between return level estimates and observations is achieved. Typical examples of quantile-quantile plots and return level estimates are shown in Figures 5-22 and 5-23.

Gauge Reference	Name	Region	Parameter stability	Quantile-Quantile	Return level
12	Baltasound No. 2	NS	13	3	2
147	Braemar	ES	14	14	3
251	Edinburgh, Blackford Hill	SS	7	1	2
326	Durham	NEE	9	11	12
606	Oxford	SEE	5	11	12
671	Ross-on-Wye	SWE	8	10	3
1530	Armagh	NI	14	14	15
4436	Stretham	CEE	14	14	14
12936	Appleby Castle	NWE	12	5	5

Table 5-3 : Value of *r* for the multivariate GEV distribution for which all parameters are stable, the best model fit occurs and the best accord between return level estimates and observations is achieved with comparison to the annual maximum values (*r*=1) as the empirical distribution

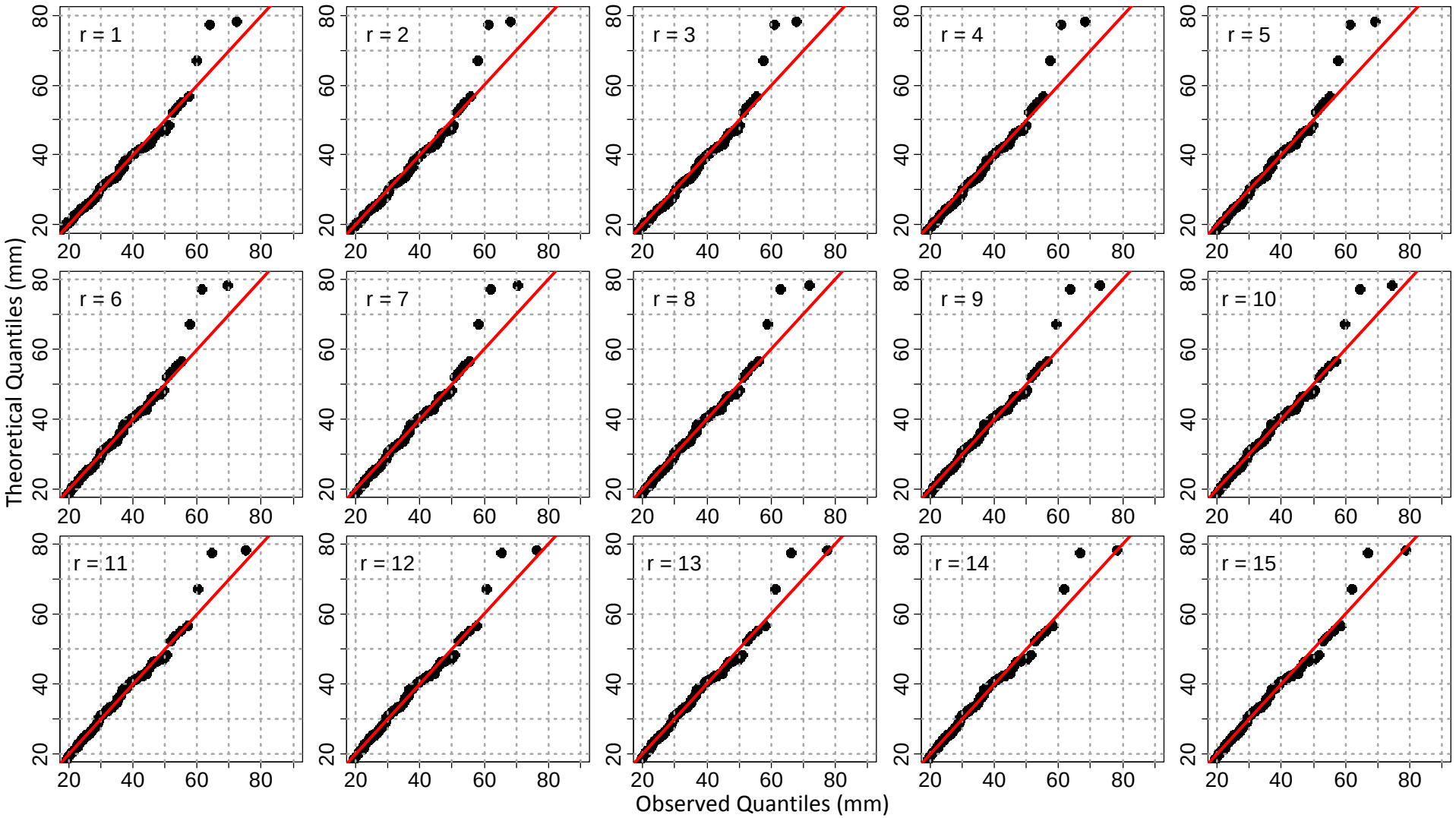

Figure 5-22 : Armagh quantile-quantile plots for the multivariate GEV distribution at different values of *r* -largest events per year, with comparison to the annual maximum values (*r*=1) as the empirical distribution

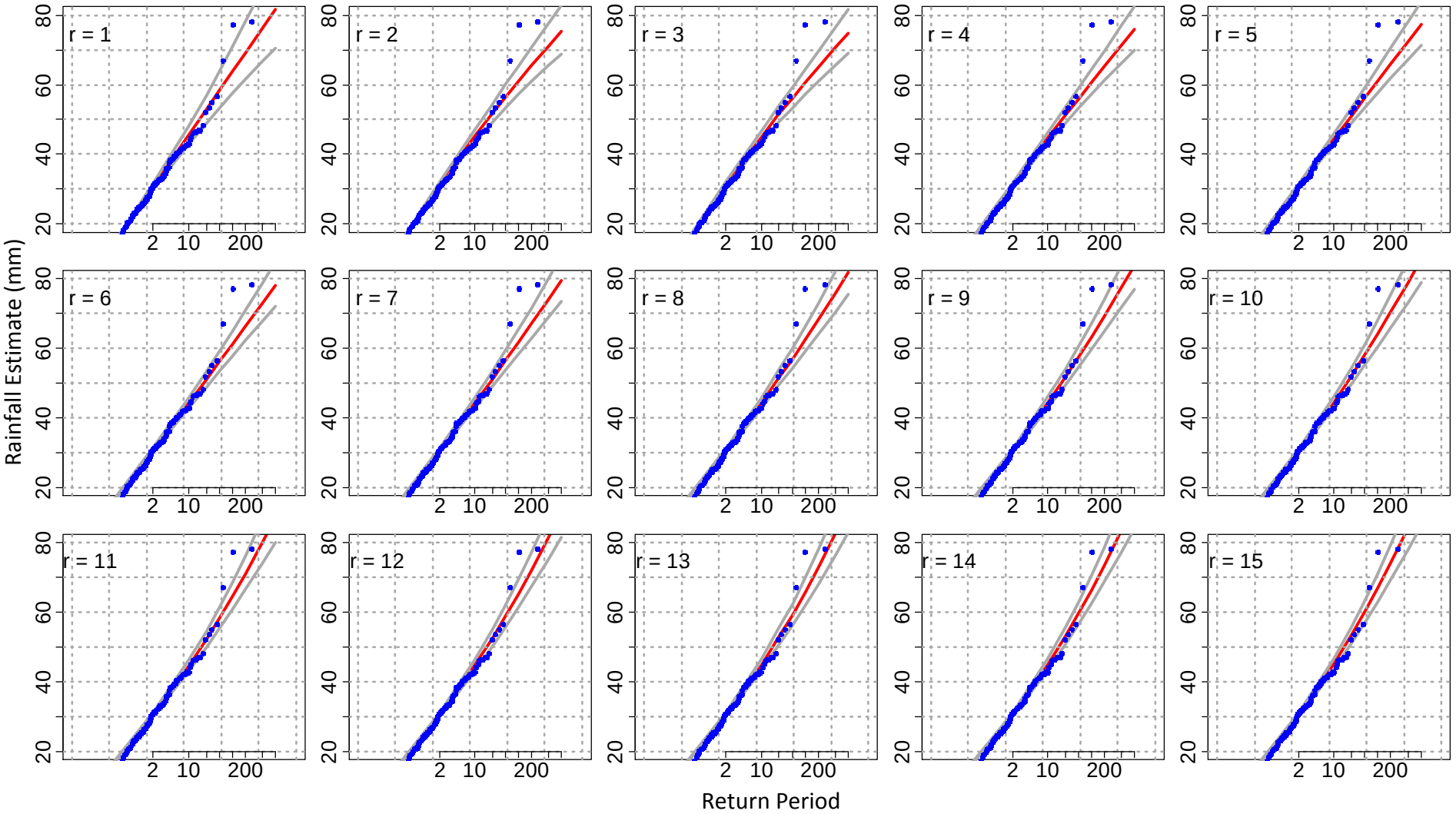

Figure 5-23 : Armagh return level estimates for the multivariate GEV distribution at different values of *r*-largest events per year using the annual maximum values (*r*=1) as the empirical distribution

Visual inspection of the proximity of the upper 5% quantiles to the theoretical best line (in red) in Figures 5-22 and 5-23, suggests that parameter estimates can be improved by using at least r=5 events per year, although there are differences between the most effective value of r for all stations. While there is some improvement compared with estimates from AMAX (r=1), all fifteen GEV distributions underestimate the upper tail. Other methods for improving parameter estimates such as regional frequency analysis (Hosking and Wallis, 1997) or excess over threshold models using only independent extreme events (Davison and Smith, 1990) may be more appropriate for extreme value distribution estimates. Table 5-2 suggested that using fewer maxima per year ($1 \leq r \leq 5$) in parameter fitting leads to better approximations of the shape parameter; similarly return period estimates from the distributions fitted to smaller values of r appear to match the observations better. Guedes Soares and Scotto (2004) assessed the influence of increasing r objectively with the deviance statistic, using three-hourly North Sea wave maxima from 1976-1999, arriving at an optimum value of r=5. Deviance statistics and the AIC indicate that the optimum value of r for GEV parameter estimates is between 13 and 15. However, the improvements in parameter estimation, and reciprocal reduction in standard error, are outweighed by the inclusion of too many non-extreme events in model fitting. The variability between different stations is also too great to apply this method homogenously to compare spatial differences in return period estimates.

5.4.1 Variance in range of r

When countering the quantile approach, Michaels *et al.* (2004) suggested examining trends in the magnitude of each r=10 largest events per year, effectively a simple form of quantile regression. They found limited evidence of changes in the wettest 10 days per year across the conterminous United States. However, their selection of r was determined from data availability rather than through subjective testing, leading to low significance of any tests as a result of the wide variability in rainfall regimes. Liu *et al.* (2011) found the choice of 10 days to be "arbitrary", opting instead to select a number, r, of events reflecting a fraction of the annual total rainfall.

Rather than analysing monotonic linear trends in each of the r-largest events per year, event magnitudes were examined in relation to each other (e.g. range of the largest magnitudes per year, occurrence month) to determine the characteristics of the heaviest

rain days. For instance, to assess whether reciprocity exists between the magnitude, e.g. in the range of r events, or timing of the events from year to year. Understanding whether particular years are more or less likely to experience large maxima would be beneficial to water resource managers, insurers and many others.

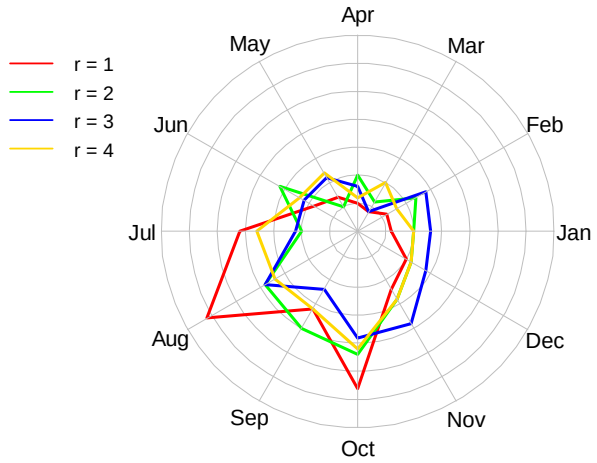

Figure 5-24 : Frequency of *r*-largest events by month for Armagh

Figure 5-24 illustrates the typical month of occurrence of the 4-largest events per year for Armagh, an r value selected from parameter stability plots of the characteristics depicted in Figures 5-25 to 5-27. This differs from the most appropriate r for use in the GEV model, where a higher number of events were required for parameter estimates. Similar temporal patterns were obtained for other stations, with more frequent maxima found either in the summer or winter, and very few of the wettest days in March or April. It is not possible to identify whether the wettest days cluster within year from this analysis as the causes of the events and inter-annual variability are too diverse to identify clear patterns. A more detailed exploration of POT seasonality, limiting the range of other drivers, is included in Chapter 7.

The mean, variance, interquartile range and median of the four largest events per year were explored for each gauge to determine whether any quantifiable relationship exists. The results for Armagh (Figure 5-25) show a high degree of year to year variability, as anticipated, in their range and mean value. Linear regressions are suggestive of an increase in either the inter-quartile range or variance of the events for a related decrease in median or mean. The results for other stations are equally noisy, with no coherent spatial pattern.

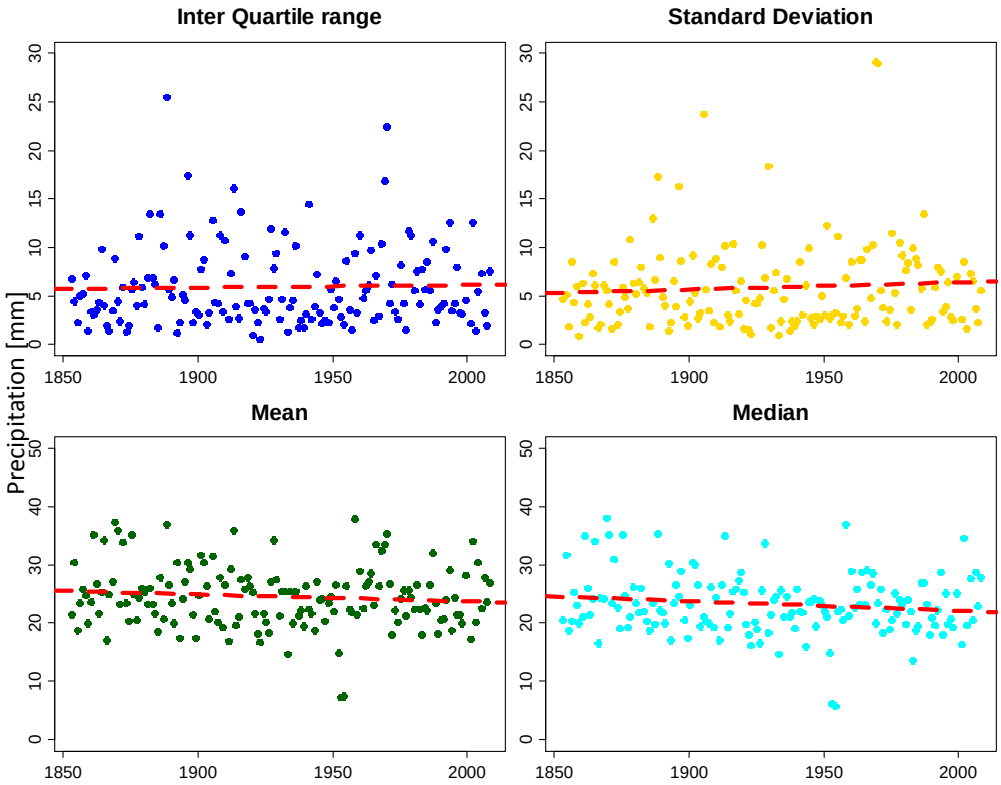

Figure 5-25 : Statistics of *r*=4 largest events per year for Armagh

All stations also have a positive correlation between the mean of the wettest four days and their variance, as typified by the plots for Armagh in Figures 5-26 and 5-27. The relationship suggests that during years with the most intense annual maximum events other peak event totals are not as large; this tallies with observed and projected variability in the magnitude of maxima, which is greatest in the extremes (Pall *et al.*, 2007; Portmann *et al.*, 2009) and likely to increase in variability (Hegerl *et al.*, 2007).

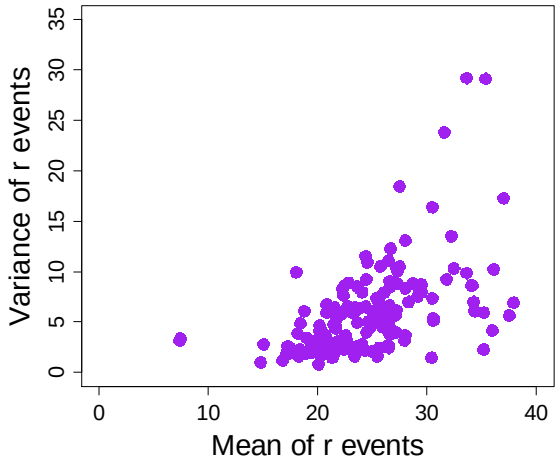

Figure 5-26 : Relationship between mean and variance of *r*-largest events for Armagh

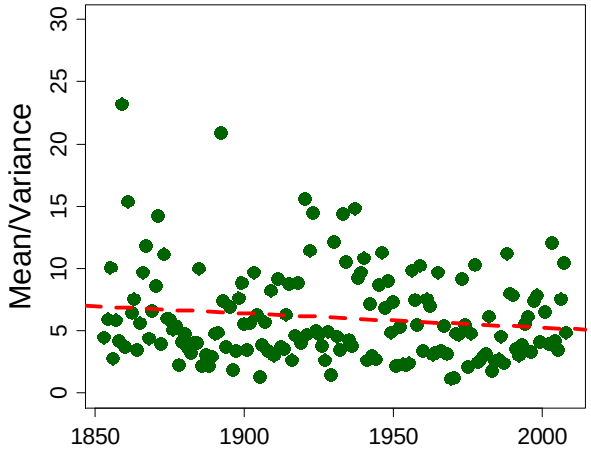

Figure 5-27 : Mean of *r*-largest totals divided by variance per year for Armagh

However, the spatial variability between gauges, as well as temporal variations, makes it difficult to interpret any patterns in the wettest day per year. There appears to be a general relationship between the r-largest events, whereby the range is greatest (least) in dry (wet) years and the events occur more (less) at random, but high temporal variability confuses this relationship. The differences from year to year make interpretation of the driving forces, whether atmospheric or seasonal, overly complex. It is believed that the method of wet days could be informative, but only once the most intense rainfall events have been fully characterised; therefore, other metrics of heavy and extreme rainfall will be examined. An alternative method to improve the GEV parameter estimates is examined in Chapter 6, while peak over threshold maxima are explored in Chapter 7. The exploratory data analyses carried out in this chapter have demonstrated that the r-largest statistical model, applied either to extreme value theory or more standard statistical analyses, is inappropriate for use in this project and so will not be employed in later chapters.

5.5 Summary

Data processing to develop a comprehensive set of daily rainfall observations was an iterative procedure, where initial quality control measures (in Chapter 4) were followed by exploratory data analyses to identify erroneous data. Tests for abrupt and gradual changes, or event randomness, highlighted remaining errors; some of these were rectified, while others identified the need to remove observation series from POT analyses. As a result, only 199 of the observation records are suitable for peak-over-threshold analyses; however all 223 AMAX series can be used as these were verifiable against other records.

Approximately half of the stations had no significant abrupt changes in the mean or the variance of the annual maxima series. Tests for gradual changes were insignificant, equated to a null trend, or identified a change after a significant change point towards the end of the observation record. The influence of identified change points will be minimised by regional pooling, a method to be used in later chapters (Hosking and Wallis, 1988), which permits all stations to be analysed without specific allowance for abrupt or gradual changes.

Exploration of various metrics of rainfall extremity established the most appropriate wet day threshold as ≥1mm for extreme events and a threshold of 95% ("very heavy") for POT analyses, to be able to characterise within year clustering. The method of volumetric quantiles was found to be unnecessarily restrictive and did not quantify frequency *and* intensity changes in extreme events, making it unsuitable for use in this project. Improvements in return period assessment using the r-largest events per year were highly variable across the stations examined and are minimal with comparison to the regionally pooled estimates explored in Chapter 6. The use of these events in a separate analysis to characterise the drivers and timing of annual Q95 events may have greater application in the future, but is overly complex for use in this project as the data include non-extreme events. Therefore, the r-largest event set will not be studied further within this thesis.

5.6 Computer Packages

The following packages were used in R for all analyses in this chapter: evd (Stephenson, 2002), fArma (Wuertz *et al.*, 2009), quantreg (Koenker, 2011), and tseries (Trapletti and Hornik, 2011).

Chapter Six Changes in Annual and Seasonal Maxima

"For the rain it raineth every day"

William Shakespeare, Twelfth Night V:i

Several notable floods in the UK in recent years have reinvigorated interest in estimating the probability of experiencing such events and whether it is possible to detect changes in the frequency (Pryor *et al.*, 2009; Stott and Trenberth, 2009) as anticipated from a changing hydrological cycle (Trenberth and Shea, 2005). Exploratory data analyses in Chapter 5 demonstrated that the simplest metrics of extremity, such as annual maxima (AMAX), combined with extreme value theory provide the most effective and readily interpretable method to assess such changes. While Chapter 3 showed that the most appropriate method to extrapolate annual maxima and estimate the return frequency of extreme events is the Generalized Extreme Value (GEV) distribution.

GEV models can be used to characterise seasonal or location specific changes in frequency or magnitude. For example, Maraun *et al.* (2009) represented UK seasonality through a multivariate GEV model with a simple sinusoidal component fitted to monthly rainfall maxima. In contrast, Fowler and Kilsby examined the implications of changes to extreme rainfall from both seasonal (2003a, henceforth FK2003a) and annual (2003b, henceforth FK2003b) event magnitudes using regional frequency analysis to fit a univariate GEV model. In common with other studies, FK2003a found a downward trend in estimated summer extreme rainfall magnitudes, particularly for 1-day events in Southeast England, and for the median seasonal maximum event (SMED). An increasing trend in estimated winter extreme rainfall magnitudes was apparent with the greatest increases in Scotland. However, in contrast with Osborn and Hulme (2002), limited change in winter extreme rainfall was apparent for England and Wales.

Changes in the seasonal occurrence of extreme rainfall events have had significant impacts on the food and drink industry in recent years with heavy rain damaging recently planted crops (Rosenzweig *et al.*, 2002), or droughts (an extreme absence of rain) occurring at unexpected times of the year, or an increased flood potential resulting from severe rainfall on either arid or saturated ground. Quantifying seasonal and regional differences in maximum rainfall behaviour, particularly being able to distinguish long term change from

natural variability, may inform those involved with adaptive action planning, from the individual farmer to the policy maker.

FK2003b used an approach based on L-moment ratios (Hosking and Wallis, 1997) to fit a GEV distribution to regionally pooled standardised AMAX data, and hence to estimate the regional rainfall growth curves for 1-, 2-, 5- and 10-day maxima. Decadal variability in the pooled AMAX was further examined using ten year moving windows and by fixed decades comparisons. It was concluded that several HadUKP regions have experienced changes, of differing scale and direction, in the magnitude of pooled extreme rainfall during the period 1961-2000. Notably, prolonged heavy rainfall events (5- or 10-days) increased in northern and western regions during the 1990s while the equivalent events decreased in magnitude in the south. It is now opportune to revisit the original work to update the analyses from 1961-2000 to 2009, and to compare the results with recent publications on UK extreme rainfall.

Here, changes in the estimated magnitude of events with specific return periods were also examined using the GEV distribution. GEV distribution curves were fitted to the 1-, 2-, 5- and 10-day seasonal and annual standardised pooled maxima using maximum likelihood estimates (MLE) of the parameters and estimated event magnitudes obtained by multiplying by the regional SMED or RMED. A comparison of the estimated GEV parameters obtained from MLE and L-moments confirmed that differences between estimates from each method are minor and well within the confidence intervals for data sets >50 years. Given the extended data set in use and the ease of calculation, it was decided to fit the GEV distribution using MLE; parameters estimated from MLE have also been found to minimise bias where strong multi-annual cycles are present (Rust, 2009). This differs from the previous work (FK2003b; FK2003a), where the L-moments of individual gauges were weighted to fit the regionally pooled GEV distributions.

Regional pools were assessed for homogeneity with the discordancy measure D_i (Hosking and Wallis, 1997) of each site in the region to ensure adequate similarity of the AMAX distribution in the pooling group. This was important as some stations have been added to the regions in this study which were not present in the previous assessments (FK2003b; FK2003a); furthermore, GIS based assessment of digital boundaries (Alexander

and Jones, 2000) identified some incorrectly allocated stations in FK2003a,b (Figure 6-1). The discordancy measure for site i, in a pool of size M, with $\mathbf{u}_i$ L-moment ratios is:

$$D_i = \frac{1}{3} M(\mathbf{u_i} - \mathbf{U})^T \mathbf{A}^{-1}(\mathbf{u_i} - \mathbf{U})$$

Equation 6-1

where $\mathbf{U}$ is a matrix of the mean L-moment ratios, $\mathbf{A}$ is a matrix of the variance in L-moment ratios and $\mathbf{A}^{-1}$ is the inverse of matrix $\mathbf{A}$. For a more detailed definition, refer to Robson (1999). A site was considered to be potentially group discordant when D_i was greater than D_{crit}, with $D = 3.0$ the critical value at the 10% significance level for a pooling group of $M \geq 15$ (after Hosking and Wallis, 1997).

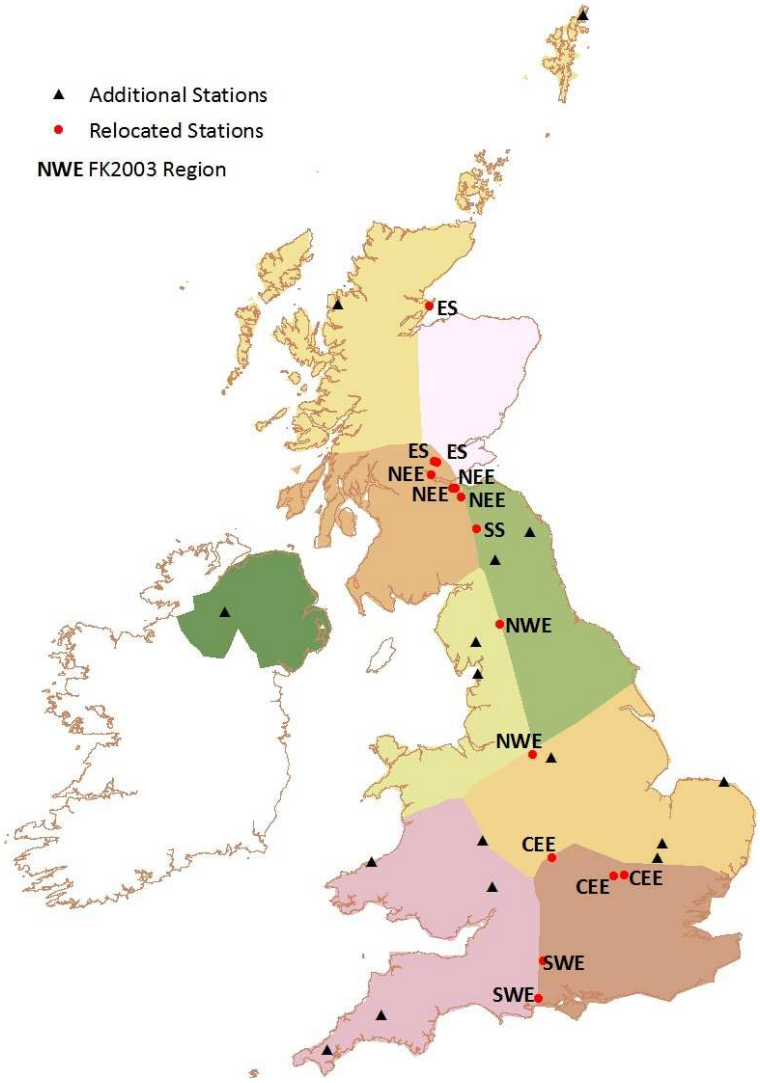

Figure 6-1 : Changes in station region in comparison with Fowler and Kilsby. Text denotes original regional allocation (FK2003b; FK2003a), red circles denote relocated stations, black triangles are additional stations

Two sites were found to have values of D_i greater than the critical value; these sites are reported in Table 6-1 together with the notable storms identified as the source of

discordancy. No changes were deemed necessary to NS as one exceptional storm does not necessarily indicate an intrinsic difference from the remainder of the pool. A GIS assessment suggested that Appleby Castle should be reallocated to NEE; however, the particularly high discordancy score recommended retaining this site within NWE where D_i dropped to 0.69.

Region	Gauge Name	Gauge Reference	Discordancy (D_i)	AMAX	Date
NS	Mull: White House of Aros	14162	3.6	70.1mm	27/03/1968
NWE	Appleby Castle	12936	4.11	79mm	24/07/1965
				61.8mm	10/08/2004

Table 6-1 : High values of discordancy measure (D_i) in the pooling regions

Regional Frequency Analysis (RFA) was then applied (Hosking and Wallis, 1997), standardising time series of individual gauge maxima by the gauge median (for 1961-1990) to remove orographic or exposure effects prior to pooling. Regional seasonal and annual medians (SMED and RMED, respectively) were calculated from the weighted mean of all gauges in the region, where individual stations were weighted according to record length to reflect the reliability of the relevant set of observations using Equation 4-1:

$$w_i = \frac{n_i}{\sum_{i=1}^{N} n_i}$$

Where w_i is the effective record length at the ith site, N the number of sites in the pooling group and n represents the number of station years.

Data were subdivided according to three different categories to examine potential changes in return level estimates and median values (annual and seasonal):

- Fixed decades (1961-1970, …, 1991-2000);
- Rolling decades (1961-1970, 1962-1971, …, 2000-2009);
- Datasets covering 1961-2000 and 1961-2009.

Examining the rolling decades enhances the resultant estimates within fixed decades by verifying that apparent changes are not merely artefacts of the selected time period. Method three allows a subjective assessment of the influence of recent maxima from 2000 to 2009 on the return period estimates. For clarity within the text, event estimates are identified with the numeric form (e.g. 5-day, 25-year) and analysis periods with the alphabetic form (e.g. ten year group).

Events considered for this study are the 1-, 2-, 5- and 10-day maximum daily totals per annum or season; return period estimates are calculated for an idealised set of 10-, 25-, 50- and 100-years for each of the fixed and rolling ten year groups, while acknowledging that estimates of 1:100 years are not necessarily reliable. Following the FEH rule of thumb (Faulkner, 1999), a dataset at least five times the length of the target return period (T) should be used in event estimation, thus T=100 exceeds the maximum valid estimate from a minimum pool of fifteen gauges for North Scotland in the period 2000-2009. Seasonal maxima and associated return period estimates were analysed using fixed seasons: Spring (MAM), Summer (JJA), Autumn (SON) and Winter (DJF).

6.1 Updated Annual and Seasonal Maxima

To determine the influence of additional data on the regionally pooled results, and identify any recent changes, the pooled standardised series were examined for differences from those produced by FK2003b before fitting the GEV as shown in Figure 6-2 for each event duration. Plotting positions, y, for the fitted distributions were determined from the Gringorten formulae (1963):

$$F_i = \frac{(i + 0.44)}{(N + 0.12)}$$
$$y = -ln(-ln(F_i))$$

Equation 6-2

where F_i is the non-exceedance probability, i the rank in ascending order and N, the number of pooled maxima.

Comparison of Figure 6-2 with FK2003b Figure 3 shows that most regions have higher extreme values of standardised annual maxima. Some of the increases in the extremes relate to annual maxima recorded during the period 1961-2000 at the nineteen supplementary gauges so preventing any direct comparison. However, several regions (CEE, NWE, NEE, SS and NS) have higher extremes resulting from recent events such as July 2007, affecting CEE and SWE with 147mm recorded over a 48-hour period at Pershore Agricultural College, September 2008 in NEE with 152mm in 48-hours at Morpeth and the UK record 24-hour total of 316.4mm recorded in Seathwaite, Cumbria in November 2009. An exception to this pattern is East Scotland, where the maxima values are now lower, arising from the re-allocation of Edinburgh Botanic Gardens to the South Scotland region; however, later results will show that the return period estimates have not been unduly influenced by this relocation.

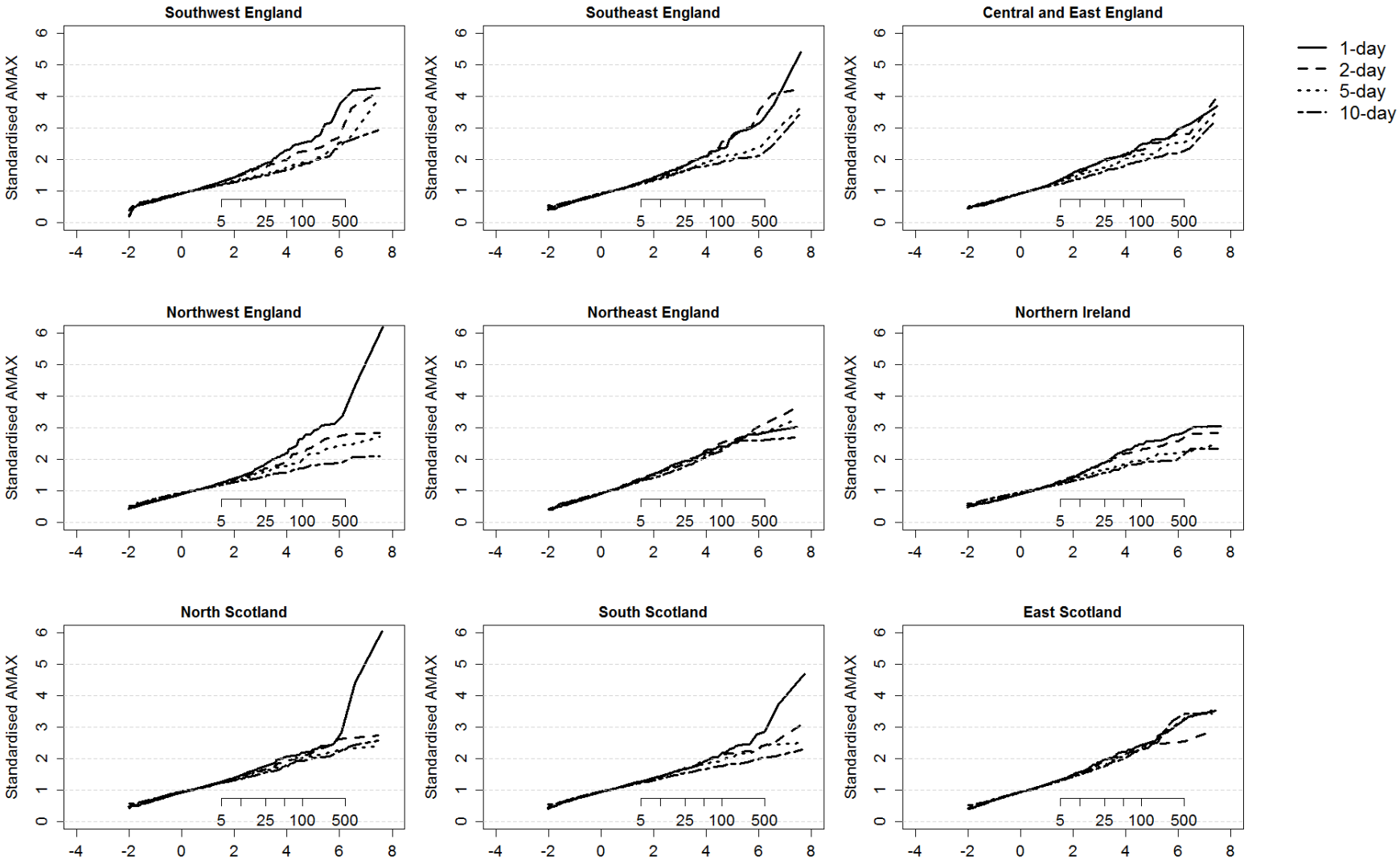

Figure 6-2 : Standardised regional annual maximum (AMAX) rainfall distributions 1961-2009 for the nine HadUK Precipitation pooling regions (from FK2003b, Figure 3)

The extra data for 2000-2009 have made most curves steeper, i.e. follow a Fréchet distribution, with the exception of Northeast England (NEE) and Northern Ireland (NI) where little change is observable. Very few significant monotonic linear trends were found in the annual maxima in Chapter 5, and none of >5mm in magnitude, in part because the data are highly variable. Before fitting GEV distributions, and to identify spatial or temporal patterns, a similar analysis was carried out on the mean regional RMED and SMED for rolling ten year periods (Figure 6-3 and 6-4). Rolling decade statistics were calculated from the first year of the ten year period analysed for the weighted regional mean 10-year median of the annual or seasonal maxima, the *x*-axis corresponds to the start year of each ten year period.

Other than NI and SEE, most regions exhibit a significant upward trend in RMED for all duration events, particularly in the north and west. South Scotland (SS) shows a significant increase of 0.75mm per year in median 10-day maxima, approximately 36mm over the period of record. Changes in SMED are more apparent in longer duration events (5- and 10-day) with significant increases across all regions in winter, again with the largest increases in SS. Spring and autumn SMED also appear to be increasing, although both the magnitude and the significance of the increase are weaker in the east; summer SMED is significantly decreasing in SEE.

Table 6-2 presents the magnitude per year of linear trends in each region, and their estimated significance in parentheses, for the regional RMED and SMED series. Trends were assessed using a two-tailed Mann-Kendall statistic, with a significance level of 5%, as rank based tests are more appropriate for non-normally distributed data (Yue and Pilon, 2004). The significance of trends in each region was also tested using a moving-block bootstrap (Efron and Tibshirani, 1993), of block length L=5, to establish the confidence intervals over each decade and reflect the relative decrease in data during the most recent decade (2000-2009). Despite the autocorrelation introduced by the rolling decade approach, the bootstrap technique did not alter the trend magnitudes or standard error estimates. Smaller trends in shorter duration events, although significant, equate to around 4mm over the period of record, and could arise from random atmospheric fluctuations (Benestad, 2003). In contrast, significant increases in winter rainfall, particularly in the longer durations, approximate 40-50mm over the period of record and could have severe implications for flood generation.

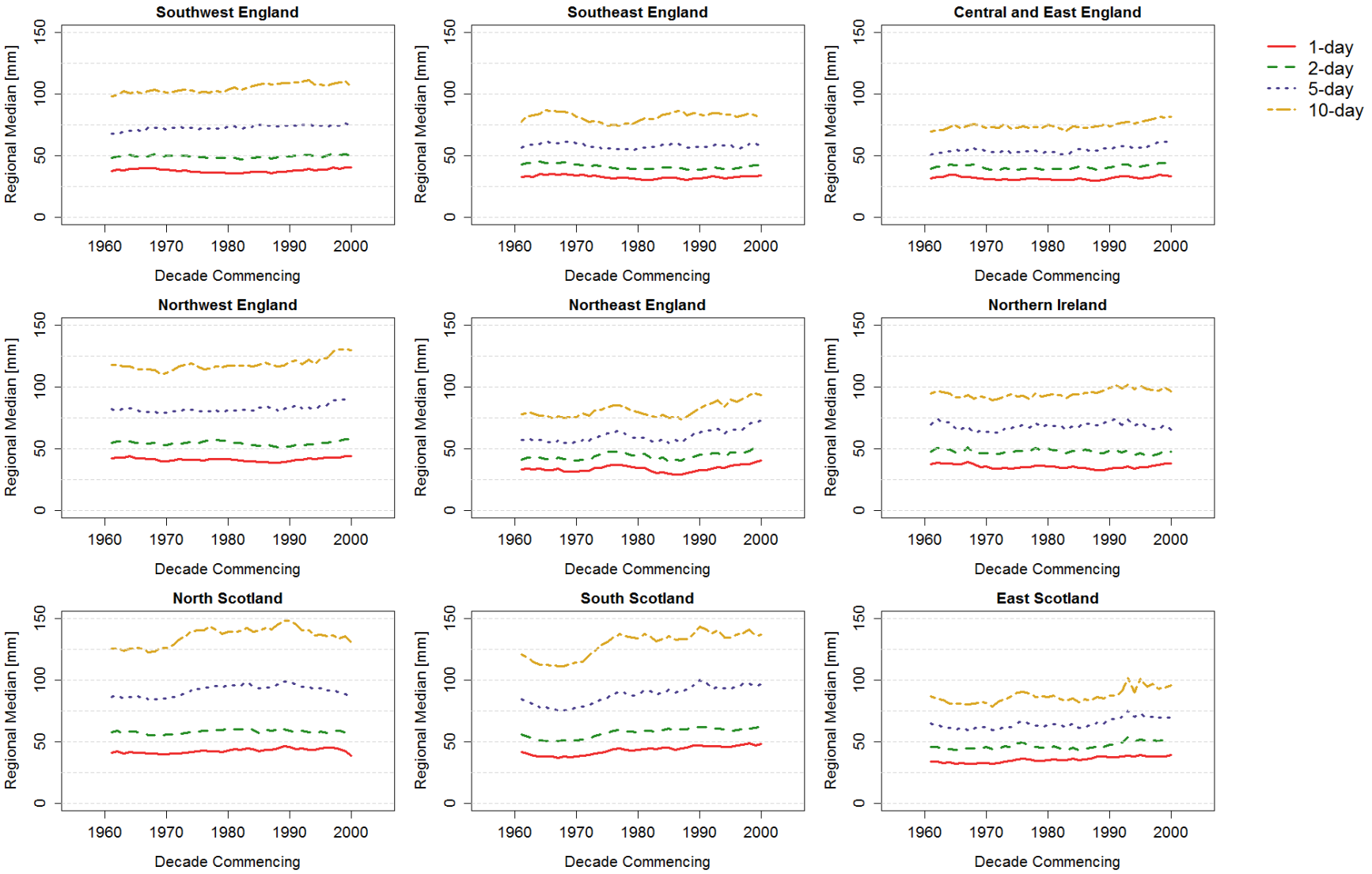

Figure 6-3 : Decadal mean Regional Median Annual Maxima (RMED)

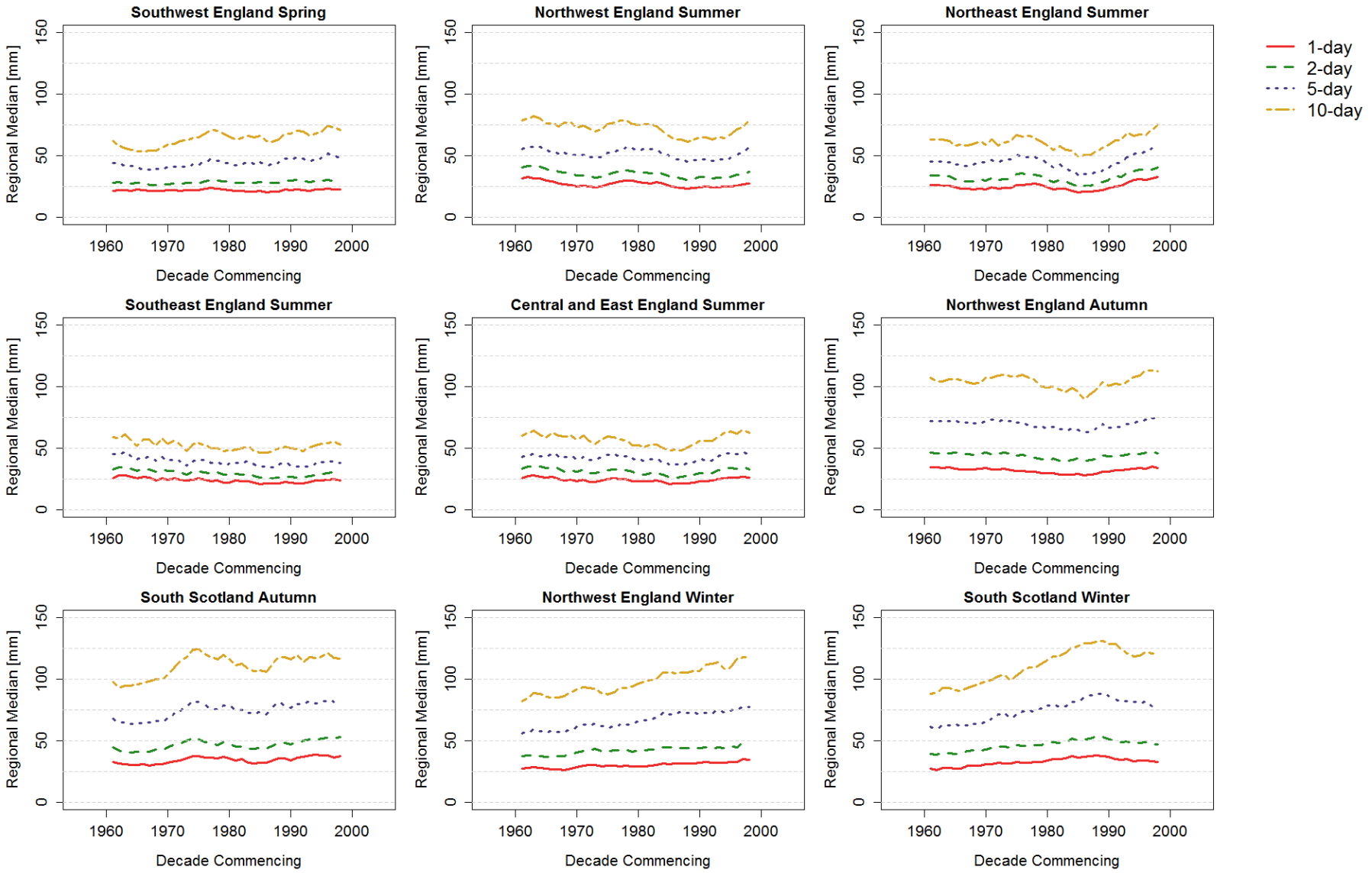

Figure 6-4 : Trends in the Regional Median Seasonal Maxima (SMED) for SWE in spring; NWE, NEE, SEE and CEE in summer; and NWE and SS in autumn and winter

Pooling Region	RMED mm/year	Spring mm/year	Summer mm/year	Autumn mm/year	Winter mm/year
(a) 1-day					
SWE	0.01 (0.66)	0.01 (0.13)	-0.07 (<0.01)	0.05 (<0.01)	0.08 (<0.01)
SEE	-0.05 (0.02)	0.01 (0.54)	-0.12 (<0.01)	0.04 (0.03)	0.09 (<0.01)
CEE	0.01 (0.78)	0.01 (0.45)	-0.05 (0.04)	0.1 (<0.01)	0.07 (<0.01)
NWE	0 (0.78)	0.02 (0.13)	-0.15 (<0.01)	-0.06 (0.01)	0.16 (<0.01)
NEE	0.08 (0.07)	-0.03 (0.29)	0.07 (0.57)	0.04 (0.13)	0.16 (<0.01)
NI	-0.05 (0.07)	0.06 (<0.01)	-0.11 (<0.01)	-0.02 (0.55)	0.07 (<0.01)
NS	0.1 (<0.01)	0.08 (<0.01)	-0.02 (0.28)	0 (0.35)	0.16 (<0.01)
SS	0.28 (<0.01)	0.16 (<0.01)	0.03 (0.15)	0.14 (<0.01)	0.23 (<0.01)
ES	0.18 (<0.01)	0.14 (<0.01)	0 (0.7)	0.16 (<0.01)	0.12 (<0.01)
(b) 2-day					
SWE	0.02 (0.38)	0.06 (<0.01)	-0.12 (<0.01)	0.1 (<0.01)	0.19 (<0.01)
SEE	-0.11 (<0.01)	0 (0.86)	-0.17 (<0.01)	0.01 (0.45)	0.19 (<0.01)
CEE	0.05 (0.03)	0.02 (0.52)	-0.08 (0.02)	0.11 (<0.01)	0.1 (<0.01)
NWE	-0.01 (0.6)	0.05 (0.01)	-0.19 (<0.01)	-0.07 (0.01)	0.23 (<0.01)
NEE	0.16 (<0.01)	-0.04 (0.25)	0.06 (0.7)	0.09 (0.04)	0.2 (<0.01)
NI	-0.04 (0.15)	0.09 (<0.01)	-0.09 (<0.01)	0.02 (0.92)	0.08 (<0.01)
NS	0.04 (0.1)	0.08 (<0.01)	-0.04 (0.16)	-0.04 (0.01)	0.22 (<0.01)
SS	0.29 (<0.01)	0.19 (<0.01)	0.04 (0.06)	0.21 (<0.01)	0.31 (<0.01)
ES	0.17 (<0.01)	0.21 (<0.01)	-0.07 (0.12)	0.22 (<0.01)	0.14 (0.04)
(c) 5-day					
SWE	0.14 (<0.01)	0.2 (<0.01)	-0.14 (<0.01)	0.29 (<0.01)	0.27 (<0.01)
SEE	-0.03 (0.41)	0.03 (0.62)	-0.21 (<0.01)	0.02 (0.38)	0.24 (<0.01)
CEE	0.16 (<0.01)	0.07 (0.05)	-0.04 (0.3)	0.14 (<0.01)	0.13 (<0.01)
NWE	0.18 (<0.01)	0.15 (<0.01)	-0.18 (<0.01)	-0.08 (0.05)	0.57 (<0.01)
NEE	0.3 (<0.01)	-0.01 (0.81)	0.08 (0.6)	0.19 (<0.01)	0.27 (<0.01)
NI	0.05 (0.17)	0.15 (<0.01)	-0.11 (<0.01)	0.09 (0.2)	0.13 (<0.01)
NS	0.21 (<0.01)	0.25 (<0.01)	0 (0.67)	-0.1 (0.05)	0.58 (<0.01)
SS	0.56 (<0.01)	0.3 (<0.01)	0.06 (0.2)	0.41 (<0.01)	0.69 (<0.01)
ES	0.26 (<0.01)	0.21 (<0.01)	-0.01 (1)	0.42 (<0.01)	0.22 (<0.01)
(d) 10-day					
SWE	0.26 (<0.01)	0.38 (<0.01)	-0.25 (<0.01)	0.34 (<0.01)	0.33 (<0.01)
SEE	0.04 (0.56)	0.1 (0.05)	-0.2 (<0.01)	0.06 (0.6)	0.23 (<0.01)
CEE	0.18 (<0.01)	0.15 (0.02)	-0.09 (0.04)	0.25 (<0.01)	0.13 (<0.01)
NWE	0.3 (<0.01)	0.24 (<0.01)	-0.36 (<0.01)	-0.03 (0.67)	0.89 (<0.01)
NEE	0.34 (<0.01)	-0.01 (0.86)	0.06 (0.65)	0.3 (<0.01)	0.37 (<0.01)
NI	0.19 (<0.01)	0.17 (0.03)	-0.05 (0.19)	0.17 (0.03)	0.13 (<0.01)
NS	0.39 (<0.01)	0.37 (<0.01)	-0.06 (0.2)	-0.2 (0.06)	1.01 (<0.01)
SS	0.75 (<0.01)	0.34 (<0.01)	0.03 (0.51)	0.56 (<0.01)	1.14 (<0.01)
ES	0.34 (<0.01)	0.31 (<0.01)	0.03 (0.36)	0.54 (<0.01)	0.25 (<0.01)

Table 6-2 : Magnitude per year of linear trends calculated with a block bootstrap, of mean decadal RMED and SMED by region over the period 1961-2009 for (a) 1-day; (b) 2-day; (c) 5-day; and (d) 10-day events. The significance measure is included in parentheses; values ≤0.025 are significant against a two-tailed Mann-Kendall test at the 5% level.

In common with FK2003a, and more recent research (Maraun *et al.*, 2009), a consistent increase in magnitude over 1961-2009 is evident in most regions for spring and autumn SMED, although the Mann-Kendall test results are only significant in northern regions. Contrasting results are apparent for the summer SMED, with the trend in some regions decreasing at first then increasing toward the end of the record (e.g. SEE, CEE) and, for others, showing overall increases (e.g. NEE). Recent summer events which have been particularly intense over southwest and central England (e.g. Boscastle 2004, Gloucester 2007) have probably influenced the rise at the end of the record in these regions. Mann-Kendall test results correspond to a significant decrease in short duration events in the summer in NI, SEE, SWE and NWE, with less conclusive results for longer durations and other regions. Winter SMED is, however, increasing, by varying amounts, most notably in NWE, NS and SS for long duration events.

Table 6-3 shows mean RMED values for each pooling region for fixed decades commencing in 1961-70. While the exact numbers differ from those published by FK2003b, the same behaviour is observed, with most regions experiencing an increase in RMED over the last two decades, particularly the north and west. The decade 1991-2000 was dominated by some exceptionally heavy long duration events, reflected by the higher rolling mean RMEDs in 5- and 10-day events. While the highest mean RMED for 10-day events generally occurred during 1991-2000, in most regions there has been a continuous increase since 1961-1970. Some of the changes in RMED are reflected in SMED values: peak short duration events in the south and east occur mostly during late summer and autumn, with the respective SMED matching RMED behaviour for these regions. By contrast, regions dominated by westerly weather, with the heaviest rainfall occurring over longer durations in the winter, are again commensurate with RMED increases.

Figure 6-5 indicates the typical seasonality of annual maxima events for 1- and 10-day duration events over the period 1961-2009. This illustrates how south-eastern areas are dominated by events in the summer (Rodda *et al.*, 2010), with 1-day events occurring later in the summer than 10-day. All other regions tend to experience short duration events (1-day) in late autumn, with little difference in timing between the regions. 10-day events have a wider range of occurrence month, ranging from late autumn to mid-winter, again with similar seasonality for all western and northern regions.

Pooling Region	1961-70	1971-80	1981-90	1991-2000	2001-09
(a) 1-day					
SWE	37.8	38.1	36.1	38.4	**40.8**
SEE	32.7	**34.6**	30.3	32.5	33.9
CEE	32.0	31.1	30.7	33.2	**33.4**
NWE	42.2	40.9	41.5	41.2	**44.1**
NEE	33.4	32.6	34.7	33.1	**40.9**
NI	37.8	34.3	36.0	34.9	**38.1**
NS	41.2	40.5	44.0	**44.3**	39.2
SS	42.0	38.7	44.4	46.7	**48.3**
ES	34.0	32.5	36.1	37.6	**39.3**
(b) 2-day					
SWE	48.5	49.9	48.4	**50.3**	50.1
SEE	43.2	**42.4**	39.7	39.6	42.1
CEE	39.5	38.6	39.7	41.8	**43.9**
NWE	54.8	54.6	54.8	53.4	**57.2**
NEE	41.5	41.0	46.1	45.4	**52.5**
NI	47.8	45.9	48.8	**49.0**	47.6
NS	57.9	56.3	**60.4**	57.7	57.9
SS	55.8	51.8	59.2	61.9	**62.5**
ES	46.1	44.3	46.9	47.8	**52.3**
(c) 5-day					
SWE	67.8	72.9	73.9	**74.4**	**74.4**
SEE	56.8	**59.6**	56.9	57.2	58.3
CEE	50.7	53.2	53.2	56.9	**61.3**
NWE	82.0	80.5	81.1	85.5	**90.3**
NEE	57.4	57.4	59.1	64.2	**72.8**
NI	70.0	63.1	68.5	**74.0**	65.6
NS	86.7	86.3	95.9	**96.8**	87.2
SS	84.7	78.6	92.4	**98.1**	96.7
ES	64.9	59.8	64.7	68.8	**70.2**
(d) 10-day					
SWE	98.3	101.9	105.3	**109.4**	106.1
SEE	77.6	79.7	80.4	**82.8**	80.2
CEE	69.8	73.3	74.1	75.9	**82.0**
NWE	117.7	113.6	117.3	121.4	**129.8**
NEE	78.2	78.6	78.2	85.9	**93.3**
NI	94.6	89.2	94.1	**101.3**	96.7
NS	125.7	128.5	139.6	**145.1**	130.5
SS	120.8	114.9	137.5	**141.1**	136.8
ES	87.3	78.8	87.6	87.4	**95.7**

Table 6-3 : Mean RMED per decade for the nine pooling regions for durations (a) 1-day; (b) 2-day; (c) 5-day; (d) 10-day. The highest value of decadal RMED is shown in bold for each case. (Update of FK2003b Table III)

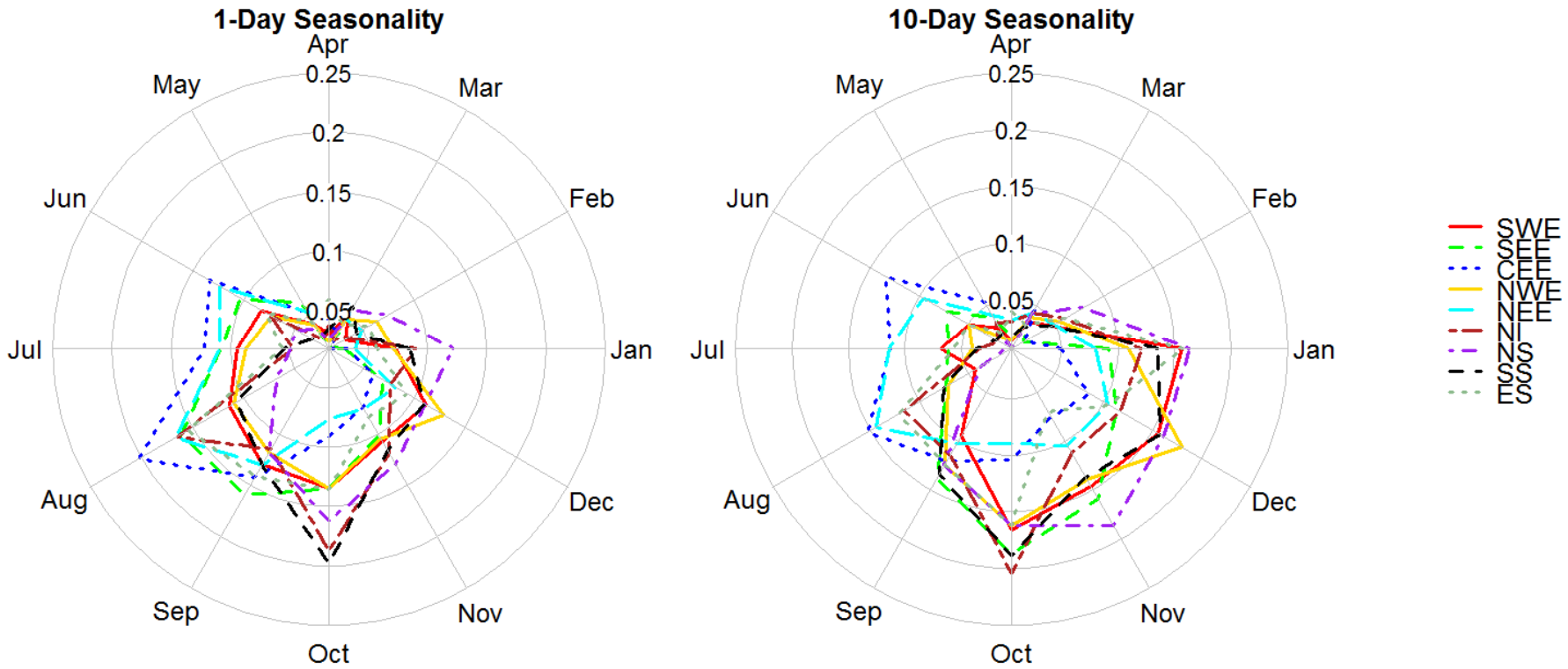

Figure 6-5 : Regional timing of extreme rainfall events over the period 1961-2009 from (a) 1-day annual maxima and (b) 10-day annual maxima. Months are arranged radially with event frequency on the horizontal axis.

The increases in a few regions in summer SMED, although statistically insignificant, contrast with climate model projections which suggest that the future climate is likely to bring hotter, drier summers (Murphy *et al.*, 2009; Hopkins *et al.*, 2010). However, the results presented above and later in this chapter are premised on seasonal maxima rather than seasonal mean rainfall and it is known that both Global and Regional Climate Models (GCM, RCM) are currently unable to simulate realistic short duration rainfall extremes, due to inadequate parameterisation of convective processes (Fowler and Ekström, 2009). Recently high resolution ($1.5km^2$) RCM have improved the spatial and temporal representation of convective rainfall, although the intensity is still over-estimated (Kendon *et al.*, 2012). The significant increases in winter SMED, especially within Scotland and more upland areas, may have arisen from less precipitation falling as snow (Jones and Conway, 1997).

6.2 Updated Return Period Estimates

6.2.1 Annual Maxima 1961-2009

Maximum Likelihood Estimates of the GEV parameters were calculated for each of the regionally pooled, standardised AMAX series together with standard error estimates. The fitted GEV curves for each region are very similar in shape and scale to those obtained by FK2003b; this emphasises that with a pool size greater than five, no individual station has a dominating influence on the final fitted distribution (Dales and Reed, 1989).

Figure 6-6 shows regional return period estimates obtained by multiplying the GEV curves by the regional RMEDs for the period 1961-2009 for each event duration. There is no coherent pattern in the differences with respect to region or event duration between Figure 5 in FK2003b (reproduced in Figure 6-7) and this update; most differences in estimated magnitude are within the confidence limits and are either attributable to natural variability or minor changes in pooling group. The SEE, NEE and ES regions present the greatest differences in return period estimates and growth curve shape. In SEE all fitted curves have become flatter, with the greatest decreases in the upper tail of 1- and 2-day storms. Similarly, fitted curves for NEE are flatter but with larger peak values for all duration events. FK2003b reported that ES had experienced very wet conditions during the late 1980s and 1990s. Recent events in East Scotland have not been as extreme and so had little influence on the return period estimates for this region; changes in station data do not appear to have affected the fitted distributions.

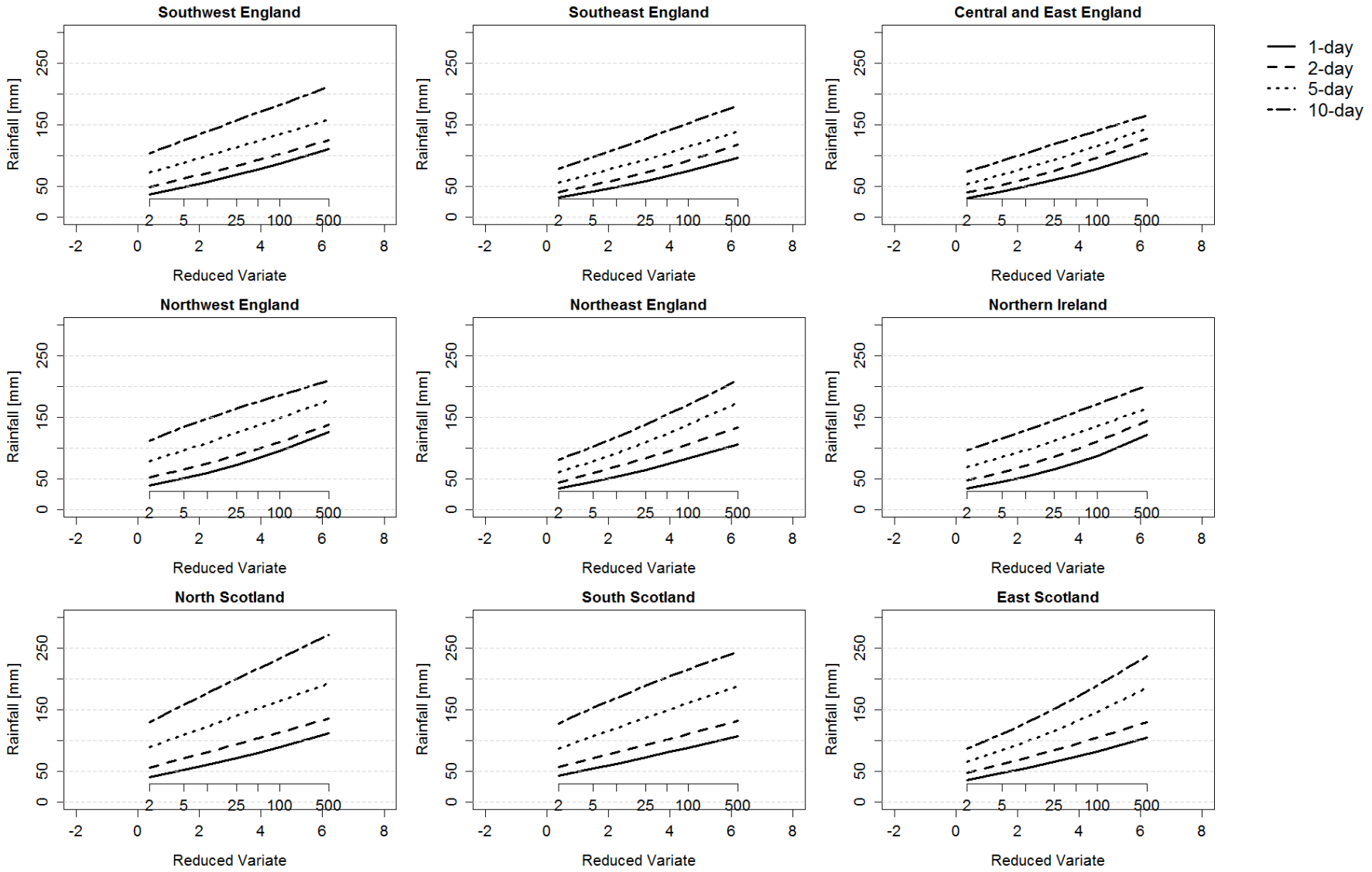

Figure 6-6 : Fitted annual maximum GEV distributions 1961-2009 (using regional mean RMEDs). Update of FK2003b Figure 5.

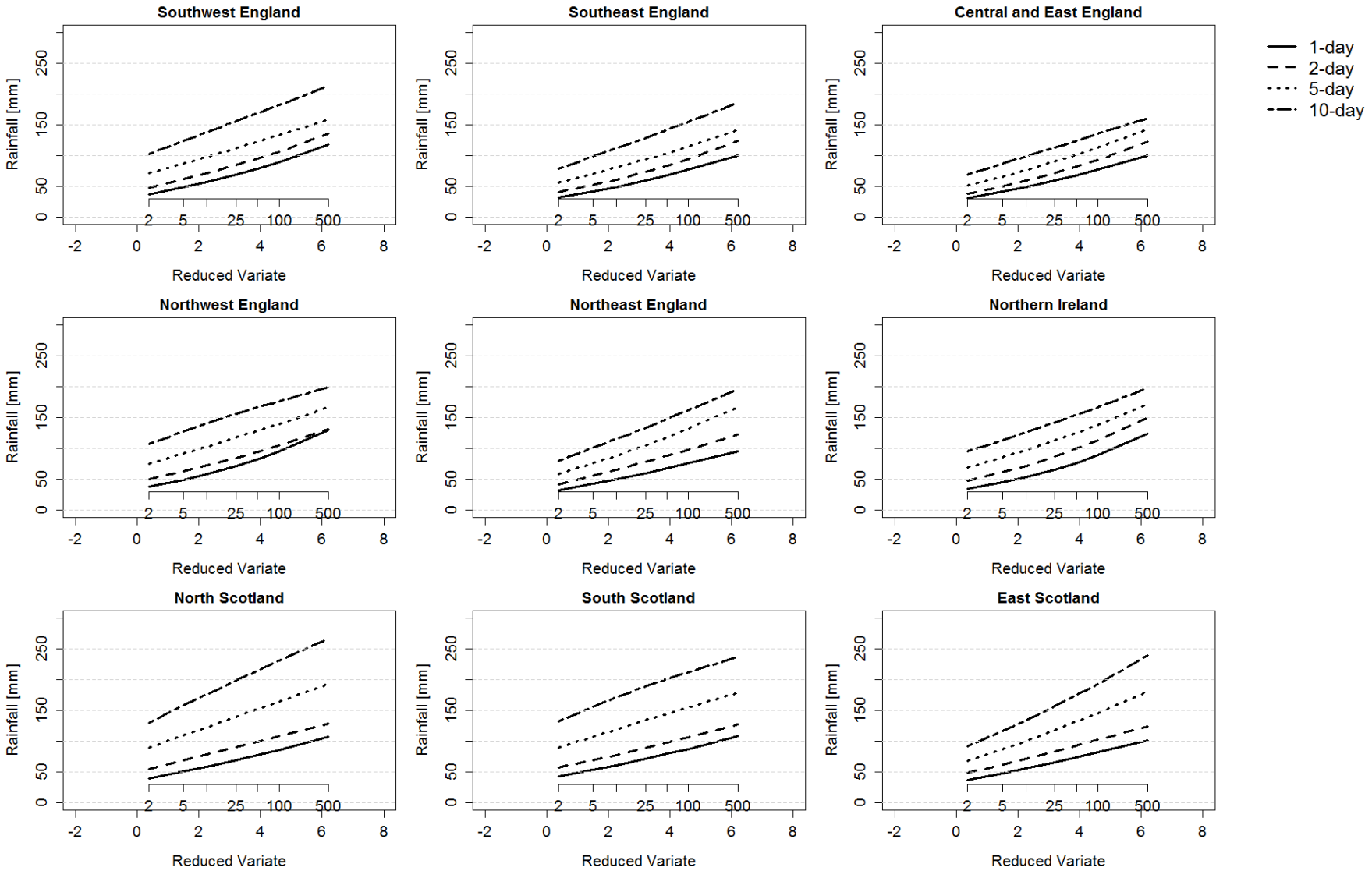

Figure 6-7 : FK2003b Figure 5 for comparison

6.2.2 Annual Maxima By Decade

Differences between FK2003b estimates and the 1961-2009 estimates were explored in greater depth using decadal analyses to ascertain whether these result from periodic fluctuations or are part of a longer term change in behaviour. Two approaches were adopted: fixed decades (years xxx1 to xxx0); and sliding ten year windows starting from 1961. The standardised AMAX for the i^{th} year of decade k, at site j (X_{ijk}) were calculated from the maximum rainfall for that year P_{ijk} and the decadal median AMAX for site j during decade k, $RMED_{jk}$, before fitting GEV distributions to regionally pooled series.

$$X_{ijk} = \frac{P_{ijk}}{RMED_{jk}}$$

Equation 6-3

The results of both analyses (Figure 6-8 and Figure 6-9) emphasise the variability between decades and the influence of exceptional years, confirming the need to use the largest dataset possible (Institute of Hydrology, 1999). A selection of regions and different event accumulations are plotted in Figures 6-8 and 6-9 which are representative of the northwest/southeast divide in regional results.

Five regions show notable increases in their rolling decadal return period estimates over the full analysis period (1961-2009): NWE, NEE, SS and ES. Some regions (e.g. NI, ES) have sharp changes which clearly indicate extreme events entering and leaving the decadal calculations. The same features are also evident in the fixed decade analyses, where growth curves for the decade around the extreme event are considerably higher than those for other decades and could, if examined in isolation, suggest a longer term change in behaviour. The most noticeable development for the last fixed decade (2001-2009) is that many significant differences between the growth curves observed for 1991-2000 are no longer significant, being nearer in magnitude to the estimates of previous decades. The variability is more prominent in north and west regions, which tend to be more responsive to weather systems over the North Atlantic and forcing from the North Atlantic Oscillation (NAO), which recently ended a prolonged positive phase (Hurrell and Deser, 2009). Other regions which display less contrast between the fixed decade estimates (e.g. SS) have much more noticeable increases when the rolling decade return period estimates are reviewed.

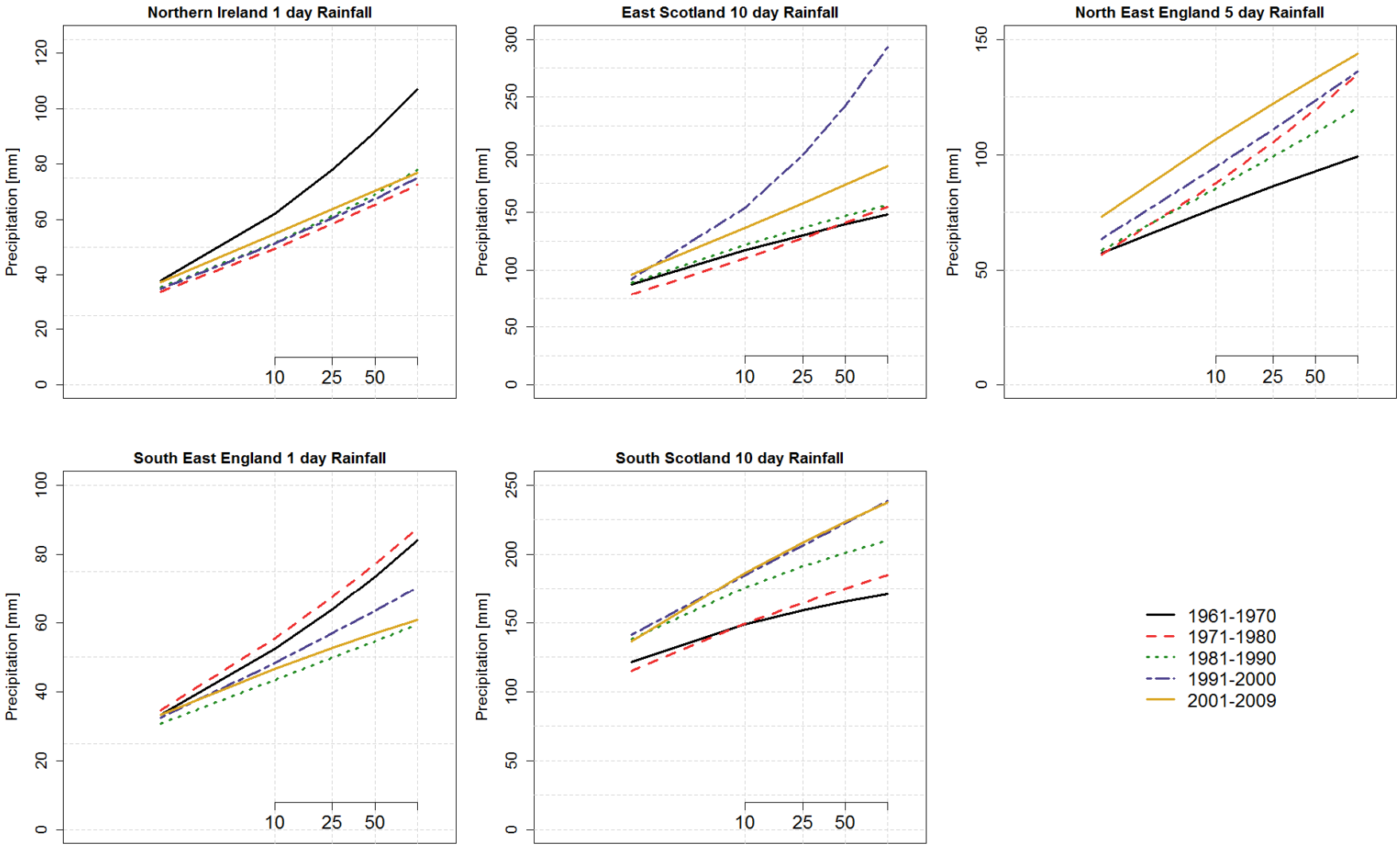

Figure 6-8 : Fixed decade changes in return period estimates using mean regional RMED: (a) NI region, 1-day; (b) ES region, 10-day; (c) NEE region, 5-day; (d) SEE region, 1-day; (e) SS region 10-day

Figure 6-9 : Rolling decadal return period estimates fitted for 1961-2009: (a) NI region, 1-day; (b) ES region, 10-day; (c) NEE region, 5-day; (d) SEE region, 1-day; (e) SS region 10-day

Fitted GEV curves for the SEE region were flatter in comparison to other regions for all durations, most notably for 1-day events. While the changes from decade to decade are small, the overall change in the 10-year event estimate since 1961 shows a significant decrease of approximately 15mm. The flatter growth curve is a result of lower skew (κ) in the data, i.e. the variance in event magnitudes is decreasing, although the mean value may be heavier for all maxima. This is also reflected in the rolling decadal analysis (Figure 6-9d) by a reducing interval between the magnitudes of return period estimates in each ten year period and an apparent downward trend in the magnitude of shorter duration events over 1961-2009.

The gradual increase in estimated event magnitude noted by FK2003b for 5- and 10-day rainfall in SS has continued into the most recent decade with a significant increase in magnitude. The magnitude of the estimated 100-year event (1% annual probability) in 1961-1970 has increased in frequency over the analysis period to approximately 10-years. Fixed decade curves, particularly for shorter duration events, are less informative and equally likely arise from natural variability and uncertainty in the distribution parameter estimates as from progressive increases since 1961 toward longer and heavier rainfall events. FK2003b noted a substantial steepening of the fitted GEV curves for 1991-2000 in all accumulations in ES, most particularly for the longer duration storms; with uncertainty limits clearly separated from all other decades. However, the curve for the 10-day event in the fifth decade, is representative of variability in all accumulations, and is considerably flatter representing more closely those of earlier decades (Figure 6-8). Changes in return period estimates for ES found by FK2003b are replicated here in the rolling decadal analysis, with a peak over the 1990s in 5- and 10-day events (related to the events of September 1995) but then declining over the last decade. Despite the recent decline, there is a significant upward trend both in the estimated range and magnitude of events, with return interval estimates increasing from 25-year (4% annual probability) to 10-year frequency. Figure 6-8 demonstrates that NEE fitted GEV distributions for fixed decades are progressively steeper since 1961-1970, although direct comparison between 1961-2000 and 1961-2009 indicates flatter curves for the longer period. Inspecting the rolling decade results shows that there has been an increase in the range of return period estimates over the whole record in NEE in addition to a significant upward trend with increases in estimated event magnitude for each return period ranging from 15mm (1-day) to 55mm (10-day) over the analysis period.

The results for NI are highly variable and reveal no conclusive changes in return period estimates. In this region, the 1- and 2-day events exhibit similar behaviour in the rolling decadal distribution estimates, with a step change in estimated magnitude at the end of the first decade (1961-1970) of around 20-30mm, before continuing to vary about a lower median. The pattern is not repeated in the 5- or 10-day event estimates, which peak later in the record; the longer duration events are more suggestive of a continuous increase in event magnitude over the full record period. The anomaly in shorter duration events is attributable to two wet years in 1968 and 1970 which have not been repeated; a widespread storm on 16 August 1970 was recorded at all gauges, with 110.5mm falling at Lough Mourne Reservoir.

Overall, the results from the rolling decadal analyses indicate increases in estimated return period magnitudes for all duration storms, particularly in the north and west as anticipated from the regional RMED results. Some regions, such as NI, are dominated by extremes which occurred within a particular decade and so the changes are less certain. The fixed return period estimates for all regions are also highly variable and dominated by exceptional events such as those of the late 1990s, as reported by FK2003b.

6.2.3 Seasonal Maxima

Seasonal return period estimates were examined in the same manner as the AMAX return period estimates. There is distinct decadal variability in the results, and some regions and seasons which were previously identified by FK2003a as showing significant increases do not show a continuation of this trend. In common with the increases in SMED, and supporting the findings of other research (Allan *et al.*, 2009; Hopkins *et al.*, 2010), the greatest increases in return period estimates appear in autumn and winter long duration events.

As few UK annual maxima occur during the spring months (Hand *et al.*, 2004) most studies of seasonal extremes have focussed on the common sources of serious flooding, that is heavy rainfall during winter or late summer and autumn months. However, FK2003a identified increases in spring extreme rainfall over the period 1961-2000 for short duration events around the UK, as well as in longer duration events in the north and west of the UK. Similarly, more recent work in the UK (Biggs and Atkinson, 2011) found that where the signal of change in spring maxima was previously weak or inconclusive, there is now evidence of long-term increases in the rainfall intensity. Estimated event magnitudes for the

10-year return period have marginally increased, for most accumulations, over the full record period in eastern regions as demonstrated in Figure 6-10. The trends are variable, with the largest significant increases in 5- and 10-day events, ranging between 5mm and 25mm for the 10-year return period, and fewer significant results than for other seasons arising from the high variability.

Recent UK observations suggest that mean summer rainfall has decreased in all regions, as has the percentage contribution of the heaviest events to total summer rainfall (Jenkins *et al.*, 2010). Similarly FK2003a reported that all durations of summer maxima consistently decreased in magnitude through the 1961-2000 period. SMED behaviour suggests that recent summer maxima and the resultant return period estimates have continued to decrease during 2000-2009 for most regions, with minor increases occurring in northern regions (NEE, SS, ES). With the exception of those regions, and in common with FK2003b, estimated return period magnitudes have significantly decreased in the south and east for longer duration events. Decreases of greater magnitude in the longer duration events are anticipated with increasing global mean temperature, as the limiting condition of available evaporable soil moisture will become an important factor (Allen *et al.*, 2002).

Burt and Ferranti (2010) found that the contribution of heavy events to total summer rainfall had increased in the northwest, corroborated here by an upward trend in estimated extreme rainfall event magnitude for 5- and 10-day durations in NI and SS. Other regional variations, such as increases in longer duration estimates in NEE and ES and little change in NS, are consistent with Perry (2006) who reported similar variability in total and maximum summer rainfall over the period 1914-2005 in approximately the same regions.

FK2003a found increases in autumn rainfall maxima across the country, a result supported by more recent work (Maraun et al., 2008; Biggs and Atkinson, 2011). Figure 6-11(a) demonstrates that the updated 25-year estimates for 10-day rainfall have a high degree of variability from decade to decade; with a significant increase in estimated event magnitude in all regions except NI, NWE and SEE. However, as the record for Northern Ireland is highly variable, with a corresponding irregularity in the estimated return periods, it is difficult to find convincing evidence of changing behaviour. In all other regions, there are increases in estimated event magnitude between the baseline period of 1961-1990 and the most recent results (Table 6-4); although some changes are persuasive they may appear

to be more significant due to the period of record examined (Chen and Grasby, 2009) as the 1960s were a period of low frequency and magnitude for extreme daily rainfall.

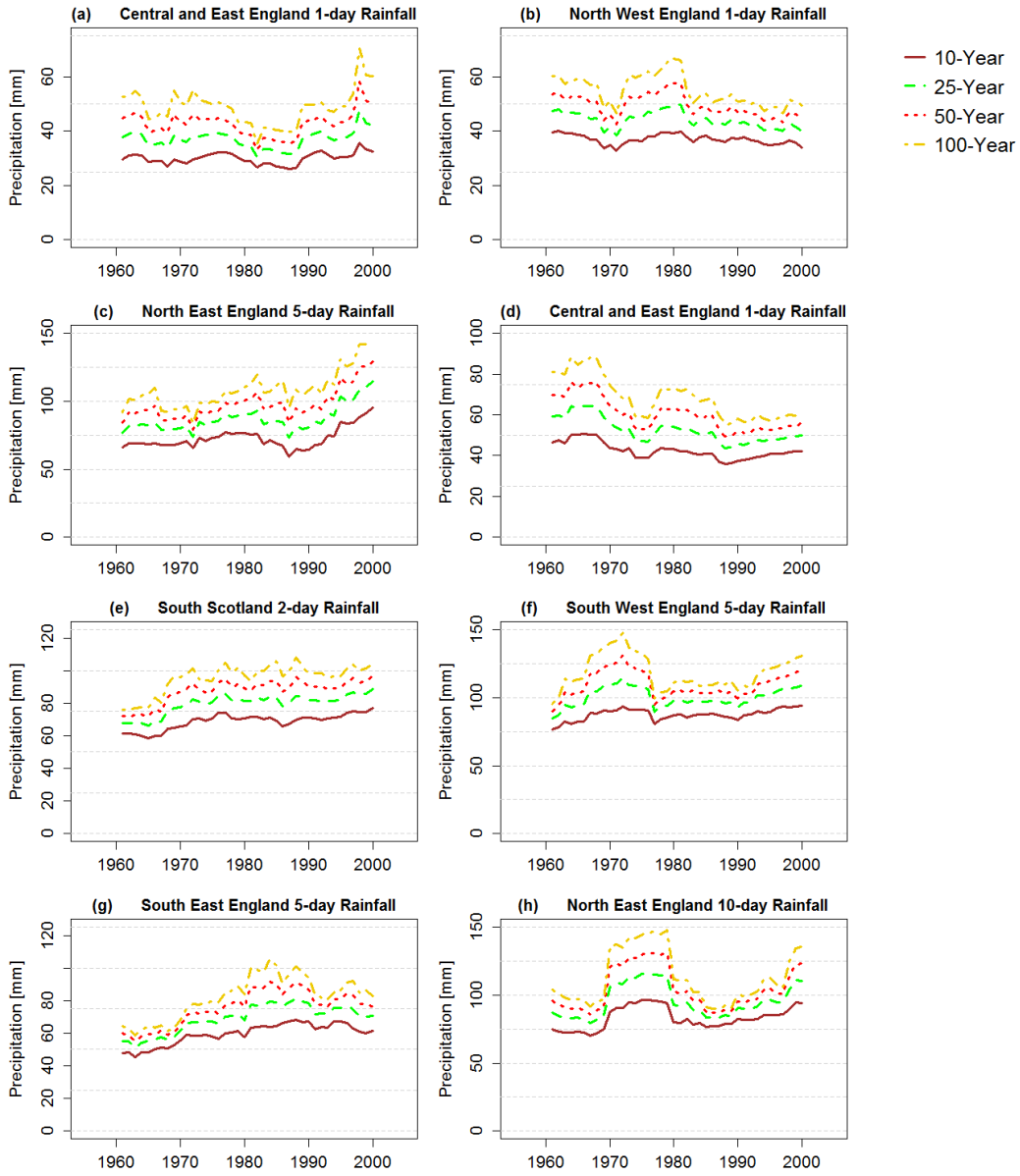

Figure 6-10 : Ten year rolling period return level estimates for 1961-2009 for Spring (a) CEE and (b) NWE regional 1-day; Summer (c) NEE 5-day, (d) CEE 1-day; Autumn (e) SS 2-day, (f) SWE 5-day; Winter (g) SEE 5-day, (h) NEE 10-day.

FK2003a identified spatially variable changes in winter extreme rainfall event magnitudes, with increases found in Scotland but little or no change found in England and Wales. Osborn and Hulme (2002), found that the proportion of rainfall from heavy events has increased during the winter season across the whole UK; this is supported for Northern Ireland and northern England by more recent research (Burt and Ferranti, 2010). Perry (2006) reported that, of all the UK regions, North Scotland experienced the largest percentage increase in winter rainfall in the period 1914-2004; increases in winter total

rainfall were also found in western parts of the UK. Future projections for winter, the season most reliably reproduced by Regional Climate Models (Fowler and Ekström, 2009), show estimated increases in magnitude of 15-30% across the UK for the 1-day 5-year event by 2070 (Fowler and Ekström, 2009). Similarly, the UK Climate Projections estimate a 50% probability of increases in both mean and wettest day winter rainfall in the order of 33% and 25%, respectively, for the medium emissions scenario (Murphy *et al.*, 2009).

Pooling region	Rainfall from the 10-year event (mm)			Rainfall from the 100-year event (mm)		
	1961-1970	2001-2009	Trend mm/year (significance)	1961-1970	2001-2009	Trend mm/year (significance)
(a) 2-day						
SWE	55.3	62.2	0.1 (<0.01)	74.6	95.5	0.1 (0.55)
SEE	59.9	52.5	-0.23 (0.01)	99.9	72.9	-0.78 (<0.01)
CEE	45.2	51.1	0.27 (<0.01)	67.5	84.7	0.72 (<0.01)
NWE	64.7	69.4	-0.05 (0.86)	87.7	99.3	-0.02 (0.81)
NEE	49.5	64.2	0.23 (<0.01)	66.5	111.5	0.49 (0.01)
NI	65.0	58.9	-0.05 (0.25)	102.8	94.3	-0.57 (<0.01)
NS	62.7	73.4	0.24 (<0.01)	80.2	103.4	0.57 (<0.01)
SS	61.4	77.2	0.33 (<0.01)	76.2	104.0	0.54 (<0.01)
ES	46.6	70.6	0.58 (<0.01)	61.2	111.9	1.06 (<0.01)
(b) 5-day						
SWE	76.4	94.0	0.2 (<0.01)	95.2	130.6	-0.04 (0.79)
SEE	77.0	75.9	-0.15 (0.04)	113.2	112.9	-0.26 (0.1)
CEE	58.0	67.0	0.32 (<0.01)	76.5	98.4	0.69 (<0.01)
NWE	98.3	104.6	0.02 (0.81)	134.1	144.6	0.18 (0.55)
NEE	68.9	84.9	0.43 (<0.01)	86.5	136.9	0.99 (<0.01)
NI	89.9	80.4	0.07 (0.55)	120.6	119.9	-0.12 (0.41)
NS	104.2	109.0	0.23 (<0.01)	134.8	150.9	0.83 (<0.01)
SS	95.6	114.6	0.8 (<0.01)	116.3	145.8	1.45 (<0.01)
ES	66.4	90.6	0.93 (<0.01)	84.2	129.4	2.02 (<0.01)

Table 6-4 : Change in the estimated magnitude of 10-year and 100-year autumn rainfall events for (a) 2-day and (b) 5-day durations for 1961-1970 and 2001-2009, with overall trend magnitude (and significance).

All regions exhibit a significant increase in estimated event intensity although with substantial inter-decadal variability, e.g. SWE. Figure 6-11(b). The increase is least apparent in short duration events in NI, CEE and NEE where summer rainfall maxima continue to dominate (Burt and Ferranti, 2010).

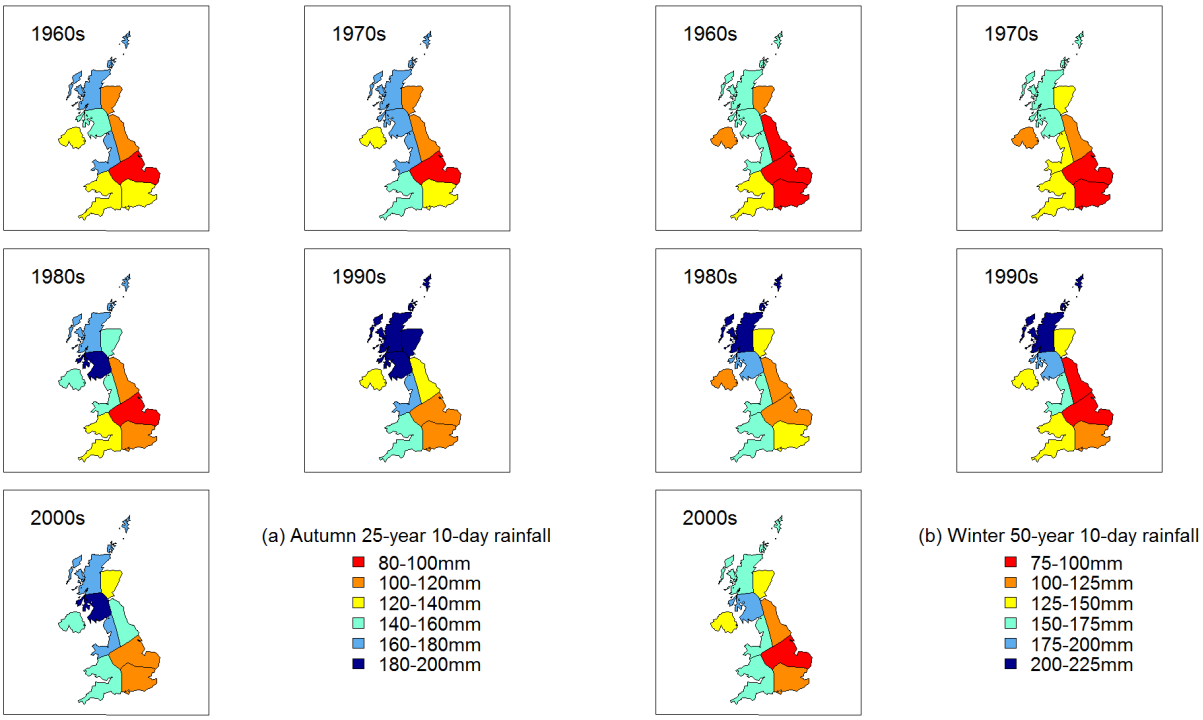

Figure 6-11: 10-day duration regional return period estimates from five decadal periods: (a) Autumn 25-year (4% probability); (b) Winter 50-year (2% probability)

Estimated changes in event magnitude for the 5- and 10-day 25-year return period events over the full record are reported in Table 6-5. With the exception of CEE and NI, where the changes are negligible, the results are supportive of previously observed increases in winter seasonal maxima, and consequent decreases in return period estimates.

Region	Change in 5-day magnitude (mm)		Change in 10-day magnitude (mm)		Estimated New Return Period
	mm/year	significance	mm/year	significance	
SWE	0.31	<0.01	0.68	<0.01	12-year
SEE	0.60	<0.01	0.91	<0.01	15-year
CEE	0.25	<0.01	0.29	<0.01	-
NWE	0.48	<0.01	0.74	<0.01	8-year
NEE	0.22	0.05	0.16	0.06	20-year
NI	0.35	<0.01	0.23	<0.01	-
NS	0.66	<0.01	1.03	<0.01	30-year
SS	1.28	<0.01	1.23	<0.01	8-year
ES	0.51	<0.01	0.37	<0.01	12-year

Table 6-5 : Trend magnitude per year and significance in estimated event magnitude for 25-year (4% probability) 5- and 10-day events in winter.

6.3 Discussion

It is always easy to determine the presence of a trend somewhere within a large data set, a phenomenon which increases in tandem with the length of record (Benestad, 2003); however, it is more difficult to discern a consistent signal of changes across multiple regions. By using several different approaches, it was possible to identify those periods of record which were exceptional, e.g. events in NI in the early 1960s, from those which may form part of a longer term change in behaviour. The influence of natural variability also made some previously clear trends (FK2003b; FK2003a) more ambiguous, e.g. winter in East Scotland. Burt and Ferranti (2010) examined the trends in heavy rainfall in several long duration records for 1900-2009 across the north of England, finding significant trends in maxima for some gauges but not for others. Regional frequency analysis has the advantage of removing the variability across a region (i.e. individual peaks from single point observations) and allowing greater certainty in magnitude estimates for high return period events by augmenting the record (Hosking and Wallis, 1993). This technique has been used to effect here to analyse regional behaviour rather than the individual station records.

UK daily and aggregated daily maxima were examined to determine whether the magnitude of extreme rainfall events has continued to evolve in the same manner presented in FK2003b and FK2003a. In some instances the perceived changes may be as much a factor of changes in the pooling group, due to station closure or change of operation, as climate change, natural climatic variability or uncertainty in the GEV parameter estimates. Significant changes in the decadal growth curves (FK2003b; FK2003a) contrast with some of those reported here where the differences between 2001-2009 and earlier decades are more muted.

Climatic variability has evidently played a major role in the decadal evolution of return period estimates, particularly evidenced by the changes in ES. FK2003b observed that the ES pooling region had experienced some notable storms during the 1990s, receiving 299% of the 1961-1990 average rainfall in September 1995 for example (FK2003b). Subsequent years have been drier, and the decadal median rainfall closer to that of the 1970s. This emphasises the importance of accounting for climatic variability over several decades, making it far harder to discern changes on shorter timescales (Chen and Grasby, 2009). Fowler and Kilsby (2002) also assessed the seasonal influence of the NAO on summer and

winter rainfall in Yorkshire, finding that the variability of rainfall during these seasons is greater during negative phases of the NAO. The NAO has been shown to have a significant impact on a decadal to multi-decadal scale on rainfall in the UK and mainland Europe (Allan et al., 2009), this seems to be a reasonable explanation for the changes in the curves in northern and western regions and will be examined in greater detail in subsequent chapters.

It could be argued that the use of fixed seasons for the analyses is not appropriate if, as reported, spring and autumn are becoming shorter in duration and so the associated seasonal maxima may not be captured. While regional differences are apparent from spring "commencing" over a period of weeks across the country, a fixed approach to the definition of seasons gives a benchmark against which to compare the maxima. Alternative approaches could include the use of rolling 30-day or 60-day maxima, or half yearly maxima which would ignore changes in spring and autumn; as spring maxima are rarely extreme (Hand *et al.*, 2004), the latter method might be appropriate. On the other hand, the timing and magnitude of heavy rainfall events is of great consequence to farmers as newly planted crops are more vulnerable to extreme rainfall (Rosenzweig *et al.*, 2002). Furthermore, several recent devastating UK floods have occurred during the autumn and would not be effectively captured by a 6-month approach. These considerations justify the use of shorter fixed seasons in this study, leading to an earlier awareness of potential changes in behaviour. Another method to encompass the seasonality of rainfall is to incorporate a seasonality index (Li *et al.*, 2011) based on the angular properties of the calendar day (Robson, 1999). This will be explored further in Chapter 7 in conjunction with peak-over-threshold maxima, to ascertain seasonal properties which have less dependence on fixed season definitions.

The upward trend in autumn maxima is of particular importance to flood defence practitioners and farmers as the timing of the events may have a considerable impact on harvests. The timing of autumn harvest and subsequent stubble burn in relation to extreme rainfall could also have major impacts on rural flooding by affecting surface runoff (Holman *et al.*, 2003). Summertime increases in event magnitude, particularly in a hotter, drier future climate, may have devastating impacts on future floods, particularly in regions with clay soils that are more sensitive to desiccation. Similarly, many sewers in the UK have a design

capacity of the 30-year event; increased urbanisation coupled with more intense rainfall will lead to increases in urban flooding. Even where flooding may not be an issue, the enhanced hydrological cycle will cause an increase in "first flush" pollution and so have a detrimental impact on river water quality.

There have been significant increases in annual maxima over the period 1961-2009, particularly in the west, confirming trends which were apparent but possibly insignificant in previously published work (FK2003b; FK2003a; Burt and Ferranti, 2010). Estimated return period frequencies for South Scotland have decreased over the period of record with events formerly having a 1% annual probability now having nearer to 10% probability of occurring. In East Scotland, estimated magnitudes for 5- and 10-day events are lower than those found by FK2003b, but there has been a sustained increase in magnitude over the full analysis period (1961-2009) and a decrease in return period estimates from a 25-year event (4% probability) to a 10-year event (10% probability).

Increases in the median seasonal maxima and the estimated return frequencies and magnitudes were found in the spring, autumn and winter seasons, emphasising the likely increase in northern latitudes of wetter conditions (Alexander *et al.*, 2006). Results for the median summer maxima, and resultant estimates of event magnitude, are variable across the country but, in general, point to an increase in the highest intensity events. This result is particularly pertinent in the light of recent summer flood events, which could be set to increase in frequency if the trend of high intensity rainfall preceded by prolonged dry spells persists. Understanding the link between the timing of very heavy rainfall and catchment runoff dynamics is likely to be beneficial to adaptation planners hoping to characterise likely developments in flood frequency (Wilby *et al.*, 2008), particularly as extreme impacts often arise from sequences of less severe events (Stephenson, 2008).

Methods to examine extreme rainfall can either quantify the changes in frequency of event and the relationship to total rainfall, or the changes in estimated event magnitude. The former, as employed by Burt and Ferranti (2010) and references therein, is statistically interesting and useful in assessing the likely insurance risk in a year. However, in adapting to the requirements of the future, practitioners require a quantifiable assessment of changes in both frequency and likely magnitude. The approach of this chapter in reviewing changes in seasonal maxima and the associated return period estimates begins to address this need,

but in concentrating on the maximum values neglects possible variations in within-year frequency. The next chapters will assess how best to examine the combination of magnitude and within-year frequency of extreme daily rainfall.

6.4 Computer Packages

The following computer packages were used for analyses in this chapter: ismev (Coles and Stephenson, 2009), evd (Stephenson, 2002), lmomco (Asquith, 2009), nsRFA (Viglione, 2011), boot (Canty and Ripley, 2011) and Kendall (McLeod, 2009).

Chapter Seven Analysis of Very Heavy Rain Day Characteristics

"And the rain it hammered down"

Nick Cave, The Carny

7.1 Introduction

The temporal and spatial distribution of heavy rainfall events are major drivers in flood development, particularly where such events are clustered around a river basin or over a sequence of days. The time-varying nature of extreme rainfall, whereby events arrive non-uniformly in time and with a high degree of reciprocity, is not often assessed despite the evident link to flooding (Li *et al.*, 2011). Having explored different extreme statistics, the aim of this chapter is to identify the characteristics of extreme 1-day rainfall which best explain the temporal variability of event frequency. A threshold exceedance model was adopted using *very heavy rainfall* (Q95) and *extremely heavy rainfall* (Q99), as outlined in Chapter 5 and defined by (Alexander *et al.*, 2006). The use of *very heavy rainfall* will be necessary to understand changes in the inter-arrival times of within-year rainfall events, as the higher threshold restricts the data to ≤1 event per year. However, the likely stimuli of extreme and very heavy rainfall frequency will be first determined using only *extremely heavy rainfall*.

While wet spells, a sequence of variable duration of consecutive wet days, are likely to have a greater influence on flood generation than individual days of rain, analyses were only carried out for single day events in this project. It is hoped that the analyses can be readily expanded to incorporate wet spells when an adequate measure of wet spell extremity can be defined. Appendix C.3 explores possible measures of wet spell intensity and relative wet spell extremity for adoption by such analyses. Individual events were considered to be independent when separated by an interval of consecutive days, of duration at least equal to the cluster index identified in Chapter 5 (Ferro and Segers, 2003), with rainfall below Q95.

The remainder of this chapter explores the seasonality of rainfall maxima to identify characteristics which can be used to define homogenous regions of extreme rainfall which are less spatially diverse than the Hadley UK Precipitation regions (HadUKP). Subsequently, the regional climatic influences on very heavy event occurrence and the interval between events, and recurrent short and long term patterns such as seasonality or inter-annual cycles, are examined in preparation for the development of statistical models in Chapter 8.

7.2 Seasonality

Individual analysis of the stations would be inefficient, yet a regional analysis using the HadUKP regions (Alexander and Jones, 2000) is inappropriate as these regions are spatially diverse and encompass several different extreme rainfall response patterns. A coherent grouping of the stations is required, for which typical characteristics which might identify regional similarities, such as the timing of extreme events, is also necessary. It is noted that the original development of the 5 England and Wales precipitation regions (Wigley *et al.*, 1984) used a principal component analysis of the mean rainfall characteristics (1861-1970) from only 55 observation stations, of which fewer than half were located in the region of interest. By using considerably more data, specifically directed at extreme daily rainfall characteristics, both the spatial coverage of the regions, and their applicability to analyses of the extremes, should be considerably enhanced.

Seasonal variability in the occurrence and intensity of UK rainfall is well recognised, with some regions known to receive the heaviest rainfall totals during the summer while others receive their largest daily totals later in the year. While seasonally driven extremes can be approximated by a sinusoidal form (Hyndman and Grunwald, 2000; Maraun *et al.*, 2009), the true distribution of extremely heavy rainfall is skewed non-uniformly towards the latter half of the year (Rodda *et al.*, 2009), with very few extremes occurring during mid to late spring, and one or two concentrated periods of peak activity. In contrast, the distribution of rainfall days tends to be skewed towards high event frequency over several winter months, with some regional differences particularly in western locations. The initial explorations, of all 199 stations, to identify extreme rainfall characteristics are illustrated by two typical stations, located in Figure 7-1; all analyses are repeated for the extreme rainfall regions in Section 7.4.

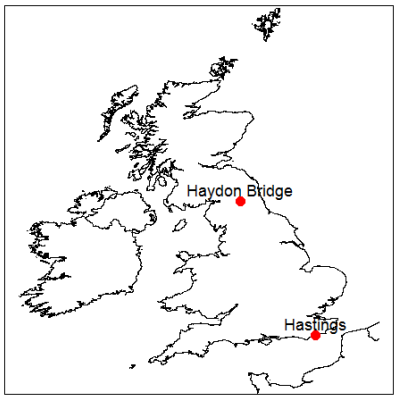

Figure 7-1 : Station locations for seasonal behaviour plots

The typical seasonality of extremely heavy rainfall per day of the year, compared with all days of rainfall, was calculated using a smoothed 30-day running mean of event frequency per day of the year. A smoothed running mean approach was adopted to account for natural chaotic behaviour, where the probability of rain on any given day follows a Poisson process which may vary from year to year in accordance with the prevailing climatic conditions (Cowpertwait *et al.*, 2002). Furthermore, as daily rainfall records are aggregated over a subjective period, the actual day of peak occurrence is somewhat arbitrary, dependent on the time of measurement (Stewart *et al.*, 1999).

Extremely wet day frequencies displayed the expected pattern of skewed distributions, with a high kurtosis, and centred approximately on the summer and early autumn months at all stations. Rodda *et al.* (2009) observed that the distribution of all extreme rain days, for the combined records of all UK stations, exhibit two peak periods – one in mid-summer and a second in late autumn. The combined records for all stations used in this project also displayed the same properties; however, there was considerable regional variation in the timing and extent of the peaks which is discussed in greater detail following the definition of the extreme rainfall regions. This seasonal variation in extreme rainfall occurrence is an important factor in understanding the clustering of heavy rainfall and will also assist in the definition of extreme behaviour regions.

Figure 7-2a shows the smoothed frequency per day of year of 1- and 5-day Q95 events for Haydon Bridge; this station has a relatively uniform distribution of days with rainfall throughout the year and a distinctive double peak in extremely wet event frequency, with the 5-day peak appearing to have greater emphasis in the winter months. The histogram is plotted with respect to 1st April to centre the peak period of activity. In contrast, Figure 7-2b plot for Hastings illustrates the high kurtosis and suggestion of a secondary event peak in early summer. However, Figure 7-2a was constructed from a record of only 50 years compared with that of Hastings (120 years) and so indicates higher variability in the smoothed daily frequency density. Both histograms are representative of all stations in the similarities of the timing and shape of the histograms for 1- and 5-day rainfall maxima. The seasonality of all days with rainfall differs considerably from that of the extreme events which tend to occur in conjunction with the seasonality of higher air temperatures.

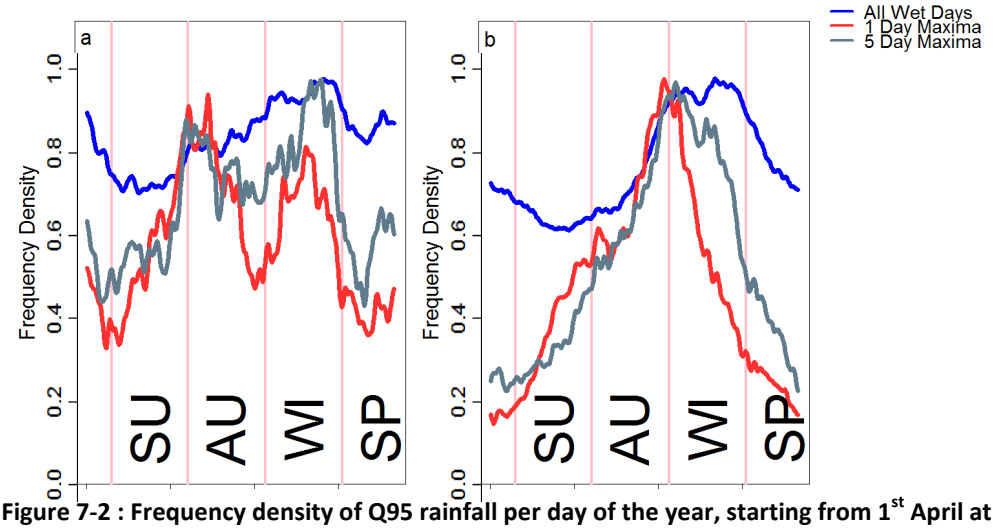

Figure 7-2 : Frequency density of Q95 rainfall per day of the year, starting from 1st April at (a) Haydon Bridge; and (b) Hastings SE England. Vertical lines indicate the first day of the season.

The long term evolution of seasonality was visualised with each Q95 event plotted by day (x-axis) and year (y-axis) of occurrence; a smoothed kernel surface was applied averaging over 20 years and 30 days to all 199 stations. Edge effects have been removed from the plots below, reducing the apparent record durations to 30 years and 100 years respectively; the same smoothing density was applied to each gauged record. The double peaks in event frequency at Haydon Bridge (Figure 7-3a) are highlighted by magenta bands in summer and winter, the single peak is highlighted in cyan in late autumn at Hastings (Figure 7-3b). Colour differences reflect the differences in rainfall frequency, with fewer events occurring in southeast England. There is also a suggestion of a long term evolution in seasonality, e.g. with Haydon Bridge now receiving more peak events later in the year. Similar patterns of shifting seasonality were also observed at many other stations, with respect to geographical distribution and different dependence on atmospheric oscillations.

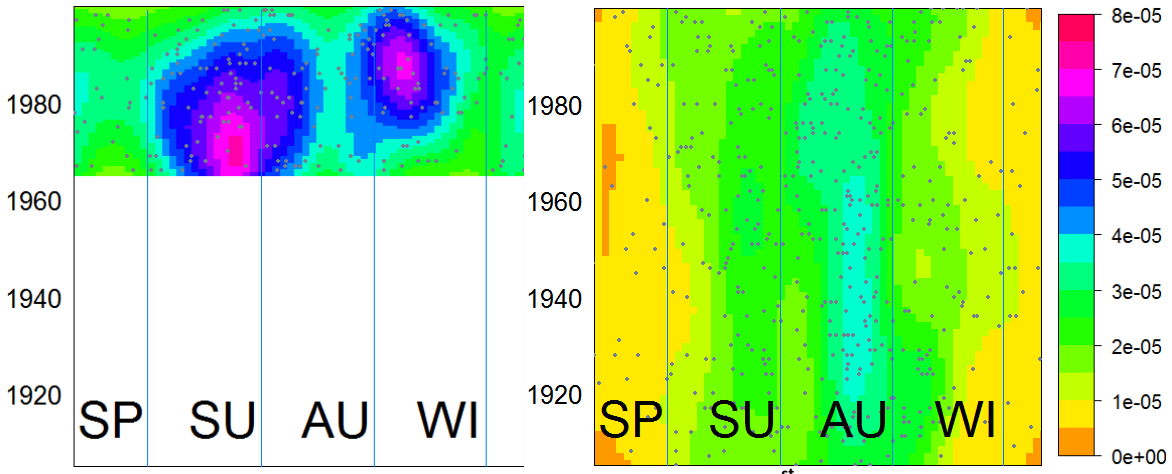

Figure 7-3 : Evolution of Q95 event occurrence by day of year from 1st April at (a) Haydon Bridge; and (b) Hastings. Grey dots represent event occurrence, coloured surface ranges from orange to red representing frequency of events within a 30 day and 20 year centred smooth.

It is evident from the above plots that extremely heavy rainfall events do not occur uniformly throughout the year, and have considerable regional variation arising from their relative dependence on the North Atlantic Oscillation or Sea Surface Temperatures; there is a marked period during the year in which events are more likely to cluster in time. However, many statistical analyses of extremes neglect seasonal irregularity and persistence as important generating processes for extreme behaviour (Stephenson, 2008). Dot plots of the evolution of events by day of year for the longer duration observation records (>75 years) demonstrate a time varying quality and are suggestive of changes in seasonal timing, which requires closer enquiry.

While seasonality is readily visualised in a horizontal manner with the calendar day approach, as above, comparisons between years and seasons may benefit from a rotational approach (Robson, 1999), refer to Appendix B.6. The most frequent day of heavy rainfall occurrence, $\bar{\theta}$, was calculated for all stations for use in the definition of extreme regions. All stations had a value of $\bar{\theta}$ approximately equal to the calendar day of the highest event frequency density typified in Figure 7-2; the seasonality vector, $\bar{r}$, was calculated from the vector components of $\bar{\theta}$. Stations such as Haydon Bridge, with two seasonal periods of peak event frequency, had low $\bar{r}$ values, indicating dispersion throughout the year; stations with one seasonal period had $\bar{r} \to 1$.

7.3 Extreme rainfall regions

The HadUKP regions outlined in Chapter 4 are effective for describing mean daily rainfall behaviour and responses to the typical weather systems which act over these general areas. However, they were developed using statistics of mean daily rainfall, and are not fully representative of sub-scale variations in extreme rainfall frequency, magnitude and seasonality. Some regions such as North West England and South West England combine several areas with very different extreme rainfall responses. More detailed regional rainfall classifications have been developed for several different applications (Bonell and Sumner, 1992; Hossell *et al.*, 2003; Neal and Phillips, 2009), using a principal component analysis of daily rainfall. However, as with the HadUKP regions, these would still require manipulation to reflect the different behaviour of extreme rainfall within each sub-division (Macdonald *et al.*, 2010) as all relate to mean behaviour.

An approach which has been used previously with success to determine the orographic and weather driven influences on extreme rainfall is to incorporate these parameters as covariates within the estimates of the extreme value distribution (Cooley *et al.*, 2007). Figure 7-4 visualises the Generalized Extreme Value distribution location parameter at each station estimated using the latitude, longitude and elevation as covariates. It is possible to pick out some of the major orographic features of the UK, including the Highlands, the Lake District and Snowdonia as well as very low areas within East Anglia. As this approach forces each station to be analysed individually, resulting in overly complex models based on limited data, it is considered that specifically defined extreme regions would be more beneficial to enable regional data pooling and enhance estimates of event frequency and magnitude.

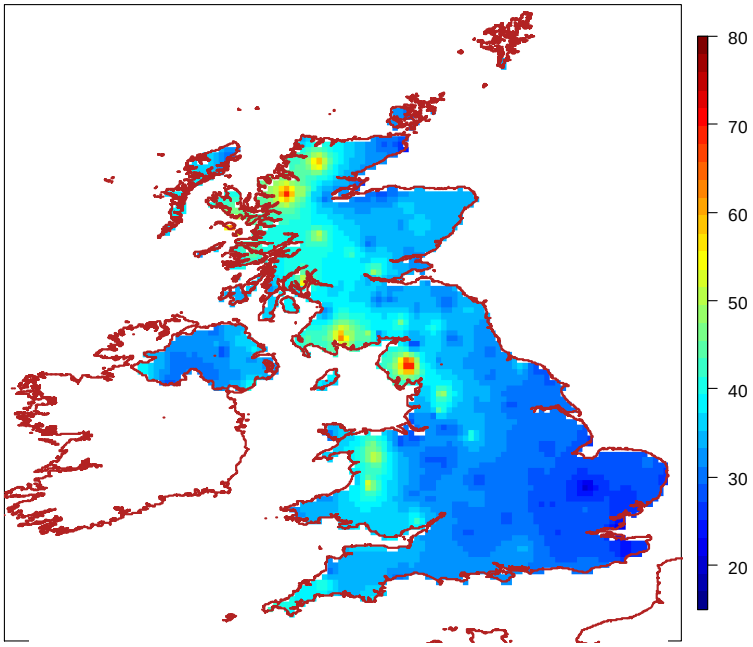

Figure 7-4 : Estimates of Location Parameter for the GEV linking elevation, longitude and latitude

Dales and Reed (1989) devised a set of extreme regions from subjectively clustering stations according to GEV distribution characteristics, RBAR (mean of annual maxima from the Flood Studies Report) and coefficient of variance. Their initial selection of regions, taken from Jackson and Larke (1974), was subdivided throughout England to reflect real differences in extreme rainfall patterns; although they acknowledged that the Wales, Scotland and Northern Ireland regions require further delineation. Applying these regional divisions to the current data set demonstrated that the groupings are inadequate with excessive sub-division in some regions, and large grouping in others, resulting in poor representation of extreme rainfall

seasonal responses. As a result, it was decided to classify daily rainfall regions from measures of extreme rainfall intensity, frequency, climatological behaviour and seasonality.

7.3.1 Principal Component Analysis

Following the approaches used by others to create regional divisions (Wigley *et al.*, 1984; Dales and Reed, 1989; Phillips and McGregor, 2002; Hossell *et al.*, 2003), a set of extreme rainfall parameters were investigated to identify the most descriptive variables which accounted for climatological influences and topographical differences without duplication. The final selection of variables (Table 7-1) was used in a principal component analysis (PCA) to classify regions with coherent behaviour. It was considered important to include various measures of seasonality to replicate the frequency of summer and winter events; the data skewness, in combination with GPD parameters, reflect responses to typical atmospheric systems (such as winter driven North Atlantic fronts) as well as the station aspect and elevation.

Variable Name	Description	Calculation
sigmahat	Shape parameter, $\hat{\sigma}$	Generalized Pareto Distribution (GPD) fitted to 99th Quantile of daily station rainfall maxima
ksi	Scale parameter, ξ	
sintheta	Angular seasonality	Rotational statistics applied to 99th Quantile of daily station rainfall maxima
costheta		
$rbar_{se}$	Seasonality vector	
g1	Skewness	Skew of individual station annual maxima
RMED	Median	Median of individual station annual maxima
R20sum	Event count	Number of summer events >20mm (May-August) 1961-1990
R20win	Event count	Number of winter events >20mm (October-March) 1961-1990
RWIN	Mean	Mean winter daily rainfall, for rainfall days ≥1mm
z	Elevation	Station elevation

Table 7-1 : Rainfall variables used in Principal Component Analysis for Extreme Regions

Excesses over the 99% wet day quantile (Q99) were adopted in preference to annual maxima to maximise the data used, and a Generalized Pareto Distribution was fitted at each station. The seasonality rotational statistics were derived from Q99 calendar days of occurrence. Neither the Q99 threshold or RBAR (as Dales and Reed, 1989) were used in the final set as these both replicate information from the fitted GPD and are too similar to the

AMAX. Maps of each of the main rainfall measures and $\hat{\sigma}$ estimates are depicted in Figure 7-5; ξ is not shown as it cannot be estimated with any accuracy and presented little regional coherence. The seasonality measures highlight the tendency for higher altitude regions to receive their maximum rainfall during the winter, and lower lying locations in the summer, while the midlands have far less distinctive seasonality (Rodda *et al.*, 2010).

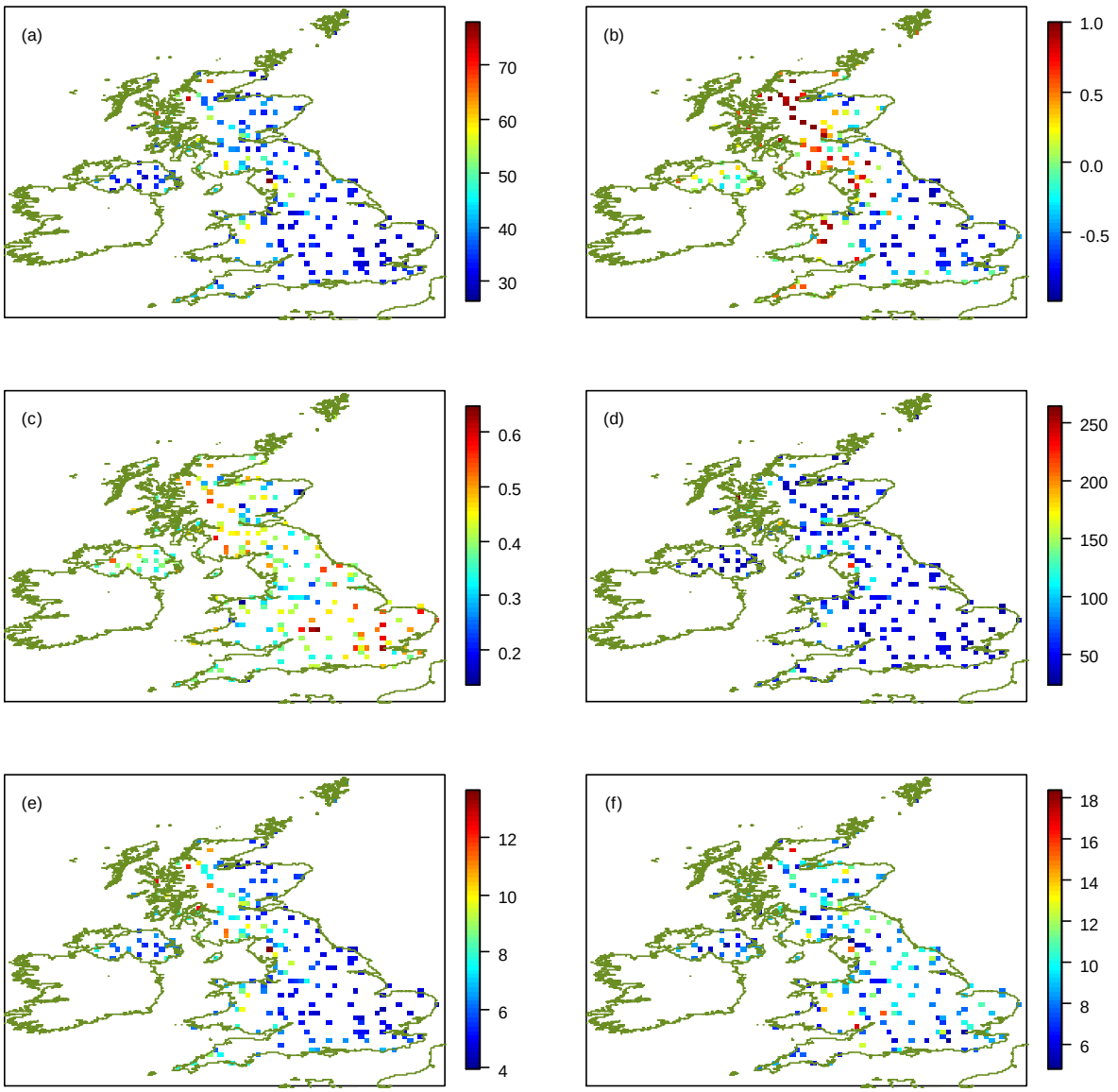

Figure 7-5 : Some measures of extreme rainfall used in a principal component analysis (a) RMED; (b) Rotational measure of day of event (c) Coherence of seasonality; (d) Count of summer days >20mm; (e) Mean winter wet day value; (f) Fitted GPD scale parameter.

Several combinations of the measures in Table 7-1 were assessed with PCA, using a minimum of four parameters (Jolliffe, 1973), eventually selecting all parameters as the most descriptive of extreme rainfall behaviour. Identifying the most appropriate number of principal components is largely subjective, based on scree plots (Figure 7-6) or a rule-of-thumb approach such as selection of components with eigenvalues >1 (Kaiser, 1960) or

eigenvalues >0.7 (Jolliffe, 1972), or the number of components required to explain some percentage of the data variance. All tests were examined and these suggested use of the first three or four components.

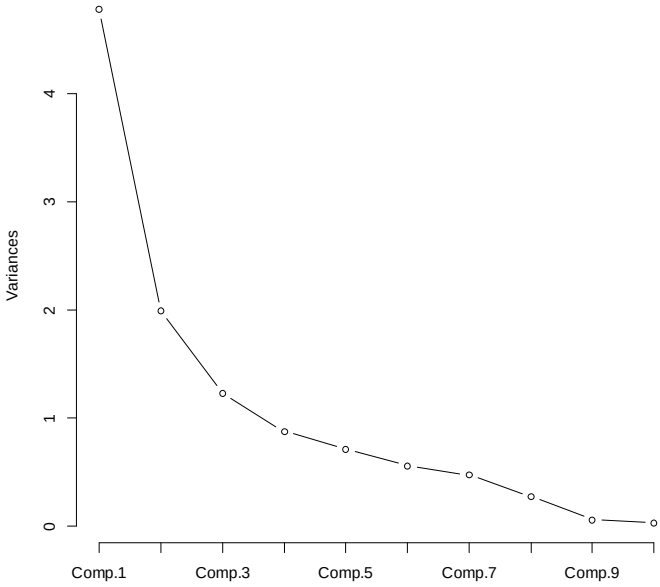

Figure 7-6 : Scree plot of principal components

The first three components explain 72.6% of the data variance, increasing to 80.1% with the fourth component; while the first three eigenvalues all exceed 1, the fourth is 0.88. Table 7-2 indicates the loadings of each variable for each of the first four components, with the two absolute largest values highlighted in bold. The first principal component (PC1) relates to the magnitude of the maxima, and the relative regional wetness or response to atmospheric circulation patterns. PC2 is more focussed on the extreme value distribution behaviour, such as skew and variability in event magnitude; PC3 describes the seasonality of events; PC4 is somewhat ambiguous but appears to describe the response to location, topography and station aspect or exposure. The smoothed scores for the first three principal components are shown in Figure 7-7.

K-means cluster analysis (Hartigan and Wong, 1979) was applied to the retained components to identify coherent groupings of the components and, thus, the stations within each region. Sensitivity testing determined that the first three principal components produced the most comprehensive regional partitioning with least randomly displaced members from the main groups. Use of only the first three components also tallies with the scree plots and eigenvalue criteria (Kaiser, 1960). A drawback of *k-means* clustering is that the optimum number of clusters must be defined by the analyst, which can be problematic

if the value is not known *a priori* (Wilks, 2005). Clusters were examined for groups between 11 < k < 20, as a minimum requirement of the regional definition is to enhance those represented by HadUKP whilst avoiding excessive sub-division.

Measure	PC1	PC2	PC3	PC4
sigmahat	0.241	**0.488**		0.188
ksi		**-0.533**	-0.385	-0.232
z	0.198		0.252	**-0.807**
sintheta	0.187	0.314	**-0.476**	
costheta	0.337	-0.232	0.176	
$rbar_{se}$		0.243	**-0.665**	-0.293
g		-0.466	-0.276	**0.342**
R20sum	0.400			0.158
R20win	**0.442**	-0.101		
RMED	**0.444**			
RWIN	0.436	-0.161		
Proportional Contribution	*0.43*	*0.18*	*0.11*	*0.08*

Table 7-2 : Loadings of each variable within the first four principal components and proportional contribution (in italic) to the variance. Bold type indicates most significant contributing variable.

Cluster analysis applies a random partitioning of the selected data, in this case the station principal component scores, centred on the initial latitude and longitude seed positions. Algorithms iterate to a solution with the smallest distance between the cluster centroid and the group members. An advantage of clustering by group means over hierarchical methods is that cluster members can be reallocated to more relevant clusters throughout the process. In common with other climatic clustering analyses, it was found that increasing the number of clusters fragmented the smaller regions rather than arriving at a more comprehensive partitioning of all stations (Corte-Real *et al.*, 1998; Blenkinsop *et al.*, 2008; Raziei *et al.*, 2011). Examination of the within sum of squares, and between sum of squares statistics for each cluster suggested an optimum partitioning of between 13 and 16 clusters; closer examination of these revealed that some of the smaller clusters could be combined, arriving at a final solution of 14 UK extreme rainfall regions shown in Figure 7-8.

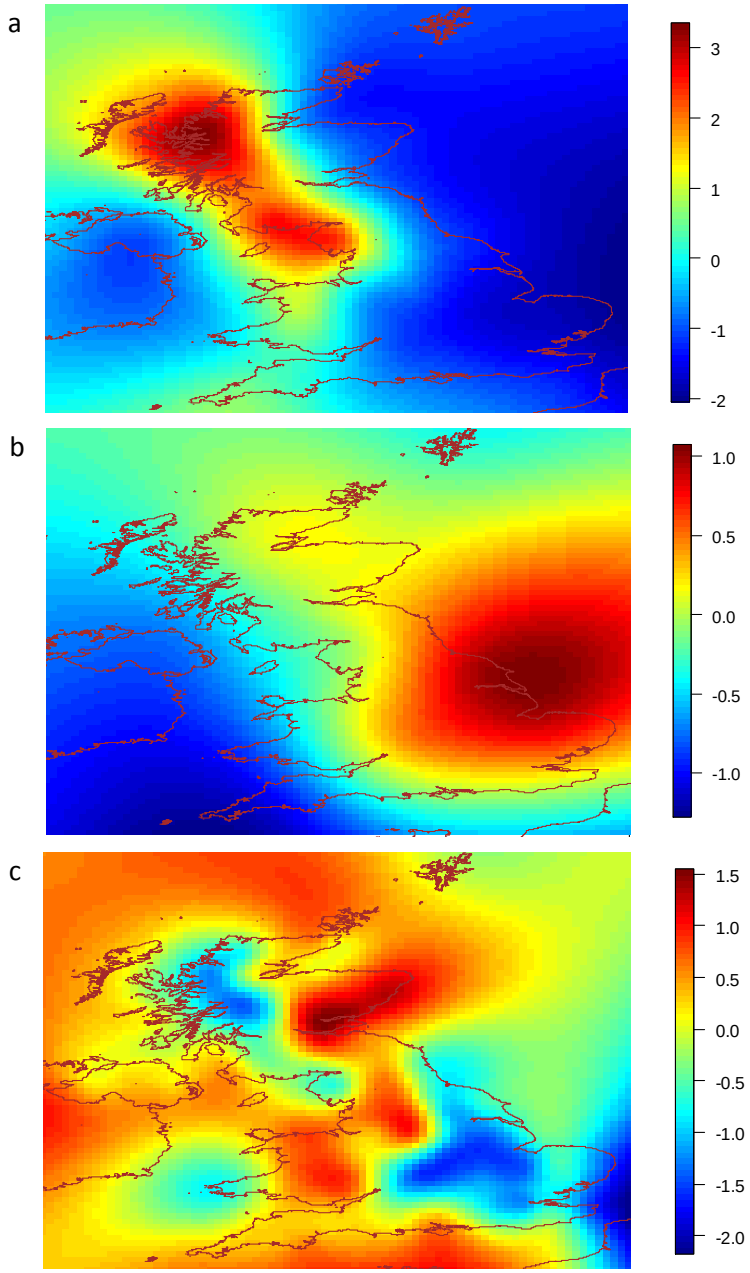

Figure 7-7 : Scores of principal components derived from the variables listed in Table 7-1 where (a) PC1 describes maxima; (b) PC2 describing variance in maxima; (c) PC2 describing seasonality

Most regions contain >10 stations with the exception of Mid Wales (MW), which only contains five stations, and Humber (HU) with nine. As shown in Chapter 4, five stations are sufficient to calculate regional frequency estimates but will also incorporate high uncertainty estimates; however, a balance must be achieved between high uncertainty and over-smoothing of the extreme characteristics.

Each region was tested for homogeneity using: the discordancy measure for each station (Hosking and Wallis, 1997), regional homogeneity statistics (Hosking and Wallis, 1993) and the Anderson-Darling rank test statistic (Stedinger *et al.*, 1993). As the

discordancy measure is a reliable estimator of homogeneity only for regions with more than 5 sites (Hosking and Wallis, 1997) it may not be applicable to MW; the Hosking and Wallis statistic is most reliable where skew between stations is low, while the Anderson-Darling measure is more appropriate for regions with a high skewness measure (Viglione *et al.*, 2007). Three Hosking and Wallis heterogeneity measures can be calculated from regional estimates of L-CV, t^R, L-skew, t_3^R, and L-kurtosis, t_4^R:

$$V = \left\{ \sum_{i=1}^{k} n_i (t^{(i)} - t^R)^2 / \sum_{i=1}^{k} n_i \right\}^{1/2}$$

$$V_2 = \left\{ \sum_{i=1}^{k} n_i (t^{(i)} - t^R)^2 + (t_3^{(i)} - t_3^R)^2 \right\}^{1/2} / \sum_{i=1}^{k} n_i$$

$$V_3 = \left\{ \sum_{i=1}^{k} n_i (t_3^{(i)} - t_3^R)^2 + (t_4^{(i)} - t_4^R)^2 \right\}^{1/2} / \sum_{i=1}^{k} n_i$$

Equation 7-1

where n_i is the record length at the ith site, obtaining the heterogeneity measure:

$$\theta_{HW} = \frac{V - \mu_v}{\sigma_v}$$

Equation 7-2

Regions were considered to be homogenous where $\theta < 1$, possibly heterogeneous for $1 \leq \theta \leq 2$ and definitely heterogeneous if $\theta \geq 2$ (Hosking and Wallis, 1997). The critical discordancy measure for individual sites within a regional pool, with relation to ≤ 15 stations, is shown in Table 7-3. The Anderson-Darling test statistic is a generalisation of the goodness of fit test, with the significance of the homogeneity score obtained from a bootstrap analysis (Viglione, 2011). The statistic was tested at a significance level of $\alpha = 95\%$, with the null hypothesis of a homogenous region being rejected for all $p > 1 - \alpha$. Viglione (2011) recommends that if L_R-skew <0.23, the first Hosking-Wallis heterogeneity measure is most appropriate and the Anderson-Darling preferable in all other cases.

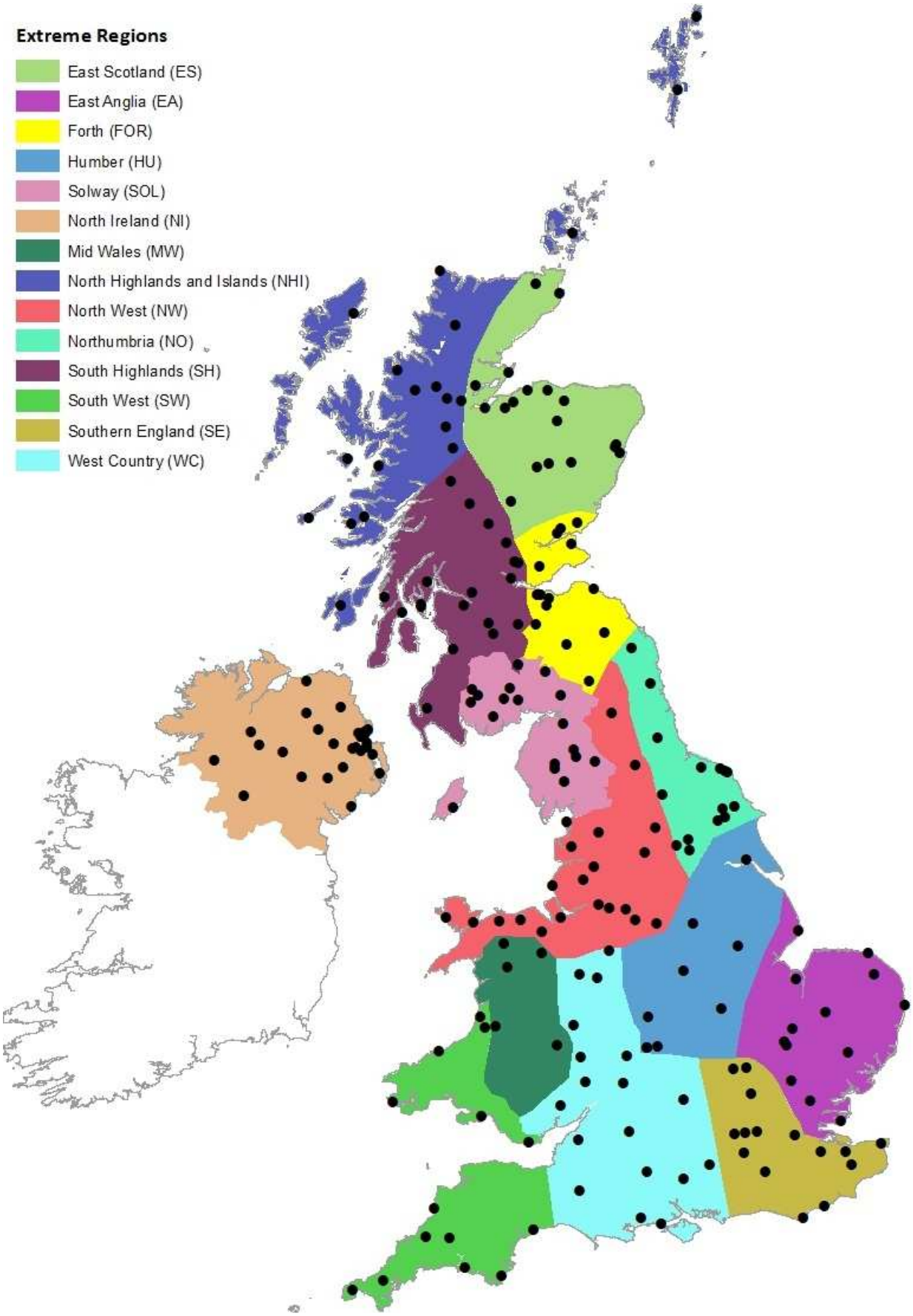

Figure 7-8 : Final selection of Extreme Rainfall Regions identified from a principal component analysis of extreme rainfall measures and homogeneity testing

Number of sites in Region	Critical Discordancy Measure (Dc)
5	1.333
6	1.648
7	1.917
8	2.140
9	2.329
10	2.491
11	2.632
12	2.757
13	2.869
14	2.971
≥15	3.000

Table 7-3 : Critical discordancy values

The results of the different homogeneity tests are outlined in Table 7-4, with regions exceeding the critical test values highlighted in bold; scores near to the critical value are in italic. The discordancy measures for all stations in each of the regions were below the critical values; although some stations had near critical discordancy measures, these all occurred in regions which are otherwise homogenous.

Extreme Region	Hosking and Wallis Test (θ_{HW})	Anderson-Darling Significance Value	Critical Discordancy value (critD)	Number of sites approaching critD
NHI	**2.57**	**0.98**	3.00	1
ES	*-1.21*	0.15	3.00	1
FOR	*1.94*	**0.98**	3.00	2
SH	-0.42	0.52	3.00	0
NW	**6.47**	0.89	3.00	1
NO	*-1.87*	0.06	2.97	0
HUM	-0.76	0.57	2.33	1
EA	*1.23*	0.51	2.87	0
SE	0.97	0.61	3.00	0
WC	1.00	0.86	3.00	0
MW	0.22	0.87	1.33	4
SOL	**2.30**	0.86	3.00	1
SW	0.27	0.71	2.97	0
NI	-0.49	0.84	3.00	1

Table 7-4 : Extreme rainfall regions tests for homogeneity using the Hosking and Wallis heterogeneity test based on L-CV, Anderson-Darling bootstrap test and discordancy measure. Bold font indicates critical test values, italic font indicates near critical values.

High discordancy scores can often arise from one anomalous rainfall event and so do not provide conclusive evidence of heterogeneity. All regions with high scores were investigated further, considering the most likely source of heterogeneity to be the most

discordant site. Given the limited data set in use, regions achieving marginal scores and containing some discordant sites were considered to be homogenous where an improvement could not be directly identified.

North West (NW) has a very high heterogeneity measure, although an insignificant Anderson-Darling score, caused by Worthington Water Works located in the centre of the region; this station was not reallocated although the score was not ascribable to a specific event. North Highlands and Islands (NHI), which is a highly skewed region, also has a significant heterogeneity measure according to all three tests. Once again, the score can be ascribed to one station which is well within the North Highlands and would not be appropriate in a separate region. Cassley, the anomalous station, recorded several high rainfall totals including 158.2mm on 22 October 1971 and 145mm on 6 February 1989. The Solway region (SOL) has a heterogeneous rating, arising from the inclusion of the Isle of Man. In the absence of supporting data, it was decided not to create a specific region for the Isle of Man, but to maintain the current allocation which is supported by the PCA scores for all stations in this cluster.

Forth (FOR) has a high discordancy score for one station, located near to the regional border, although the Hosking and Wallis heterogeneity measure indicates possible heterogeneity. The location of this site recommends that two adjacent stations of similar characteristics should also be reallocated, to South Highlands (SH), if the regional border were relocated. Although the other two stations do not have high discordancy measures, the revised homogeneity scores were calculated for changed regional boundaries moving these stations into SH. The revised allocations marginally improved the homogeneity ratings for both regions and have been adopted in the final regional definition.

It is possible that there are too few gauges in some regions to characterise the differences in behaviour or to be confident that the regions are fully homogenous. However, the allocation is considered sufficiently robust to analyse the pooled regional extreme behaviour. Where boundaries were not dictated by station location, they were adopted in common with those used by Dales and Reed (1989) and the UK Climate Change Impacts Programme (Murphy *et al.*, 2009), shown in Figure 7-9. The boundary definition used in the remainder of this project is pragmatic and would benefit from more detailed analysis and refinement with a considerably larger data set.

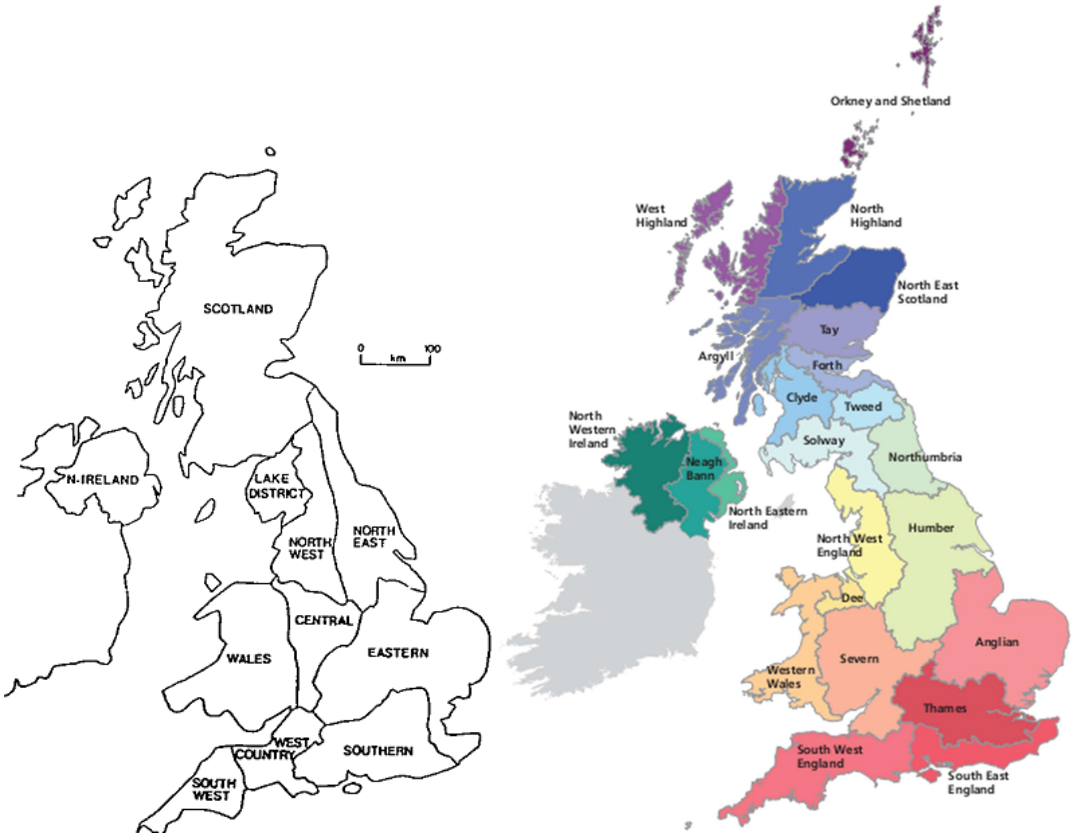

Figure 7-9 : Rainfall regions defined by (a) Dales and Reed (1989) and UKCP09 (Murphy *et al.*, 2009)

7.4 Regional behaviour

While the extreme rainfall regions were defined using Q99, this threshold may reduce the subset of maxima to one or fewer events per year, preventing within year clustering analysis. Extreme events do not arrive unprovoked but arise either from an unusual combination of circumstances or as an evolution of several common occurrences (Stephenson, 2008). Establishing the characteristics and sensitivity of very heavy rainfall to different variables will, it is hoped, facilitate greater insight into the evolution of extreme events. The remaining analyses will assess the characteristics and time-varying qualities of rainfall exceeding Q95.

Figure 7-10 combines the histograms of event frequency per day of year, as explored in Section 7.2, for all stations within each region. Several regions appear to have a lack of coherence in the seasonal pattern between the different stations, such as East Scotland (ES) or North West (NW). This may in part be due to the spatial extent of the regions, as well as incorporating stations with shorter records (<40 years) where natural fluctuations and chaotic behaviour may be more apparent than regular seasonal patterns.

Some features consistently stand out for all regions. For instance the double peak in seasonality, whether equally dominant or with one peak dominant in either summer or late autumn, is more in evidence in regions bordering the North Sea. In contrast, exposed western regions (notably NHI, SH, SW and SOL) exhibit one long peak period commencing in early autumn. Stations in southeast England (SE and EA) demonstrate much clearer double periods, with a principal peak in mid- to late-summer and a secondary peak period during the autumn. In general terms, the northern regions are dominated by a wide ranging peak period over late autumn and early winter. South and eastern stations are dominated by a peak in the summer preceded or succeeded by a secondary peak, while stations in the south west experience the peak period in the autumn. Overall each regional group appears to encompass the correct stations to allow the definition of seasonal characteristics.

To establish the overall seasonal attributes for each region, station records were pooled and the process repeated (Figure 7-11); these results demonstrate much clearer east-west and north-south seasonal event timing. Various weighting criteria to account for spatial dependence (Hosking and Wallis, 1997; Alexander *et al.*, 2006) were examined but all were found to concentrate on event magnitude rather than timing, as a result no weighting was applied to the station records. The regional pools are likely to experience the same synoptic events and so will not contain completely independent records; including several stations with events from the same storm gives reassurance that the data are not erroneous. It was also considered that in common with the regional frequency analysis approach, including several similar records may increase the standard error in magnitude estimates, but should not affect the regional bias (Hosking, 1995a).

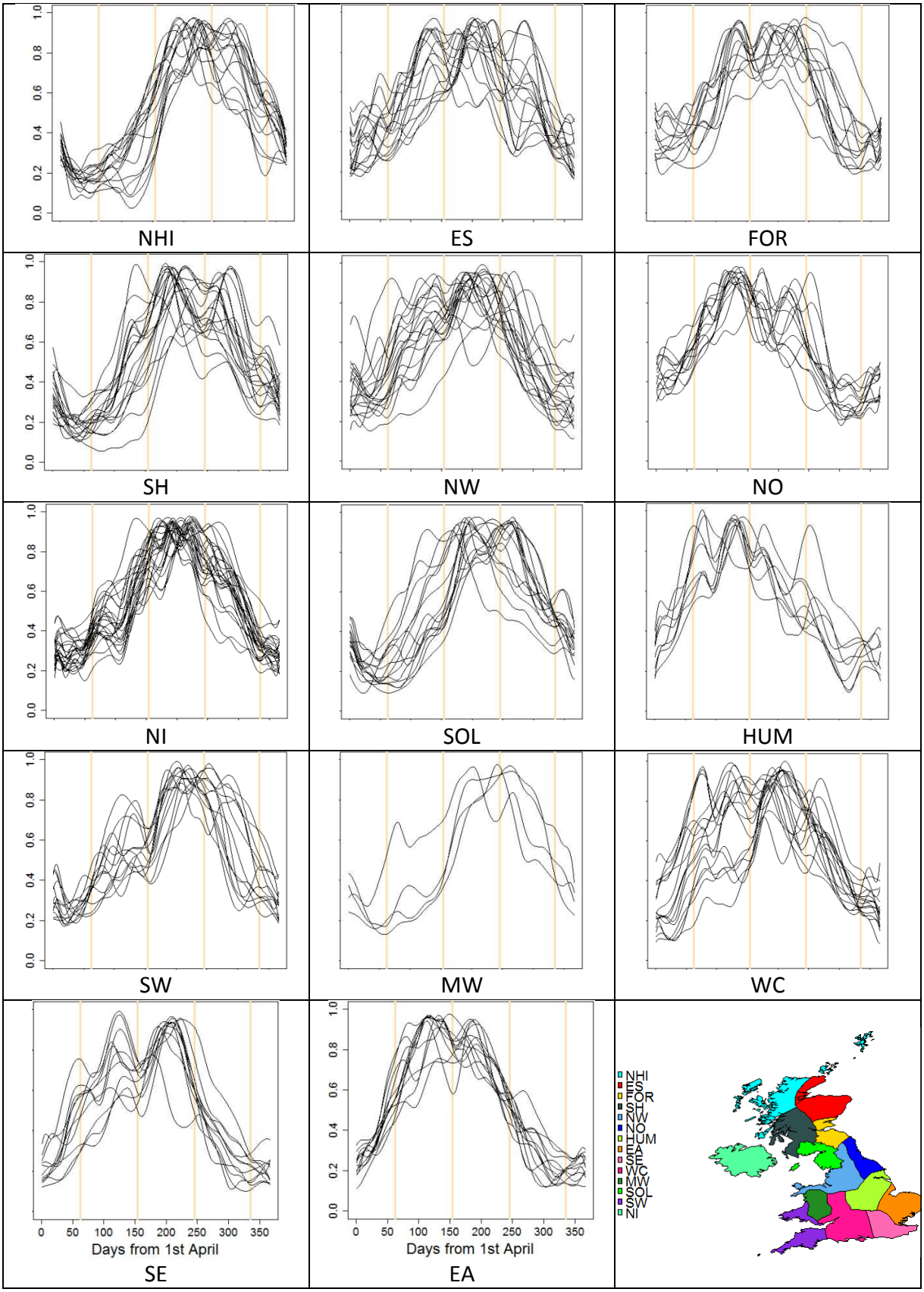

Figure 7-10 : Frequency density plots of 1-day events per day of year for each station in each extreme rainfall regions : North Highlands and Islands (NHI), East Scotland (ES), Forth (FOR), South Highlands (SH), North West (NW), Northumbria (NO), North Ireland (NI), Solway (SOL), Humber (HU), South West (SW), Mid Wales (MW), West Country (WC), Southern England (SE), East Anglia (EA).
Vertical lines denote start day of each season.

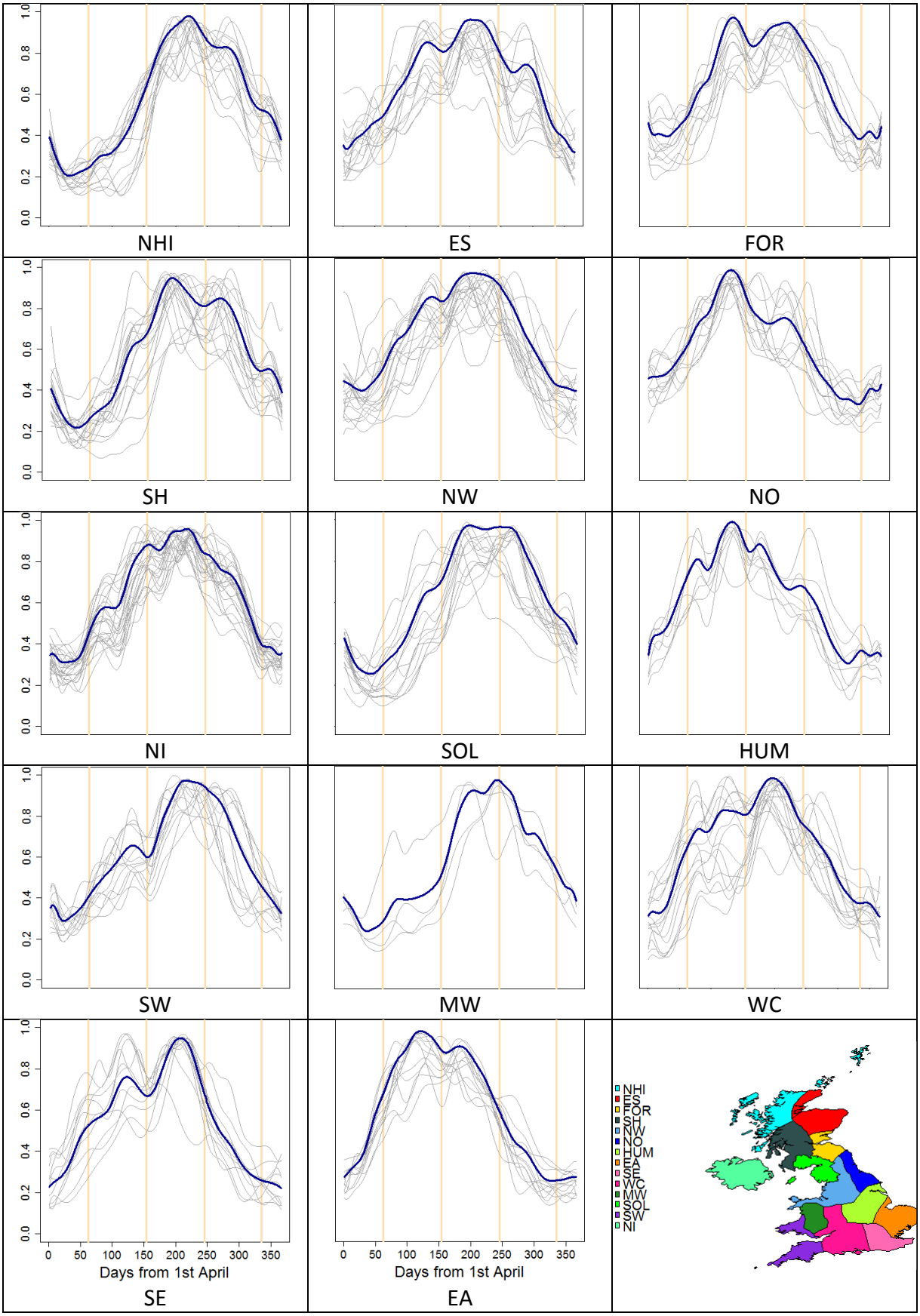

Figure 7-11 : As Figure 7-10 but using regionally pooled data in dark blue lines. Pale grey lines denote individual stations.

Examination of the possible long term changes is more valid when using a regionally pooled data set than from the individual series. Not only is it possible to examine the apparent changes in one location in the context of longer records, but natural variability is easier to discern from true regional patterns. The pooled data were examined for patterns in the highest frequency density of event occurrence over the collective period of record, although no weighting was applied to the individual station events prior to pooling. Figure 7-12 compares the individual station results of events per day of year for Wisley, a station in southern England, with its counterpart regional plot (SE) over the common period of record containing the most stations. The additional regional data clarifies that an apparent clustered period in early summer in Wisley (cyan) and the secondary period in autumn are also important for the whole region (dark blue and magenta) demonstrating a good match between the station and regional event timing. The darker shading in Figure 7-12b merely reflects the additional number of events used for the pooled analysis. This is repeated for all stations in all regions, giving confidence in the extreme rainfall region definitions.

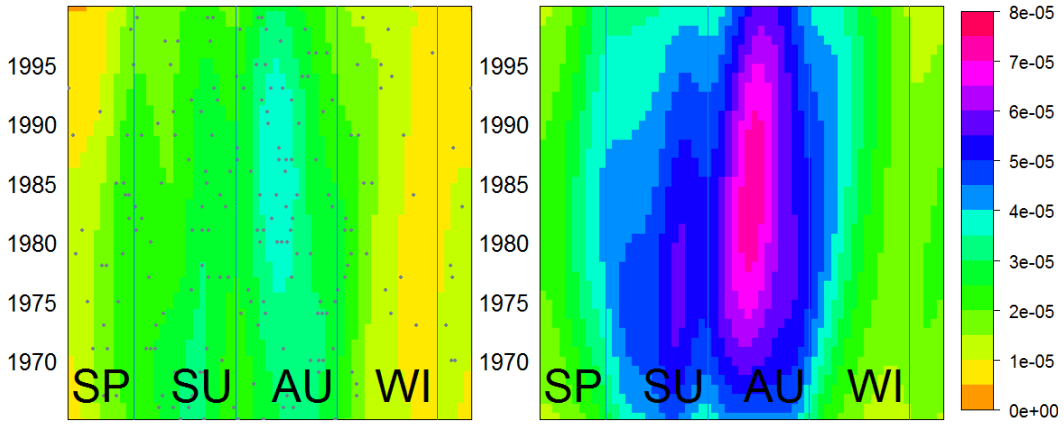

Figure 7-12 : Events per day of year for (a) Wisley 1960-2000, (b) Southern England (1960-2000). Scale bar represents frequency density.

Figure 7-13 illustrates the regionally pooled records for the period covered by most stations (1965-1995); however, some of the plots have considerable "edge effects" in the smoothing where the density of stations within the region reduced from the year 2000 (e.g. NHI). The whole record for each pooled region is not shown as scaling the smoothed surface to reflect the number of contributing stations would give a false impression of the relative smoothing errors at different periods; it is more robust to consider only the period containing all stations. Many of the regions appear to show a shift in extreme rainfall seasonality in recent decades, either combining two clustered seasons in the 1960s into a single period later on (e.g. ES) or occurring later in the year (e.g. NI).

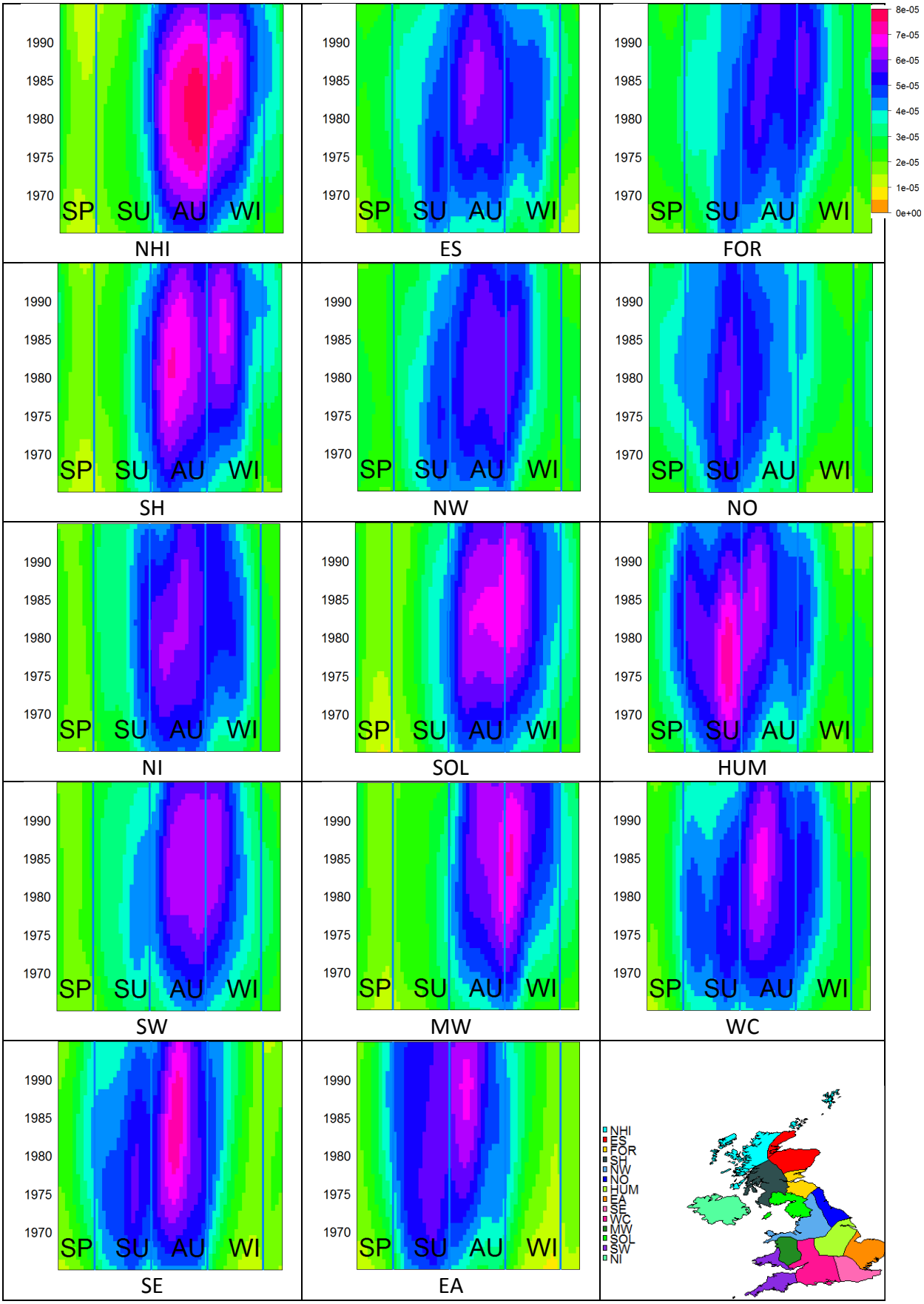

Figure 7-13 : Events per day of year, each year for regionally pooled data 1965-1995.

The areas of darker blue in each plot in Figure 7-13 correspond with the peak event activity indicated in Figure 7-11. It is more obvious from the long term evolution in some regions (NHI, EA) that secondary maxima in event frequency per day of the year is an artefact of the seasonal response to external influences; in other regions (SH, HUM, FOR) it may be that a second period of heavy rainfall only occurs when certain atmospheric conditions prevail, such as those experienced during highly positive NAO years. A change in the clustered process, where more events occur in a shorter seasonal period, could have serious implications for flooding as the timing of events over a river catchment is a critical factor in flood generation. While a change in the timing of the seasonal clustered process may have less impact on flood generation, it could still have severe consequences for agriculture, for instance through intense rain over recently planted crops or enhanced agricultural drought.

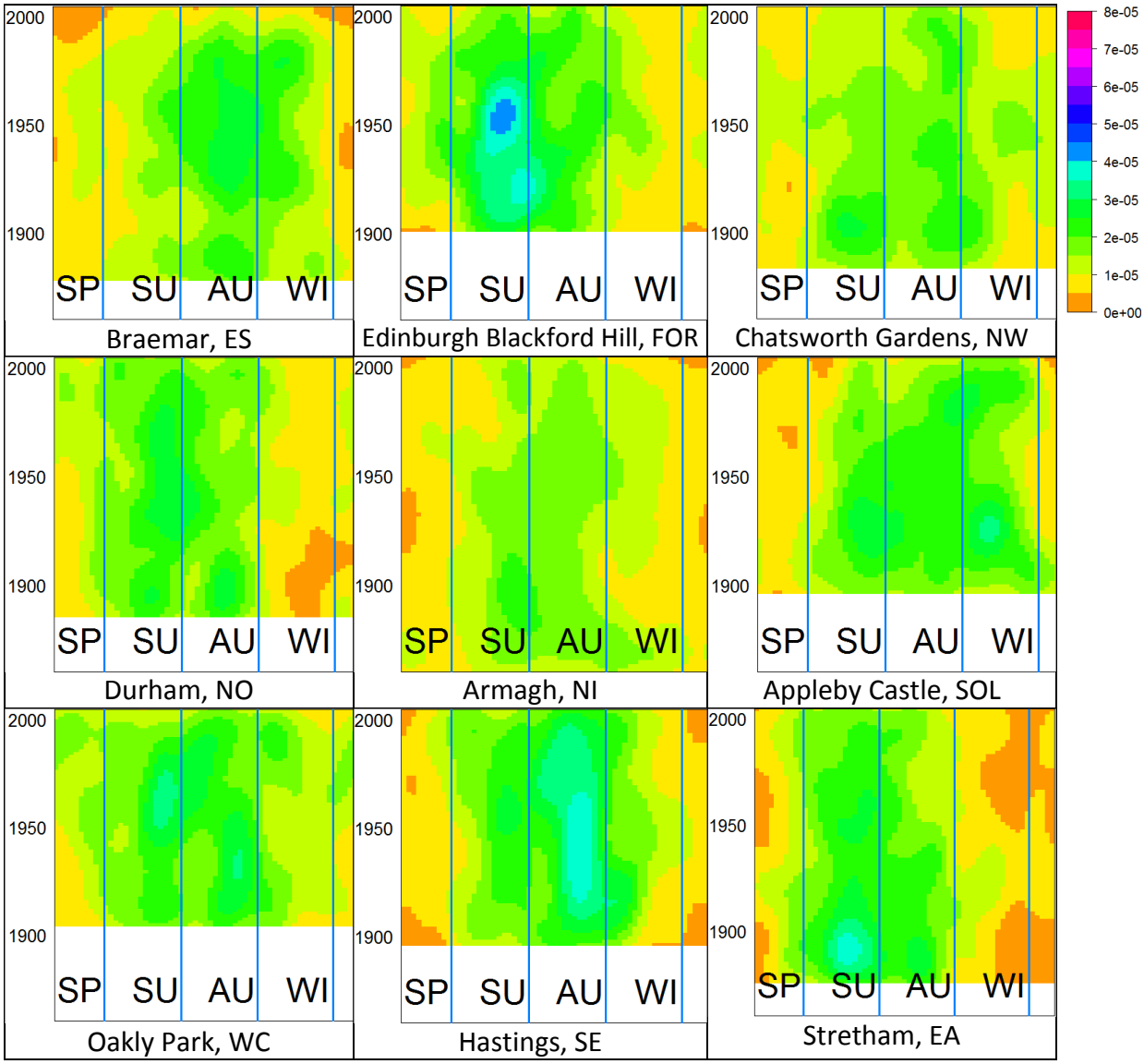

Figure 7-14 : Events per day of year each year for record length >75 years in each region (1860-2005)

Similar plots for the longest station, with >75 years of data, within each region were used to assess whether any of the apparent changes in regional behaviour are clearer in the longer records or reflective of periodic behaviour. The selected stations are those with the longest record in each region; three regions (NHI, MW, HUM) had no station records >75 years and have not been included as inter-annual patterns are less apparent in shorter records (Kundzewicz and Robson, 2004). The resultant plots, commencing between 1853 and 1911 and ending in 2005, are shown in Figure 7-14. Most of the stations do appear to change from around 1960 with respect to the longer period of record, with the figures either suggestive of a less concentrated peak seasonal behaviour (ES, EA), or definite shifts towards extreme rainfall earlier (SE) or later (NI) in the season. However, this visual assessment is not robust and will be better examined with specific statistical tools in Chapter 8.

The influence of the North Atlantic Oscillation (NAO) on the frequency of very wet day rainfall was confirmed by a Poisson regression analysis in Chapter 5; other studies have also established a connectivity with the NAO for summer rainfall (Linderholm *et al.*, 2009) in addition to the better known winter connectivity (Allan *et al.*, 2009; Bartolini *et al.*, 2009). An initial examination was carried out of very wet day occurrence in relation to the coincident upper (lower) 20% of the monthly NAO distribution.

Individual stations were assessed for these years, plotting each event by day of year, per year of record, with the event magnitude represented by the scale of the dot. Figure 7-15 illustrates the plots for two such gauges in northwest and southeast England; blue (red) dots represent negative (positive) NAO indices. Gaps in the plot on the right (left) correspond to years where events did not coincide with very negative (positive) NAO indices.

The results for Hastings, which tends to receive more continental driven weather patterns or summer convective storms, suggests little correspondence between the NAO index and event timing or magnitude. As convective events are very short lived, the daily NAO signal coincident with the event is likely to be masked by monthly averaging; use of a sub-monthly NAO index, which is an atmospheric signal, is considered inappropriate as short timescales reflect weather patterns rather than atmospheric processes. Rainfall responses for summer convective events are likely to correspond better to sea surface or land surface temperatures. In contrast, the influence of the positive NAO index can be seen in the longer

duration Appleby Castle winter events. Little is clear from either station regarding the relationship between magnitude or interval between events and the NAO index.

While there are insufficient data to make a definitive statement about the influence of NAO phase on very heavy rainfall, both Figure 7-15 and the Poisson regression analyses suggest that the NAO correlates well with the frequency of very heavy rainfall. Scatter plots of the magnitude of very heavy events plotted against day of the year and NAO index (Figure 7-16) are also suggestive of a positive correlation. The influence of air temperature, and therefore seasonality, on the magnitude of events is borne out by the plot of event magnitude with respect to calendar day; there is also a suggestion that very heavy rainfall does not often occur during particularly negative NAO years. However, as shown by Hurrell (2003), NAO<-4 is very rare, with a consecutive negative index for all winter months (NDJFM), occurring for only five winters between 1890 and 2010. Thus, the lack of extremely low values in Figure 7-16b may be a distributional quality rather than seasonal characteristic.

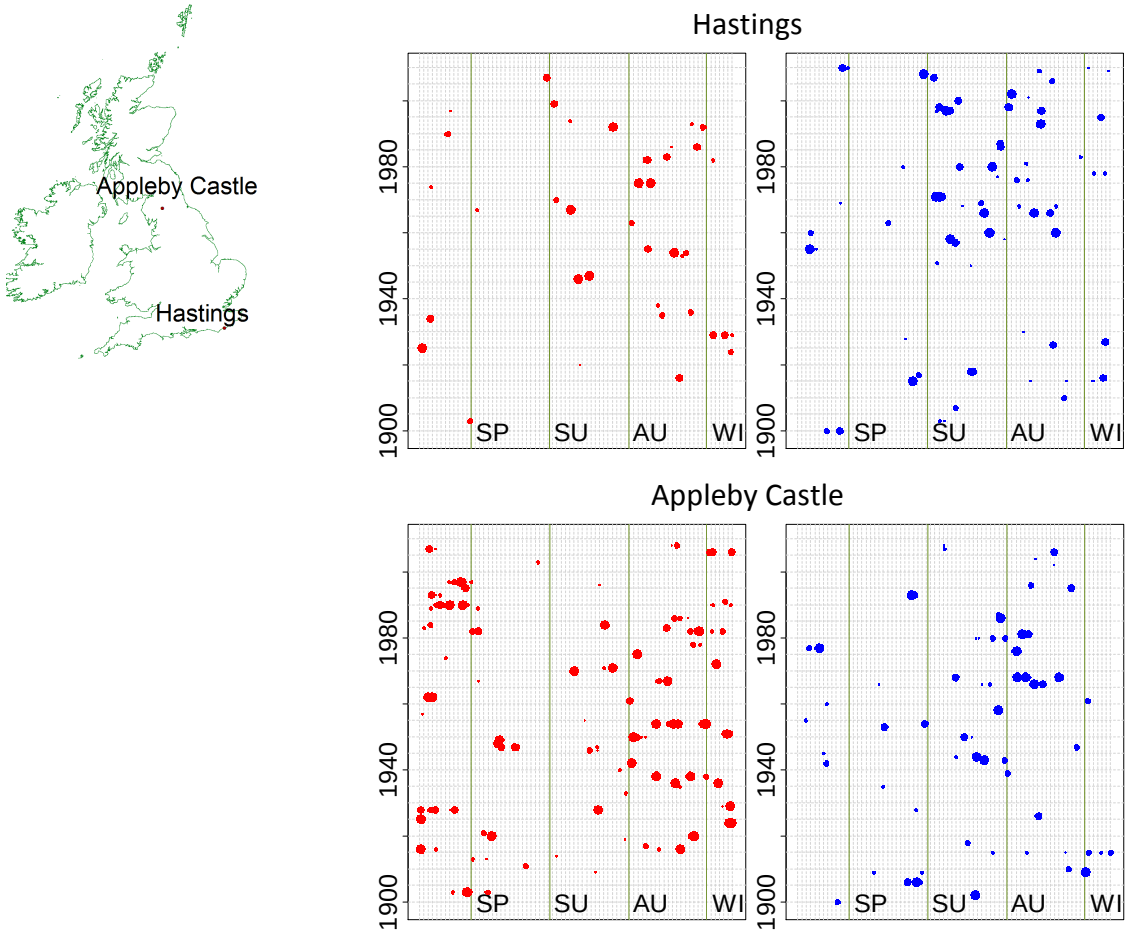

Figure 7-15 : Influence of Positive and Negative phase NAO on very heavy rainfall, events corresponding to a positive (negative) monthly index are shown in red (blue) on the left (right). Event magnitude is represented by the scale of the dot.

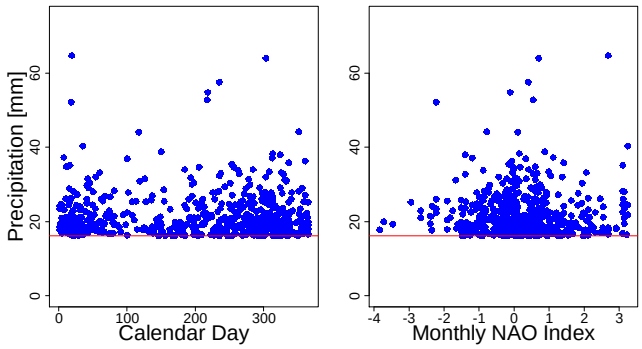

Figure 7-16 : Scatter plots of events exceeding a threshold - magnitude against (a) calendar day or (b) coincident NAO index for Stornoway (North Scotland)

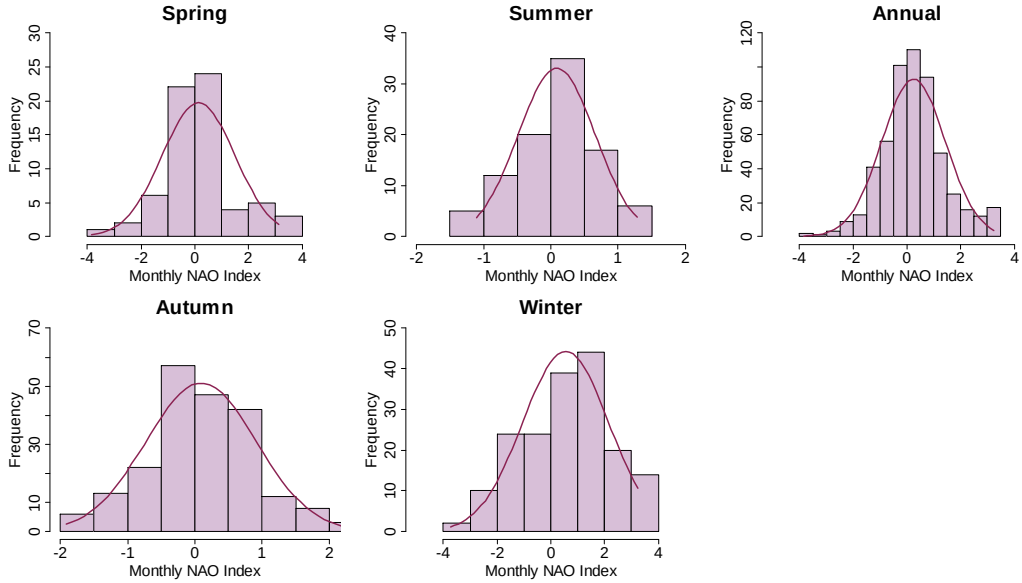

Figure 7-17 : Frequency of very heavy rainfall in relation to monthly NAO index (Hurrell and Van Loon, 1997) at Stornoway (North Scotland) with fitted Normal distribution

The annual distribution of the monthly NAO index coincident with event occurrence is approximately normal, with a slight positive skew highlighting the high intra-year variability in the NAO index (Figure 7-17). Both autumn and winter NAO indices have a distinct positive skew, emphasising the North Atlantic influence on event occurrence in north Scotland during these months; in contrast, the NAO indices for summer and spring are very small and heavily concentrated about zero. However, Folland *et al.* (2009) found that the July-August NAO index has a very strongly significant negative correlation with rainfall in the UK and northwest European regions, causing anticyclonic low rainfall conditions during positive phase summers. Bladé *et al.* (2012) found a strong positive correlation with summer rainfall in the Mediterranean region, concurring with Folland *et al.* (2009) that the June NAO index differs substantially in behaviour from that of July and August. These analyses emphasise that

meteorological responses cannot be characterised from a single seasonal value (Hurrell and Deser, 2009) and that the use of monthly aggregates or different seasonal combinations would be more appropriate.

To characterise the intensity of regional rainfall as well as the frequency, a regional frequency analysis approach was applied to the Q99 events to develop regional return period estimates. Most examples in the literature of pooling excesses over a high threshold assume complete homogeneity of the stations within the pool and so do not standardise the observation series. This is not appropriate for the regional pools under consideration, where considerable differences in elevation and aspect can exist between stations. An adaptation of the Regional Frequency Analysis (Hosking and Wallis, 1997) approach has been adopted here, whereby the Q99 events are standardised by the Q99 threshold for the station prior to pooling. L-moments were fitted to the individual station, i, series for all stations, N, in the region before deriving the regional L-moments from the weighted station average values as follows:

$$\hat{\theta} = \sum_{i=1}^{N} w_i \hat{\theta}_i$$

$$\text{and} \qquad w_i = \frac{n_i}{\sum_{i=1}^{N} n_i}$$

Equation 7-3

where n represents the effective years of station record and $\hat{\theta}$ the parameter estimate. Years were rejected where either >3 days were missing per month, or >10 days in the whole year as it is not possible to estimate whether any events exceeding the threshold occurred during those times (Stewart *et al.*, 1999). The location parameter is known to be the threshold used to extract the data; in this case a regionally weighted value of $\hat{u}$, calculated from all station thresholds was adopted. Regional Generalized Pareto Distribution (GPD) parameters were derived from the regionally weighted L-moments (Hosking, 1990); refer also to Appendix B.4. An estimate of RMED for each station was obtained from the fitted GPDs (Robson, 1999) with the regional RMED calculated from their weighted mean.

Return period estimates for a full range of events were then calculated using the regionally weighted RMED, shown in Figure 7-18; for comparison, regional GEV distributions were also fitted to annual maxima and the return periods estimated. Inter-site dependence is not explicitly accounted for as it has been shown that including dependent events only

increases the uncertainty surrounding the return period estimates and not their bias (Hosking and Wallis, 1997). A spatial dependence model applying a radial weighting to each station in relation to the centroid of the region (e.g. Alexander *et al.*, 2006) may reduce the uncertainty, but introduces additional unnecessary complexity for distributions derived from excesses over a threshold (Svensson and Jones, 2010).

The calculated return period estimates for most regions follow a similar distributional shape and attain comparable magnitude estimates with both the GP (applied to Q99 events) and GEV (applied to AMAX) models. The AMAX values were those used in Chapter 5 for all 223 stations, while the Q99 events are peak over threshold rainfall extracted for only 199 stations. It has been shown that for shorter time series, or small pools of data, return period estimates obtained from the GP model are more robust to outliers (Davison and Smith, 1990), while with larger data sets there is little difference between the two methods. Four regions exhibit considerable differences in return period estimate magnitude between the GEV and GP models: NI and EA appear to be underestimated while SE, NO and SOL appear to be overestimated. It is likely that these discrepancies have arisen from differences between the data sets, as annual maxima for missing years were included when they could be verified from British Rainfall or other sources, while the equivalent missing years of POT data were omitted completely. In general, the results are similar to those reported in Chapter 6, with the steeper curves and highest magnitudes in higher altitude regions (NHI, SOL), or regions which receive intense summer convective events (HUM, SE, EA). Regions with flatter curves, such as MW or WC, are representative of regions receiving high annual totals of rainfall, but with a smaller range in the magnitude of events.

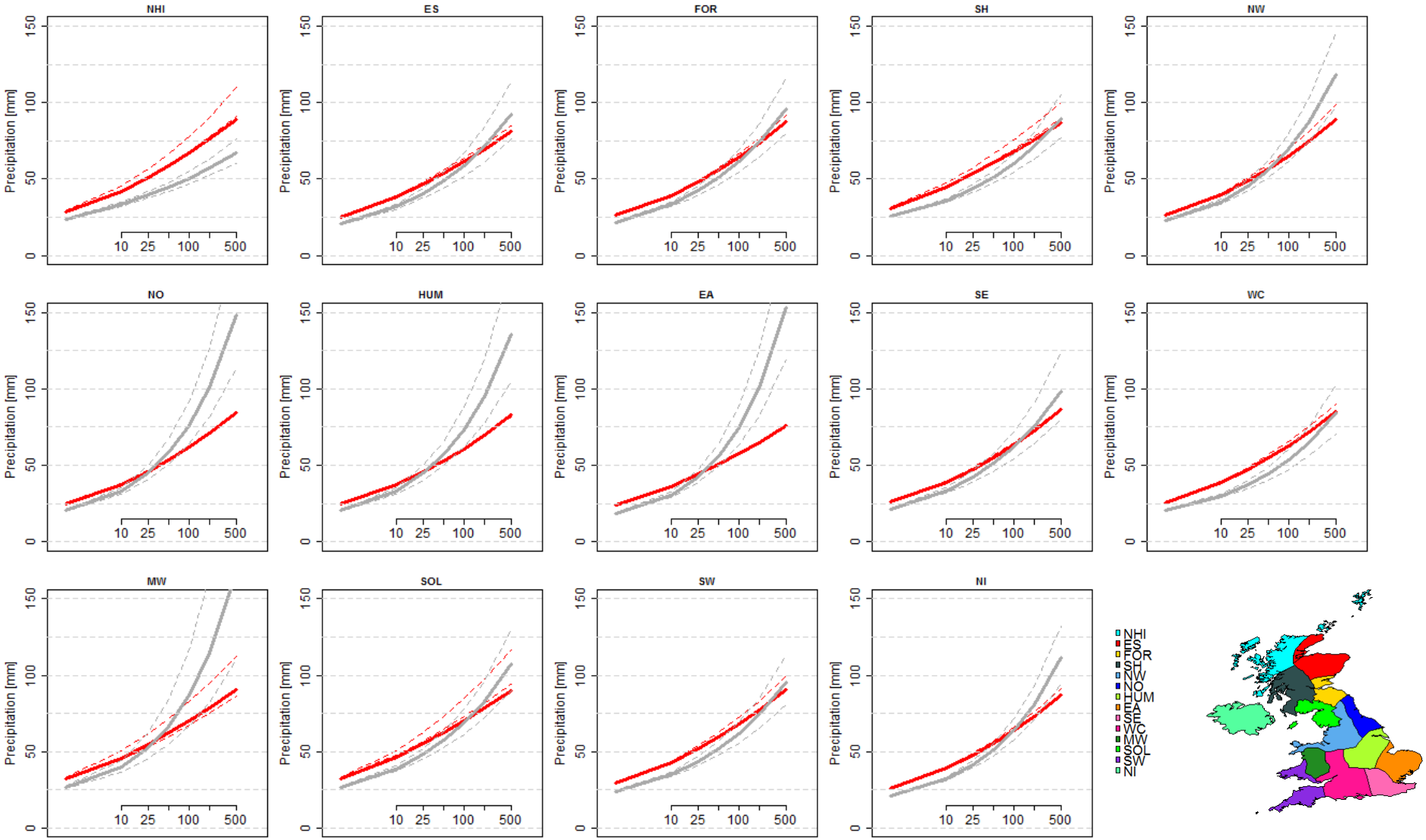

Figure 7-18 : Regional return period estimates generated from the regional Generalized Pareto distribution fitted to Peaks over the 99th Quantile (red) and regional Generalized Extreme Value distribution fitted to AMAX (grey) for all years of maxima. Dashed lines denote uncertainty estimates.

7.5 Multiple Wet Days

Analyses of partial duration series are premised on independence assumptions, such that either all consecutive events are included or only the sequence maximum (Stewart *et al.*, 1999). Both approaches have merits and drawbacks: the former enhances distribution estimates but includes duplicate information, introducing bias; while the latter minimises bias yet discards some important maxima. Where a 24 hour event occurs over two days, duplication can be avoided by multiplying the maximum total by 1.16 (Faulkner, 1999). Alternatively, multiple wet days (wet spells) could be assessed from the aggregated totals such as 2-, 5-, or 10-days (Fowler and Kilsby, 2003b). While fixed aggregate events facilitate simple comparison, longer aggregates may contain a period of dry days with considerably different properties from a continuous wet spell, making direct comparison less effective.

Figure 7-19 explores the similarities between seasonality of 1-day (red line) and 5-day grey) very heavy rainfall, compared with mean days with rainfall (black). The *mean rainfall day count* incorporates wet spells of duration >1-day as data were not de-clustered. The plots suggest that there is little appreciable difference between the frequency of very heavy rainfall in relation to the event duration, because the multiple day maximum is usually heavily influenced by one heavy day. It is also apparent that the seasonality of very heavy days differs considerably from that of rainfall days as the highest frequency of mean rainfall days occurs during autumn and winter months. In the south the period with the highest frequency of Q95 events coincides with the start of the highest frequency of mean rainfall days; further north the range of the mean wet day frequency density per year is smaller than in the south. The most frequent mean rainfall days coincide with the most frequent Q95 1- and 5-day events in Atlantic facing regions, which are coincidentally those with higher elevation; regions bordering the North Sea have a dislocation between summer Q95 events and autumn/winter mean wet day frequency.

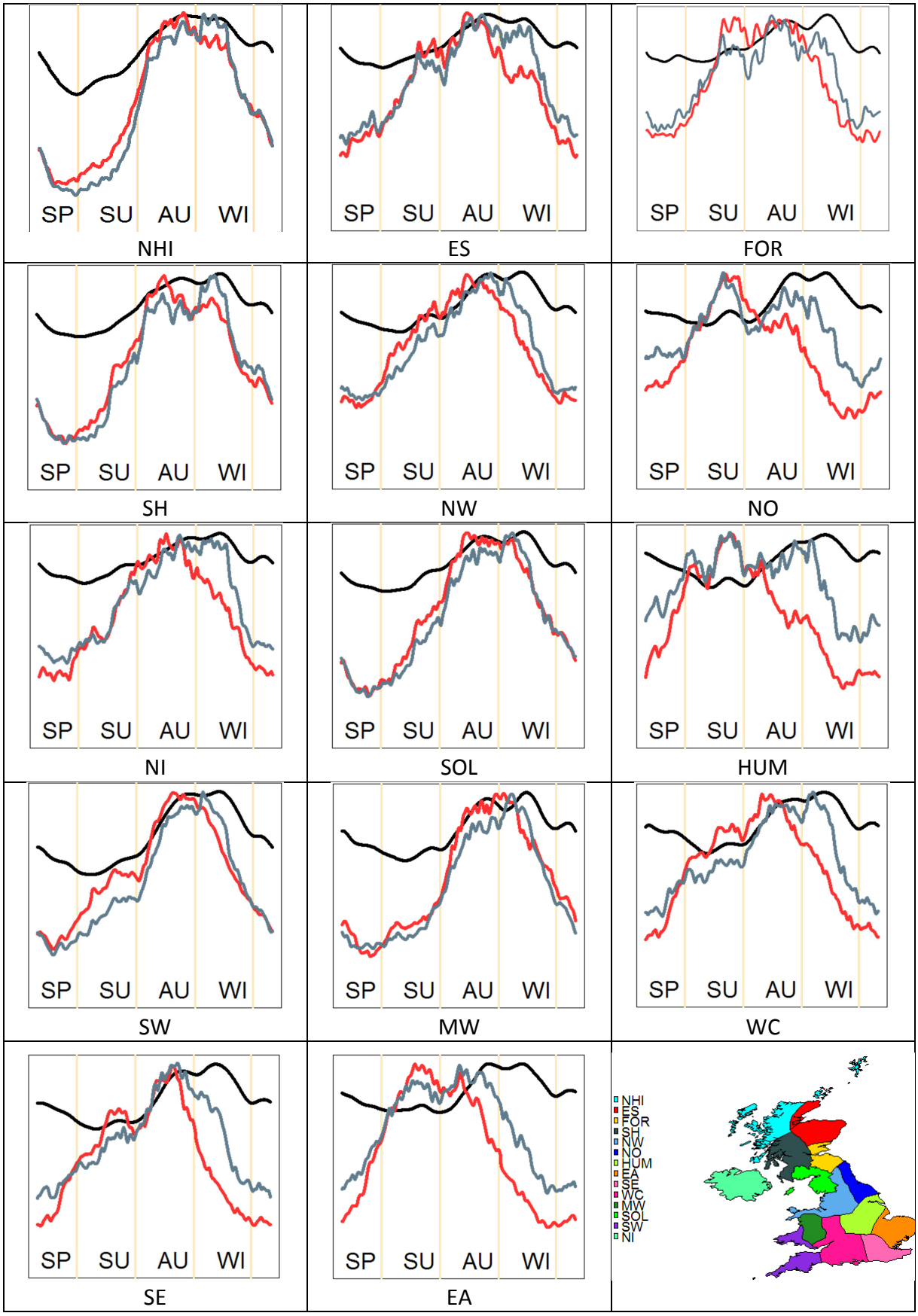

Figure 7-19 : Regional frequency of day of year for rainfall days (black), 1-day very heavy rain (red) and 5-day very heavy rain (grey)

Heavy rainfall has several time-varying characteristics: the events arrive non-uniformly in time (Cowpertwait *et al.*, 2002); the interval between successive wet spells is also non-uniform; and the duration of wet spells is inconstant. These time-varying characteristics are seldom examined in depth, particularly the inter-dependence of successive heavy rainfall events, and yet extreme events often develop from several dependent non-extreme events (Stephenson, 2008). Multiple day heavy events, arriving in succession are a frequent cause of flooding and characterising their driving triggers would be beneficial to all involved in flood risk management. However, wet spells of varying duration are complex and not readily comparable. A long wet spell with 0.5RMED per day may be relatively rare but not severe, although repetition could generate an extreme response. By comparison a single daily total of 253mm, as at Seathwaite in Cumbria in 2009, is both rare and severe; the associated flooding was compounded by the preceding extended wet spell (Met Office, 2010a).

It is evident that some measure is required to identify the relative extremity of different wet spells, regardless of duration; possible approaches include the use of some concentration parameter (Li *et al.*, 2011) or a development of the flood and drought precipitation index (McKee *et al.*, 1993). A potential definition for wet spells and their relative extremity is outlined in Appendix C.3. While this approach would enable wet spells to be categorised and the combinations of wet spell duration and intensity most likely to have negative consequences identified, characterising the drivers would be highly complex. Extreme wet spells arise from different governing climatic conditions, assessment of which would necessitate further sub-classification, with the application of multiple extreme value distributions to the different maxima (Sornette, 2009). It is concluded that this additional complexity lies outside the scope of the current study, and so the statistical models will only be applied to 1-day maxima.

7.6 Conclusions

A pivotal output from this chapter was the development of rainfall regions formulated from metrics of extreme rainfall. While the HadUKP regions (Alexander and Jones, 2000) are effective in describing mean daily rainfall behaviour, they are not fully representative of sub-scale variations in extreme rainfall. Daily rainfall observations from 199 stations were used to develop earlier extreme region characterisations (Jackson and Larke, 1974; Dales and Reed, 1989) into 14 regions, representing the temporal, orographic and atmospheric

drivers affecting UK extreme rainfall. A paucity of records in upland areas such as the North Highlands and Islands or Mid Wales dictated that the regional boundaries are pragmatic at present, although these could be enhanced through the use of additional data. The regional classifications were used as a spatial tool to explore variations in heavy and extreme daily rainfall characteristics.

Heavy and extreme daily rainfall are time variant in relation to inter- and intra-annual occurrence rate and wet spell duration. Although mean wet day frequency follows a homogenous Poisson process, the same is not true of heavy or extreme events which tend to cluster by season, and are not well represented by linear forms (Yee and Stephenson, 2007). Seasonality of the day of maxima occurrence was explored in great detail in addition to the relationship with atmospheric drivers and, more briefly, with temperature to identify the most likely drivers of extreme events. Some spatial characteristics were also assessed and a pragmatic selection of regions collating stations with similar extreme rainfall characteristics (in relation to magnitude and event timing) was formulated. By pooling extreme rainfall data from similar stations, it was possible to verify whether the apparent seasonal event frequency was representative or simply the result of a randomly generated process.

Questions remain after this exploratory analysis, such as the impact of different atmospheric conditions on the frequency of events or the long term evolutions in behaviour. Developing a frequency model to determine event probability based on the governing atmospheric conditions would be beneficial to water resource or risk managers. Similarly, characterising the atmospheric relationships may assist with adaptation planning, as projected changes in the hydrological cycle or driving conditions could be used to identify likely changes in the patterns of event frequency. The aim of Chapter 8 will be to develop such a model from the governing processes identified in this chapter.

7.7 Computer packages

Packages used for analyses in this chapter include nsRFA (Viglione, 2011), fields (Furrer *et al.*, 2012), moments (Komsta and Novomestky, 2011), lmomco (Asquith, 2009), cluster (Maechler *et al.*, 2011), and extRemes (Gilleland *et al.*, 2009).

Chapter Eight Modelling Very Heavy Rain Days

"When you have eliminated the impossible, whatever remains, however improbable*, must be the truth"*

Sir A. C. Doyle, The Sign of the Four

8.1 Introduction

The characteristics examined in Chapter 7, describing seasonality, long-term behavioural patterns and dependence on atmospheric drivers, present a highly complex relationship which cannot be examined with standard statistical tools. Improved estimates of event frequency and magnitude could be achieved using extreme value parameters estimated from linear covariates of terms such as seasonality (Tramblay *et al.*, 2011). Linear models facilitate improved absolute estimates of the covariates and can describe any long-term changes in behaviour; however, the model terms do not explain how the changes transpire, only the result of the change (Underwood, 2009). Furthermore, the complex relationship between the characteristic variables driving the non-homogenous rate of event occurrence demands a flexible statistical model which encompasses non-linear behaviour. This is better achieved with a Generalized Additive Model (GAM; Wood and Augustin, 2002).

The comparative benefits of Generalized Additive and Generalized Linear Models (GAM, GLM) were explored in Chapter 3, concluding that Vector Generalized Additive Models (VGAM) will provide flexibility both in parameter choice and underlying model definition. GAMs have gained gaining popularity in assessing data with a strong time-varying component and atmospheric dependence (Hyndman and Grunwald, 2000), as well as for identifying whether long-term behavioural changes are occurring (Underwood, 2009). GAMs have been widely employed in other disciplines to model the health impacts of air pollution or long term variability in biota spatial density, but rarely applied in hydrology (Morton and Henderson, 2008; Underwood, 2009). Their direct application in extreme value distributions is computationally difficult, achieved through incorporating matrix transformed basis functions in the distribution parameter estimates using multiple b-splines (Chavez-Demoulin and Davison, 2005). VGAMs use vector splines, a form of p-spline, to extend the GAM domain of application beyond the mean of the distribution (Yee and Stephenson, 2007). As a result, VGAMs have been selected for use in this thesis to analyse the complex temporal responses of very heavy rainfall to non-linear atmospheric patterns in a flexible manner.

This chapter applies the VGAMs to very heavy daily rainfall totals (Q95) to: assess how the arrival rate of heavy rainfall varies throughout the year; evaluate whether long term trends exist in the frequency distribution; and quantify apparent changes in the seasonal distribution. While two of the most effective methods to pool regional peak over threshold maxima are weighted L-moments (Hosking and Wallis, 1997) or Bayesian estimation centred on a single site of interest (Ribatet *et al.*, 2007), neither are supported by the R (R Development Core Team, 2011) package VGAM v.0.8-4 (Yee, 2011). Therefore, the statistically correct, but less efficient point process method was adopted using the relationship between the GEV and GPD (refer to Appendix B.2.3). A point process applied to normalised pooled block maxima and pooled POT event frequency to simulate event rate and intensity (Katz *et al.*, 2002; Eastoe and Tawn, 2010) is considered an appropriate alternative pooling method, provided that both models are derived from the same controlling covariates to aid interpretation (Coles, 2001).

While Maraun *et al.* (2011) developed similar models of monthly rainfall maxima dependent on proxies of atmospheric circulation patterns, their sinusoidal Vector Generalized Linear Models (VGLM) over-simplified the seasonal responses identified in Chapter 7 and did not examine event frequency. The benefit of the VGAM over linear model covariates is the resultant parameter flexibility, allowing temporal variation throughout the year with respect to multiple influences, and better seasonal clustering representation. This approach is novel in several respects. Primarily, GAMs have rarely been applied to hydrological series, and the extension to extreme value distributions through VGAMs has seldom been applied to daily rainfall extremes. Regionally pooling the hydrological extremes assessed with VGAMs, to enhance seasonal frequency and magnitude estimates, does not appear to have been attempted elsewhere within the literature.

To effectively assess within-year clustering, the frequency of events must be analysed. As extreme rainfall events are randomly distributed and described by a Poisson Process, with a rate which varies throughout the year, the frequency of 1-day Q95 rainfall maxima were assessed with a non-homogenous Poisson-VGAM. The magnitude of such events is well approximated by extreme value distributions, such as the Generalized Pareto Distribution (GPD) or the Generalized Extreme Value (GEV) distribution. Regional pooling of event maxima is not possible using the selected software, therefore, event magnitudes were

assessed using a GEV-VGAM fitted to regionally pooled annual maxima to form a flexible orthogonal point process model. The notation arises from the property of orthogonality between Λ and parameters σ and ξ for all independent data (Katz *et al.*, 2002; Chavez-Demoulin and Davison, 2005).

The remainder of this chapter describes the selection of the VGAM parameters and regional extreme value distributions. The VGAM orthogonal point process models were then used to explore different properties of the rainfall distribution such as long term seasonal behaviour and perceived within year clustering.

8.2 Method

VGAM supporting theory and the advantages in relation to simpler linear and additive models are presented in Chapter 3 and Appendix B.2.3. This section outlines the basics of the model formulation, the selection of smoothing and link functions specifically related to the regional daily rainfall maxima, and the final model selection.

8.2.1 Model Parameters

Chapter 5 demonstrated that the arrival rate, Λ, of POT events follows a non-homogenous Poisson distribution, with a higher frequency at different periods of the year giving the impression of clustering. Runs testing confirmed that the events are randomly distributed, although further exploration in Chapter 7 suggested that Λ is primarily dependent on the season. In Chapter 7 it was shown that inter-annual fluctuations in event frequency appear to be influenced by ocean-atmosphere coupling and variability, while some regions also showed changes in their seasonal patterns, representative of a longer term behavioural evolution. These attributes suggest that covariates which should be included in the model should encompass, as a minimum, the calendar day and an atmospheric component. Spatial differences in behaviour were well represented by the 14 extreme regions, obviating the requirement for specific locational components. Smoothing functions within the VGAMs applied to the covariates will reduce the effective contribution of insignificant parameters to zero, allowing a common regional model to be constructed rather than several location specific models. Various measures of temperature and atmospheric circulation were selected a priori for inclusion as covariates in the model to describe extreme daily rainfall frequency and intensity, as these variables are well-predicted by climate models (Christensen *et al.*, 2007); this will be beneficial for future iterations of

the statistical models to project changes to properties of extreme rainfall with greater accuracy than is currently achievable (Fowler and Ekström, 2009).

The analyses presented in this thesis so far have focussed on the monthly NAO index coincident with the event occurrence; and the coincident normalised monthly mean sea level pressure (MSLP) and coincident monthly sea surface temperature (SST), for the nearest 5°x5° grid cells. The response of extreme and very heavy daily rainfall to the coincident monthly NAO index may, however, duplicate those driven by coincident monthly MSLP. Sub-seasonal NAO indices may be more descriptive of the immediate weather rather than atmospheric patterns (Hurrell and Deser, 2009) accordingly, a set of seasonal indices combining the most common winter (Hurrell, 1996) and summer (Folland *et al.*, 2009) indices with new aggregates for spring and autumn were also investigated. A brief exploration of the monthly and seasonal NAO patterns suggested that a spring index comprising April-June and an autumn index of September-October are most appropriate; the November NAO index was found to be more closely aligned with the winter index and is sometimes included in the winter aggregate (Rodriguez-Fonseca and de Castro, 2002). While lagged values of the seasonal NAO index, particularly winter, may be skilful in predicting summer stream flow (Wilby *et al.*, 2004), this is likely due to the influence of winter rainfall on the base flow in groundwater catchments and is not considered as a driver of extreme rainfall. As a result, the NAO indices investigated further as predictors were coincident month and coincident seasonal mean, where seasons are defined as November-March, April-June, July-August and September-October.

Research suggests that monthly SST is strongly correlated with daily rainfall frequency and intensity in the south of the UK (Phillips and McGregor, 2002). SST lagged by up to 6 months and SST anomalies over a wider Atlantic region (Wilby *et al.*, 2002) have also proved to be effective predictors of summer stream flow; all variations were investigated in the VGAM. Although daily air temperature may better represent the atmospheric fluctuations which control the onset of short duration rainfall than monthly measurements, daily data also introduce far more noise, with little improvement in the modelled representation of event frequency or magnitude. Therefore, the VGAMs investigated the dependence of rainfall frequency and intensity on monthly grid box averaged maximum and minimum air temperature, for the nearest 5° UK grid cell, and maximum monthly air temperature range.

The variables examined for importance in the regional VGAMs are listed in Table 8-1.

Covariate	Term	Definition	
Year	T_t		where t is the event
Day of the year	d_t		
Linear seasonality: sine	S_{kt}	$\sin(dt')$	$t' = 2\pi t/365.25$
Linear seasonality: cosine	C_{kt}	$\cos(dt')$	$t' = 2\pi t/365.25$
Event intensity	r_t	x_t-u	Where x_t is daily total
Event occurrence	y_t	y=[0,1]	When $x_t \geq u$
NAO index	N_t		N_t monthly or seasonal
Sea Surface temperature	SS_t		SS_t coincident or ≤ 6 months lag
Normalised mean sea level pressure	SP_t		SP_t coincident or ≤ 6 months lag
Monthly max air temperature	Θ_{TX}		Grid box average maximum
Monthly min air temperature	Θ_{TN}		Grid box average minimum
Monthly maximum range	Θ_{DR}	$\Theta_{TX} - \Theta_{TN}$	

Table 8-1 : Terms used in the Vector Generalized Additive Models

To enhance the reliability of frequency and intensity estimates through the use of a larger data set, VGAMs were applied to regionally pooled rainfall data. Individual station maxima were de-clustered by an interval ≥1day between successive events, selecting the maximum of any wet spell to ensure that only independent rainfall maxima were included in the analyses. Stations were not standardised prior to fitting the Poisson model to Q95 events, as event frequency is a binomial sequence which is directly comparable between stations when a station specific threshold has been adopted. However, the extreme value regional models for event intensity were standardised by the station RMED prior to fitting regional GEV distributions. Given the size of the extreme rainfall regions defined in Chapter 7, it is likely that one storm will be recorded by several stations within a regional pool, either on the same or a consecutive day. However, it has been shown that using repeated events within a pool of hydrological data does not increase the bias in estimates of rate or magnitude, although there is an increase in the standard error estimate (Hosking, 1990; Morton and Henderson, 2008). Thus, event duplicates (following station de-clustering) were not removed as this would unreasonably reduce the size of the data set and negate the advantage of using regional pools for model fitting.

8.2.2 Model Framework

Penalized maximum likelihood methods for parameter estimation, which are the default option in the computer software (Yee, 2011), were used to fit VGAMs to each region. Penalized maximum likelihood is computationally efficient and highly flexible in the

selection of model parameters (Wood, 2000), aiding model parameter interpretation due to the resultant simplicity of the model. A smoothing parameter is not used directly within VGAM for model fitting, rather the maximum model degrees of freedom are specified to achieve a suitable balance between model over-fitting and excessive parsimony. The number of effective degrees (edf) of freedom dictate the response of the term, with edf=1 representing a linear response; the default minimum in VGAM is edf=3 (Yee, 2011). Modified vector backfitting, where $f(x_t)$ is decomposed into linear and non-linear components, was used to fit the smooth functions, to improve the model convergence rate and numerical stability (Yee, 2011).

Three general methods can be adopted to incorporate smoothed functions of the covariates in a GAM :

- all terms are additive of the form $f_1(x) + f_2(y)$ with independent smoothing for each covariate;
- variable coefficients $z + zf(x)$ where x varies smoothly, but its effect is modified by the constant covariate z (Hastie and Tibshirani, 1990);
- bivariate smoothing $f(x, y)$ where x and y vary jointly to represent a more complex interaction of covariates. This option is not available in VGAM.

The smoothing parameters can be fitted with ordinary cubic regression splines, polynomial splines, or linear based natural cubic splines; cubic regression splines are the default option in VGAM and outperformed the other options in efficiency and efficacy. The polynomial smoother over-fitted the model to the data, while linear base smoothers are only valid for use in linear models.

Covariates were included in the model in the order of greatest explanation of data variance. The greatest source of repeatable variability had been identified as seasonality; d_t was, therefore, the first smoothed covariate term. Subsequent model terms were included as combinations of those listed in Table 8-1, dependent on the relative importance, as identified from the model score, and signficance of the correlation between the parameters rainfall frequency. It can be complex to determine which of several, possibly similar, covariates to include within the model as there is a need to balance the overall model goodness of fit against parsimony (Marra and Wood, 2011). Wood and Augustin (2002) state

that a term should be dropped from the model if all three of the following criteria are satisfied:

- the term edf is close to its lower limit;
- the confidence region for the smooth contains zero everywhere;
- removing the term reduces the deviance statistic, or other relative comparison measure such as AIC (Akaike, 1974).

Stepwise iteration to reject unnecessary covariates (Hastie and Tibshirani, 1990) is time consuming, particularly when many covariates are involved, so a modified approach was used where only the significant terms from less complex models were included in later multivariate models.

Parameter link functions were selected automatically within the package to ensure that the Poisson arrival rate, $\Lambda > 0$, and GEV parameters for location, $\mu > 0$, scale, $\sigma > 0$ and shape, $\xi > -0.5$ (Mestre and Hallegatte, 2009); log-link was used here to obtain positive parameters to maintain model stability, although a wide range of other parameter link functions are available. Link functions increase the rate and success of model convergence by avoiding numerical problems, for instance with negative rate parameter estimates, and lead to improvements in the log-likelihood functions and standard error estimates (Yee, 2010).

8.3 Model Fitting and Selection

Parameter definitions for the Poisson-GEV model were initially established from $X_1, \ldots, X_q$ covariates as:

$$\log \Lambda(X) = \beta_{0(1)} + f_{1(1)}(X_1) + f_{2(1)}(X_2) + \ldots f_{q(1)}(X_q)$$
$$\mu(X) = \beta_{0(2)} + f_{1(2)}(X_1) + f_{2(2)}(X_2) + \ldots f_{q(2)}(X_q)$$
$$\log \sigma(X) = \beta_{0(3)} + f_{1(3)}(X_1) + f_{2(3)}(X_2) + \ldots f_{q(3)}(X_q)$$
$$\log(\xi + \frac{1}{2}) = \beta_{0(4)}$$

Equation 8-1

ξ is modelled as an intercept only term with a log link and offset to minimise numerical instability (Katz *et al.*, 2002; Yee and Stephenson, 2007) and satisfy the asymptotic normally distribution and asymptotic covariance constraints of maximum likelihood estimation (Chavez-Demoulin and Davison, 2005). Direct modelling of over-

dispersed event frequency with a negative-binomial distribution, as suggested by Lang (1999), was initially considered but rejected in favour of a Poisson distribution with time-varying rate parameter as being more representative of the physical processes driving event occurrence (Chavez-Demoulin and Davison, 2005). If a sequence of events arrive with a rate Λ_{ij} on day j in year i, the probability of an event on any particular day is approximately zero, and the probability of an event over the whole year is also small $Pr(x) = \sum_{j=0}^{365} \Lambda_{ij}$, following the governing laws of a discrete distribution. Allowing the arrival rate to vary reflects the independence of the maxima and their non-identical distribution throughout the year.

Most regional models were only fitted to a sub-set of stations covering the full record period 1961-2009 to minimise the influence of varying numbers of stations per year in the pool. The only exceptions were Humber (HUM) and Mid Wales (MW) where, due to their small original size, the whole pool was employed. Longer data series were used with the fitted models to examine changes in seasonal behaviour.

8.3.1 Covariate Selection

To compare the relative importance of the different covariates, the initial models comprised a response variable, y_t, representing event occurrence or magnitude, and only one explanatory variable. Table 8-2 summarises the results for a Poisson VGAM fitted in one region; significant variables with the lowest deviance scores are in bold. The results suggest that the SST one month prior to an event (Lag 1) is more powerful as a covariate than coincident SST; the 6-month lag normalised SLP and maximum monthly air temperature range were also found to be powerful covariates. SST achieved the lowest deviance scores although the significance of the parameter varied between regions, with the lowest scoring covariate not always significant at the 5% test level. The importance of air temperature metrics also varied between regions, with minimum temperature or monthly temperature range achieving the lowest deviance scores. Table 8-2 suggests that including seasonality as a rotated statistic (Robson, 1999) is statistically better than the calendar day, as demonstrated by the model scores, but it was found to represent the seasonal cycle poorly and severely increased the computational demand when used in combination with another covariate. The coincident monthly NAO index was found to be more important than its

seasonal counterpart in all regions. The year of occurrence is replicated by variations in the other covariates and so was not selected for more complex model evolutions.

Selecting the most appropriate covariates for the GEV model was complicated by the differing importance of some covariates compared with the Poisson model. In keeping with the orthogonal approach (Coles, 2001), the Poisson model was fitted first to represent event frequency followed by the GEV model using the same covariates for the GEV model as for the Poisson model; this approach aids model interpretation.

Variables were included in the VGAMs in increasing combinations to determine their relative importance or redundancy as interactive terms. SLP was removed from the explanatory variables as it detracted from model performance in combination with all other covariates; the information provided from SLP was also replicated by including the monthly NAO as a covariate. The aim was to achieve the best data representation whilst minimising measures such as the deviance statistic or AIC and, therefore, model iterations included simplifications with covariates included as linear or quadratic terms to improve model parsimony. The final model includes a combination of flexible, semi- and fully-linear covariates. The variables selected for their explanatory power of frequency and magnitude in all regions are: day of year (d_t), monthly NAO index (N_t), lagged monthly SST ($ST1_t$) and monthly air temperature range (Θ_{DR}). Air temperature will be particularly beneficial for adaptation planning using climate projections, as confidence in projections of this variable are much higher than for extreme daily precipitation (Christensen et al., 2007; Fowler and Ekström, 2009). Known relationships with seasonality and the NAO may also aid seasonal forecasting and planning by improving the probability of accurately forecasting one or more extreme events in the year.

The smooth terms from the fully flexible model indicated that only SST required a flexible representation. Therefore, the final model adopted a flexible smoothing parameter for $f_2(ST1_t)$; the other covariates were represented by linear terms (NAO and Θ_{DR}), and a piece-wise linear regression spline or hinge function model for $f_1(d_t)$. Deviance testing indicated that this simplified model was sufficiently representative of the data. A similar iterative approach was adopted for the GEV distribution models to determine the need for flexibility in modelling the location and scale parameters. As discussed in Section 8.2.1, the

shape parameter is notoriously difficult to fit accurately and is often fit as a constant value; when modelling complex multi-variate distributions, it has also been found that allowing the scale parameter, σ, to be flexible introduces unnecessary complexity (Cooley, 2009). Therefore, to minimise computational instability and maintain a degree of parsimony in the VGAM, σ was modelled as an intercept only term. The GEV models were more variable than the Poisson counterparts with respect to the number and nature of covariates: in some regions a parsimonious model constructed from only one covariate achieved the lowest AIC score, while others favoured more complex models. Although the model with the same structure as the Poisson VGAM did not outperform all simpler versions in all regions, it is one of the most representative models where the covariates are all statistically significant and so has been adopted here.

Model	Terms	Effective degrees of freedom						Residual Deviance	χ^2	p-value
		d_t	T_d	N_t	SS_t	SP_t	θ_t			
M1	f(d_t)	11						6512	199	<0.01
M1.01	f(S_{kt}, C_{kt})	11						**2.95**	21243	**<0.01**
M1.1	f(N_t)			11				**1970**	4695	**<0.01**
M1.11	f(N_{sea})			5				3234	4510	<0.01
M1.2	f(ST_t)				11			4.28	84	<0.01
M1.21	f($ST1_t$)				11			**1.99**	68	**<0.01**
M1.22	f($ST2_t$)				11			4.86	91	<0.01
M1.23	f($ST3_t$)				11			5.16	95	<0.01
M1.24	f($ST4_t$)				11			8.4	133	<0.01
M1.25	f($ST5_t$)				11			9	143	<0.01
M1.26	f($ST6_t$)				11			8.8	147	<0.01
M1.3	f(SP_t)					11		1698	4332	<0.01
M1.31	f($SP1_t$)					11		1864	4535	<0.01
M1.32	f($SP2_t$)					11		2044	4644	<0.01
M1.33	f($SP3_t$)					11		1933	4684	<0.01
M1.34	f($SP4_t$)					11		1778	4531	<0.01
M1.35	f($SP5_t$)					11		1831	4516	<0.01
M1.36	f($SP6_t$)					11		**1672**	4469	**<0.01**
M1.4	f(Θ_{TXM})						11	31.5	342	<0.01
M1.41	f(Θ_{TNM})						11	628	1865	<0.01
M1.42	f(Θ_{DRM})						11	**0.87**	30.5	**<0.01**
M1.5	f(Θ_{TXD})						11	**116**	671	**<0.01**
M1.51	f(Θ_{TND})						11	1258	2947	<0.01
M1.52	f(Θ_{TGD})						11	523	30.5	<0.01
M1.6	f(T_d)		4					6793	7.5	<0.01

Table 8-2 : Model summaries and effective degrees of freedom for Poisson VGAM models in EA using individual descriptors to identify the relative importance of different parameters

8.3.2 Final Model Selection

Statistical testing of the VGAM model from four covariates, which achieved the lowest deviance and AIC scores, against a more parsimonious model, dependent only on d_t and ST1, suggested that the difference between the models was negligible and the simpler model should be selected. Comparison of the predicted terms from the models corresponded well with the observations, but the smoothed representation of the covariates differs between each model. The simpler model over-emphasised events occurring at the beginning of the year, while the more complex model better reflected seasonality. As a subjective review of data representation is an important factor in model selection (Villarini and Serinaldi, 2011), the more complex model was selected, using the same model for all regions to ensure consistency.

Poisson and GEV distribution model parameters, listed in Table 8-3, are of the form:

$$\log \Lambda(x) = \beta_{0(1)} + f_{1(1)}(d_t) + f_{2(1)}(ST1_t) + \beta_{3(1)} N_t + \beta_{4(1)} \Theta_t$$
$$\mu(x) = \beta_{0(2)} + f_{1(2)}(d_t) + f_{2(2)}(ST1_t) + \beta_{3(2)} N_t + \beta_{4(2)} \Theta_t$$

$$\log \sigma = \beta_{0(3)}$$
$$\log(\xi + 0.5) = \beta_{0(4)}$$

Equation 8-2

d_t was the most important covariate for most regions and models, explaining 45-90% of the variability; the next most important variable was Θ_t, followed by ST1 or N_t (dependent on location). The importance of NAO was greatest in northern and Atlantic facing regions, while SST dominated in southern regions. Air temperature range was more important than the calendar day in south eastern regions, which tend to receive more summertime convective storms driven by temperature gradient.

Figures 8-1 and 8-2 are examples of the smoothing functions which were fitted to each regional Poisson and GEV VGAM shown here only for the Northern Ireland (NI) region; ±2 standard error bars are indicated by dashed lines. The strong seasonality observed in both the frequency and magnitude of events is well replicated by d_t. The linear term for air temperature range is indicative of a negative correlation between air temperature range and event magnitude or frequency, which is consistent with observations of the most intense rainfall during the summer when the diurnal temperature range is lowest (Zhou *et al.*, 2009). Event frequency has a positive correlation with lagged SST for all regions. The SST relationship

is less well defined in the GEV model, where southern regions have a positive correlation and there is a more variable relationship in northern and Atlantic facing regions.

Region	Estimated Model Terms											
	Poisson					Generalized Extreme Value						
	$\log \Lambda$					μ					$\log \sigma$	$\log(\xi) + \frac{1}{2}$
	β_0	d_t	$ST1_t$	N_t	θ_t	β_0	d_t	$ST1_t$	N_t	θ_t	β_0	β_0
NHI	-1.90	**-1.04**	0.10	0.21	-0.20	0.81	**-0.11**	$2.0e^{-2}$	$-2.5e^{-2}$	$-1.8e^{-2}$	-1.53	-0.47
ES	-0.57	-0.23	0.01	0.05	**-0.28**	0.76	**0.67**	$2.3e^{-2}$	$-2.7e^{-2}$	$-3.5e^{-2}$	-1.46	-0.47
FOR	-0.88	**0.84**	0.03	0.07	-0.34	0.94	**0.12**	$1.2e^{-2}$	$-2.8e^{-2}$	$-3.1e^{-2}$	-1.39	-0.64
SH	-0.64	**-1.07**	0.03	0.25	-0.28	0.93	**-0.17**	$2.2e^{-4}$	$-2.9e^{-3}$	$3.0e^{-3}$	-1.58	-0.63
NW	-1.20	**0.47**	0.03	0.08	-0.23	0.92	**0.12**	$6.9e^{-5}$	$-1.0e^{-2}$	$-5.2e^{-3}$	-1.49	-0.52
NO	-2.91	**0.85**	0.16	-0.14	-0.28	1.06	**-0.19**	$7.9e^{-3}$	$-3.7e^{-2}$	$-3.5e^{-2}$	-1.39	-0.57
HUM	-3.25	**2.39**	0.05	-0.19	-0.24	1.09	**-0.38**	$-2.2e^{-3}$	$-3.2e^{-2}$	$-1.5e^{-2}$	-1.39	-0.54
EA	-2.86	**4.69**	0.07	-0.06	-0.25	0.84	$4.2e^{-2}$	$1.9e^{-3}$	**-0.05**	$-7.2e^{-4}$	-1.37	-0.58
SE	-2.54	**3.37**	0.10	-0.02	-0.31	0.67	**0.39**	$6.2e^{-3}$	$-9.1e^{-3}$	$6.3e^{-3}$	-1.54	-0.41
WC	-2.07	**1.43**	0.06	-0.03	-0.24	0.71	**-0.07**	$2.2e^{-2}$	$-1.5e^{-2}$	$-9.7e^{-3}$	-1.54	-0.61
MW	-2.09	**2.47**	0.01	0.17	-0.29	1.17	**0.51**	$-1.9e^{-2}$	$-1.6e^{-2}$	$-2.5e^{-2}$	-1.56	-0.53
SOL	-0.85	-0.23	0.02	0.18	**-0.27**	1.01	**0.15**	$-5.1e^{-4}$	$-1.0e^{-3}$	$-1.7e^{-2}$	-1.68	-0.45
SW	-1.48	**0.93**	0.06	0.01	-0.26	0.51	**0.14**	$2.8e^{-2}$	$3.0e^{-3}$	$9.0e^{-3}$	-1.58	-0.36
NI	-2.21	-0.15	0.10	-0.03	**-0.20**	1.01	**0.04**	$-1.2e^{-3}$	$-2.0e^{-2}$	$-1.6e^{-2}$	-1.54	-0.46

Table 8-3 : Contributions of atmospheric variables (model term covariates) to distribution parameters, with the most influential covariate highlighted in bold for each extreme rainfall region : North Highlands and Islands (NHI), East Scotland (ES), Forth (FOR), South Highlands (SH), North West (NW), Northumbria (NO), North Ireland (NI), Solway (SOL), Humber (HU), South West (SW), Mid Wales (MW), West Country (WC), Southern England (SE), East Anglia (EA).

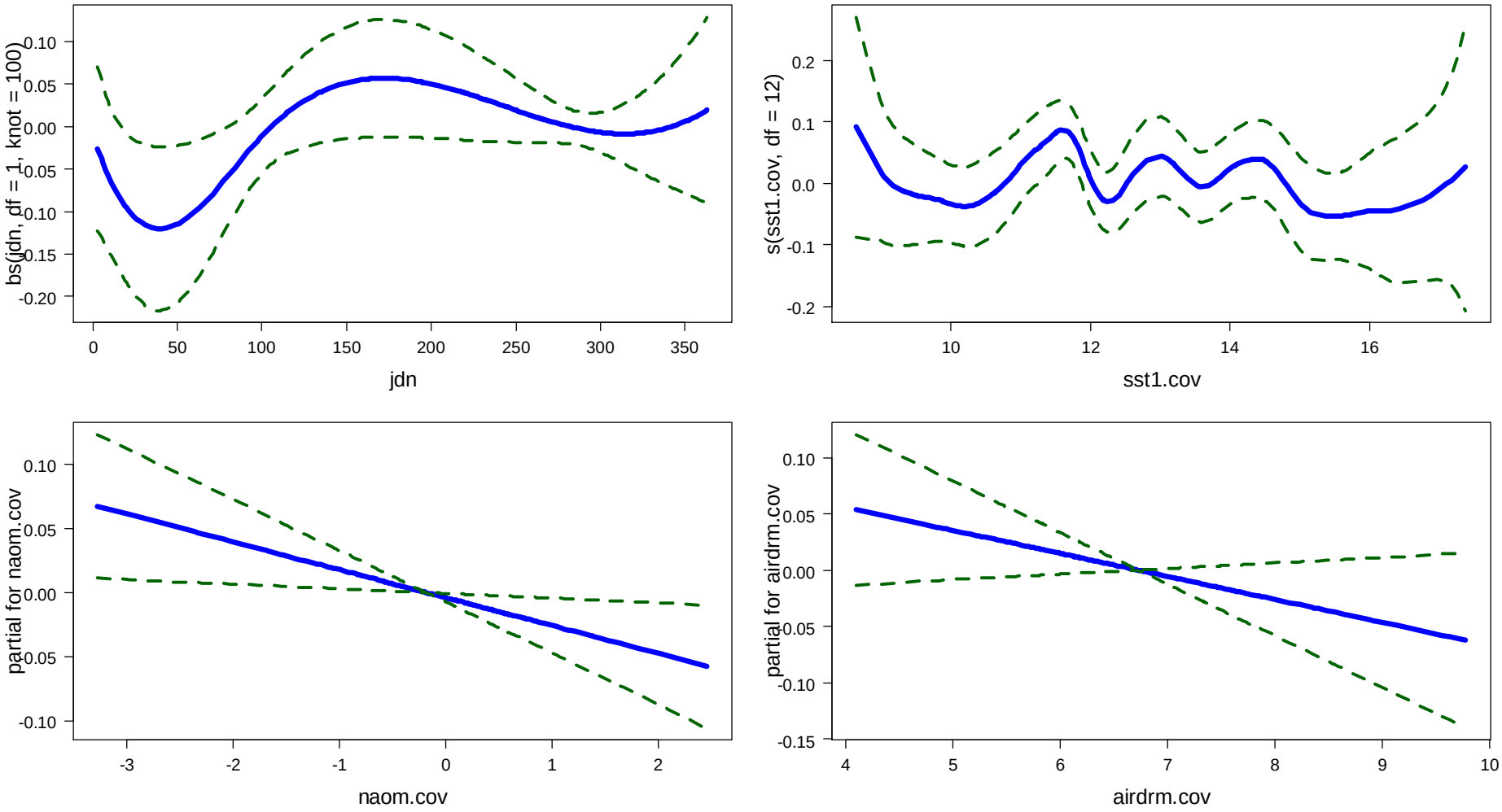

Figure 8-1 : Generalized Extreme Value VGAM fitted to the Northern Ireland Region annual maxima rainfall to model event intensity. Lagged SST (sst1.cov) has 12 degrees of freedom (edf), day of year (jdn) is piece-wise linear centred about a knot at days 100 and 300 and edf=12, NAO (naom.cov) and monthly air temperature range (airdrm.cov) are both linear. The *dashed lines* are ±2 SE bands. From top left going clockwise, the fitted functions are $\widehat{\beta}(d_t), \widehat{f_{1(1)}}(ST1_t), \widehat{\beta}\Theta_t, \widehat{\beta}N_t$

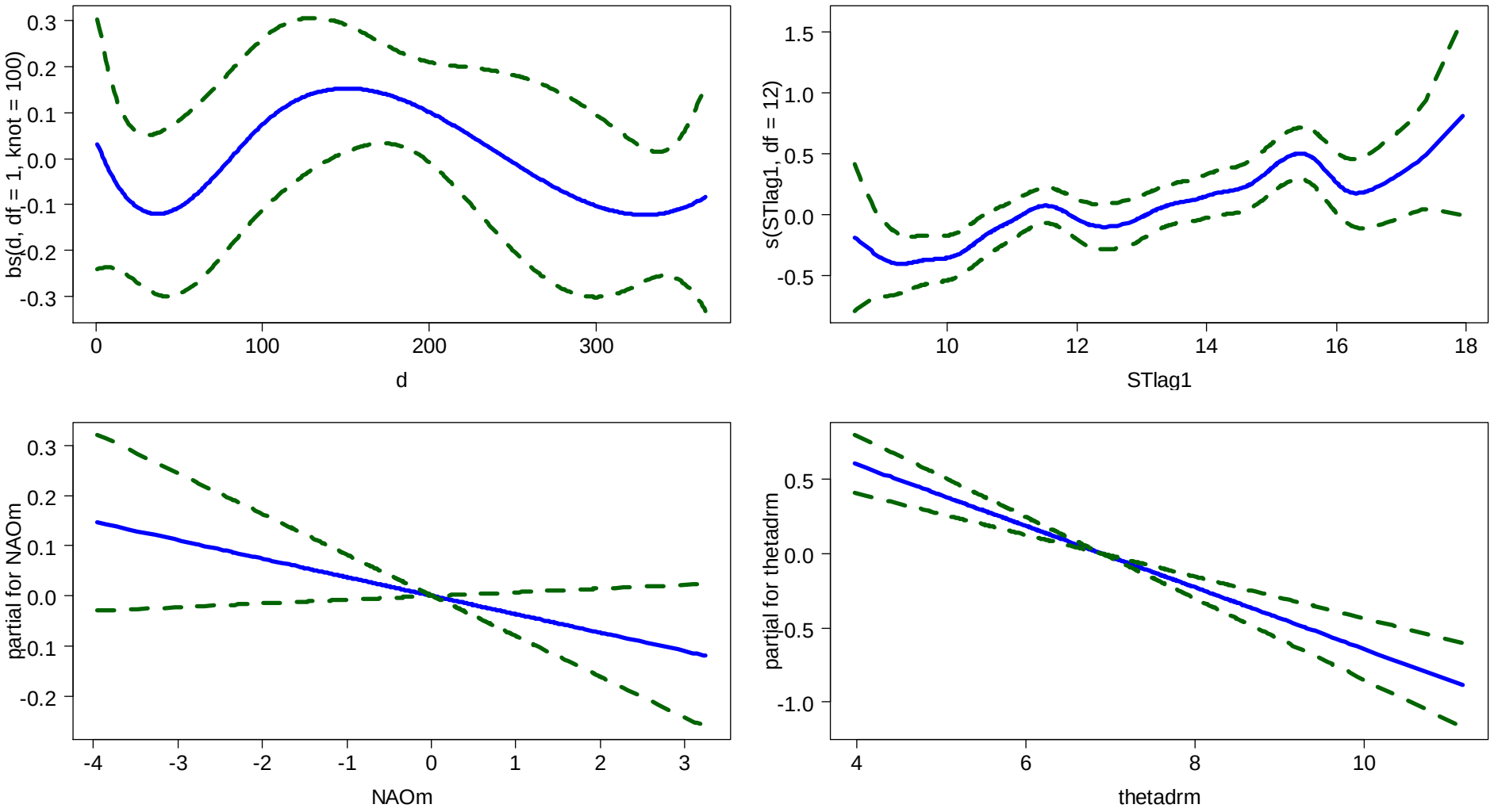

Figure 8-2 : Poisson VGAM fitted to the Northern Ireland Region Q95 rainfall to model event frequency. The terms are a combination of smoothed, piece-wise linear and fully linear functions as for the GEV VGAM. The *dashed lines* are ±2 SE bands. From top left going clockwise, the fitted functions are $\widehat{\beta}(d_t), \widehat{f_{1(1)}}(ST1_t), \widehat{\beta}\Theta_t, \widehat{\beta}N_t$

8.4 Model Verification

The ability of each regional orthogonal point process model to represent observed event frequency throughout the year (the Poisson models) and magnitude (the GEV models) was checked by simulating a large number of events from each VGAM distribution. Hypothesised changes in event seasonality, frequency and intensity cannot be examined if the observed base distribution is modelled incorrectly. Visual tools such as quantile-quantile plots and comparisons of the model outputs with observed data were then used to verify the model's adequacy.

8.4.1 Event frequency and seasonality

Figure 8-3 compares the frequency of observed events per day of year with the simulated frequency using covariate data for the same period of record (1961-2000). The two distributions match well without excessive reproduction of noise (which would suggest an over-fitted model (Wood, 2006)), attaining maximum and minimum frequency in the correct periods. The regional models are able to replicate the observed double peak in event frequency, arising from the interaction and changing importance of the covariates throughout the year. Two regions which are less well represented by the model, MW and HUM, were derived from the smallest data set; each having fewer than five stations with complete records between 1961-2009. However, in both regions the model is able to simulate the correct timing, duration, and magnitude of maximum and minimum event frequencies.

Each VGAM produced a sequence of daily Poisson rate parameter estimates, dependent on the relevant monthly or lagged monthly covariate data; thus, it is not possible to compare the observed and simulated event frequency directly as the latter is the median value from 500 random draws from the appropriate Poisson distribution while the former was an individual observation. Many draws from the simulated distributions were required to characterise objectively the variability present in the observation, and to replicate the randomness with which events may occur given different driving atmospheric conditions. The quantile-quantile plots depicted in Figure 8-4 are derived from the standardised distributions of observed frequency against that simulated from 500 random draws. These show good correlation for most regions, with the exception of SW, ES, NHI and FOR; a few other regions are less well represented at the lower tail of event frequency. As these regions

tend to be dominated by the influence of the North Atlantic Oscillation on storm occurrence and intensity, it is likely that the discrepancies have arisen through the model bias towards SST flexibility rather than NAO index.

8.4.2 Intensity

A similar exercise was carried out for the regionally standardised annual maxima, sampling from the fitted GEV-VGAMs 500 times to establish a range of possible event magnitudes. The results are indicated in Figure 8-5, with standardised observed events plotted within the 95% confidence limits established from the model simulations. Figure 8-6 illustrates the quantile-quantile plots obtained from the same data; these regional plots are generally representative of the observed maxima. As with the Poisson model, tail end maxima are not well represented within one or two regions which show under- or over-estimated maxima; but, for the most part, the confidence bounds surround the desired 1:1 line, with the exceptions of ES and FOR. A likely cause of the discrepancies is the use of a homogenously applied model, which does not apply preferential weighting to covariates in different regions. The disparate nature of station observations within some larger regions, such as NHI, where lack of data precluded further regional sub-division, also has an impact on the regional model fit. The latter may be resolved when regional boundary definitions are improved with additional station information. In contrast, the apparently simple solution to the former, introducing regional weights on different covariates would augment the model complexity as accurate representation would require the weighting to vary temporally in response to different covariate combinations. The potentially limited return for such an increase in complexity was not considered worthwhile.

As a final comparison, annual return period magnitudes were estimated from the simulated model quantiles for each region, using covariate data for 1961-2000, and are shown in Figure 8-7. The shape and steepness of each estimated curve compares well with the approximate growth curves obtained from the observed annual maxima in Figure 8-5. Similarly, the estimated magnitudes for each year and region are close to those obtained in Chapters 6 and 7, providing reassurance that the model is adequate in its representation of event frequency and magnitude.

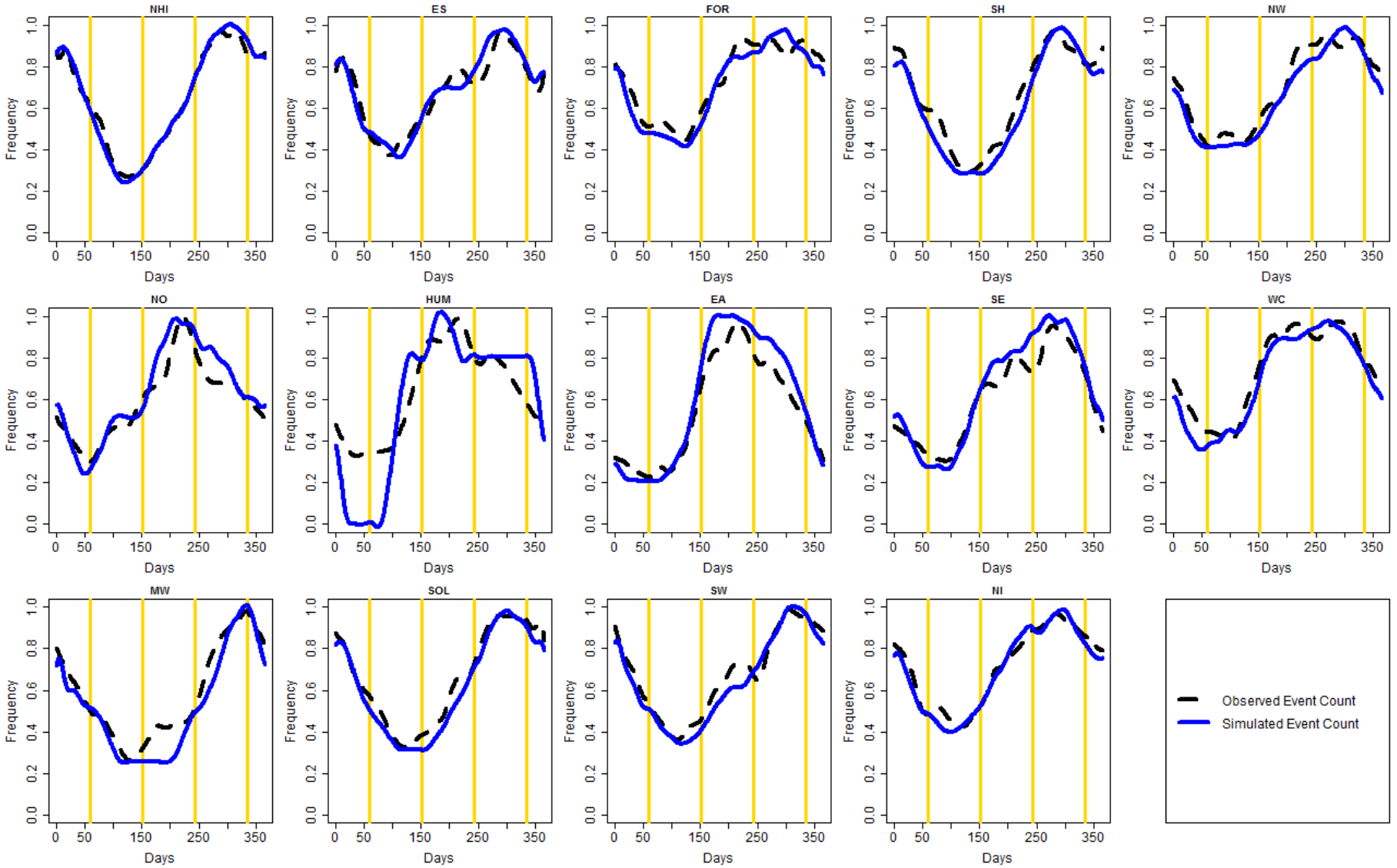

Figure 8-3 : Comparison of mean event frequency per day of year from observations and simulated from the Poisson VGAM

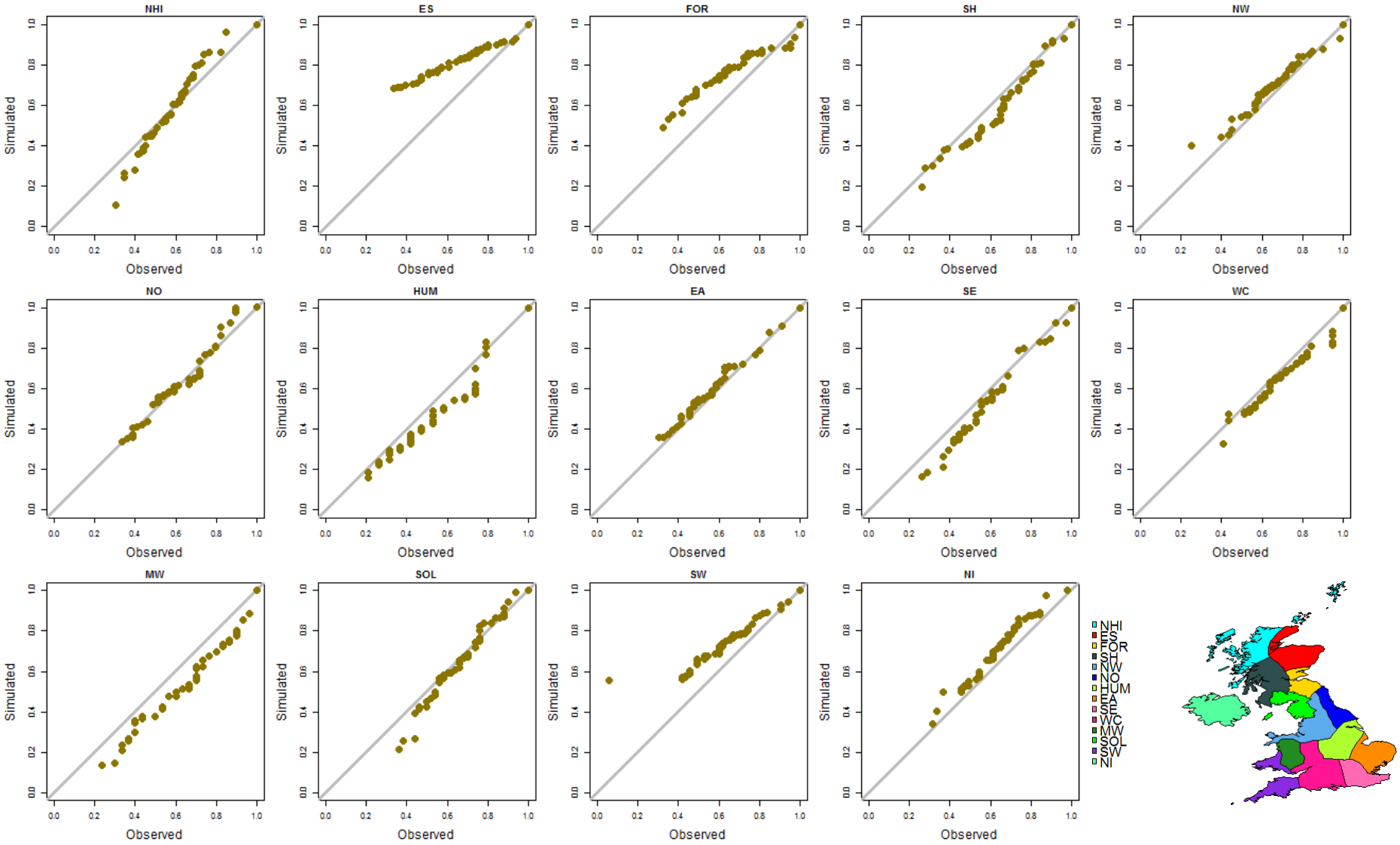

Figure 8-4 : Quantile-quantile plots of standardised frequency from observations and drawn from the Poisson VGAM

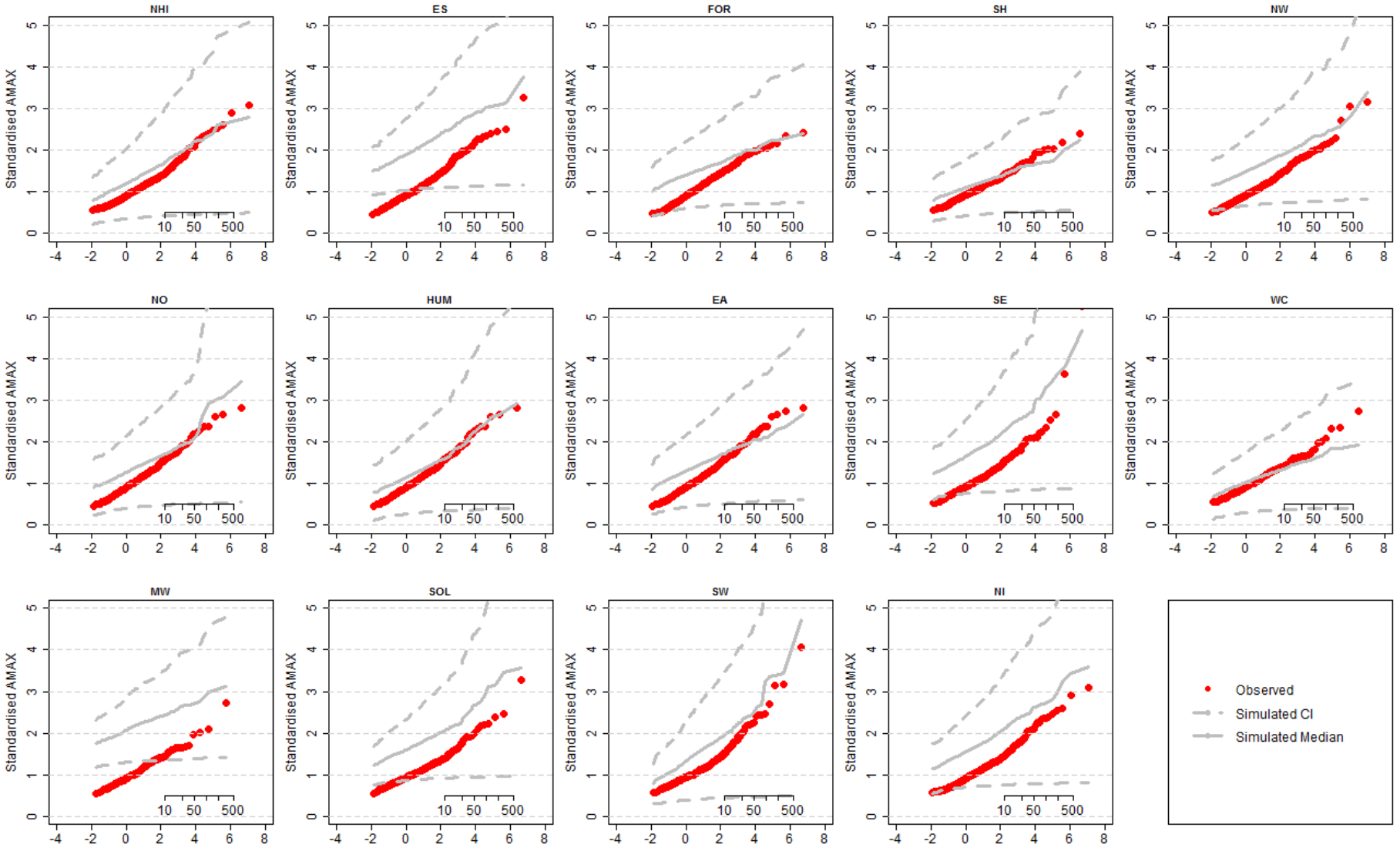

Figure 8-5 : Comparison of standardised regional annual maxima with confidence envelope from 500 simulations of the GEV VGAM distribution

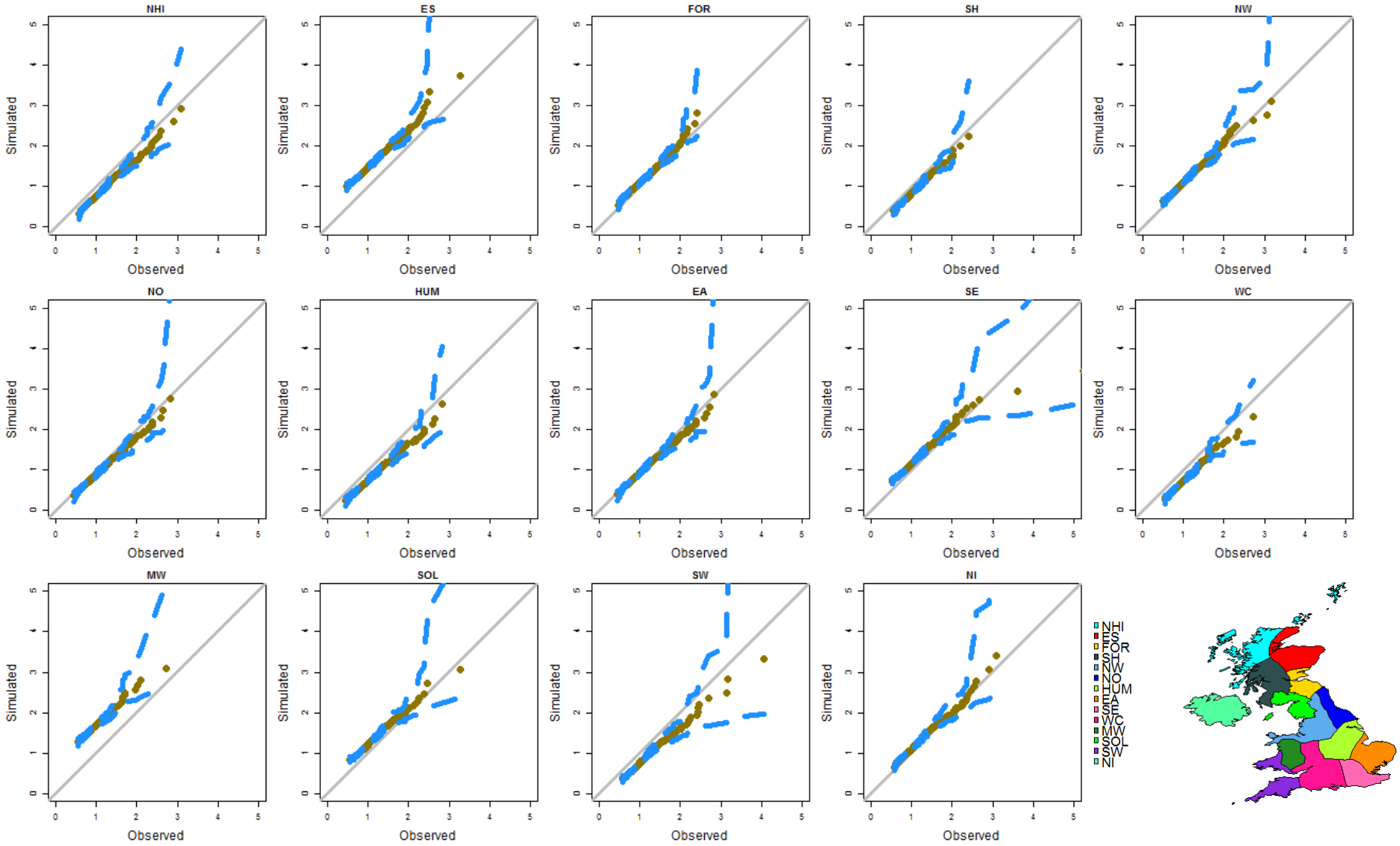

Figure 8-6 : Quantile-quantile plots of observed event magnitude (gold) with 95% confidence bounds (blue) simulated from the GEV VGAM

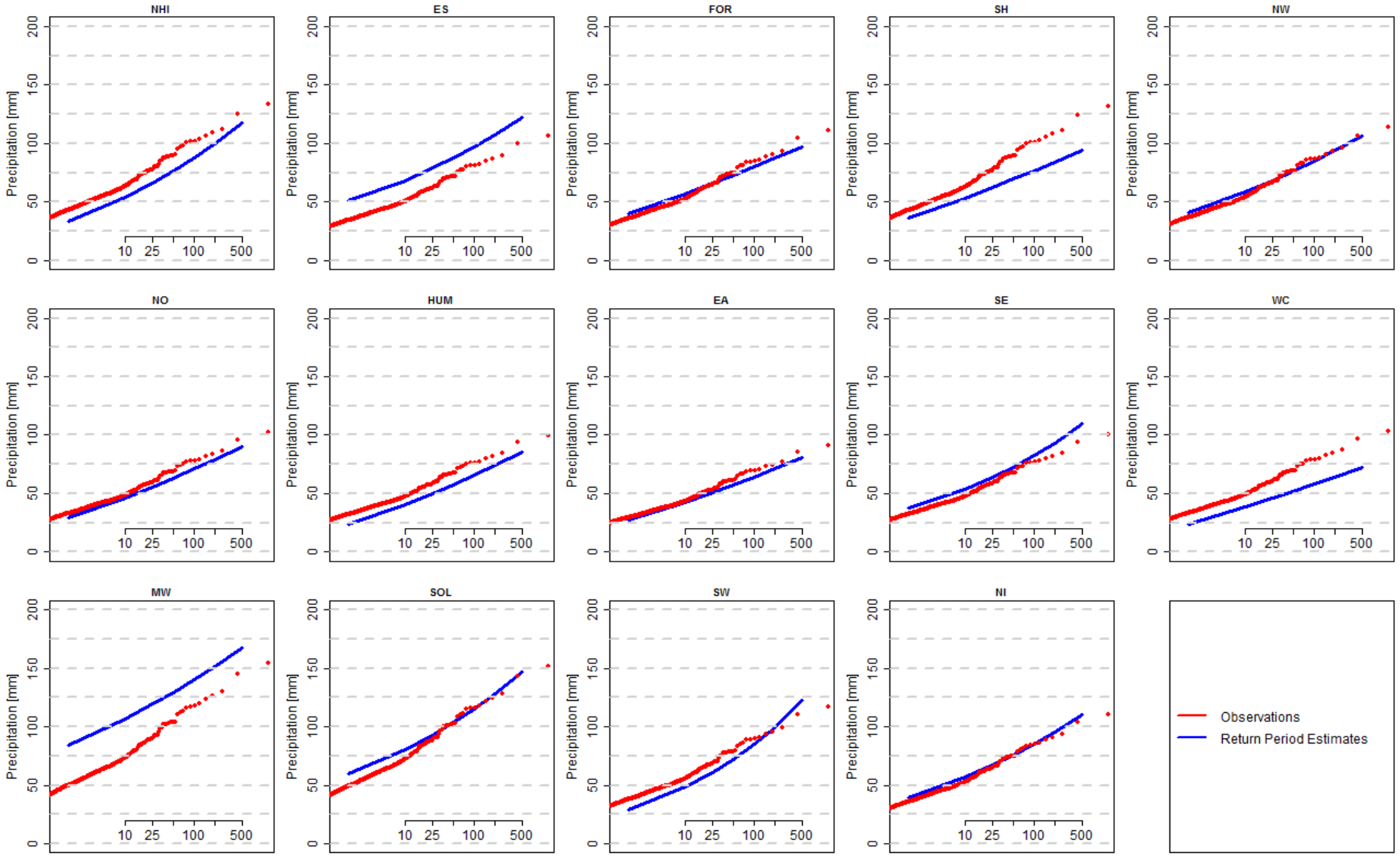

Figure 8-7 : Estimated annual return period magnitudes using parameters estimated from the GEV VGAM for 1961-2009

8.5 Long-term Changes

The visual representation of events per day of year by year presented in Chapter 7, were suggestive of changes in seasonality over the course of the observational record. In some regions there appeared to be a more concentrated period of events, suggesting increases in within-year event clustering, while in others events appeared more dispersed throughout the calendar. Both could have considerable implications on water resource management if true. Although the contoured plots of observed daily frequency shown in Chapter 7 are highly suggestive of changes, the pooled regional plots encompassed only the common period of record for all stations (1961-2000) which is insufficient to determine trends. Monthly observations of SST, air temperature range and NAO for the period 1901-2010 were used as covariates in the VGAMs to test whether these apparent changes in seasonal timing and in within year frequency were true or arose from natural climate variability.

8.5.1 Event Seasonality

The relationships in the Poisson-VGAM model were developed from correlations between regionally pooled observed rainfall frequency and time series of observed covariates for the period 1961-2000. 'Predictions' of event probability per day of each year, both those which occurred and all likely variations given the driving conditions, were obtained by applying the Poisson VGAM to a time series of observed covariate data from 1901-2009. 500 random draws were taken from each of the resultant 39812 Poisson distributions, to accumulate a time series of daily occurrences per year. Day of year vs. year plots per region were developed from the resultant event counts, shown in Figure 8-8 to compare with Figure 7-13. A direct comparison between the two figures is not possible given the scale differences between a series of pooled observations per day and multiple simulations per day. That is, the frequency density per year obtained from the pooled observations (Figure 7-13) reflects the mean value of an empirical distribution with wide confidence bounds; this is also well illustrated by the multiple grey lines on the frequency density plot in Figure 7-11 compared with the regional mean frequency density. In contrast, Figure 8-8 depicts the mean frequency density from a statistical distribution with narrower confidence bounds; therefore, the maximum values do not appear to be as large.

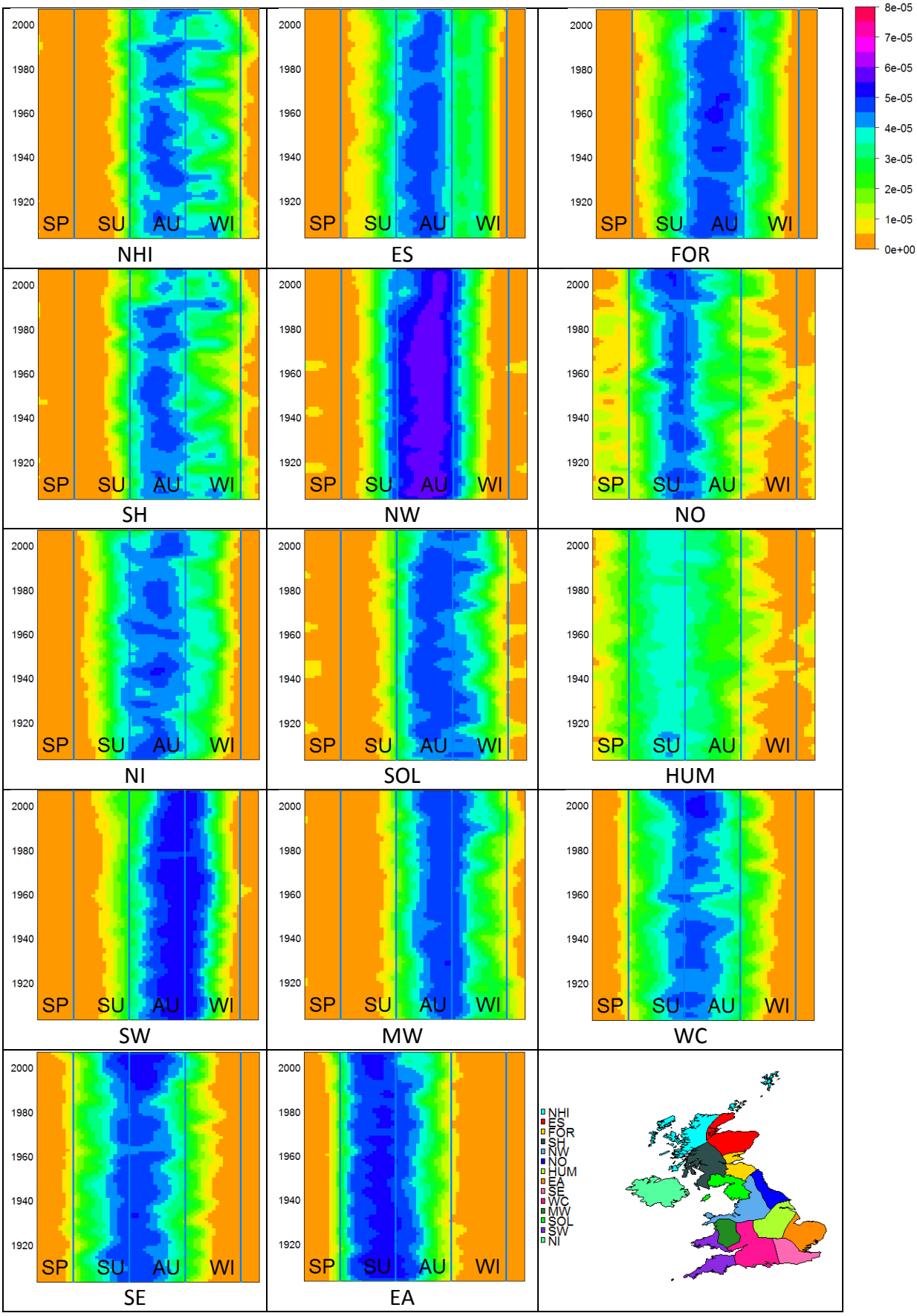

Figure 8-8 : Q95 Events per day of year simulated from Poisson VGAM for 1901-2009. Day of year is shown along the x-axis starting from 1st April. Vertical lines delineate the first day of each season.

Concentrating only on the top third (1971-2010) of Figure 8-8, it is possible to recognise some similarities between the simulations and the observations. For instance the dual seasonality of peak events in some regions is apparent, as is the dependence on atmospheric patterns. Simulation results between 1901 and 1970 reveal that the diagonal shift of observed event frequency (Figure 7-14) from autumn into winter in NHI and EA is more reflective of prevailing atmospheric conditions and cyclic variability, indicated in Figure 8-8 by the repeated pattern over several decades, than a behavioural shift. It is concluded that the apparent changes in seasonality were visual only, and are not significant; this is further demonstrated in Section 8.5.3 with estimates of frequency per day of year.

As suggested by the figures in Chapter 7, many of the regional plots also demonstrate increases in simulated event frequency in the most recent decades - indicated by purple and darker blue areas, at the end of the record, within the deep blue patch. This is suggestive of increased within-year clustering as event probability is heightened in certain seasons, and is formally tested in Section 8.5.3.

8.5.2 Estimated Event Magnitudes

As with the Poisson-VGAM, the relationships in the GEV model were developed from correlations between regionally pooled observed rainfall frequency and time series of observed covariates for the period 1961-2000. 'Predictions' of event intensity per day of each year, both those which occurred and all likely variations given the driving conditions, were obtained by applying the GEV-VGAM to a time series of observed covariate data from 1901-2009 and deriving the relevant distribution parameters. 500 random draws were then taken from each of the resultant GEV distributions, to accumulate a time series of daily occurrences per year which was then cut to form decadal time slices for periods 1901-1910,…,2001-2009.

Estimates of events with specified return periods were calculated for each region using the decadal regional RMED values together with the predicted GEV parameters. Regional RMED estimates were calculated using weighted station AMAX, as in Chapter 6. Where fewer than 5 station AMAX series extended prior to 1961, the station median value was multiplied by its ratio to the 1961-1900 regional RMED value to estimate an equivalent decadal RMED closer to the regional value rather than the station specific value. In those regions which did not have observations prior to 1950, e.g. NHI, the earliest decadal RMED value was adopted for all preceding decades; that is the 1950s regional RMED was also used

for 1900, 1910,… etc. This has resulted in some artificial similarities between earlier decades. The return period estimates by decade are presented in Figure 8-9; return period estimates for rolling ten year groups are shown in Figure 8-10

Eight of the fourteen regions show negligible differences between estimates for each decade. The results reflect those presented in Chapter 6 where changes per decade were not evident in some eastern and southern regions when using fixed decade estimates. For some regions, FOR, MW, SOL and SH, the results are suggestive of an increase in event magnitude over the past century; results which, although not directly comparable, are similar to those presented in Chapter 6. NHI displays a range of return period estimates reflective of cyclic variability, similar to those previously reported in observations and in Chapter 6. In contrast SH and ES indicate decreases in event magnitude over the course of the century. The results for SH demonstrate the importance of using the newly derived extreme rainfall regions, as this result reflects observations reported elsewhere (Jenkins *et al.*, 2010) but contradicts the significant increases for the region presented in Chapter 6.

Fitted standardised GEV distributions from the simulated VGAM parameters, per day of year, are shown in Figure 8-11; there are insufficient observations to estimate RMED per day of year. Some regions display a tendency toward heavier winter rainfall (MW, SW, NHI) and others toward heavier summer events (NO, FOR, HUM), although seasonal differences in magnitude are not as distinct for the whole data set as for event frequency or individual decades. The variability throughout the year reflects changes in the different contributing covariates and their interactions; although the differences do not appear to be as great as expected from the analyses in previous chapters. Changes per decade in the estimated 50-year return period event by day of year, combining the analyses above, are displayed in Figure 8-12. Again there is considerable variability, but little significant difference between each decade.

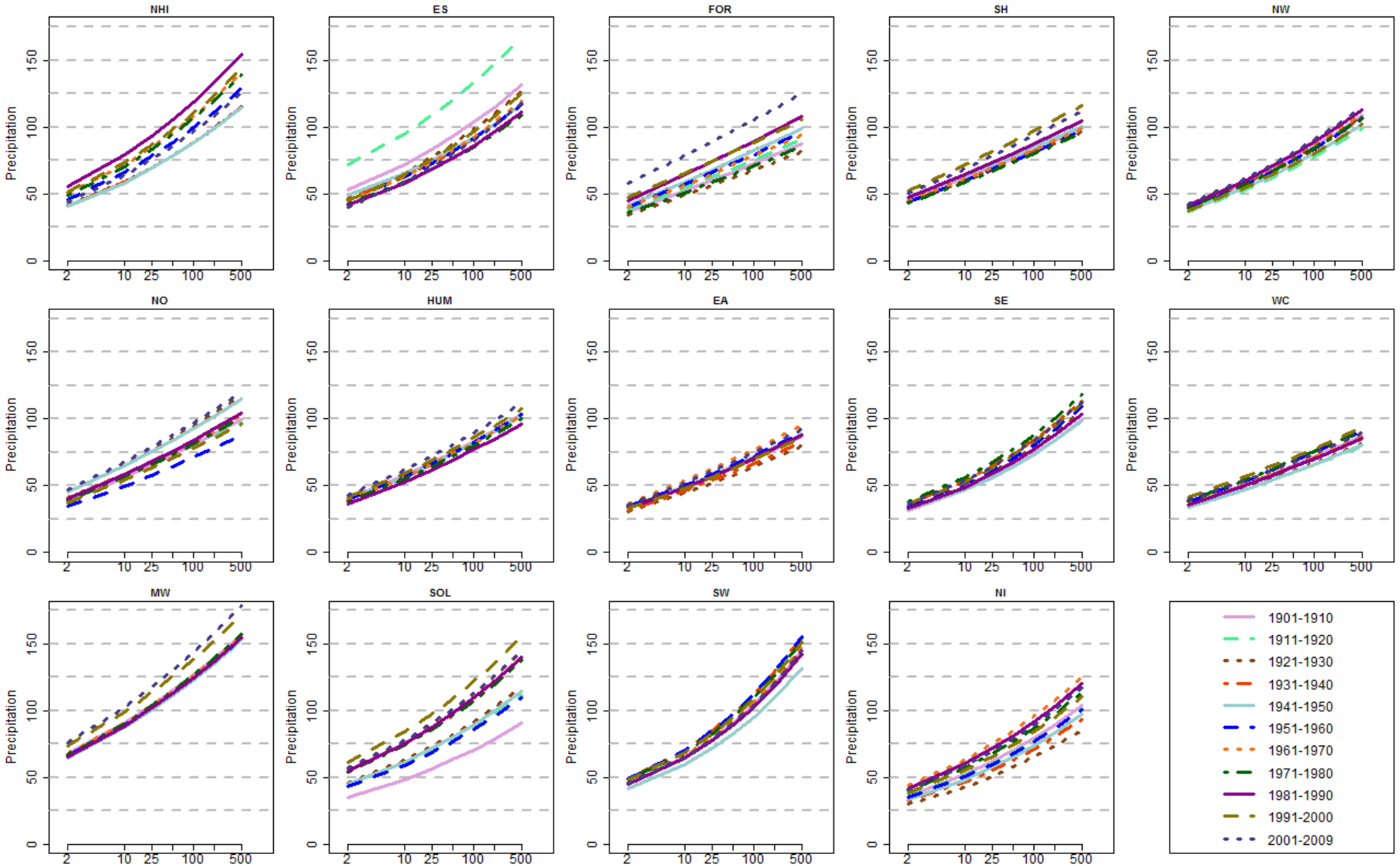

Figure 8-9 : Estimated Annual Return Period Magnitudes using parameters from the GEV VGAM for each decade

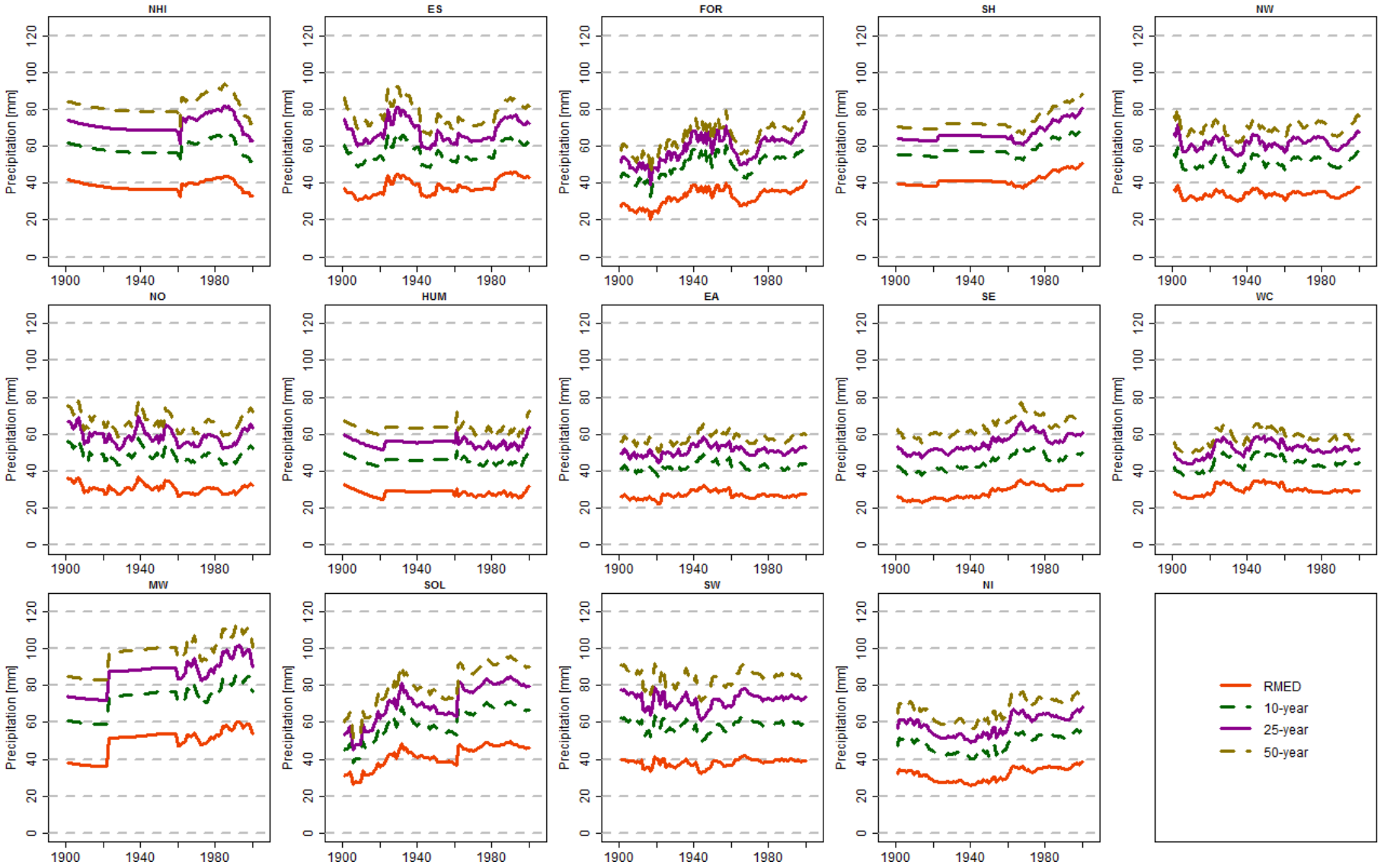

Figure 8-10 : Estimated Annual Return Period magnitudes using parameters from the GEV VGAM for rolling ten year periods

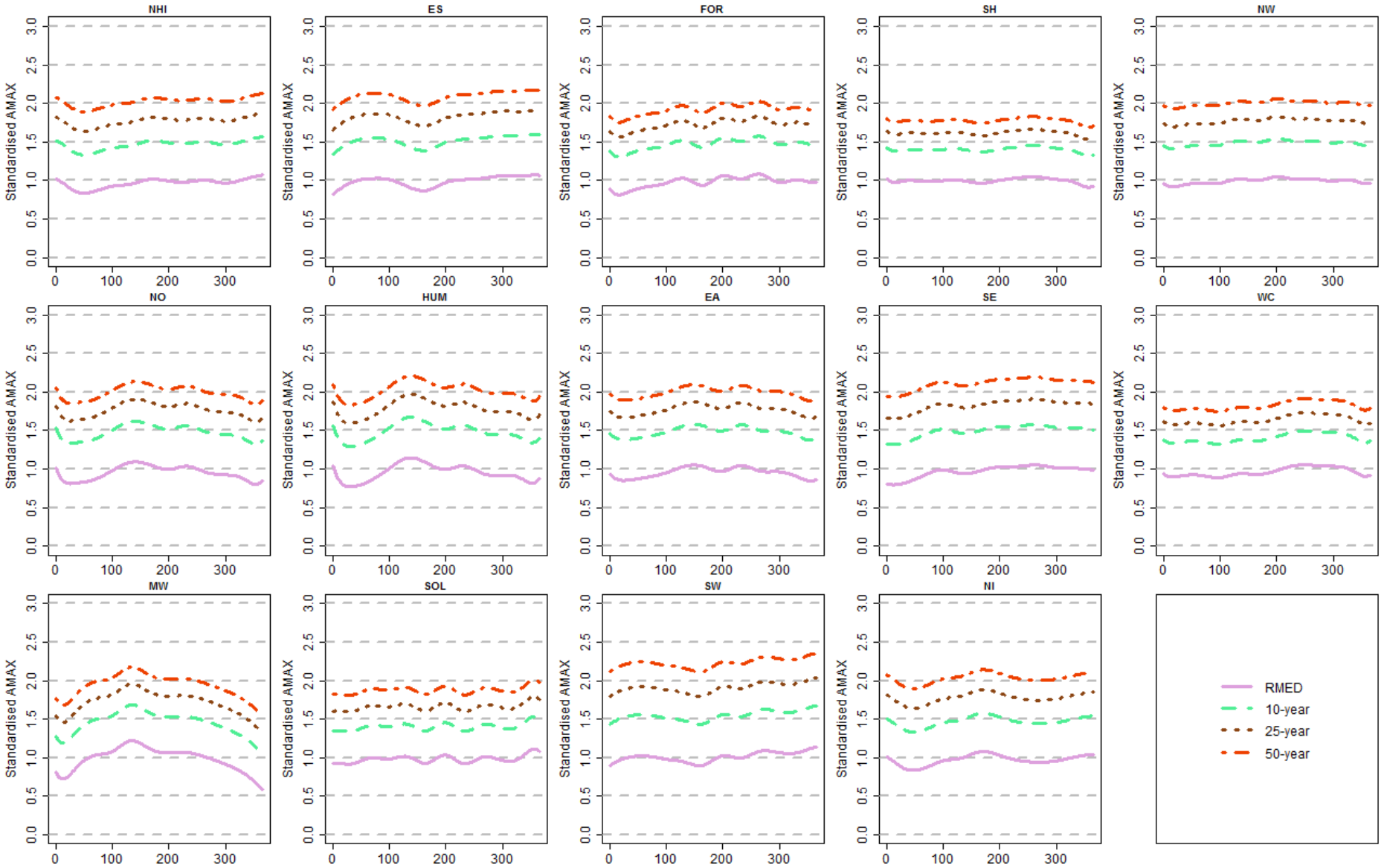

Figure 8-11 : Standardised quantiles of fitted GEV VGAM, per day of year, for events equivalent to 2-, 10-, 25- and 50-year frequency

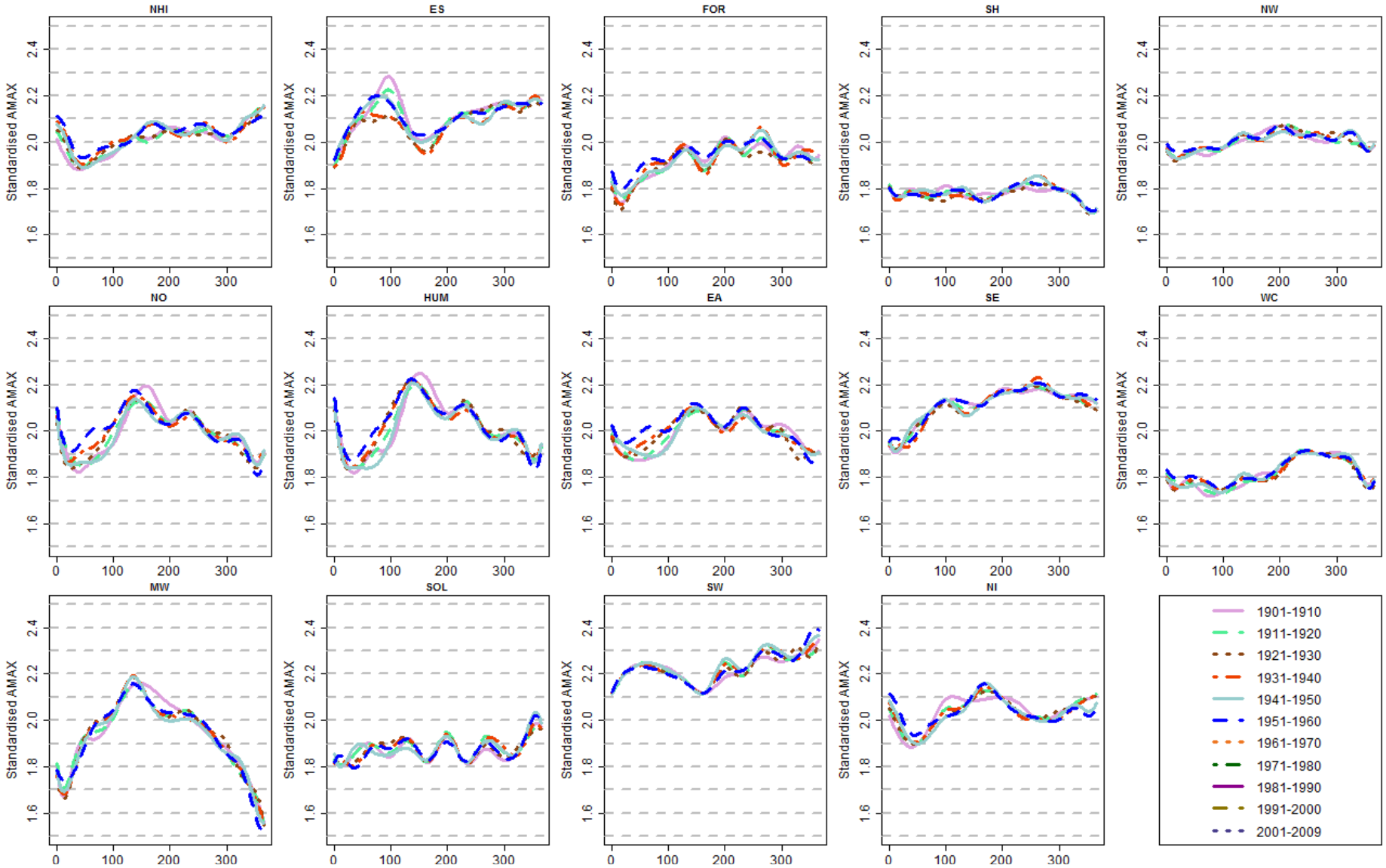

Figure 8-12 : Standardised magnitude estimates per day of year equivalent to the 50-year event, simulated by decade from GEV VGAM parameters

8.5.3 Within-year Clustering

Decadal time series of observed covariates were again used to generate a time series of daily Poisson rate estimates, which were sampled 500 times to assess changes in the daily frequency of events, shown in Figure 8-13. There is more decadal variability apparent in the probability of an event per day of the year than for the equivalent return period estimates, although the differences between decades are statistically negligible. Regions with the greatest variability in the timing of the peak event frequency seem to repeat the patterns from Figure 8-8 where cyclic patterns were apparent in the frequency and spread of events over the year. The minor differences between the daily probabilities for each decade confirm that the period of higher probability of events has not changed shape or timing. It is concluded that apparent changes in seasonality are not significant; the relative probability per day of year is distributed according to a non-homogenous Poisson process, dependent on calendar day and varying atmospheric patterns.

While there is no significant temporal change in the relative probability per day, the actual probability of an event per day may have increased, leading to enhanced within-year clustering. The most frequent day of observed maxima ($\bar{\theta}$) was calculated from rotated seasonal statistics (Robson, 1999); this tallies with the period of highest frequency obtained from many simulations. The combination of monthly observed covariates and $\bar{\theta}$, which averages to a period of several days around the actual day, approximate the conditions of highest event probability per year; any increase in event probability in this period equates to heighted probability of consecutive extreme events and, hence, clustering. The predicted values of Λ for each region on $\bar{\theta}$ per annum were simulated from the Poisson VGAM, and plotted in Figure 8-14 with the smoothed event probability, from a five year running mean. Several regions (NW, HUM, WC, SW) have no significant changes over the 109 year simulated series, despite considerably variability. Others appear to fluctuate with a peak in the central period (ES, FOR, SOL) or at either end (EA). A simple linear trend analysis in SE implies that there is no increase in event frequency, although inspection of the running mean contradicts this. Three regions (NHI, SH, NO) have significant increases in event probability on $\bar{\theta}$, confirming that the probability of several events occurring in rapid succession (clustering) has increased.

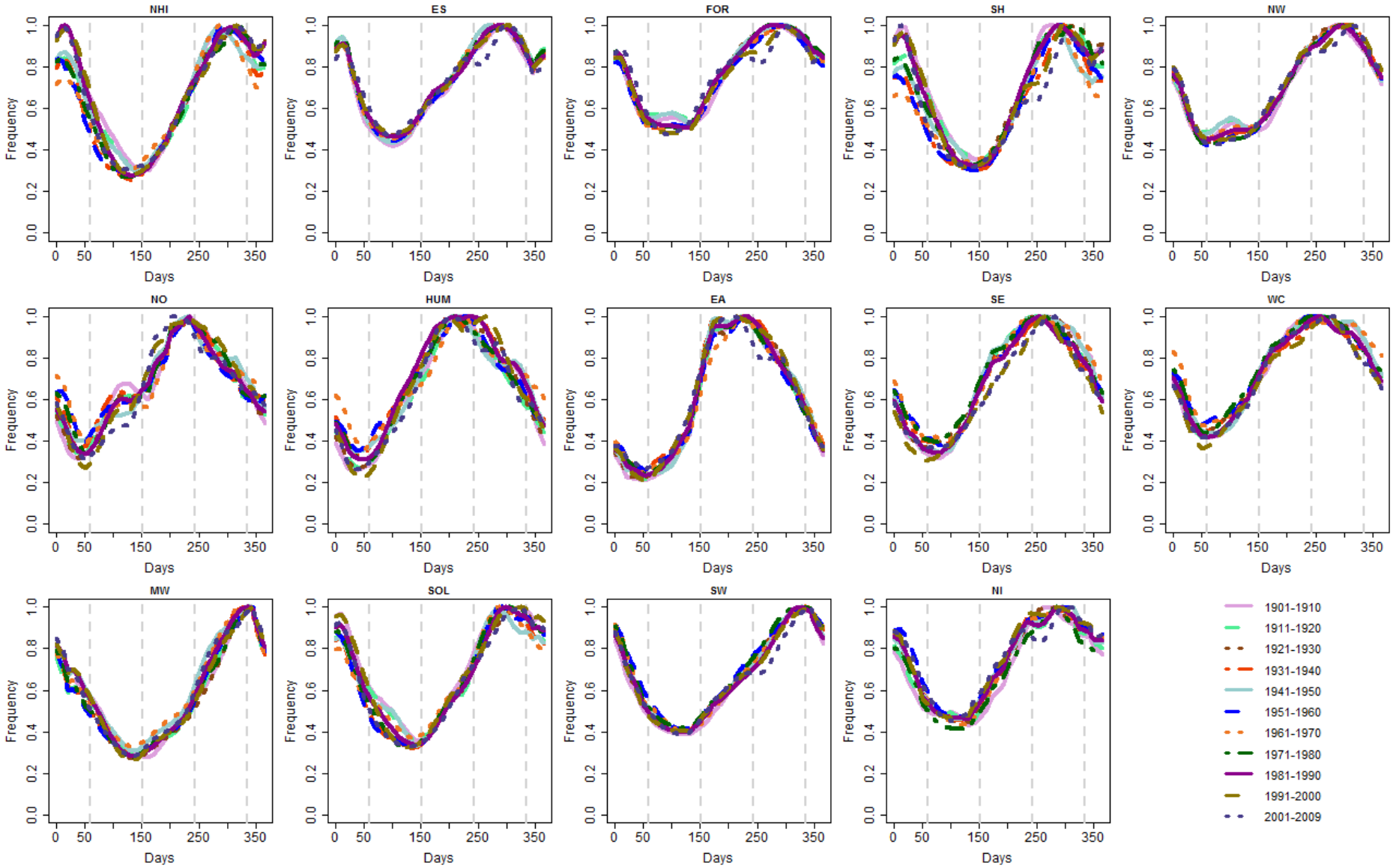

Figure 8-13 : Predicted event frequency per day of year simulated per decade from fitted Poisson VGAM

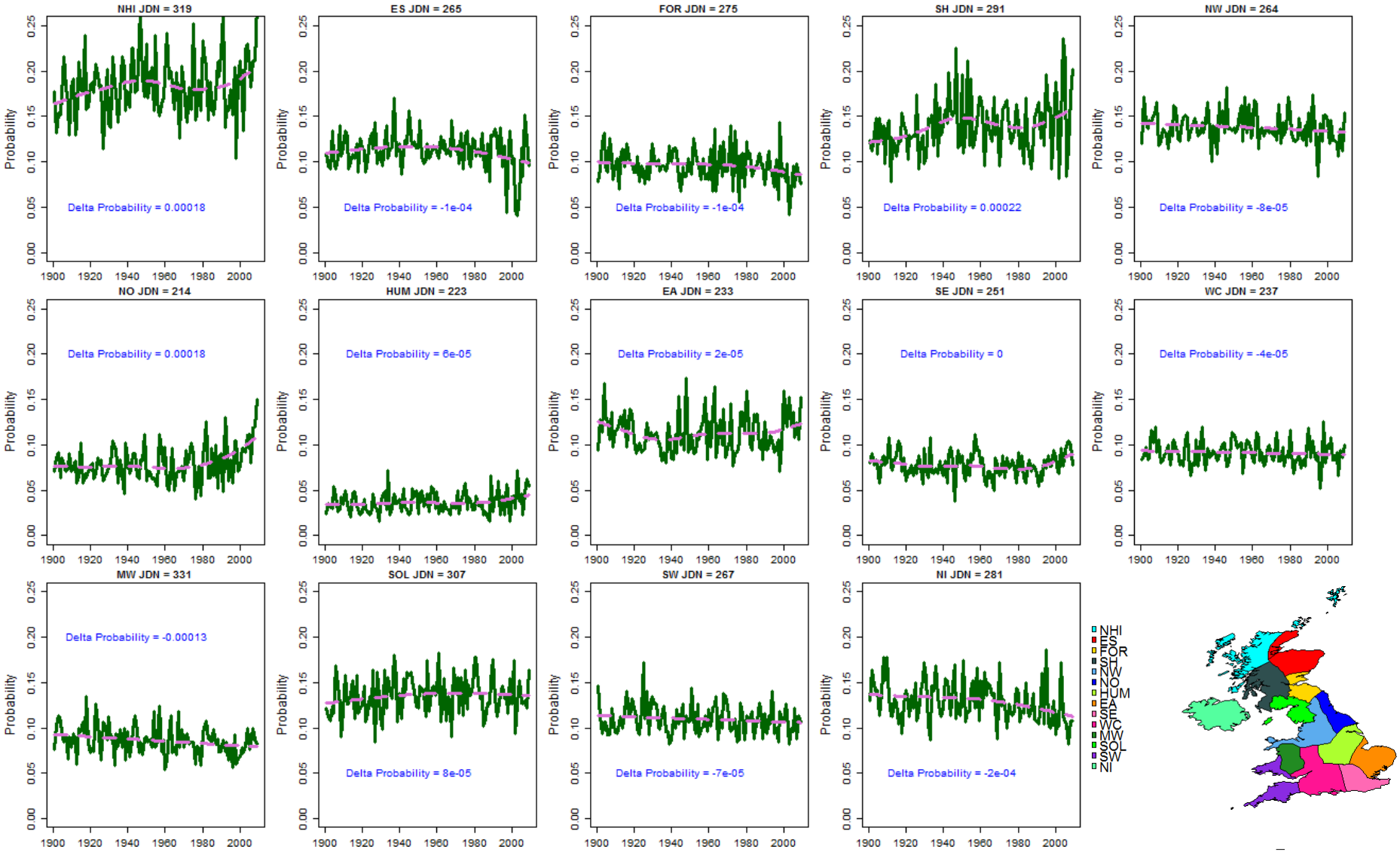

Figure 8-14 : Simulated annual changes in probability on the day of the year with the highest probability of event occurrence (Selected JDN From $\bar{\theta}$), with smooth fit and linear trend estimate in pink.

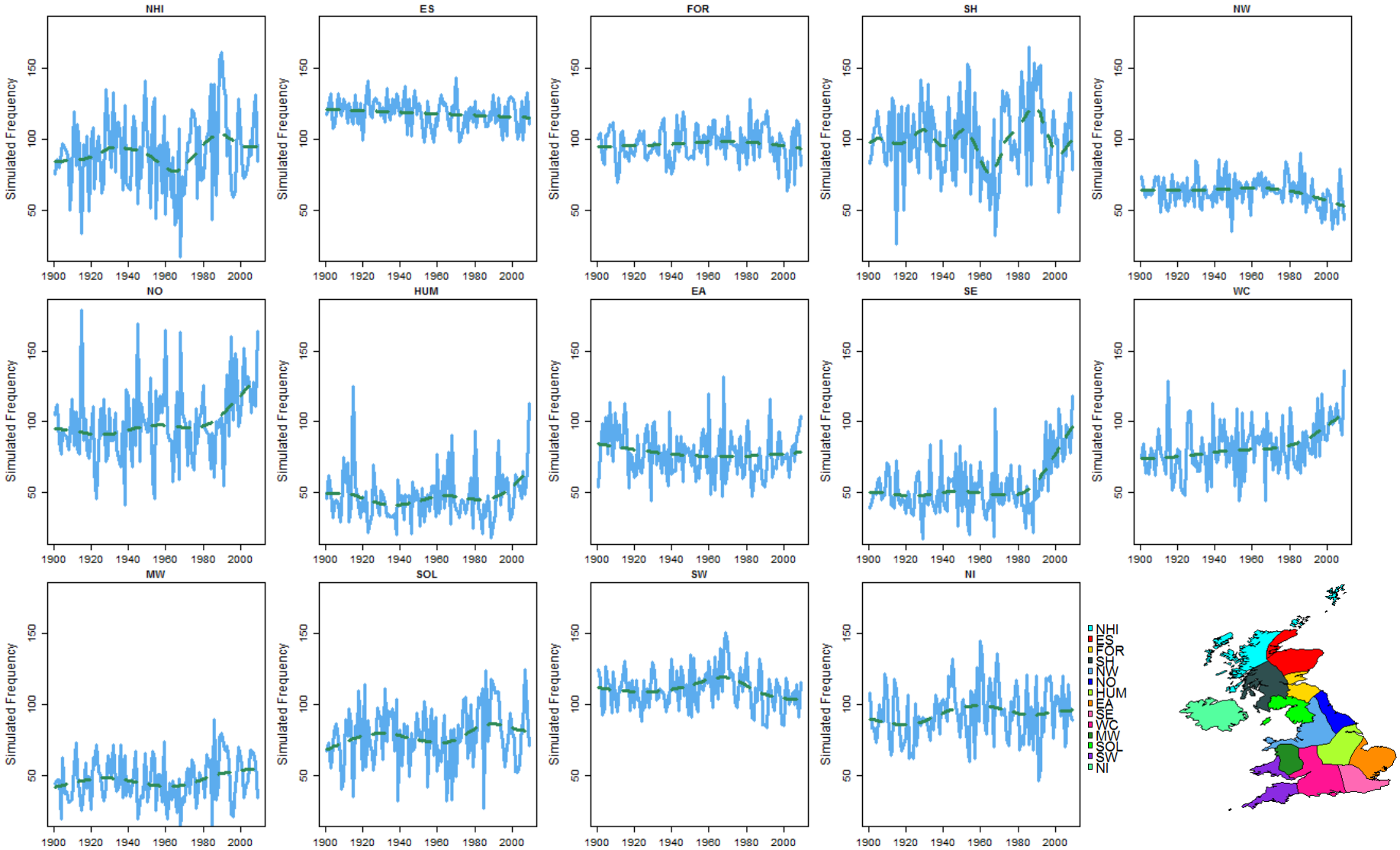

Figure 8-15 : Changes In Event Frequency Per Year From 500 Random Draws Per Year From Fitted Poisson Distribution

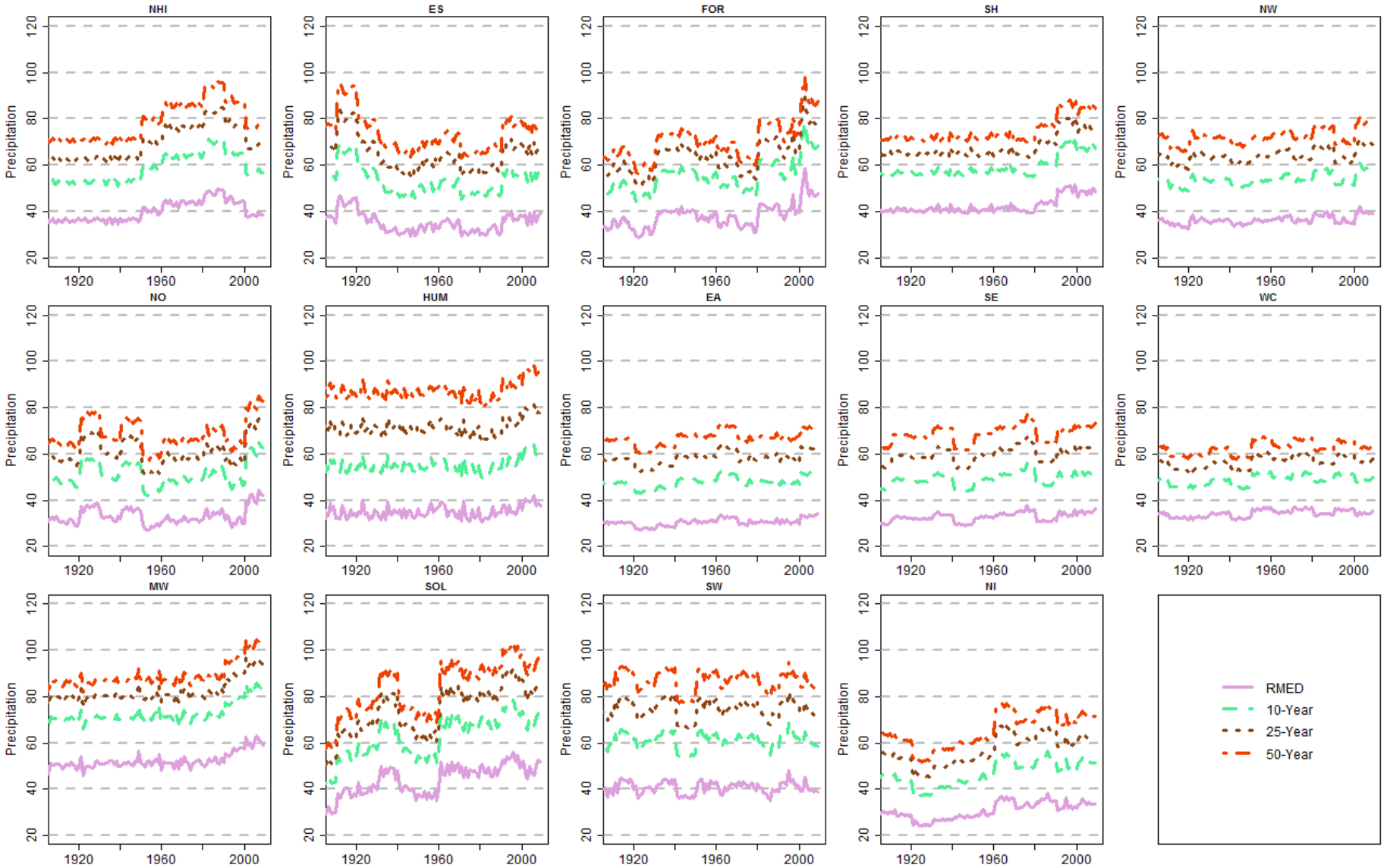

Figure 8-16 : Simulated annual changes in event magnitude on the on the day of the year with the highest probability of event occurrence (Selected JDN From $\bar{\theta}$)

500 samples were drawn from each of the daily individual Poisson distributions with the cumulative total per year plotted in Figure 8-15. This shows a significant increase in event frequency in 8 regions, again demonstrating enhanced clustering. It is hard to distinguish common regional patterns in the changes, for instance sensitivity to SST driven events, although there is possibly a north-south difference with increased clustering in the north.

Figure 8-16 illustrates estimates of event magnitude on $\bar{\theta}$ per annum using fixed decade estimates of regional RMED value, as employed in Figure 8-9. As before, the decadal estimates of RMED have influenced the apparent return period magnitudes in regions with insufficient observations (NHI, MW, SH). The influence of very large events in individual decades on regional RMED estimates is also visible, in addition to cyclic variability in the driving processes. Changes in event intensity appear to parallel those in event frequency, with regions demonstrating significant upwards trends in frequency also increasing in magnitude.

8.6 Conclusions

Allowance for non-stationarity in regional rainfall or flood estimates has been addressed by the research community, but is far from common practice (Jakob *et al.*, 2011). This chapter has presented a new approach to accommodate non-stationarity in frequency and magnitude estimates. Allowing the parameters to vary temporally, in response to external covariates, represents the non-identically distributed nature of independent rainfall maxima over the course of the year and over several different years. A Vector Generalized Additive Model for Poisson and GEV distributions, dependent on external covariates such as sea surface temperature, was developed to allow for the non-stationarity in observed event intensity and frequency to assess apparent changes in the distributions; this is an effective method to address the stationarity paradigm (Milly *et al.*, 2008; Lins and Cohn, 2011). Fitting a statistical model to observed data enabled the use of observed atmospheric and meteorological conditions to simulate event probability many hundred times to establish whether the observed responses were random or part of a longer term change. In combination with regional climate projections of the covariates, the models could be used to assess likely future changes in extreme rainfall intensity and frequency.

8.6.1 Model Development

Many different parameters were investigated for use in the VGAM using covariate information identified in previous chapters; the final model incorporated four components of varying flexibility. Model summaries and deviance statistics were used to confirm the importance of each covariate in the model, as well as their adequacy in representing observed data. To aid model interpretation, an orthogonal point process of Poisson and GEV distributions was adopted, with the same base covariate set, to estimate event frequency and magnitude.

The contribution of each covariate to the estimated parameters confirmed that calendar day is the principal driver of event frequency, with monthly air temperature range having second most importance; calendar day and air temperature jointly encompass the twin seasonality in event frequency demonstrated in several regions in Chapter 7 as air temperature is, perforce, seasonally driven. SST and NAO differ in importance between regions, displaying a north-south divide with northern Atlantic regions dominated by the NAO and south eastern regions by SST. Calendar day was also the most important covariate in the GEV model in all but two regions, which are known to be more responsive to SST driven summer convective storms. The balance between the remaining three covariates was more equal in the GEV model than in the Poisson model.

A negative relationship exists in the models between monthly air temperature range and both event frequency and magnitude. This parallels the observed relationship between frequency and magnitude of summer convective events (Zhou *et al.*, 2009) and confirms that the probability of extreme rainfall is higher, and events are more likely to be intense, during times of elevated temperature when the diurnal temperature range is at its lowest. Climate projections suggest that increases in global mean temperature will also bring a reduction in diurnal air temperature range (Christensen *et al.*, 2007). In combination with the positive relationship with SST, this implies that short duration rainfall will increase in frequency and intensity with increases in global mean temperature.

8.6.2 Results

The Poisson and GEV models were tested for their adequacy using a variety of statistical and subjective tools (Villarini and Serinaldi, 2011). The Poisson models replicated the observed frequency well, without over-fitting the model, and the regional GEV models

reproduced event maxima satisfactorily. Weaknesses in the two distribution fits were observed in the two regions containing the smallest input data set, but both still replicated the key periods of peak event frequency and estimated magnitudes well.

Long term changes in event frequency and magnitude were tested from many hundred simulations from the distributions parameters. Tests for changes in daily event frequency per year concluded that there was no significant change in very heavy rainfall seasonality from 1901 to 2009. However, the probability of a very heavy rainfall event on the day of the year with the highest probability of event occurrence has increased significantly in at least 8 regions, resulting in enhanced within-year clustering.

Event magnitude characteristics confirmed that seasonal signal differences in magnitude are less apparent than for event frequency; primarily due to the additional variability introduced by the NAO. The changing interactions between the driving covariates justify the use of an additive structure, to allow the importance of different signals to vary over the course of the year. Changes in magnitude were assessed by decade, finding increasing trends in event magnitude in only seven regions. However, the dependence on SST and air temperature is indicative of likely increases in event magnitude in all regions with projected increases in SST.

8.6.3 Uses

The relationships between atmospheric circulation patterns, temperature and extreme rainfall established with this statistical modelling technique could be of benefit in many applications. The models could be employed in conjunction with seasonal forecasts of the NAO and temperature indices to aid water resource management on an annual basis: for instance, controlling water levels in reservoirs during years likely to receive many intense rainfall events.

Climate change adaptation plans are often unclear about the implications of projected changes in extreme rainfall frequency and magnitude. The models developed here could be used with RCM outputs as the driving covariate set to assist adaptation planning, by improving projections of the likely changes in very heavy rainfall event frequency and intensity. Secondary impacts of changes in water resources, such as the consequences to agricultural practices or health impacts could be evaluated more effectively with better projections of the rainfall extremes.

Improvements to statistical downscaling for regional climate models adopt a two-pronged approach: enhanced model resolution and using improved input parameters. Refined understanding of the interactions between rainfall extremes and driving mechanisms could assist model parameterisation and so lead to improvements in regional climate projections.

8.7 Computer Packages

The packages used for analyses in this chapter were VGAM (Yee, 2011), extRemes (Gilleland *et al.*, 2009) and plotrix (Lemon, 2006).

Chapter Nine Conclusions

"Human history becomes more and more a race between education and catastrophe."

H.G. Wells, The Outline of History

9.1 Summary

This thesis has investigated changes in the temporal behaviour of UK extreme and very heavy daily rainfall through analysing different extreme metrics and responses to large scale atmospheric and oceanic drivers and correlated responses (temporal and spatial). The temporal patterns which were examined focussed on the frequency and temporal proximity (or clustering) of events both within-year and over several years. Characterising extreme rainfall responses, both frequency and magnitude, in relation to larger atmospheric circulation patterns, enabled the current behaviour of extreme rainfall events to be understood in the context of natural climate variability and climate change. Furthermore, by using climatological observation series which are well represented in Global Circulation Models and Regional Climate Models (GCM, RCM) it should be possible to improve projections of extreme rainfall intensity and frequency through enhanced statistical downscaling and facilitate more effective adaptation action planning in the hydrological domain. In a similar manner, improved understanding of the drivers of extreme rainfall should lead to better representation of extreme rainfall within GCMs and RCMs, by using comparative relationships between the atmospheric circulation patterns and extreme rainfall in the models and in the observations to enhance the models.

A coherent grouping of the extreme rainfall records was required to identify spatial patterns in extreme rainfall behaviour, and the responses to atmospheric circulation patterns. To this end a new set of extreme rainfall regions was developed using typical characteristics, such as the timing and magnitude of extreme events. The 14 regions are the first to encompass the orographic and atmospheric spatial differences of extreme daily rainfall characteristics for the whole of the UK.

Statistical models were developed from the relationships between the driving oceanic and atmospheric circulation patterns and observed extreme rainfall frequency and intensity in each of the 14 regions. These models were used to explain observed randomness in extreme rainfall frequency and magnitude as a result of natural climatic variability and to quantify

apparent trends in the observations. This is the first time that such models have been used to identify changes in within-year event frequency (clustering) and to test trends using time series of the observed drivers to "generate" daily event frequency and magnitude for each year of a 110 year series. No trends were found in the seasonal patterns of extreme and very heavy daily rainfall event frequency, identifying instead considerable randomness and natural variability. However, an increased probability of extreme rainfall events, during the period of the year when most extreme rainfall events occur, was identified which is suggestive of increased event clustering; this will have considerable implications for current flood risk management and with respect to future climate change.

The earliest chapters outlined the context of the project and the tools to be employed in the analyses of extreme and very heavy daily rainfall described in later chapters; while later chapters assessed trends in extreme rainfall behaviour, and characterised the responses to atmospheric and oceanic circulation patterns. The principal conclusions are:

- Extreme and very heavy rain days in the UK display a distinctive seasonal pattern in their frequency, with regional differences in the timing of the peak period.
- The probability of extreme and very heavy rainfall events within those peak periods is increasing, resulting in amplified within-year clustering of events.
- Seasonal characteristics for event magnitude are less clear primarily due to the additional influence of the North Atlantic Oscillation (NAO). The NAO enhances the variability of event frequency and intensity in Atlantic facing regions; in southern and eastern regions the effect is moderated by sea surface temperatures, which reduce the variability in event frequency.
- Changes to annual estimated event magnitudes are also uncertain. This is thought to be a result of the variability in their driving influences. There are statistically significant increases in five (of fourteen) regions, decreases in two and no change in the remainder.
- The strong dependency of UK extreme daily rainfall on monthly air temperature and lagged sea surface temperature is suggestive of likely future increases in frequency and intensity under global warming.

The remainder of this section synthesises the results from each chapter, then discusses the likely impacts of future changes. The chapter concludes with possible extensions to this thesis.

9.1.1 Development of a comprehensive data set of UK daily rainfall

A review of UK daily rainfall data sets revealed various inadequacies, leading to the development of a new comprehensive set of daily rainfall observations extending to 2009. The data set comprises 223 stations, each with a minimum record duration of 40 years, distributed across the UK, and spanning the period 1856-2010 with a latest start date of 1961; 19 stations cover only the period 1961-2000. A regional frequency analysis (RFA) was used to test the sensitivity of regionally pooled statistics to the number of gauges included in the pool, confirming that ≥5 stations are required for reasonable extreme value estimates and that confidence estimates stabilise for ≥15 stations (Hosking and Wallis, 1988).

Data processing to develop a comprehensive set of daily rainfall observations was an iterative procedure, where initial quality control measures were followed by exploratory data analyses to identify remaining problems within the data. Many tests for changes in the data or randomness of extreme occurrences highlighted anomalies within individual station records which were either rectified with focussed quality control measures, or necessitated the removal of the series. Approximately half of the stations had no significant abrupt changes in the mean or the variance of the annual maxima series; while tests for gradual changes were insignificant or meaningless for all station series. Runs testing established that only 199 of the observation records were suitable for peak over threshold (POT) analyses; the remaining 24 station records contained too many consecutive missing years of observations. However, cross-verification of station maxima using sources such as *British Rainfall* enabled the use of all 223 stations for analyses based on annual maxima.

9.1.2 Identification of metrics of extreme daily rainfall for examining changes in event frequency and magnitude

Exploration of various metrics of rainfall extremity defined a wet day threshold of ≥1mm and established that the definition of a higher threshold is highly dependent on the eventual application. Although a threshold equal to 99% of the mean wet day distribution is "extremely heavy" (Alexander *et al.*, 2006), the subset of $\lesssim 1$ event per year (i.e. the annual maximum series, AMAX) was insufficient to characterise within-year clustering; as such a lower 95% ("very heavy") threshold was adopted for POT analyses to identify more events per year. The method of volumetric quantiles was also examined and found to be unnecessarily restrictive as it did not quantify changes in both the frequency *and* intensity of extreme rainfall. The r-largest events method to improve return period estimates was also examined, obtaining

highly variable results across the stations examined and proved to give minimal improvements with comparison to regionally pooled estimates. The use of the r-largest events to characterise inter-annual variability in the heaviest rain days per year may have greater application in the future, but was found to be overly complex for this project as non-extreme events are included in the analysis set.

9.1.3 Update existing analyses of annual and seasonal maxima

Regional frequency analysis of daily and aggregated daily annual maxima in the UK rainfall regions (Wigley *et al.*, 1984) was employed to estimate likely return frequencies from the Generalized Extreme Value (GEV) distribution. The purpose was to determine whether the changes in the magnitude of extreme rainfall events reported by Fowler and Kilsby (2003b; 2003a) have continued; the results found here contrast with the previous study, as the differences between return period estimates for 2001-2009 and earlier decades are more muted.

Climatic variability has played a major role in the decadal evolution of return period estimates. For instance, considerable increases in East Scotland return period estimates during the 1990s arose from some notable storms (Fowler and Kilsby, 2003b) which have not been repeated. This emphasises the importance of accounting for climatic variability over several decades and the use of multiple analysis methods to understand any changes.

There have been significant increases in annual maxima over the period 1961-2009, particularly in the west of the UK, confirming trends which were apparent but insignificant in previously published work (Fowler and Kilsby, 2003b; Fowler and Kilsby, 2003a; Burt and Ferranti, 2010). Estimated return period frequencies for South Scotland have decreased over the period of record with events which formerly had a 1% annual probability now having nearer to 10% probability of occurring. In East Scotland, estimated magnitudes for 5- and 10-day events are lower than those found by Fowler and Kilsby (2003b), but there has been a sustained increase in magnitude over the full analysis period (1961-2009) and a commensurate decrease in return period estimates from around a 25-year event (4% probability) to a 10-year event (10% probability). Increases in both the median seasonal maxima and estimated event return frequency and magnitude were found in the spring, autumn and winter. Results for median summer maxima, and resultant estimates of event

magnitude, were variable across the country but in general pointed to an increase in the highest intensity events.

The results of these analyses revealed two material deficiencies in the analysis approach. Firstly, the use of spatially disparate rainfall regions, which can experience very different extremes and consequences, is inappropriate. Secondly, practitioners require a quantifiable assessment of changes in both the frequency and likely magnitude of extreme rainfall to determine appropriate protection measures. A regional frequency analysis based only on event magnitudes does not incorporate this critical knowledge surrounding temporal variability in those hydrological events which may have the greatest societal impacts (Tebaldi *et al.*, 2006).

9.1.4 Development of a new set of UK extreme rainfall regions

A pivotal output was the development of UK rainfall regions specifically formulated from metrics of extreme rainfall. Daily rainfall observations from the 199 stations which had no missing years of data were used to identify a set of 14 extreme rainfall regions representing the temporal, orographic and atmospheric drivers affecting extreme rainfall in the UK. The regions were tested using a selection of measures and found to be homogenous; however, the specific boundaries for some regions were a pragmatic adoption of other classifications, and could be considerably enhanced through the use of additional station data. The regional classifications were then used to explore spatial variations in very heavy and extreme daily rainfall characteristics.

9.1.5 Identification of atmospheric and oceanic drivers of extreme daily rainfall

Very heavy and extreme daily rainfall events were shown to be time variant in relation to the occurrence rate and display a distinctive seasonal clustering pattern. In many regions the peak in event frequency occurs over the middle and late autumn months, with a quiet period in April or May. Several highly complex relationships with atmospheric drivers, temperature and seasonality were explored to identify the most likely drivers of extreme events for use in later statistical models. Seasonality was identified as the most common driving characteristic for event frequency, arising from the dependence on seasonal temperatures. Different measures of the NAO were explored as drivers of event frequency, finding that the index derived from principal component analyses of sea level pressure measurements better represented the event frequency. Using this measure, a significant

positive relationship with daily extreme rainfall frequency was identified in Atlantic facing regions and significant negative relationship elsewhere.

9.1.6 Development of multivariate statistical models from daily rainfall observations, and atmospheric and oceanic drivers

Pooled regional maxima contributed to the development of extreme value multivariate models representing the frequency and magnitude of events in each region. Increasing the number of data used in the estimation of distribution parameters was found to improve the model representations of event magnitude and seasonally driven frequency. A Vector Generalized Additive Model (VGAM) was selected for a flexible representation of non-stationarity in observed event intensity and frequency and dependency on external covariates. Two models were fitted, combining to form an orthogonal Poisson process model: a Poisson-VGAM to simulate the variability in event frequency and a GEV-VGAM to simulate the variability in event intensity.

The initial covariates which were tested for inclusion in the models were those identified from earlier exploratory analyses; progressive iteration of the models to include more variables and objective statistical testing were used to identify the most descriptive covariates. The selected covariates included in the Poisson-VGAM were calendar day, one month lagged sea surface temperature (SST), concurrent monthly NAO and concurrent monthly air temperature range. The percentage contribution of each covariate to the estimated distribution parameters confirmed that seasonality is the principal driver of event frequency, explaining between 45-90% of the variability. The second most important covariate was monthly air temperature range; calendar day and air temperature jointly encompass the observed double peak in event frequency. SST and NAO were found to differ in importance between regions displaying a north-south divide with northern Atlantic regions dominated by the NAO index and south eastern regions by SST. The same covariates were applied to the GEV-VGAM, with a more equal balance between the latter three covariates reflecting the range of influences on event magnitude.

9.1.7 Identification of sources of non-stationarity in extreme daily rainfall behaviour

A negative correlation was found between monthly air temperature range and event frequency and magnitude, suggesting that the probability and intensity of extreme rainfall are higher during times of elevated temperature, when the diurnal temperature range is also at its lowest. In southern and eastern regions a strong positive correlation was found

between SST and event frequency and magnitude; the relationship with monthly NAO was more variable by region.

Poisson models based on VGAM parameters were able to replicate observed event frequency well, without over-fitting the model; regional GEV-VGAM models reproduced event maxima satisfactorily. Many hundred simulations of event probability, from known atmospheric or meteorological conditions, were conducted with the statistical models to establish whether apparent changes in extreme behaviour response were random or part of a longer term change. Tests for changes in event frequency per day of year concluded that there has been no significant change in seasonality over the record period. However, the probability of an event occurring within the most active extreme event season has increased, leading to an increase in within-year clustering. Exploration of event magnitudes confirmed that the seasonal signal is not strong; the highest intensity events are as likely in summer as in winter and are dependent on the controlling atmospheric conditions. Changes in magnitude were then assessed by decade, finding significant increasing trends in only five regions.

9.2 Discussion

The increasing trend found in the GEV analyses of spring maxima is of great consequence to farmers as newly planted crops are more vulnerable to extreme rainfall than better established plants (Rosenzweig *et al.*, 2002). The upward trend in the same analysis of autumn maxima is of particular importance to farmers water resource managers and, indirectly, flood defence practitioners as the timing of the events may have a considerable impact on the timing and quality of autumn harvests as well as affecting surface runoff (Holman *et al.*, 2003). Summertime increases in event magnitude, particularly in combination with a hotter, drier future climate, may have devastating impacts on future floods in regions with clay soils that are more sensitive to desiccation and so enhanced runoff generation. Similarly, many sewers in the UK have a design capacity of only the 30-year event; increased urbanisation coupled with more intense rainfall will lead to increases in urban flooding. Even where flooding may not be an issue, the enhanced hydrological cycle will cause an increase in “first flush” pollution and so have a detrimental impact on river water quality (Woods-Ballard *et al.*, 2007)

Allowance for non-stationarity in regional rainfall or flood estimates has been addressed by the research community, but is far from common practice (Jakob *et al.*, 2011); most analyses of extreme rainfall have focussed on traditional extreme value analyses to estimate the likely return frequency of specific events (Ghil *et al.*, 2011). A statistical examination of event frequency and intensity assessing intra-annual frequency, where the parameters vary temporally in response to external covariates, is therefore timely. Climate change adaptation plans are often unclear with respect to projected changes in extreme rainfall as statistical models often underestimate extreme rainfall and the associated uncertainty (Fowler *et al.*, 2007). However, the multivariate point process model developed in this thesis represents the intra- and inter-year non-identically distributed nature of independent rainfall maxima in a manner which could be repeated using climate projections to assist with adaptation planning to quantify likely impacts from changes in extreme daily rainfall.

The importance of air temperature range and sea surface temperature as covariates in the GEV and Poisson based VGAM models confirms the hypothesis that warmer years may bring more intense and more frequent rainfall (Trenberth, 2011). Climate projections suggest that increases in global mean temperature will also cause a reduction in diurnal air temperature range (Christensen *et al.*, 2007). In combination with the positive relationship with Sea Surface Temperature, the implication of this is that short duration rainfall will become more clustered and will increase in intensity in the future.

The drivers of UK extreme rainfall established using this statistical modelling technique could also be of practical benefit for extant flood resilience schemes. For instance, seasonal forecasts of the covariates could be used as predictors within models to assist with short term water resource or flood risk management planning. In addition to the social impacts, which cannot be assigned a true monetary value, recent floods in Europe and worldwide have had major financial consequences (Maynard, 2006). The insurance industry considers consecutive events occurring within a short duration, say 15 days, to be the same event. Using the information from this statistical model suggests that such an approach is erroneous as the probability of several independent events occurring during this period is increasing; this could lead to high costs in years with a higher probability of extreme events.

Insurers should consider revising their window of significance accounting for independent events to account both for natural seasonal clustering and likely future increases.

An outcome of this research which would benefit practitioners involved with flood defence design and water resource management, would be design guidelines encompassing year-to-year variability in event frequency, seasonal clustering, and their likely increases in the future. Current design guidelines which focus only on the single largest event per year are evidently not sufficient in areas which are sensitive to rapid runoff. Policy makers should consider embedding such guidelines in legislation, for example through the Planning Policy Statements relating to development in flood plains. Similarly, a revision of urban water drainage systems to place less reliance on storage capacity within the sewer network is necessary, as existing systems cannot meet the current demands of frequent intense rainfall. Those involved with adaptation planning should give greater emphasis to solutions such as Sustainable Urban Drainage Systems to enable better water resource management and flood risk management in the future.

Statistical downscaling for regional climate models benefits from a bi-directional approach: improvements in model resolution (down) and improvements in input parameters (up). While this project will have little impact on the model resolution, enhancing the interactions between rainfall extremes and their driving mechanisms in regional climate models will lead to improvements in regional climate projections for use in adaptation planning. Comparing the results presented in this thesis with those obtained from climate projections for the control period would be a useful exercise to establish whether the physical processes driving extreme rainfall are correctly represented in climate models. A responsibility also lies with those in power to ensure that the observation network is properly financed and maintained as improvements to the climate models can only be effective with sufficient validation data for comparison.

9.3 Project Developments

Some immediate developments to this project which are likely to be carried out in the short term are:

- A short comparison of the changes in annual and seasonal maxima reported in Chapter 6 with a complementary study carried out for the newly defined extreme rainfall regions.
- Application of covariate information from the UKCP09 climate projections (Murphy et al., 2009) within the VGAMs to identify the likely future behaviour of extreme rainfall frequency and intensity in the UK, and hence the likely consequences for future flood risk.

In addition to these immediate developments, the following paragraphs summarise research interests which were not pursued due to time constraints. If developed thoroughly, all three projects would be of benefit for those applying climate research, such as the insurance industry, adaptation planners, or water resource managers.

9.3.1 Wet days and wet spells

This thesis only examined the clustering of one day rainfall maxima using a seasonally driven Point Process model. However, a formal assessment of the dependence between event magnitude and arrival rate to identify whether the intensity and frequency of very heavy and extremely heavy rainfall are inextricably linked as part of the clustered process (Mumby *et al.*, 2011), thereby heightening the probability of flooding, would also be beneficial to flood risk managers.

Heavy rainfall has several time-varying characteristics: events arrive non-uniformly in time, dependent on a seasonal cluster process; the interval between successive periods forming a wet spell is also non-uniform, governed by the controlling atmospheric systems; and the duration of wet spells is inconstant. These time-varying characteristics are seldom examined in depth, particularly the inter-dependence of successive rainfall, and yet extreme events often develop from several dependent non-extreme events (Stephenson, 2008). Multiple-day heavy rainfall events, arriving in succession are a frequent cause of flooding; a characterisation of their driving processes would be of great benefit to all involved in risk management.

This project focussed on single and fixed day aggregates of extreme rainfall, which facilitated a simple comparison of known quantities and extremes. However, these aggregates may contain a period of dry days within the accumulated total. More useful would be an analysis of only the rainfall days contributing to the high total by considering varying duration wet spells. Wet spells of varying duration are complex and not readily comparable: a wet spell lasting > 15 days with 10mm per day may be relatively rare but not severe, although several wet spells in succession (i.e. *chronic severe*; Stephenson, 2008) could generate an extreme response. By comparison a single daily total of 253mm, as at Seathwaite in Cumbria in 2009, is both rare and severe (*acute severe*; Stephenson, 2008); the associated flooding in this case was compounded by the preceding extended wet spell (Met Office, 2010a).

Other evaluations of wet spell duration have principally concentrated on the mean duration of daily rainfall wet spells (Dai *et al.*, 1998; Zolina *et al.*, 2010) or monthly aggregates (Kruger, 2006). Spell durations are often analysed for drought or temperature excesses, employing a combination of Generalised Linear Models and extreme value theory to determine spell duration and event frequency (Furrer *et al.*, 2010). This approach is suitable for data which are reasonably continuous and dependent on the previous day, but cannot be used for daily rainfall extremes (Cowpertwait *et al.*, 2002). A beneficial development, particularly for disaster alleviation or risk management planning, would be to characterise the drivers of different types of wet spells. An initial definition for wet spells and their severity is outlined in Appendix C.3.

Once the extreme wet spells have been identified, it should be possible to apply the models developed for 1-day maxima to characterise the wet spell behaviour, incorporating a linear model for the spell duration. While the wet spells may all be classified as extreme, the severity of the event is very different and may arise from different governing climatic conditions. Characterisation of the different governing atmospheric conditions would necessitate classification of the wet spells to allow the effective application of multiple extreme value distributions (Sornette, 2009).

9.3.2 Agricultural responses to extreme rainfall

Little research has been completed linking trends in phenology with meteorology, with the exception of the direct impacts of increasing temperature (Gouveia *et al.*, 2008). Many

studies have reviewed trends in the advancement of seasons, timing of pollen releases and flowering dates; some have also examined correlations between mean seasonal vegetation fluctuations and atmospheric teleconnection patterns. However, the secondary impacts of changes in rainfall, particularly extremely heavy rain, are poorly understood; yet increasing combinations of drought and flood can have devastating consequences on crop development and harvests and can have the greatest impacts on society (Tebaldi *et al.*, 2006).

Quantifying the impacts of extreme rainfall on harvest times, quantity and quality, in terms of their sensitivity to extreme daily rainfall, using the extreme rainfall models developed in this thesis may be of interest to adaptation planners. By enhancing the characterisation of current and lagged responses (i.e. the preceding season or year) to extreme rainfall, agricultural adaptation plans might focus on realistic improvements rather than generic solutions (Eakin and Patt, 2011).

9.3.3 Co-dependent extremes

Climatic extremes pose multi-dimensional hazards to critical infrastructure and the most vulnerable sectors of society as extreme events arrive non-uniformly in time, in clusters or in parallel with other extremes. The direct health costs of climate related extreme events incurred in the US between 2002-2009 is estimated at $14bn (Natural Resources Defense Council, 2011), and are indicative of the likely repercussions of increased intensity, frequency, duration and spatial extent of extreme climate events (CCSP, 2008). Yet appropriate risk and hazard management strategies for climate change cannot be devised without a proper understanding of the current impacts and vulnerability to non-stationary and clustered extreme climatic events, or of the driving atmospheric processes. Flexible decision making can only be effected with tools which account for both complexity and uncertainty (Wilby and Dessai, 2010).

Enhancements of single-type extreme event analyses to assess multi-dimensional risks largely ignore the tendency for climatic extremes to cluster in time (von Storch and Zwiers, 1999), although these have major repercussions on remedial work, or a collective impact far greater than their individual influence (Vitolo *et al.*, 2009). The temporal risk of sequences of extreme events, particularly the composite impact of multivariate extremes, is poorly represented in traditional analyses which are premised on event independence. The

alternative approach estimates the likely magnitude or impact of specific individual hazards with a predefined probability of occurrence (Fowler and Ekström, 2009). The two approaches are rarely, if ever, considered in tandem even though both are required for resilient disaster risk management (McEvoy *et al.*, 2010).

A major development of the ideas explored in this thesis would be to examine the temporal relationship between several different extreme phenomena. For instance the relationship between extremes of heat and precipitation is not well understood; characterising the interplay between extremes of differing natures may improve event representation in climate models. Applying spatial tools to examine the concurrence of events of different nature at similar times would also enable appropriate risk and hazard management strategies to be developed. Flood receptor systems have embedded memory, for instance channel realignment or sediment movement following a flood event, subsequent flooding after the failure of manmade or natural flood defences, or the financial consequences of a secondary flood during the business recovery period. Understanding the spatial and temporal interplay between these memory processes and likely changes in the frequency and intensity of extreme events, with particular reference to flood risk, is a research topic which is about to commence in the Water Group, School of Civil Engineering and Geosciences.

Appendix A Summary of Equations and Methods

Clausius-Clapeyron relationship:

$$\frac{de_s}{dT} = \frac{L_v e_s}{R_v T^2}$$

for saturation water vapour pressure (e_s); temperature (T); latent heat of evaporation (L_v) and water vapour gas constant (R_v) Equation 2-1 p23

Pettit Test for Change Points:

$$U_{t,T} = \sum_{t=1}^{t} \sum_{j=t+1}^{T} D_{ij} \qquad \text{where} \qquad D_{ij} = (X_i - X_j)$$
$$= 2W_t - t(T+1)$$

For a time series X of duration T at time t Equation 3-1 p39

Aggregated variance test for Long Range Dependence:

$$X^m(k) = \frac{1}{m} \sum_{i=(k-1)m+1}^{km} X(i) \qquad k = 1, 2, \ldots,$$

$$Var(^m)\ \sigma^2 m^{2H-2}$$

For a time series X_i in m blocks; giving the sample variance with Hurst exponent H.

Equation 3-3 p40

Mann-Kendall test for trends:

$$Z = \begin{cases} (S-1)/Var(S)^{1/2} & \text{for } S > 0 \\ 0 & \text{for } S = 0 \\ (S+1)/Var(S)^{1/2} & \text{for } S < 0 \end{cases}$$

$$\tau = \frac{2S}{n(n-1)}$$

For the test statistic T of n points and a critical value τ Equation 3-4 p42

Wald-Wolfowitz test for randomness:

$$E(R) = 1 + \tfrac{2nm}{n+m} \qquad \text{and} \qquad \sigma^2(R) = \tfrac{2nm(2nm-n-m)}{(n+m)^2(n+m-1)}$$

$$Z = \frac{R - E(R)}{\sqrt{\sigma^2(R)}}$$

For a sequence of runs R with m failures and n successes and test statistic Z Equation 3-5 p43

Generalized Extreme Value (GEV) distribution:

$$G(x;\mu;\sigma;\xi) = \exp\left[-\left(1 + \frac{\xi(x-\mu)}{\sigma}\right)^{-1/\xi}\right] \qquad \text{where } 1 + \frac{\xi(x-\mu)}{\sigma} > 0$$

for location $-\infty < \mu < \infty$, scale $\sigma > 0$ and shape $-\infty < \xi < \infty$ Equation 3-7 p45

Generalized Pareto Distribution (GPD):

$$H(y) = 1 - \left(1 + \frac{\xi y}{\tilde{\sigma}}\right)^{-1/\xi}$$

For threshold *u*, scale $\tilde{\sigma} > 0$ and shape $-\infty < \xi < \infty$ Equation 3-8 p46

GPD relationship to GEV:

$$\xi_{GPD} = \xi_{GEV}$$

$$\ln \Lambda = -1/\xi \ln \left[1 + \frac{\xi(u-\mu)}{\sigma}\right]$$

$$\tilde{\sigma} = \sigma + \xi(u - \mu)$$

For arrival rate Λ, threshold *u*, GPD scale $\tilde{\sigma} > 0$ and GEV scale $\sigma > 0$ Equation B. 9 p223

Regional Frequency Analysis record weighting:

$$w_i = \frac{n_i}{\sum_{i=1}^{N} n_i}$$

For number of annual maxima *n* at *N* stations Equation 4-1 p66

Site discordancy measure:

$$D_i = \frac{1}{3} M (\mathbf{u_i} - \mathbf{U})^T \mathbf{A}^{-1} (\mathbf{u_i} - \mathbf{U})$$

For site i, in pool size M, with $\mathbf{u}_i$ L-moment ratios, matrix of the mean L-moment ratios $\mathbf{U}$, and matrix of the variance in L-moment ratios $\mathbf{A}$ Equation 6-1 p108

Gringorten Formulae for return level plotting:

$$F_i = \frac{(i + 0.44)}{(N + 0.12)}$$

$$y = -ln(-ln(F_i))$$

For the *i*th ranked position of *N* maxima and non-exceedance probability *F* Equation 6-2 p110

Rotational seasonal statistics:

$$\theta = (\mathrm{JDN} - 0.5)\frac{2\pi}{\mathrm{LENYR}}$$

$$\bar{x} = \frac{1}{n}\sum_{i=1}^{N} \cos\theta_i \qquad \bar{y} = \frac{1}{n}\sum_{i=1}^{N} \sin\theta_i$$

$$\bar{r} = \sqrt{\bar{x}^2 + \bar{y}^2}$$

$$\bar{\theta} = \begin{cases} \tan^{-1}\frac{\bar{y}}{\bar{x}} & \bar{x} \geq 0 \quad \bar{y} \geq 0 \\ \tan^{-1}\frac{\bar{y}}{\bar{x}} + \pi & \bar{x} < 0 \\ \tan^{-1}\frac{\bar{y}}{\bar{x}} + 2\pi & \bar{x} \geq 0 \quad \bar{y} < 0 \end{cases}$$

For the angular position θ of the calendar day JDN and N events at i stations. Equation B. 24 p227

L-moment ratios:

$$\lambda_1 = \beta_0$$
$$\lambda_2 = 2\beta_1 - \beta_0$$
$$\lambda_3 = 6\beta_2 - 6\beta_1 + \beta_0$$
$$\lambda_4 = 20\beta_3 - 30\beta_2 + 12\beta_1 - \beta_0$$
$$\tau_3 = \lambda_3/\lambda_2 \qquad \text{and} \qquad \tau_4 = \lambda_4/\lambda_2$$

For the mean λ_1, coefficient of variation λ_2, skewness τ_3 and kurtosis τ_4 Equation B. 15 p225

GPD parameters from L-moment ratios:

$$\xi = 2 - \frac{(\lambda_1 - \hat{u})}{\lambda_2}$$
$$\tilde{\sigma} = (1 - \xi)(\lambda_1 - \hat{u})$$

For threshold $\hat{u}$, scale $\tilde{\sigma}$ and shape ξ, mean λ_1, coefficient of variation λ_2 Equation B. 16 p225

Hosking and Wallis regional heterogeneity statistics:

$$V = \left\{ \sum_{i=1}^{k} n_i (t^{(i)} - t^R)^2 / \sum_{i=1}^{k} n_i \right\}^{1/2}$$
$$\theta_{HW} = \frac{V - \mu_v}{\sigma_v}$$

For the site statistic V_i, with record length n_i using the mean L-moment t and skew L-moment t^R
Equation 7-2 p146

Final parameter definition for Vector Generalized Additive Poisson and GEV models:

$$\log \Lambda(x) = \beta_{0(1)} + f_{1(1)}(d_t) + f_{2(1)}(ST1_t) + \beta_{3(1)} N_t + \beta_{4(1)} \Theta_t$$
$$\mu(x) = \beta_{0(2)} + f_{1(2)}(d_t) + f_{2(2)}(ST1_t) + \beta_{3(2)} N_t + \beta_{4(2)} \Theta_t$$
$$\log \sigma = \beta_{0(3)}$$
$$\log(\xi + 0.5) = \beta_{0(4)}$$

For arrival rate Λ, location μ, scale σ and shape ξ with covariates day of year d_t, lagged Sea Surface Temperature $ST1_t$, coincident monthly NAO N_t and monthly air temperature range Θ_t
Equation 8-2 p177

Appendix B Statistical Tools

B.1 Bootstrapping

Bootstrapping is only suitable for use where the dataset size is >10 (Efron, 1979). The basic bootstrap method relies on a Monte Carlo simulation to generate a large number of random samples from a known process or series of data; summarised as follows (Alexander *et al.*, 2009):

1. Construct a sample probability distribution $\hat{F}$
2. Generate a random sample, $\boldsymbol{X^*_j}$, size n, from $\hat{F}$ with replacement.
3. Evaluate $\hat{\alpha}$, the parameter or test statistic for the sample.
4. Repeat steps 2 and 3 a large number, say 1000, of times.

The x_j^{th} observation drawn from $\boldsymbol{X^*_j}$, may occur multiple times, while x_i may not appear.

B.2 Statistical Distributions

B.2.1 Discrete distributions

The *Binomial distribution* is formulated from n independent Bernoulli trials, sampled from a population N, with a stationary probability of event occurrence is:

$$X \sim Bin(N,p) \rightarrow P(n|N) = \binom{N}{n} p^n (1-p)^{N-n} \qquad n = 0,1,2\ldots$$

Equation B. 1

For all non-negative integer values, the probability of events following the *negative binomial distribution* is:

$$X \sim NegBin(N,p) \rightarrow P(X=n) = \frac{\Gamma(x+n)}{n!\Gamma(x)} p^x (1-p)^n \qquad n = 0,1,2\ldots$$

Equation B. 2

Where $\Gamma(x)$ is the gamma function, shown in Equation 3-3, $0 \leq p \leq 1$ and $x > 0$.

The *Poisson distribution* has $E[X] = Var[X] = \Lambda > 0$ with probability density function:

$$Pr(X=x) = \frac{\Lambda^x e^{-\Lambda}}{x!} x = 0,1,2,\ldots$$

Equation B. 3

B.2.2 Gamma distribution

The *gamma distribution* is a continuous distribution controlled by the dimensionless shape parameter, α, and scale parameter, β, and described by:

$$f(x) = \frac{(x/\beta)^{\alpha-1}\, exp\,(-x/\beta)}{\beta\Gamma(\alpha)} \quad \text{where} \quad x, \alpha, \beta > 0 \quad \text{and} \quad \Gamma(\alpha) = \int_0^\infty t^{\alpha-1} e^{-t} dt$$

Equation B. 4

B.2.3 Extreme Value distributions

GEV Extension to the R-largest model

The series of maxima M_n from the set $(X_1, \ldots, X_2, \ldots, X_n)$ may be expanded to incorporate the *r* largest statistics by defining $M_n^{(r)} = r^{\text{th}}$ largest of $(X_1, X_2, ...X_n)$ with limiting behaviour, for fixed *r,* as $n \to \infty$ (Coles, 2001). Fitting this series into the GEV distribution function, G, using constants $a_n > 0$ and b_n:

$$Pr\{(M_n^{(r)} - b_n)/a_n \geq z\} \to G_k(z)$$

Equation B. 5

where

$$G_k(z) = \exp\{-\tau(z)\} \sum_{s=0}^{k-1} \frac{\tau(z)^s}{s!}$$

Equation B. 6

with

$$\tau(z) = \left[1 + \xi\left(\frac{z-\mu}{\sigma}\right)\right]^{-1/\xi}$$

Equation B. 7

Peak-over-threshold (POT) Maxima

By Poisson's law of small numbers, the excesses of a distribution over the threshold, u, are a countable sum of binary events $N$with mean n. If u is defined at a high enough level such that $\lim_{n\to\infty} nPr(x > u) = \Lambda(0, \infty)$, then N can be approximated by a Poisson variable. The *Point Process* relationship can be combined with the GPD to define both the frequency and magnitude of events exceeding the threshold, with the occurrence rate, Λ, following:

$$\Lambda = \left[1 + \frac{\xi}{\sigma}(u - \mu)\right]^{-1/\xi}$$

Equation B. 8

With the parameters directly linked to the GEV as (Davison and Smith, 1990):

$$\xi_{GPD} = \xi_{GEV}$$
$$\ln \Lambda = -1/\xi \ln \left[1 + \frac{\xi(u-\mu)}{\sigma}\right]$$
$$\tilde{\sigma} = \sigma + \xi(u-\mu)$$

Equation B. 9

B.3 Linear and Additive Models

B.3.1 Generalized Linear Models

The ordinary linear regression model is a special case of the Generalized Linear Model (GLM), where only one explanatory variable exists and it is confined to the Gaussian distribution (Dobson, 2002). For a set of independent variables $Y_1, \ldots, Y_n$, the mean $E(Y_i) = \mu_i$ follows an exponential family and is dependent on a single parameter Φ (Nelder and Wedderburn, 1972) such that

$$g(\Phi_i) = \eta \mathbf{x} = \beta_\mathbf{0} + \beta_\mathbf{1}\mathbf{x_1} + \ldots + \beta_\mathbf{n}\mathbf{x_n}$$

Equation B. 10

The parameters Φ_i are functions of the explanatory variables βX and $g(\Phi_i)$ is the link function giving the residuals from the model as

$$r_i = \frac{y_i - \widehat{\Phi_i}}{\sqrt{\widehat{\Phi_i}}}$$

Equation B. 11

VGLMs extend the available model families beyond the exponential to extreme value distributions, applying the $\eta_i(\mathbf{x})$ directly to the distribution parameters using link functions g_j and parameters Φ_j. Several different link functions may be assigned to each parameter.

$$\eta_1 = \mu$$
$$\eta_2 = \log \sigma$$
$$\eta_i = g_j(\Phi_j)$$

Equation B. 12

The vector smoothers are estimated using combined quasi-Newton and iteratively reweighted least squares (IRLS) algorithms with Fisher scoring for numerical stability (Yee, 2010).

B.3.2 Generalized Additive Models

A more flexible enhancement is the Generalized Additive Model (GAM, Hastie and Tibshirani, 1990). The linear predictor term $g(\Phi_i)$ involves a sum of smooth non-linear functions f_j of the covariates of an exponential family:

$$g(\Phi_i) = \eta(\mathbf{x_{ij}}) = \beta_0 + f_1(x_1) + \ldots + f_n(x_n)$$

Equation B. 13

where the relationship between η and x_{ij} is constrained to be smooth through a non-negative smoothing parameter λ_j.

The smoothness for the model f_i, is transformed into a linear model with a basis function b covering the space of functions where f is an element for a set of parameters $(\beta_1, \ldots, \beta_n)$.

$$f(x) = \sum_{j=1}^{q} b_j(x)\beta_j$$

Equation B. 14

P-splines are recommended to define an appropriate smoothing function (Hastie and Tibshirani, 1990). The aim is to choose a smoothing parameter, λ_j, and basis dimension as close to f as possible so that data are neither over or under smoothed.

The vector smoothers used in VGAMs fit a vector of smooth functions $f(.)$ to the vector measurements model $\mathbf{y_i} = f_i(\mathbf{x_i}) + \epsilon_\mathbf{i}$, while b-splines minimise the quantity with a two term penalty on the lack of fit and λ_j using a penalised likelihood term. These were defined from penalized regression smoothers, of the form $f(y_t) = \sum_{m=1}^{M} b_m(x_t)\beta_m$ where $b_m(x_t)$ are linear basis functions and β_m are the non-linear parameters (Yee, 2011).

B.4 Parameter Estimation

For a vector x of observations and θ of parameters (in the parameter space Ω) the likelihood function is $L(\theta; \mathrm{x})$. The estimator $\hat{\theta}$ is the maximum of the likelihood function, tending to the best parameter grouping with $L(\hat{\theta}; x) \geq L(\theta, x)$ for all θ in Ω (Wilks, 2005). The likelihood function is similar to the probability distribution function, the difference is that fixed values are estimated from unknown parameters with the former.

Probability weighted moments of data values X_1, X_2, …, X_i arranged in a linearly

ascending order are given by $\beta_r = \int x(F(x)^r dF(x)$, where $r = 1, 2, \ldots$. L-moments, and their ratios, of the probability distribution defined in terms of the weighted probability moments are then given by:

$$\lambda_1 = \beta_0$$
$$\lambda_2 = 2\beta_1 - \beta_0$$
$$\lambda_3 = 6\beta_2 - 6\beta_1 + \beta_0$$
$$\lambda_4 = 20\beta_3 - 30\beta_2 + 12\beta_1 - \beta_0$$
$$\tau_3 = \lambda_3/\lambda_2 \qquad \text{and} \qquad \tau_4 = \lambda_4/\lambda_2$$

Equation B. 15

Where λ_1 is equivalent to the mean of the distribution and λ_2 is the coefficient of variation. L-moment ratios calculated from the higher order L-moments describe the skewness (τ_3) and kurtosis (τ_4) of the distribution. Coefficients of the parameters are those of the "shifted Legendre polynomials" (Hosking, 1995b). Sample L-moments for data samples are calculated in a similar manner with corresponding notation and definitions, e.g. $l_1 = b_0; l_2 = 2b_1 - b_0$ etc.

Generalised Pareto distribution scale, $\tilde{\sigma}$, and shape, ξ, parameters can be derived from L-moments, assuming a known location parameter (Hosking, 1990):

$$\xi = 2 - \frac{(\lambda_1 - \hat{u})}{\lambda_2}$$
$$\tilde{\sigma} = (1 - \xi)(\lambda_1 - \hat{u})$$

Equation B. 16

B.5 Model Testing

The Kolmogorov non-parametric test for the goodness of fit of a probability distribution, with statistic D_n, and critical value, C_ν, are defined for significance ν at the K_ν level of significance.

$$D_n = \overset{\max}{x} |F_n(x) - F(x)|$$

$$C_\nu = \frac{K_\nu}{\sqrt{n} + 0.12 + \frac{0.11}{\sqrt{n}}}$$

Equation B. 17

The χ^2 test assesses model fit for counts of data falling into pre-defined classes against the χ^2 distribution with ν degrees of freedom; for $\nu =$ number of classes - number of parameters - 1.

$$\begin{aligned}\chi^2 &= \sum_{classes} \frac{(\text{Observed - Expected})^2}{\text{Expected}} \\ &= \sum_{classes} \frac{(\text{Observed - } n\Pr(\text{data in class}))^2}{n\Pr(\text{data in class})}\end{aligned}$$

Equation B. 18

The deviance statistic compares the ratio of fitted model likelihood functions θ for significant differences against the χ^2 distribution.

$$D = -2\ln\frac{\theta_{\text{model 1}}}{\theta_{\text{model 2}}}$$

Equation B. 19

For each model j with k dimensions, the AIC (Akaike, 1974) is defined from the maximum likelihood functions as:

$$AIC_j = -2\theta + 2k_j$$

Equation B. 20

While the BIC (Schwarz, 1978) includes a term for the number of observations n:

$$BIC_j = -2\theta + \frac{1}{2}k_j\log(n)$$

Equation B. 21

The Generalized Cross Validation (GCV) score is obtained by rotating the ordinary cross validation score through an optimum angle to the point where the row lengths are equal to obtain:

$$\upsilon_g = \frac{n||\mathbf{y} - \hat{\mu}||^2}{(n - (\mathbf{A}))^2}$$

Equation B. 22

The smoothing parameter estimate is selected from the minimum GCV score. In a similar manner, the unbiased risk estimator is given by (Wood, 2006)

$$\upsilon(\lambda) = \frac{||y - \mathbf{A}\mathbf{y}||^2}{n} - \frac{\sigma^2 + 2(\mathbf{A}\sigma^2}{n}$$

Equation B. 23

B.6 Rotated Seasonal Statistics

If θ represents the angular position of the calendar day (at noon) in radians, JDN the Julian Day number of the event and LENYR the length of the year (calculated as 365.25):

$$\theta = (\mathrm{JDN} - 0.5)\frac{2\pi}{\mathrm{LENYR}}$$

Equation B. 24

then for Nevents at i stations the centroid of the events, $\bar{\theta}$, can be calculated from

$$\bar{x} = \frac{1}{n}\sum_{i=1}^{N}\cos\theta_i \qquad \bar{y} = \frac{1}{n}\sum_{i=1}^{N}\sin\theta_i$$

$$\bar{r} = \sqrt{\bar{x}^2 + \bar{y}^2}$$

$$\bar{\theta} = \begin{cases} \tan^{-1}\frac{\bar{y}}{\bar{x}} & \bar{x} \geq 0 \quad \bar{y} \geq 0 \\ \tan^{-1}\frac{\bar{y}}{\bar{x}} + \pi & \bar{x} < 0 \\ \tan^{-1}\frac{\bar{y}}{\bar{x}} + 2\pi & \bar{x} \geq 0 \quad \bar{y} < 0 \end{cases}$$

Equation B. 25

$\bar{r} \to 1$ indicates a regular seasonal concentration of events and $\bar{r} \to 0$ indicates weak seasonality.

Appendix C Definitions

C.1 Treatment of Uncertainty

The following definitions for uncertainty and probability have been used in the thesis, following the Guidance Note for Lead Authors of the IPCC Fifth Assessment Report on Consistent Treatment of Uncertainties (2010).

The assessed probability trends or future behaviour is categorised as:

Term	Likelihood of Outcome
Virtually certain	99-100% probability
Very likely	90-100% probability
Likely	60-100% probability
About as likely as not	33-66% probability
Unlikely	0-33% probability
Very unlikely	0-10% probability
Exceptionally unlikely	0-1% probability

Confidence in the evidence and agreement of research are depicted with a sliding confidence scale; increases in confidence are suggested by the increased strength of shading.

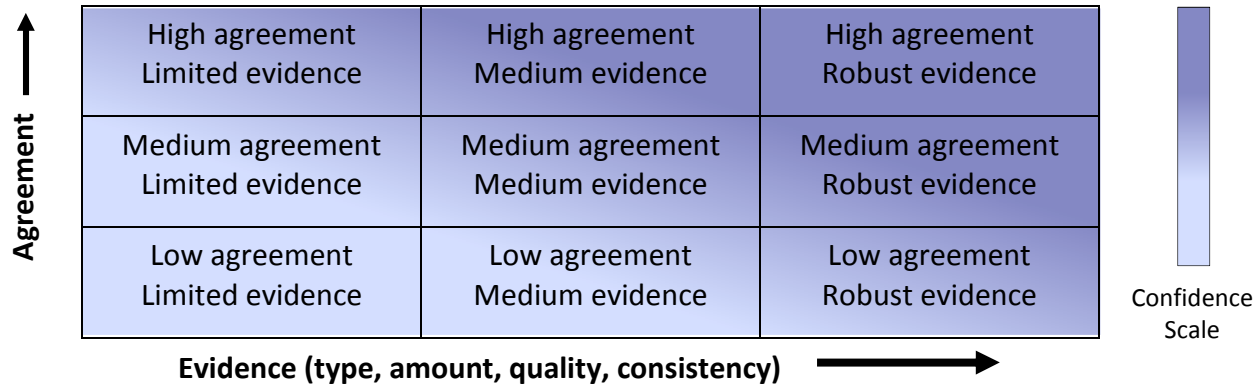

C.2 Phenology

The Oxford English Dictionary (*Volume XI Ow - Poisant*, 1989) defines "phenology" and related words as:

> **"Phenological** *a*. Also *phaen-* [f. phenol + logical: rendering Ger. phänologisch, used by Dr. C. Fritsch in Jarhb d.k.k. Central-Anstalt für Meteorologie, 1853, Vienna 1888].
>
> Of or pertaining to phenology or to the objects of its study. So **phenologic** a.; **phenology**, the study of the times of recurring natural phenomena (see quot. 1884), esp. in relation to climatic conditions; **phenologist**, one who studies phenology.
>
> **1875** (*title*) Instructions for the observation of Phenological Phenomena, published by the Council of the Meteorological Society. **1883** (*Nature*) 4 Jan 234/2 The most important feature of the phenological year was the mild winter. **1884** (*Ibid*) 9 Oct 558/2 Phenology, the observation of the first flowering and fruiting of plants, the foliation and defoliation of trees, the arrival, nesting, and departure of birds, and such like, has attracted the attention of naturalists from time to time for nearly 150 years. **1894** (*Naturalist*) 241 Phenological notes and statistical tables of rainfall and temperature. **1897** WILLIS *Flower Pl.* I 155 The study of periodic phenomena of vegetation is termed *phenology*. **1974** (*Nature*) I Mar 42/1 This proposed sequence of major volcanic eruptions followed by several years of cold summers and then by glacial advance is supported by historic and phenological data."

In the context of this thesis, where reference may be made to phenology, the focus is on the "periodic phenomena" of flora and fauna with respect to water resource availability.

C.3 Wet spells

To characterise extreme wet spells several components require definition: the duration of the event; the minimum rain on any of the days within the spell; an intensity measure to be able to compare events; and some measure of extremity. As wet spells of varying duration are complex and not readily comparable: the wet spell definition for extremity must also account for rarity and severity (Stephenson, 2008). Severity may have a rapid onset and conclusion such as Boscastle 2004 (*acute*), or slow to develop and either of prolonged duration such as Gloucester 2007 or repeated occurrence (*chronic*).

A wet spell, X_i, is considered to be any duration, D_i, of *>1 day* with contiguous daily rainfall totals exceeding *1mm per day*, with intervals between independent wet spells greater than the cluster index (Ferro and Segers, 2003) or one day, whichever is longer. The

event magnitude, P_i, is the total rainfall over the wet spell ($\sum P_{Di}$), and D is the total number of rainfall days per year or period under consideration (Shinohara *et al.*, 2010), giving standardised intensity, η, and wet spell durations, λ:

$$\eta = \frac{P_i}{D_i}$$

$$\lambda = \frac{D_i}{D}$$

Equation C. 1

Sensitivity testing demonstrated that a running 20-day accumulation period identifies most wet spells without encroaching into monthly responses; increasing the duration to account for longer events did not enhance the extreme data set. Employing fewer days in the running mean increased the sensitivity of deviations of long wet spells from mean conditions.

Extreme departures could be identified in a number of ways, for instance the monthly Standardised Precipitation Index (SPI) could be used to identify extreme wet spells as those with SPI>2, or the monthly concentration index (Li *et al.*, 2011) could be adapted to represent sub-monthly values. To develop this measure into one of multiple day wet spells, rather than a measure of individual daily rainfall would necessitate an assessment of the mean number of days taken to contribute to different magnitudes of events. By fitting a gamma distribution to the frequency of days contributing to varying magnitudes of events, a measure of the standard error can be derived to identify outlying events. If the goal is to understand the atmospheric processes driving each extreme event, further work is then required to classify the severity of the events.

Bibliography

Abaurrea, J., Asin, J., Cebrián, A. C. and Centelles, A. (2007) 'Modeling and forecasting extreme hot events in the central Ebro valley, a continental-Mediterranean area', *Global and Planetary Change,* **57**, pp. 43-58.

Akaike, H. (1974) 'A new look at the statistical model identification', *Automatic Control, IEEE Transactions on,* **19**, (6), pp. 716-723.

Alexander, L. V. and Jones, P. D. (2000) 'Updated precipitation series for the U.K. and discussion of recent extremes', *Atmospheric Science Letters,* **1**, (2), pp. 142-150.

Alexander, L. V., Tapper, N., Zhang, X., Fowler, H. J., Tebaldi, C. and Lynch, A. (2009) 'Climate extremes: progress and future directions', *International Journal of Climatology,* **29**, (3), pp. 317-319.

Alexander, L. V., Zhang, X., Peterson, T. C., Caesar, J., Gleason, B., Klein Tank, A. M. G., Haylock, M., Collins, D., Trewin, B., Rahimzadeh, F., Tagipour, A., Rupa Kumar, K., Revadekar, J., Griffiths, G., Vincent, L., Stephenson, D. B., Burn, J., Aguilar, E., Brunet, M., Taylor, M., New, M., Zhai, P., Rusticucci, M. and Vazquez-Aguirre, J. L. (2006) 'Global observed changes in daily climate extremes of temperature and precipitation', *J. Geophys. Res.,* **111**, (D5), pp. D05109.

Allamano, P., Laio, F. and Claps, P. (2011) 'Effects of disregarding seasonality on the distribution of hydrological extremes', *Hydrol. Earth Syst. Sci.,* **15**, pp. 3207-3215.

Allan, R. and Ansell, T. (2006) 'A New Globally Complete Monthly Historical Gridded Mean Sea Level Pressure Dataset (HadSLP2): 1850–2004', *Journal of Climate,* **19**, (22), pp. 5816-5842.

Allan, R., Tett, S. and Alexander, L. (2009) 'Fluctuations in autumn-winter severe storms over the British Isles: 1920 to present', *International Journal of Climatology,* **29**, (3), pp. 357-371.

Allan, R. P. and Soden, B. J. (2008) 'Atmospheric Warming and the Amplification of Precipitation Extremes', *Science,* **321**, (5895), pp. 1481-1484.

Allen, M., Ingram, W. and Stainforth, D. (2002) 'Constraints on future changes in climate and the hydrologic cycle, Nature Insight article,' *Nature,* **419**, pp. 224-232.

Ammann, C. M., Joos, F., Schimel, D. S., Otto-Bliesner, B. L. and Tomas, R. A. (2007) 'Solar influence on climate during the past millennium: Results from transient simulations with the NCAR Climate System Model', *Proceedings of the National Academy of Sciences,* **104**, (10), pp. 3713-3718.

Anselmo, V., Galeati, G., Palmieri, S., Rossi, U. and Todini, E. (1996) 'Flood risk assessment using an integrated hydrological and hydraulic modelling approach: a case study', *Journal of Hydrology,* **175**, (1-4), pp. 533-554.

Archer, D. R. and Fowler, H. J. (1999) 'Spatial and temporal variations in precipitation in the Upper Indus Basin, global teleconnections and hydrological implications', *Hydrol. Earth Syst. Sci.,* **8**, (1), pp. 47-61.

Asquith, W. H. (2009) *lmomco: L-moments, Trimmed L-moments, L-comments, and Many Distributions*

Atkinson, M. D., Kettlewell, P. S., Poulton, P. R. and Hollins, P. D. (2008) 'Grain quality in the Broadbalk Wheat Experiment and the winter North Atlantic Oscillation', *The Journal of Agricultural Science,* **146**, (05), pp. 541-549.

Baede, A. M. P. (2007) 'Glossary', in *Climate Change 2007: The Physical Science Basis. Contribution of Working Group I to the Fourth Assessment Report of the*

Intergovernmental Panel on Climate Change. Cambridge University Press, Cambridge, United Kingdom and New York, NY, USA.
Baines, P. G. and Folland, C. K. (2007) 'Evidence for a Rapid Global Climate Shift across the Late 1960s', *Journal of Climate,* **20**, (12), pp. 2721-2744.
Barnston, A. G. and Livezey, R. E. (1987) 'Classification, Seasonality and Persistence of Low-Frequency Atmospheric Circulation Patterns', *Monthly Weather Review,* **115**, (6), pp. 1083-1126.
Bartolini, E., Claps, P. and D'Odorico, P. (2009) 'Interannual variability of winter precipitation in the European Alps: relations with the North Atlantic Oscillation', *Hydrol. Earth Syst. Sci.,* **13**, (1), pp. 17-25.
Beguería, S. (2005) 'Uncertainties in partial duration series modelling of extremes related to the choice of the threshold value', *Journal of Hydrology,* **303**, (1-4), pp. 215-230.
Benestad, R. E. (2003) 'How often can we expect a record event?', *Climate Research,* **25**, (1), pp. 3-13.
Benestad, R. E. (2006) 'Can We Expect More Extreme Precipitation on the Monthly Time Scale?', *Journal of Climate,* **19**, (4), pp. 630-637.
Bengtsson, L., Hodges, K. I. and Keenlyside, N. (2009) 'Will Extratropical Storms Intensify in a Warmer Climate?', *Journal of Climate,* **22**, (9), pp. 2276-2301.
Beniston, M., Stephenson, D., Christensen, O., Ferro, C., Frei, C., Goyette, S., Halsnaes, K., Holt, T., Jylhä, K., Koffi, B., Palutikof, J., Schöll, R., Semmler, T. and Woth, K. (2007) 'Future extreme events in European climate: an exploration of regional climate model projections', *Climatic Change,* **81**, (0), pp. 71-95.
Beran, M. (2002) 'On breaking weather records: Part 1: The past', *Weather,* **57**, (8), pp. 303-309.
Berg, P., Haerter, J. O., Thejll, P., Piani, C., Hagemann, S. and Christensen, J. H. (2009) 'Seasonal characteristics of the relationship between daily precipitation intensity and surface temperature', *J. Geophys. Res.,* **114**, (D18), pp. D18102.
Biggs, E. M. and Atkinson, P. M. (2011) 'A characterisation of climate variability and trends in hydrological extremes in the Severn Uplands', *International Journal of Climatology,* **31**, (11), pp. 1634-1652.
Bindoff, N. L., Willebrand, J., Artale, V., Cazenave, A., J., G., Gulev, S., Hanawa, K., Le Quere, C., Levitus, S., Nojiri, Y., Shum, C. K., Talley, T. D. and Unnikrishnan, A. (2007) 'Observations: Oceanic Climate Change and Sea Level', in *Climate Change 2007: The Physical Science Basis. Contribution of Working Group I to the Fourth Assessment Report of the Intergovernmental Panel on Climate Change.* Cambridge University Press, Cambridge, UK.
Bladé, I., Liebmann, B., Fortuny, D. and van Oldenborgh, G. (2012) 'Observed and simulated impacts of the summer NAO in Europe: implications for projected drying in the Mediterranean region', *Climate Dynamics,* **38**, pp. 1-19.
Blenkinsop, S., Fowler, H. J., Dubus, I. G., Nolan, B. T. and Hollis, J. M. (2008) 'Developing climatic scenarios for pesticide fate modelling in Europe', *Environmental Pollution,* **154**, (2), pp. 219-231.
Blöschl, G. and Montanari, A. (2010) 'Climate change impacts—throwing the dice?', *Hydrological Processes,* **24**, (3), pp. 374-381.
Bocheva, L., Marinova, T., Simeonov, P. and Gospodinov, I. (2009) 'Variability and trends of extreme precipitation events over Bulgaria (1961-2005)', *Atmospheric Research,* **93**, (1-3), pp. 490-497.

Bolch, T., Buchroithner, M., Pieczonka, T. and Kunert, A. (2008) 'Planimetric and volumetric glacier changes in the Khumbu Himal, Nepal, since 1962 using Corona, Landsat TM and ASTER data', *Journal of Glaciology,* **54**, (187), pp. 592-600.

Bonell, M. and Sumner, G. (1992) 'Autumn and winter daily precipitation areas in Wales, 1982–1983 to 1986–1987', *International Journal of Climatology,* **12**, (1), pp. 77-102.

Dartmouth Flood Observatory. [Brackenridge, G. R.], Global Active Archive of Large Flood Events, (2011), Available from: http://floodobservatory.colorado.edu/Archives/index.html

Briffa, K. R., van der Schrier, G. and Jones, P. D. (2009) 'Wet and dry summers in Europe since 1750: evidence of increasing drought', *International Journal of Climatology,* **29**, (13), pp. 1894-1905.

Brönnimann, S. (2007) 'Impact of El Niño & Southern Oscillation on European climate', *Rev. Geophys.,* **45**, (3), pp. RG3003.

Brönnimann, S., Xoplaki, E., Casty, C., Pauling, A. and Luterbacher, J. (2007) 'ENSO influence on Europe during the last centuries', *Climate Dynamics,* **28**, (2), pp. 181-197.

Brown, S. J., Caesar, J. and Ferro, C. A. T. (2008) 'Global changes in extreme daily temperature since 1950', *J. Geophys. Res.,* **113**, (D5), pp. D05115.

Buishand, T. A. (1977) *Stochastic modelling of daily rainfall sequences.* thesis. Veenman.

Buishand, T. A. (1984) 'Bivariate extreme-value data and the station-year method', *Journal of Hydrology,* **69**, (1-4), pp. 77-95.

Burauskaite-Harju, A., Grimvall, A. and Brömssen, C. v. (2012) 'A test for network-wide trends in rainfall extremes', *International Journal of Climatology,* **32**, (1), pp. 86-94.

Burt, T. P. and Ferranti, E. J. S. (2010) 'Changing patterns of heavy rainfall in upland areas: a case study from northern England', *International Journal of Climatology,* **32**, (4), pp. 518–532.

Burt, T. P. and Horton, B. P. (2007) 'Inter-decadal variability in daily rainfall at Durham (UK) since the 1850s', *International Journal of Climatology,* **27**, (7), pp. 945-956.

Burt, T. P. and Shahgedanova, M. (1998) 'An historical record of evaporation losses since 1815 calculated using long-term observations from the Radcliffe Meteorological Station, Oxford, England', *Journal of Hydrology,* **205**, (1-2), pp. 101-111.

Butler, A., Heffernan, J. E., Tawn, J. A., Flather, R. A. and Horsburgh, K. J. (2007) 'Extreme value analysis of decadal variations in storm surge elevations', *Journal of Marine Systems,* **67**, (1-2), pp. 189-200.

Cade, B. S. and Noon, B. R. (2003) 'A gentle introduction to quantile regression from ecologists', *Front Ecol. Environ.,* **1**, (8), pp. 412-420.

Caesar, J., Alexander, L. V., Trewin, B., Tse-ring, K., Sorany, L., Vuniyayawa, V., Keosavang, N., Shimana, A., Htay, M. M., Karmacharya, J., Jayasinghearachchi, D. A., Sakkamart, J., Soares, E., Hung, L. T., Thuong, L. T., Hue, C. T., Dung, N. T. T., Hung, P. V., Cuong, H. D., Cuong, N. M. and Sirabaha, S. (2011) 'Changes in temperature and precipitation extremes over the Indo-Pacific region from 1971 to 2005', *International Journal of Climatology,* **31**, (6), pp. 791-801.

Canty, A. and Ripley, B. D. (2011) *boot: Bootstrap R (S-Plus) Functions* (1.3-1)

Carreau, J., Naveau, P. and Sauquet, E. (2009) 'A statistical rainfall-runoff mixture model with heavy-tailed components', *Water Resour. Res.,* **45**, (10), pp. W10437.

Casty, C., Wanner, H., Luterbacher, J., Esper, J. and Böhm, R. (2005) 'Temperature and precipitation variability in the European Alps since 1500', *International Journal of Climatology,* **25**, (14), pp. 1855-1880.

CCSP. (2008) *Weather and Climate Extremes in a Changing Climate. Regions of Focus: North America, Hawaii, Caribbean, and U.S. Pacific Islands.*, in T. R. Karl, G. A. Meehl, C. D. Miller, S. J. Hassol, A. M. Waple and W. L. Murray (ed),^(eds) Washington D.C., USA. Department of Commerce, NOAA's National Climatic Data Center pp. 164.

Cebrián, A. C. and Abaurrea, J. (2006) 'Drought Analysis Based on a Marked Cluster Poisson Model', *Journal of Hydrometeorology,* **7**, (4), pp. 713-723.

Chandler, K. N. (1952) 'The Distribution and Frequency of Record Values', *Journal of the Royal Statistical Society. Series B (Methodological),* **14**, (2), pp. 220-228.

Chavez-Demoulin, V. and Davison, A. C. (2005) 'Generalized additive modelling of sample extremes', *Journal of the Royal Statistical Society: Series C (Applied Statistics),* **54**, (1), pp. 207-222.

Chen, Z. and Grasby, S. E. (2009) 'Impact of decadal and century-scale oscillations on hydroclimate trend analyses', *Journal of Hydrology,* **365**, (1-2), pp. 122-133.

Choi, G., Collins, D., Ren, G., Trewin, B., Baldi, M., Fukuda, Y., Afzaal, M., Pianmana, T., Gomboluudev, P., Huong, P. T. T., Lias, N., Kwon, W.-T., Boo, K.-O., Cha, Y.-M. and Zhou, Y. (2009) 'Changes in means and extreme events of temperature and precipitation in the Asia-Pacific Network region, 1955–2007', *International Journal of Climatology,* **29**, (13), pp. 1906-1925.

Christensen, J. H., Hewitson, B., Busuioc, A., Chen, A., Gao, X., Held, I. M., Jones, R., Kolli, R. K., Kwon, W.-T., Laprise, R., Magana Rueda, V., Mearns, L. O., Menendez, C. G., Raisanen, J., Rinke, A., Sarr, A. and Whetton, P. (2007) 'Regional Climate Projections', in *Climate Change 2007: The Physical Science Basis. Contribution of Working Group I to the Fourth Assessment Report of the Intergovernmental Panel on Climate Change.* Cambridge University Press, Cambridge, UK.

Christensen, O. B. and Christensen, J. H. (2004) 'Intensification of extreme European summer precipitation in a warmer climate', *Global and Planetary Change,* **44**, (1-4), pp. 107-117.

Cohn, T. A. and Lins, H. F. (2005) 'Nature's style : Naturally trendy', *Geophysical research letters,* **32**, (23), pp. 23402.23401-23402.23405.

Coles, S. (2001) *An Introduction to Statistical Modeling of Extreme Values.* Springer-Verlag,Berlin.

Coles, S., Heffernan, J. and Tawn, J. (1999) 'Dependence Measures for Extreme Value Analyses', *Extremes,* **2**, (4), pp. 339-365.

Coles, S. G. and Stephenson, A. (2009) *ismev: An Introduction to Statistical Modelling of Extreme Values*

Colman, A. (1997) 'Prediction of summer central England temperature from preceding North Atlantic winter sea surface temperature', *International Journal of Climatology,* **17**, (12), pp. 1285-1300.

Cooley, D. (2009) 'Extreme value analysis and the study of climate change', *Climatic Change,* **97**, (1), pp. 77-83.

Cooley, D., Nychka, D. and Naveau, P. (2007) 'Bayesian Spatial Modeling of Extreme Precipitation Return Levels', *Journal of the American Statistical Association,* **102**, (479), pp. 824-840.

Cooley, D. and Sain, S. (2010) 'Spatial Hierarchical Modeling of Precipitation Extremes From a Regional Climate Model', *Journal of Agricultural, Biological, and Environmental Statistics,* **15**, (3), pp. 381-402.

Corte-Real, J., Qian, B. and Xu, H. (1998) 'Regional climate change in Portugal: precipitation variability associated with large-scale atmospheric circulation', *International Journal of Climatology,* **18**, (6), pp. 619-635.
Costa, A. C. and Soares, A. (2008) 'Trends in extreme precipitation indices derived from a daily rainfall database for the South of Portugal', *International Journal of Climatology,* **29**, (13), pp. 1956-1975.
Cowpertwait, P. S. P. (2001) 'A renewal cluster model for the inter-arrival times of rainfall events', *International Journal of Climatology,* **21**, (1), pp. 49-61.
Cowpertwait, P. S. P., Kilsby, C. G. and O'Connell, P. E. (2002) 'A space-time Neyman-Scott model of rainfall: Empirical analysis of extremes', *Water Resour. Res.,* **38**, (8), pp. 1-14.
Dai, A. (2011) 'Drought under global warming: a review', *Wiley Interdisciplinary Reviews: Climate Change,* **2**, (1), pp. 45-65.
Dai, A., Trenberth, K. E. and Karl, T. R. (1998) 'Global variations in droughts and wet spells: 1900-1995', *Geophys. Res. Lett.,* **25**, pp. 2659-2663.
Dales, M. Y. and Reed, D. W. (1989) *Regional flood and storm hazard assessment.* Institute of Hydrology,Wallingford, Oxfordshire, OX10 8BB.
Davis, R. A. and Mikosch, T. (2008) *The Extremogram: a correlogram for extreme events.*
Davison, A. C. and Smith, R. L. (1990) 'Models for Exceedances over High Thresholds', *Journal of the Royal Statistical Society. Series B (Methodological),* **52**, (3), pp. 393-442.
DEFRA. (2012) *The UK Climate Change Risk Assessment 2012 Evidence Report.* DEFRA, London, UK.
Della-Marta, P., Luterbacher, J., von Weissenfluh, H., Xoplaki, E., Brunet, M. and Wanner, H. (2007) 'Summer heat waves over western Europe 1880–2003, their relationship to large-scale forcings and predictability', *Climate Dynamics,* **29**, (2), pp. 251-275.
Dessai, S., Hulme, M., Lempert, R. and Pielke, R. (2009) 'Do we need more precise and accurate predictions in order to adapt to a changing climate?', *Eos,* **90**, (13), pp. 111-112.
Dobson, A. J. (2002) *An introduction to generalized linear models.* Chapman & Hall/CRC.
Eakin, H. C. and Patt, A. (2011) 'Are adaptation studies effective, and what can enhance their practical impact?', *Wiley Interdisciplinary Reviews: Climate Change,* **2**, (2), pp. 141-153.
Eastoe, E. F. and Tawn, J. A. (2010) 'Statistical models for overdispersion in the frequency of peaks over threshold data for a flow series', *Water Resour. Res.,* **46**, (2), pp. W02510.
Efron, B. (1979) 'Bootstrap Methods: Another Look at the Jackknife', *The Annals of Statistics,* **7**, (1), pp. 1-26.
Efron, B. and Tibshirani, R. J. (1993) *An Introduction to the Bootstrap.* Chapman & Hall,London.
Englehart, P. J. and Douglas, A. V. (2006) 'Defining Intraseasonal Rainfall Variability within the North American Monsoon', *Journal of Climate,* **19**, (17), pp. 4243-4253.
Environment Agency. (2012) *Drought management briefing.* in (ed),^(eds) Environment Agency
Faraway, J. J. (2006) *Extending the linear model with R: generalized linear, mixed effects and nonparametric regression models.* Chapman & Hall/CRC.
Faulkner, D. S. (1999) *Rainfall frequency estimation.* Wallingford, Oxfordshire, OX10 8BB, UK.
Faulkner, D. S. and Prudhomme, C. (1997) *Rainfall Frequency Estimation in England and Wales. Phase 2: Production.* in (ed),^(eds) Bristol, UK. Environment Agency

Fawcett, L. and Walshaw, D. (2008) 'Bayesian inference for clustered extremes', *Extremes,* **11**, (3), pp. 217-233.
Ferro, C. A. T. and Segers, J. (2003) 'Inference for clusters of extreme values', *Journal of the Royal Statistical Society: Series B (Statistical Methodology),* **65**, (2), pp. 545-556.
Folland, C. K., Knight, J., Linderholm, H. W., Fereday, D., Ineson, S. and Hurrell, J. W. (2009) 'The Summer North Atlantic Oscillation: Past, Present, and Future', *Journal of Climate,* **22**, (5), pp. 1082-1103.
Forster, P., Ramaswamy, V., Artaxo, P., Berntsen, T., Retts, R., Fahey, D. W., Haywood, J., Lean, J., Lowe, D. C., Myhre, G., Nganga, J., Prinn, R., Raga, G., Schulz, M. and Van Dorland, R. (2007) 'Changes in Atmospheric Constituents and in Radiative Forcing', in *Climate Change 2007: The Physical Science Basis. Contribution of Working Group I to the Fourth Assessment Report of the Intergovernmental Panel on Climate Change.* Cambridge University Press, Cambridge, UK.
Fowler, H., Cooley, D., Sain, S. and Thurston, M. (2010) 'Detecting change in UK extreme precipitation using results from the climateprediction.net BBC climate change experiment', *Extremes,* **13**, (2), pp. 241-267.
Fowler, H. J. and Archer, D. R. (2006) 'Conflicting Signals of Climatic Change in the Upper Indus Basin', *Journal of Climate,* **19**, (17), pp. 4276-4293.
Fowler, H. J., Blenkinsop, S. and Tebaldi, C. (2007) 'Linking climate change modelling to impacts studies: recent advances in downscaling techniques for hydrological modelling', *International Journal of Climatology,* **27**, (12), pp. 1547-1578.
Fowler, H. J. and Ekström, M. (2009) 'Multi-model ensemble estimates of climate change impacts on UK seasonal precipitation extremes', *International Journal of Climatology,* **29**, (3), pp. 385-416.
Fowler, H. J. and Kilsby, C. G. (2002) 'Precipitation and the North Atlantic Oscillation: a study of climatic variability in northern England', *International Journal of Climatology,* **22**, (7), pp. 843-866.
Fowler, H. J. and Kilsby, C. G. (2003a) 'Implications of changes in seasonal and annual extreme rainfall', *Geophys. Res. Lett.,* **30**, (13), pp. 1720-1723.
Fowler, H. J. and Kilsby, C. G. (2003b) 'A regional frequency analysis of United Kingdom extreme rainfall from 1961 to 2000', *International Journal of Climatology,* **23**, (11), pp. 1313-1334.
Fowler, H. J. and Wilby, R. L. (2010) 'Detecting changes in seasonal precipitation extremes using regional climate model projections: Implications for managing fluvial flood risk', *Water Resour. Res.,* **46**, (3), pp. W03525.
Frei, C. and Schar, C. (2001) 'Detection probability of trends in rare events: Theory and application to heavy precipitation in the Alpine region', *Journal of Climate,* **14**, (7), pp. 1568-1584.
Frei, C., Schöll, R., Fukutome, S., Schmidli, J. and Vidale, P. L. (2006) 'Future change of precipitation extremes in Europe: Intercomparison of scenarios from regional climate models', *J. Geophys. Res.,* **111**.
Frich, P., Alexander, L., Della-Marta, P., Gleason, B., Haylock, M., Klein Tank, A. and Peterson, T. (2002) 'Observed coherent changes in climatic extremes during the second half of the twentieth century', *Climate Research,* **19**, (3), pp. 193-212.
Furrer, E. M., Katz, R. W., Walter, M. D. and Furrer, R. (2010) 'Statistical modeling of hot spells and heat waves', *Climate Research,* **43**, (3), pp. 191-205.
Furrer, R., Nychka, D. and Sain, S. (2012) *fields: Tools for spatial data* (6.6.3)

Gallant, A. J. E., Hennessy, K. J. and Risbey, J. S. (2007) 'Trends in rainfall indices for six Australian regions: 1910-2005', *Aust. Meteorol. Mag.,* **56**, pp. 223-239.
Gao, P., Zhang, X., Mu, X., Wang, F., Li, R. and Zhang, X. (2010) 'Trend and change-point analyses of streamflow and sediment discharge in the Yellow River during 1950–2005', *Hydrological Sciences Journal,* **55**, (2), pp. 275-285.
Gershunov, A., Cayan, D. R. and Iacobellis, S. F. (2009) 'The Great 2006 Heat Wave over California and Nevada: Signal of an Increasing Trend', *Journal of Climate,* **22**, (23), pp. 6181-6203.
Gershunov, A. and Douville, H. (2008) 'Extensive summer hot and cold extremes under current and possible future climatic conditions: Europe and North America', in *Climate Extremes and Societ.* Cambridge University Press.
Ghil, M., Yiou, P. H., S., Malamud, B. D., Naveau, P., Soloviev, A., Friederichs, P., Keilis-Borok, V., Kondrashov, D., Kossobokov, V., Mestre, O., Nicolis, C., Rust, H. W., Shebalin, P., Vrac, M., Witt, A. and Zaliapin, I. (2011) 'Extreme events: dynamics, statistics and prediction', *Nonlin. Processes Geophys.,* **18**, (3), pp. 295-350.
Gilleland, E. and Katz, R. W. (2011) 'New software to analyze how extremes change over time', *Eos,* **92**, (2), pp. 13-14.
Gilleland, E., Katz, R. W. and Young, G. (2009) *extRemes: Extreme value toolkit* (1.60) [R package].
Gong, D. and Wang, S. (1999) 'Definition of Antarctic Oscillation Index', *Geophys. Res. Lett.,* **26**, (4), pp. 459-462.
Goosse, H., Barriat, P. Y., Lefebvre, W., Loutre, M. F. and Zunz, V. (2009) *Introduction to climate dynamics and climate modelling - Online textbook* [Online]. Available at: http://www.climate.be/textbook (Accessed: 16/03/09).
Gouveia, C., Trigo, R. M., DaCamara, C. C., Libonati, R. and Pereira, J. M. C. (2008) 'The North Atlantic Oscillation and European vegetation dynamics', *International Journal of Climatology,* **28**, (14), pp. 1835-1847.
Gregory, J. M., Jones, P. D. and Wigley, T. M. L. (1991) 'Precipitation in Britain: An analysis of area-average data updated to 1989', *International Journal of Climatology,* **11**, (3), pp. 331-345.
Gregory, S. (1975) 'On the delimitation of regional patterns of recent climatic fluctuations', *Weather,* **30**, (9), pp. 276-287.
Gringorten, I. I. (1963) 'A Plotting Rule for Extreme Probability Paper', *J. Geophys. Res.,* **68**, (3), pp. 813-814.
Groisman, P. Y., Karl, T. R., Easterling, D. R., Knight, R. W., Jamason, P. F., Hennessy, K. J., Suppiah, R., Page, C. M., Wibig, J., Fortuniak, K., Razuvaev, V. N., Douglas, A., Førland, E. and Zhai, P.-M. (1999) 'Changes in the Probability of Heavy Precipitation: Important Indicators of Climatic Change', *Climatic Change,* **42**, (1), pp. 243-283.
Groisman, P. Y. and Knight, R. W. (2008) 'Prolonged Dry Episodes over the Conterminous United States: New Tendencies Emerging during the Last 40 Years', *Journal of Climate,* **21**, (9), pp. 1850-1862.
Groisman, P. Y., Knight, R. W. and Karl, T. R. (2001) 'Heavy Precipitation and High Streamflow in the Contiguous United States: Trends in the Twentieth Century', *Bulletin of the American Meteorological Society,* **82**, (2), pp. 219-246.
Guedes Soares, C. and Scotto, M. G. (2004) 'Application of the r largest-order statistics for long-term predictions of significant wave height', *Coastal Engineering,* **51**, (5-6), pp. 387-394.

Hamed, K. H. and Ramachandra Rao, A. (1998) 'A modified Mann-Kendall trend test for autocorrelated data', *Journal of Hydrology,* **204**, (1-4), pp. 182-196.
Hand, W. H., Fox, N. I. and Collier, C. G. (2004) 'A study of twentieth-century extreme rainfall events in the United Kingdom with implications for forecasting', *Meteorological Applications,* **11**, (1), pp. 15-31.
Hanna, E., Mayes, J., Beswick, M., Prior, J. and Wood, L. (2008) 'An analysis of the extreme rainfall in Yorkshire, June 2007, and its rarity', *Weather,* **63**, (9), pp. 253-260.
Hannaford, J., Lloyd-Hughes, B., Keef, C., Parry, S. and Prudhomme, C. (2011) 'Examining the large-scale spatial coherence of European drought using regional indicators of precipitation and streamflow deficit', *Hydrological Processes,* **25**, (7), pp. 1146-1162.
Hannaford, J. and Marsh, T., J. (2008) 'High-flow and flood trends in a network of undisturbed catchments in the UK', *International Journal of Climatology,* **28**, (10), pp. 1325-1338.
Hansen, J., Ruedy, R., Sato, M. and Lo, K. (2002) 'Global Warming Continues', *Science,* **295**, (5553), pp. 275.
Hartigan, J. A. and Wong, M. A. (1979) 'Algorithm AS 136: A K-Means Clustering Algorithm', *Journal of the Royal Statistical Society. Series C (Applied Statistics),* **28**, (1), pp. 100-108.
Hastie, T. J. and Tibshirani, R. J. (1990) *Generalized Additive Models.* Taylor and Francis.
Haylock, M. R., Hofstra, N., Klein Tank, A. M. G., Klok, E. J., Jones, P. D. and New, M. (2008) 'A European daily high-resolution gridded data set of surface temperature and precipitation for 1950–2006', *JOURNAL OF GEOPHYSICAL RESEARCH,* **113**.
Hegerl, G., Zwiers, F. W., Braconnot, P., Gillett, N. P., Luo, Y., Marengo Orsini, J. A., Nicholls, N., Penner, J. E. and Stott, P. A. (2007) 'Understanding and Attributing Climate Change', in *Climate Change 2007: The Physical Science Basis. Contribution of Working Group I to the Fourth Assessment Report of the Intergovernmental Panel on Climate Change.* Cambridge University Press, Cambridge, UK.
Hegerl, G. C., Zwiers, F. W., Stott, P. A. and Kharin, V. V. (2004) 'Detectability of Anthropogenic Changes in Annual Temperature and Precipitation Extremes', *Journal of Climate,* **17**, (19), pp. 3683-3700.
Held, I. M. (1993) 'Large-Scale Dynamics and Global Warming', *Bulletin of the American Meteorological Society,* **74**, (2), pp. 228-241.
Hess, A., Iyer, H. and Malm, W. (2001) 'Linear trend analysis: a comparison of methods', *Atmospheric Environment,* **35**, (30), pp. 5211-5222.
Hess, S. L. (1959) *Introduction to Theoretical Meteorology.* Holt,New York.
Holman, I. P., Hollis, J. M., Bramley, M. E. and Thompson, T. R. E. (2003) 'The contribution of soil structural degradation to catchment flooding: a preliminary investigation of the 2000 floods in England and Wales', *Hydrol. Earth Syst. Sci.,* **7**, (5), pp. 755-766.
Hopkins, J., Warburton, J. and Burt, T. (2010) 'Placing heavy rainfall events in context using long time series: An example from the North York Moors', *Weather,* **65**, (4), pp. 88-94.
Hosking, J. R. M. (1990) 'L-Moments: Analysis and Estimation of Distributions Using Linear Combinations of Order Statistics', *Journal of the Royal Statistical Society. Series B (Methodological),* **52**, (1), pp. 105-124.
Hosking, J. R. M. (1995a) 'The use of L-moments in the analysis of censored data', in *Recent advances in life-testing and reliability.* CRC Press, Boca Raton, Fla, pp. 545-564.
Hosking, J. R. M. (1995b) http://www.research.ibm.com/people/h/hosking/lmoments.html (Accessed: 17/06/09)

Hosking, J. R. M. and Wallis, J. R. (1988) 'The Effect of Intersite Dependence on Regional Flood Frequency Analysis', *Water Resources Research,* **24**, (4), pp. 588-600.
Hosking, J. R. M. and Wallis, J. R. (1993) 'Some statistics useful in regional frequency analysis', *Water Resour. Res.,* **29**, (2), pp. 271-281.
Hosking, J. R. M. and Wallis, J. R. (1997) *Regional frequency analysis: an approach based on L-moments.* Cambridge University Press,Cambridge, UK.
Hossell, J. E., Riding, A. E. and Brown, I. (2003) 'The creation and characterisation of a bioclimatic classification for Britain and Ireland', *Journal for Nature Conservation,* **11**, (1), pp. 5-13.
Hsing, T. (1988) 'On the extreme order statistics for a stationary sequence', *Stochastic Processes and their Applications,* **29**, (1), pp. 155-169.
Hurrell, J. W. (1995) 'Decadal Trends in the North Atlantic Oscillation: Regional Temperatures and Precipitation', *Science,* **269**, (5224), pp. 676-679.
Hurrell, J. W. (1996) 'Influence of Variations in Extratropical Wintertime Teleconnections on Northern Hemisphere Temperature', *Geophys. Res. Lett.,* **23**.
Hurrell, J. W. (2003) *The North Atlantic oscillation: climatic significance and environmental impact.* American Geophysical Union.
Hurrell, J. W. and Deser, C. (2009) 'North Atlantic climate variability: The role of the North Atlantic Oscillation', *Journal of Marine Systems,* **78**, (1), pp. 28-41.
Hurrell, J. W., Kushnir, Y. and Visbeck, M. (2001) 'The North Atlantic Oscillation', *Science,* **291**, (5504), pp. 603-605.
Hurrell, J. W. and Van Loon, H. (1997) 'Decadal variations in climate associated with the North Atlantic Oscillation', *Climatic Change,* **36**, (3), pp. 301-326.
Hurst, H. E. (1951) 'Long-term storage capacities of reservoirs', *Trans. Am. Soc. Civil Eng,* **116**, (3), pp. 770-799.
Husak, G. J., Michaelsen, J. and Funk, C. (2007) 'Use of the gamma distribution to represent monthly rainfall in Africa for drought monitoring applications', *International Journal of Climatology,* **27**, (7), pp. 935-944.
Hyndman, R. J. and Grunwald, G. K. (2000) 'Applications: Generalized Additive Modelling of Mixed Distribution Markov Models with Application to Melbourne's Rainfall', *Australian & New Zealand Journal of Statistics,* **42**, (2), pp. 145-158.
Institute of Hydrology. (1975) *Flood Studies Report.* Natural Environment Research Council.
Institute of Hydrology. (1999) *Flood Estimation Handbook (Procedures for Flood Frequency Estimation).* Institute of Hydrology, Wallingford, Oxfordshire OX10 8BB, UK.
IPCC. (2007a) *Climate Change 2007: Synthesis Report. Contribution of Working Groups I, II and III to the Fourth Assessment Report of the Intergovernmental Panel on Climate Change.* in R. K. Pachauri and A. Reisinger (ed),^(eds) Geneva, Switzerland. IPCC pp. 104.
IPCC. (2007b) *Climate Change 2007: Impacts, Adaptation and Vulnerability : Contribution of Working Group II to the Fourth Assessment Report of the Intergovernmental Panel on Climate Change.* in M. L. Parry, O. F. Canziani, J. P. Palutikof, P. J. van der Linden and C. E. Hanson (ed),^(eds) Geneva, Switzerland. IPCC (9780521880107). pp. 976.
IPCC. (2011) 'Summary for Policy Makers', in *Special Report for Managing the Risks of Extreme Events and Disasters to Advance Climate Change Adaptation. Contribution of Working Group II.* Intergovernmental Panel on Climate Change.
Jackson, M. C. and Larke, P. R. (1974) *Frequencies of specified rainfall amounts within specified elevation over England and Wales.* in Met Office (ed),^(eds)

Jakob, D., Karoly, D. J. and Seed, A. (2011) 'Non-stationarity in daily and sub-daily intense rainfall - Part 2: Regional assessment for sites in south-east Australia', *Nat. Hazards Earth Syst. Sci.,* **11**, pp. 2273-2284.

Jenkins, G., Perry, M. and Prior, J. (2010) *The climate of the UK and recent trends*. [Online]. Available at: http://ukclimateprojections.defra.gov.uk/content/view/816/500 (Accessed: 23/03/11).

Jiménez, P. A., González-Rouco, J. F., Montávez, J. P., García-Bustamante, E. and Navarro, J. (2009) 'Climatology of wind patterns in the northeast of the Iberian Peninsula', *International Journal of Climatology,* **29**, (4), pp. 501-525.

Jolliffe, I. T. (1972) 'Discarding Variables in a Principal Component Analysis. I: Artificial Data', *Journal of the Royal Statistical Society. Series C (Applied Statistics),* **21**, (2), pp. 160-173.

Jolliffe, I. T. (1973) 'Discarding Variables in a Principal Component Analysis. II: Real Data', *Journal of the Royal Statistical Society. Series C (Applied Statistics),* **22**, (1), pp. 21-31.

Jones, P. D. (2011) http://www.cru.uea.ac.uk/cru/info/warming/ (Accessed: 20/04/2011)

Jones, P. D. and Conway, D. (1997) 'Precipitation in the British Isles: An analysis of area-averaged data updated to 1995', *International Journal of Climatology,* **17**, (4), pp. 427-438.

University of East Anglia Climatic Research Unit (CRU). [Jones, P. D. and Harris, I.], CRU Times Series (TS) high resolution gridded datasets., (2008), *09/03/12*. Available from:

Jones, P. D., Jonsson, T. and Wheeler, D. (1997) 'Extension to the North Atlantic oscillation using early instrumental pressure observations from Gibraltar and south-west Iceland', *International Journal of Climatology,* **17**, (13), pp. 1433-1450.

Jones, P. D. and Lister, D. (2004) 'The development of monthly temperature series for Scotland and Northern Ireland', *International Journal of Climatology,* **24**, (5), pp. 569-590.

Jones, P. D., Osborn, T. J. and Briffa, K. R. (2003) 'Pressure-based measures of the North Atlantic Oscillation (NAO): A comparison and an assessment of changes in the strength of the NAO and in its influence on surface climate parameters', in *The North Atlantic Oscillation: Climatic Signifiicance and Environmental Impact Geophysical Monograph 134.* American Geophysical Union, Washington, DC, pp. 51-62. .

Jones, P. D., Parker, D. E., Osborn, T. J. and Briffa, K. R. (2011) *Global and hemispheric temperature anomalies—land and marine instrumental records.* in (ed),^(eds) Carbon Dioxide Information Analysis Center, Oak Ridge National Laboratory, U.S. Department of Energy, Oak Ridge, Tenn., U.S.A.

Kaiser, H. F. (1960) 'The application of electronic computers to factor analysis', *Educational and Psychological Measurement,* **20**, pp. 141-151.

Kanji, G. K. (1999) *100 statistical tests.* Sage Publications.

Karl, T. R. and Knight, R. W. (1998) 'Secular Trends of Precipitation Amount, Frequency, and Intensity in the United States', *Bulletin of the American Meteorological Society,* **79**, (2), pp. 231-241.

Karnauskas, K. B. and Busalacchi, A. J. (2009) 'The Role of SST in the East Pacific Warm Pool in the Interannual Variability of Central American Rainfall', *Journal of Climate,* **22**, (10), pp. 2605-2623.

Katsoulis, B. D. and Hatzianastassiou, N. (2005) 'Analysis of hot spell characteristics in the Greek region', *Climate Research,* **28**, (3), pp. 229-241.

Katz, R. W. (1999) 'Extreme value theory for precipitation: sensitivity analysis for climate change', *Advances in Water Resources,* **23**, (2), pp. 133-139.

Katz, R. W., Parlange, M. B. and Naveau, P. (2002) 'Statistics of extremes in hydrology', *Advances in Water Resources,* **25**, (8-12), pp. 1287-1304.
Kendall, M. G. (1962) *Rank correlation methods.* Hafner Pub. Co.
Kendon, E. J., Roberts, N. M., Senior, C. A. and Roberts, M. J. (2012) 'Realism of rainfall in a very high resolution regional climate model', *Journal of Climate*.
Kenyon, J. and Hegerl, G. C. (2008) 'Influence of Modes of Climate Variability on Global Temperature Extremes', *Journal of Climate,* **21**, (15), pp. 3872-3889.
Kettlewell, P. S., Easey, J., Stephenson, D. B. and Poulton, P. R. (2006) 'Soil moisture mediates association between the winter North Atlantic Oscillation and summer growth in the Park Grass Experiment', *Proceedings of the Royal Society B: Biological Sciences,* **273**, (1590), pp. 1149-1154.
Klein Tank, A. M. G., Wijngaard, J. B., Können, G. P., Böhm, R., Demarée, G., Gocheva, A., Mileta, M., Pashiardis, S., Hejkrlik, L., Kern-Hansen, C., Heino, R., Bessemoulin, P., Müller-Westermeier, G., Tzanakou, M., Szalai, S., Pálsdóttir, T., Fitzgerald, D., Rubin, S., Capaldo, M., Maugeri, M., Leitass, A., Bukantis, A., Aberfeld, R., van Engelen, A. F. V., Forland, E., Mietus, M., Coelho, F., Mares, C., Razuvaev, V., Nieplova, E., Cegnar, T., López, J. A., Dahlström, B., Moberg, A., Kirchhofer, W., Ceylan, A., Pachaliuk, O., Alexander, L. V. and Petrovic, P. (2002) 'Daily dataset of 20th-century surface air temperature and precipitation series for the European Climate Assessment', *International Journal of Climatology,* **22**, (12), pp. 1441-1453.
Klemes, V. (1974) 'The Hurst Phenomenon: A Puzzle?', *Water Resour. Res.,* **10**, (4), pp. 675-688.
Knox, J. C. (2000) 'Sensitivity of modern and Holocene floods to climate change', *Quaternary Science Reviews,* **19**, (1-5), pp. 439-457.
Koenker, R. (2011) *quantreg: Quantile Regression* (4.71) [R package].
Komsta, L. and Novomestky, F. (2011) *moments: Moments, cumulants, skewness, kurtosis and related tests* (0.12)
Können, G. P., Jones, P. D., Kaltofen, M. H. and Allan, R. J. (1998) 'Pre-1866 Extensions of the Southern Oscillation Index Using Early Indonesian and Tahitian Meteorological Readings', *Journal of Climate,* **11**, (9), pp. 2325-2339.
Kottegoda, N. T., Natale, L. and Raiteri, E. (2008) 'Stochastic modelling of periodicity and trend for multisite daily rainfall simulation', *Journal of Hydrology,* **361**, (3-4), pp. 319-329.
Koutsoyiannis, D. (2002) 'The Hurst phenomenon and fractional Gaussian noise made easy', *Hydrological Sciences Journal,* **47**, (4), pp. 573-595.
Koutsoyiannis, D. (2003) 'Climate change, the Hurst phenomenon, and hydrological statistics', *Hydrological Sciences Journal,* **48**, (1), pp. 3-24.
Koutsoyiannis, D. (2006) 'Nonstationarity versus scaling in hydrology', *Journal of Hydrology,* **324**, (1-4), pp. 239-254.
Krebs, J., Dlugolecki, A., Fankhauser, S., Hall, J. W., Johnson, A., Palmer, T., Parry, M. and Wynne, G. (2011) *Adapting to Climate Change in the UK: Measuring Progress.* in Adaptation Sub-Committee (ed),^(eds) Adaptation Sub-Committee
Krebs, J., Dlugolecki, A., Fankhauser, S., Hall, J. W., Johnson, A., Palmer, T., Parry, M., Wynne, G. and Young, B. (2010) *How well prepared is the UK for Climate Change?* , in Adaptation Sub-Committee (ed),^(eds) London. Adaptation Sub-Committee
Kruger, A. C. (2006) 'Observed trends in daily precipitation indices in South Africa: 1910-2004', *International Journal of Climatology,* **26**, (15), pp. 2275-2285.

Kundzewicz, Z. W. and Robson, A. (2000) *Detecting trend and other changes in hydrological data.* World Meteorological Organization.

Kundzewicz, Z. W. and Robson, A. J. (2004) 'Change detection in hydrological records—a review of the methodology', *Hydrological Sciences Journal,* **49**, (1), pp. 19.

Kunkel, K. E., Easterling, D. R., Redmond, K. and Hubbard, K. (2003) 'Temporal variations of extreme precipitation events in the United States: 1895-2000', *Geophys. Res. Lett.,* **30**, (17), pp. 1900.

Lamb, H. H. (1972) *British Isles Weather types and a register of daily sequence of circulation patterns, 1861-1971.* in (ed),^(eds) pp. 85.

Lana, X., Martínez, M. D., Burgueño, A., Serra, C., Martín-Vide, J. and Gómez, L. (2006) 'Distributions of long dry spells in the iberian peninsula, years 1951-1990', *International Journal of Climatology,* **26**, (14), pp. 1999-2021.

Lang, M. (1999) 'Theoretical discussion and Monte-Carlo simulations for a Negative Binomial process paradox', *Stochastic Environmental Research and Risk Assessment,* **13**, (3), pp. 183-200.

Lavers, D. A., Allan, R. P., Wood, E. F., Villarini, G., Brayshaw, D. J. and Wade, A. J. (2011) 'Winter floods in Britain are connected to atmospheric rivers', *Geophys. Res. Lett.,* **38**, (23), pp. L23803.

Le Treut, H., Somerville, R. C. J., Cubasch, U., Ding, C., Mauritzen, A., Mokssit, A., Peterson, T. and Prather, M. (2007) 'Historical Overview of Climate Change', in *Climate Change 2007: The Physical Science Basis. Contribution of Working Group I to the Fourth Assessment Report of the Intergovernmental Panel on Climate Change.* Cambridge University Press, Cambridge, UK.

Leadbetter, M. R. (1983) 'Extremes and local dependence in stationary sequences', *Probability Theory and Related Fields,* **65**, (2), pp. 291-306.

Lemon, J. (2006) 'Plotrix: a package in the red light district of R', *R-News,* **6**, (4), pp. 8-12.

Lenderink, G. and van Meijgaard, E. (2008) 'Increase in hourly precipitation extremes beyond expectations from temperature changes', *Nature Geosci,* **1**, (8), pp. 511-514.

Lenton, T. M., Held, H., Kriegler, E., Hall, J. W., Lucht, W., Rahmstorf, S. and Schellnhuber, H. J. (2008) 'Tipping elements in the Earth's climate system', *Proceedings of the National Academy of Sciences,* **105**, (6), pp. 1786-1793.

Li, X., Jiang, F., Li, L. and Wang, G. (2011) 'Spatial and temporal variability of precipitation concentration index, concentration degree and concentration period in Xinjiang, China', *International Journal of Climatology,* **31**, (11), pp. 1679-1693.

Linderholm, H. W., Folland, C. K. and Walther, A. (2009) 'A multicentury perspective on the summer North Atlantic Oscillation (SNAO) and drought in the eastern Atlantic Region', *Journal of Quaternary Science,* **24**, (5), pp. 415-425.

Lins, H. F. and Cohn, T. A. (2011) 'Stationarity: Wanted Dead or Alive?', *JAWRA Journal of the American Water Resources Association,* **47**, (3), pp. 475-480.

Liu, B., Henderson, M., Xu, M. and Zhang, Y. (2011) 'Observed changes in precipitation on the wettest days of the year in China, 1960–2000', *International Journal of Climatology,* **31**, (4), pp. 487–503.

Liu, S. C., Fu, C., Shiu, C.-J., Chen, J.-P. and Wu, F. (2009) 'Temperature dependence of global precipitation extremes', *Geophys. Res. Lett.,* **36**, (17), pp. L17702.

Logan, J. A., Macfarlane, W. W. and Willcox, L. (2010) 'Whitebark pine vulnerability to climate-driven mountain pine beetle disturbance in the Greater Yellowstone Ecosystem', *Ecological Applications,* **20**, (4), pp. 895-902.

Lowe, J. A., Howard, T., Pardaens, A., Tinker, J., Jenkins, G., Ridley, J., Leake, J., Holt, J., Wakelin, S., Wolf, J., Horsburgh, K., Reeder, T., Milne, G., Bradley, S. and Dye, S. (2009) *UK Climate Projections science report: Marine and coastal projections.* Met Office Hadley Centre,Exeter, UK.

Macdonald, N., Jones, C. A., Davies, S. J. and Charnell-White, C. (2010) 'Historical weather accounts from Wales: an assessment of their potential for reconstructing climate', *Weather,* **65**, (3), pp. 72-81.

Madden, R. and Julian, P. (1971) 'Detection of a 40-50 day oscillation in the zonal wind in the tropical Pacific', *Journal of Atmospheric Sciences,* **28**, pp. 702-708.

Madden, R. and Julian, P. (1972) 'Description of global-scale circulation cells in the tropics with a 40-50 day period', *Journal of Atmospheric Sciences,* **28**, pp. 1109-1123.

Madden, R. and Julian, P. (1994) 'Observations of the 40-50 day tropical oscillation: a review', *Mon. Weather Rev.,* **122**, pp. 814-837.

Maechler, M., Rousseeuw, P., Struyf, A., Hubert, M. and Hornik, K. (2011) *cluster: Cluster Analysis Basics and Extensions* (1.14.1)

Mailier, P. J., Stephenson, D. B., Ferro, C. A. T. and Hodges, K. I. (2006) 'Serial clustering of extratropical cyclones', *Mon. Weather Rev.,* **134**, (8), pp. 2224-2240.

Mandelbrot, B. B. and Wallis, J. R. (1968) 'Noah, Joseph, and Operational Hydrology', *Water Resour. Res.,* **4**, (5), pp. 909-918.

Manley, G. (1974) 'Central England temperatures: monthly means 1659 to 1973. ', *Quarterly Journal of the Royal Meteorological Society*
100, pp. 389-405.

Mantua, N. J., Hare, S. R., Zhang, Y., Wallace, J. M. and Francis, R. C. (1997) 'A Pacific Interdecadal Climate Oscillation with Impacts on Salmon Production', *Bulletin of the American Meteorological Society,* **78**, (6), pp. 1069-1079.

Maraun, D. (2009) RE: Maraun et al. (2008), definition of percentile thresholds, 24/03/2009.

Maraun, D., Osborn, T. and Rust, H. (2011) 'The influence of synoptic airflow on UK daily precipitation extremes. Part I: Observed spatio-temporal relationships', *Climate Dynamics,* **36**, (1), pp. 261-275.

Maraun, D., Osborn, T. J. and Gillett, N. P. (2008) 'United Kingdom daily precipitation intensity: improved early data, error estimates and an update from 2000 to 2006', *International Journal of Climatology,* **28**, (6), pp. 833-842.

Maraun, D., Rust, H. W. and Osborn, T. J. (2009) 'The annual cycle of heavy precipitation across the United Kingdom: a model based on extreme value statistics', *International Journal of Climatology,* **29**, (12), pp. 1731-1744.

Marra, G. and Wood, S. N. (2011) 'Practical variable selection for generalized additive models', *Computational Statistics & Data Analysis,* **55**, (7), pp. 2372-2387.

Marsh, T. (2008) 'A hydrological overview of the summer 2007 floods in England and Wales', *Weather,* **63**, (9), pp. 274-279.

Marsh, T. J. and Dale, M. (2002) 'The UK Floods of 2000–2001: A Hydrometeorological Appraisal', *Water and Environment Journal,* **16**, (3), pp. 180-188.

Marshall, G. J. (2003) 'Trends in the Southern Annular Mode from Observations and Reanalyses', *Journal of Climate,* **16**, (24), pp. 4134-4143.

Mastrandrea, M. D., Field, C. B., Stocker, T. F., Edenhofer, O., Ebi, K. L., Frame, D. J., Held, H., Kriegler, E., Mach, K. J., Matschoss, P. R., Plattner, G.-K., Yohe, G. and Zwiers, F. W. (2010) *Guidance Note for Lead Authors of the IPCC Fifth Assessment Report on*

Consistent Treatment of Uncertainties. in (ed),^(eds) Geneva, Switzerland. Intergovernmental Panel on Climate Change (IPCC)

Matalas, N. C. (1997) 'Stochastic Hydrology in the Context of Climate Change', *Climatic Change,* **37**, (1), pp. 89-101.

Maynard, T. (2006) *Climate Change: Adapt or Bust.* in (ed),^(eds) www.lloyds.com/360. Lloyd's

McEvoy, D., Matczak, P., Banaszak, I. and Chorynski, A. (2010) 'Framing adaptation to climate-related extreme events', *Mitigation and Adaptation Strategies for Global Change,* **15**, (7), pp. 779-795.

McKee, T. B., Doesken, N. J. and Kleist, J. (1993) '*The relationship of drought frequency and duration to time scales',* In: Proc. *Eighth Conference on Applied Climatology.* Anaheim, California, 17-22 January 1993. pp.

McLeod, A. I. (2009) *Kendall: Kendall rank correlation and Mann-Kendall trend test* (2.1) [R package].

McWilliams, T. P. (1990) 'A Distribution-Free Test for Symmetry Based on a Runs Statistic', *Journal of the American Statistical Association,* **85**, (412), pp. 1130-1133.

Meehl, G. A., Arblaster, J. M. and Tebaldi, C. (2005) 'Understanding future patterns of increased precipitation intensity in climate model simulations', *Geophys. Res. Lett.,* **32**.

Meehl, G. A., Stocker, T. F., Collins, W. D., Friedlingstein, P., Gaye, A. T., Gregory, J. M., Kitoh, A., Knutti, R., Murphy, J., Noda, A., Raper, S. C. B., Watterson, I. G., Weaver, A. J. and Zhao, Z.-C. (2007) 'Global Climate Projections', in *Climate Change 2007: The Physical Science Basis. Contribution of Working Group I to the Fourth Assessment Report of the Intergovernmental Panel on Climate Change.* Cambridge University Press, Cambridge, UK.

Mestre, O. and Hallegatte, S. (2009) 'Predictors of Tropical Cyclone Numbers and Extreme Hurricane Intensities over the North Atlantic Using Generalized Additive and Linear Models', *Journal of Climate,* **22**, (3), pp. 633-648.

Met Office. (2010a) http://www.metoffice.gov.uk/climate/uk/interesting/nov2009/ (Accessed: 11/08/2011)

Met Office. (2010b) http://www.metoffice.gov.uk/climate/uk/interesting/nov2009/ (Accessed: 19/07/2011)

Met Office. (2011a) http://badc.nerc.ac.uk/data/ukmo-midas/ukmo_guide.html (Accessed: 11/11/2011)

Met Office. (2011b) 'United Kingdom', in *Climate: Observations, projections and impacts.* Exeter, UK.

Met Office. (2011c) http://www.metoffice.gov.uk/research/climate/climate-impacts/regional-climate (Accessed: 11 April 2012)

Michaels, P. J., Knappenberger, P. C., Frauenfeld, O. W. and Davis, R. E. (2004) 'Trends in precipitation on the wettest days of the year across the contiguous USA', *International Journal of Climatology,* **24**, (15), pp. 1873-1882.

Mills, J. N., Gage, K., L. and Khan, A. S. (2010) 'Potential influence of climate change on vector-borne and zoonotic diseases: a review and proposed research plan', *Environ. Health Perspect,* **118**, pp. 1507-1514.

Mills, T. C. (2005) 'Modelling precipitation trends in England and Wales', *Meteorological Applications,* **12**, (2), pp. 169-176.

Milly, P. C. D., Betancourt, J., Falkenmark, M., Hirsch, R. M., Kundzewicz, Z. W., Lettenmaier, D. P. and Stouffer, R. J. (2008) 'CLIMATE CHANGE: Stationarity Is Dead: Whither Water Management?', *Science,* **319**, (5863), pp. 573-574.

Min, S.-K., Zhang, X., Zwiers, F., Friederichs, P. and Hense, A. (2009) 'Signal detectability in extreme precipitation changes assessed from twentieth century climate simulations', *Climate Dynamics,* **32**, (1), pp. 95-111.

Min, S.-K., Zhang, X., Zwiers, F. W. and Hegerl, G. C. (2011) 'Human contribution to more-intense precipitation extremes', *Nature,* **470**, (7334), pp. 378-381.

Mitchell, T. D. and Jones, P. D. (2005) 'An improved method of constructing a database of monthly climate observations and associated high-resolution grids', *International Journal of Climatology,* **25**, (6), pp. 693-712.

Moberg, A. and Jones, P. D. (2005) 'Trends in indices for extremes in daily temperature and precipitation in central and western Europe, 1901-99', *International Journal of Climatology,* **25**, (9), pp. 1149-1171.

Moncel, R., Joffe, P., McCall, K. and Levin, K. (2011) *Building the climate change regime: Survey and analysis of approaches.* in W. R. Institute (ed),^(eds) United Nations Environment Programme

Morton, R. and Henderson, B. L. (2008) 'Estimation of nonlinear trends in water quality: An improved approach using generalized additive models', *Water Resour. Res.,* **44**, (7), pp. W07420.

Mosley-Thompson, E., Readinger, C. R., Craigmile, P., Thompson, L. G. and Calder, C. A. (2005) 'Regional sensitivity of Greenland precipitation to NAO variability', *Geophys. Res. Lett.,* **32**.

Mumby, P. J., Vitolo, R. and Stephenson, D. B. (2011) 'Temporal clustering of tropical cyclones and its ecosystem impacts', *Proceedings of the National Academy of Sciences,* **108**, (43), pp. 17626-17630.

Murphy, J., Sexton, D., Jenkins, G., Boorman, P., Booth, B., Brown, K., Clark, R., Collins, M., Harris, G. and Kendon, L. (2009) *Climate change projections.* July 2nd 2009 ed Met Office Hadley Centre,Exeter.

Muza, M. N., Carvalho, L. M. V., Jones, C. and Liebmann, B. (2009) 'Intraseasonal and Interannual Variability of Extreme Dry and Wet Events over Southeastern South America and the Subtropical Atlantic during Austral Summer', *Journal of Climate,* **22**, (7), pp. 1682-1699.

Natural Resources Defense Council. (2011) *Health and Climate Change: Accounting for Costs.*

Naveau, P., Guillou, A., Cooley, D. and Diebolt, J. (2009) 'Modelling pairwise dependence of maxima in space', *Biometrika,* **96**, (1), pp. 1-17.

Neal, R. A. and Phillips, I. D. (2009) 'Summer daily precipitation variability over the East Anglian region of Great Britain', *International Journal of Climatology,* **29**, (11), pp. 1661-1679.

Nelder, J. A. and Wedderburn, R. W. M. (1972) 'Generalized Linear Models', *J. R. Statist. Soc. A,* **135**, (3), pp. 370.

Nelson, D. R. (2011) 'Adaptation and resilience: responding to a changing climate', *Wiley Interdisciplinary Reviews: Climate Change,* **2**, (1), pp. 113-120.

New, M., Todd, M., Hulme, M. and Jones, P. D. (2001) 'Precipitation measurements and trends in the twentieth century', *International Journal of Climatology,* **21**, (15), pp. 1889-1922.

Nicholls, N. (2001) 'commentary and analysis: The Insignificance of Significance Testing', *Bulletin of the American Meteorological Society,* **82**, (5), pp. 981-986.
NOAA. (2005) http://www.cpc.ncep.noaa.gov/data/teledoc/nao_pmap.shtml (Accessed: 07/08/11)
NOAA. (2011) http://www.cpc.ncep.noaa.gov/data/teledoc/telecontents.shtml (Accessed: 28/09/2011)
Nordli, Ø., Lie, Ø., Nesje, A. and Benestad, R. E. (2005) 'Glacier Mass Balance in Southern Norway Modelled by Circulation Indices and Spring-Summer Temperatures ad 1781-2000', *Geografiska Annaler: Series A, Physical Geography,* **87**, (3), pp. 431-445.
O'Gorman, P. A. and Schneider, T. (2009) 'The physical basis for increases in precipitation extremes in simulations of 21st-century climate change', *Proceedings of the National Academy of Sciences,* **106**, (35), pp. 14773-14777.
Onof, C. and Wheater, H. S. (1994) 'Improvements to the modelling of British rainfall using a modified Random Parameter Bartlett-Lewis Rectangular Pulse Model', *Journal of Hydrology,* **157**, (1-4), pp. 177-195.
Osborn, T. J. and Hulme, M. (2002) 'Evidence for Trends in Heavy Rainfall Events over the UK', *Philosophical Transactions: Mathematical, Physical and Engineering Sciences,* **360**, (1796), pp. 1313-1325.
Overeem, A., Buishand, A. and Holleman, I. (2008) 'Rainfall depth-duration-frequency curves and their uncertainties', *Journal of Hydrology,* **348**, (1-2), pp. 124-134.
Overpeck, J. T. (2000) 'Climate change: The hole record', *Nature,* **403**, (6771), pp. 714-715.
Oxford Dictionary of Modern Quotations. (2008) Ed. E. Knowles Oxford University Press.
Page, E. S. (1957) 'On Problems in which a Change in a Parameter Occurs at an Unknown Point', *Biometrika,* **44**, (1/2), pp. 248-252.
Pall, P., Aina, T., Stone, D. A., Stott, P. A., Nozawa, T., Hilberts, A. G. J., Lohmann, D. and Allen, M. R. (2011) 'Anthropogenic greenhouse gas contribution to flood risk in England and Wales in autumn 2000', *Nature,* **470**, (7334), pp. 382-385.
Pall, P., Allen, M. and Stone, D. (2007) 'Testing the Clausius–Clapeyron constraint on changes in extreme precipitation under CO2 warming', *Climate Dynamics,* **28**, (4), pp. 351-363.
Parker, D. E. (2010) 'Uncertainties in early Central England temperatures', *International Journal of Climatology,* **30**, (8), pp. 1105-1113.
Parker, D. E., Legg, T. P. and Folland, C. K. (1992) 'A new daily Central England Temperature series, 1772–1991', *International Journal of Climatology,* **12**, (4), pp. 317-342.
Pedgley, D. E. (2010) 'The British Rainfall Organization, 1859–1919', *Weather,* **65**, (5), pp. 115-117.
Perreault, L., Bernier, J., Bobée, B. and Parent, E. (2000a) 'Bayesian change-point analysis in hydrometeorological time series. Part 1. The normal model revisited', *Journal of Hydrology,* **235**, (3-4), pp. 221-241.
Perreault, L., Bernier, J., Bobée, B. and Parent, E. (2000b) 'Bayesian change-point analysis in hydrometeorological time series. Part 2. Comparison of change-point models and forecasting', *Journal of Hydrology,* **235**, (3-4), pp. 242-263.
Perry, M. (2006) *A spatial analysis of trends in the UK climate since 1914 using gridded datasets.* in N. C. I. Centre (ed),^(eds) Exeter, UK. Met Office
Perry, M., Hollis, D. and Elms, M. (2009) *The Generation of Daily Gridded Datasets of Temperature and Rainfall for the UK.* in (ed),^(eds) National Climate Information Centre

Peterson, T. C., Easterling, D. R., Karl, T. R., Groisman, P., Nicholls, N., Plummer, N., Torok, S., Auer, I., Boehm, R., Gullett, D., Vincent, L., Heino, R., Tuomenvirta, H., Mestre, O., Szentimrey, T., Salinger, J., Førland, E. J., Hanssen-Bauer, I., Alexandersson, H., Jones, P. and Parker, D. (1998) 'Homogeneity adjustments of in situ atmospheric climate data: a review', *International Journal of Climatology,* **18**, (13), pp. 1493-1517.

Peterson, T. C., Folland, C. K., Gruza, G., Hogg, W., Mokssit, A. and Plummer, N. (2001) *Report on the Activities of the Working Group on Climate Change Detection and Related Rapporteurs 1998-2001.* in WMO (ed),^(eds) Geneve, Switzerland. pp. 143.

Pettitt, A. N. (1979) 'A Non-Parametric Approach to the Change-Point Problem', *Journal of the Royal Statistical Society. Series C (Applied Statistics),* **28**, (2), pp. 126-135.

Pezzulli, S., Stephenson, D. B. and Hannachi, A. (2005) 'The Variability of Seasonality', *Journal of Climate,* **18**, (1), pp. 71-88.

Phillips, I. D. and McGregor, G. R. (2002) 'The relationship between monthly and seasonal South-west England rainfall anomalies and concurrent North Atlantic sea surface temperatures', *International Journal of Climatology,* **22**, (2), pp. 197-217.

Pnevmatikos, J. D. and Katsoulis, B. D. (2006) 'The changing rainfall regime in Greece and its impact on climatological means', *Meteorological Applications,* **13**, (4), pp. 331-345.

Portmann, R. W., Solomon, S. and Hegerl, G. C. (2009) 'Spatial and seasonal patterns in climate change, temperatures, and precipitation across the United States', *Proceedings of the National Academy of Sciences,* **106**, (18), pp. 7324-7329.

Prasad, V. K., Badarinath, K. V. S. and Eaturu, A. (2008) 'Effects of precipitation, temperature and topographic parameters on evergreen vegetation greenery in the Western Ghats, India', *International Journal of Climatology,* **28**, (13), pp. 1807-1819.

Prudhomme, C. and Genevier, M. (2011) 'Can atmospheric circulation be linked to flooding in Europe?', *Hydrological Processes,* **25**, (7), pp. 1180-1190.

Pryor, S. C., Howe, J. A. and Kunkel, K. E. (2009) 'How spatially coherent and statistically robust are temporal changes in extreme precipitation in the contiguous USA?', *International Journal of Climatology,* **29**, (1), pp. 31-45.

R Development Core Team. (2011) *R: A Language and Environment for Statistical Computing*

Rayner, N. A., Brohan, P., Parker, D., Folland, C. K., Kennedy, J. J., Vanicek, M., Ansell, T. J. and Tett, S. (2005) 'Improved analyses of changes and uncertainties in sea surface temperature measured in situ since the mid-nineteenth century: The HadSST2 Dataset', *J. Climate,* **19**, pp. 446-469.

Raziei, T., Bordi, I., Pereira, L. S., Corte-Real, J. and Santos, J. A. (2011) 'Relationship between daily atmospheric circulation types and winter dry/wet spells in western Iran', *International Journal of Climatology*.

Reeves, J., Chen, J., Wang, X. L., Lund, R. and Lu, Q. Q. (2007) 'A Review and Comparison of Changepoint Detection Techniques for Climate Data', *Journal of Applied Meteorology and Climatology,* **46**, (6), pp. 900-915.

Revfeim, K. J. A. (1983) 'On the analysis of extreme rainfalls', *Journal of Hydrology,* **62**, (1-4), pp. 107-117.

Ribatet, M., Sauquet, E., Grésillon, J.-M. and Ouarda, T. (2007) 'A regional Bayesian POT model for flood frequency analysis', *Stochastic Environmental Research and Risk Assessment,* **21**, (4), pp. 327-339.

Robinson, M. E. and Tawn, J. A. (1997) 'Statistics for Extreme Sea Currents', *Journal of the Royal Statistical Society. Series C (Applied Statistics),* **46**, (2), pp. 183-205.

Robson, A. J. (1999) *Statistical procedures for flood frequency estimation.* Wallingford, Oxfordshire, OX10 8BB, UK.
Robson, A. J. (2002) 'Evidence for trends in UK flooding', *Philosophical Transactions - A - Mathematical Physical and Engineering Sciences,* **360**, (1796), pp. 1327.
Rodda, H. J. E., Little, M. A., Wood, R. G., MacDougall, N. and McSharry, P. E. (2009) 'A digital archive of extreme rainfalls in the British Isles from 1866 to 1968 based on British Rainfall', *Weather,* **64**, (3), pp. 71-75.
Rodda, J. C., Little, M. A., Rodda, H. J. E. and McSharry, P. E. (2010) 'A comparative study of the magnitude, frequency and distribution of intense rainfall in the United Kingdom', *International Journal of Climatology,* **30**, (12), pp. 1776-1783.
Rodionov, S. N. (2004) 'A sequential algorithm for testing climate regime shifts', *Geophys. Res. Lett.,* **31**, (9), pp. L09204.
Rodionov, S. N. (2005) '*Detecting regime shifts in the mean and variance: methods and specific examples',* In: Proc. *Large-Scale Disturbances (Regime Shifts) and Recovery in Aquatic Ecosystems: Challenges for Management Toward Sustainability.* Varna, Bulgaria, 14-16 June 2005. pp. 68-72.
Rodriguez-Fonseca, B. and de Castro, M. (2002) 'On the connection between winter anomalous precipitation in the Iberian Peninsula and North West Africa and the summer subtropical Atlantic sea surface temperature', *Geophys. Res. Lett.,* **29**, (18), pp. 1863.
Rodríguez-Puebla, C. and Nieto, S. (2010) 'Trends of precipitation over the Iberian Peninsula and the North Atlantic Oscillation under climate change conditions', *International Journal of Climatology,* **30**, (12), pp. 1807-1815.
Rogers, J. C. (1997) 'North Atlantic storm track variabiltiy and its association to the North Atlantic Oscillation and climate variability of Northern Europe.', *Journal of Climate,* **10**, (7), pp. 1635-1647.
Rosenzweig, C. (2011) 'All Climate is Local', *Scientific American,* **305**, pp. 70-73.
Rosenzweig, C., Solecki, W. D., Hammer, S. A. and Mehrotra, S. (2011) *Climate Change and Cities: First Assessment Report of the Urban Climate Change Research Network.* Cambridge University Press.
Rosenzweig, C., Tubiello, F. N., Goldberg, R., Mills, E. and Bloomfield, J. (2002) 'Increased crop damage in the US from excess precipitation under climate change', *Global Environmental Change,* **12**, pp. 197-202.
Rubin, G., McCulloch, C. E. and Shapiro, M. A. (1990) 'Multinomial Runs Tests to Detect Clustering in Constrained Free Recall', *Journal of the American Statistical Association,* **85**, (410), pp. 315-320.
Rummukainen, M. (2010) 'State-of-the-art with regional climate models', *Wiley Interdisciplinary Reviews: Climate Change,* **1**, (1), pp. 82-96.
Rust, H. W. (2009) 'The effect of long-range dependence on modelling extremes with the generalised extreme value distribution', *The European Physical Journal - Special Topics,* **174**, (1), pp. 91-97.
Rust, H. W., Maraun, D. and Osborn, T. J. (2009) 'Modelling seasonality in extreme precipitation', *The European Physical Journal - Special Topics,* **174**, (1), pp. 99-111.
Saji, N. H., Goswami, B. N., Vinayachandran, P. N. and Yamagata, T. (1999) 'A dipole mode in the tropical Indian Ocean', *Nature,* **401**, (6751), pp. 360-363.
Sakalauskiene, G. (2003) 'The Hurst Phenomenon in Hydrology', *Environmental research, engineering and management,* **25**, (3), pp. 16-20.

Salter, M. C. S. (1921) *The rainfall of the British Isles.* University of London Press, Ltd.
Sang, H. and Gelfand, A. (2009) 'Hierarchical modeling for extreme values observed over space and time', *Environmental and Ecological Statistics,* **16**, (3), pp. 407-426.
Sapiano, M. R. P., Stephenson, D. B., Grubb, H. J. and Arkin, P. A. (2006) 'Diagnosis of Variability and Trends in a Global Precipitation Dataset Using a Physically Motivated Statistical Model', *Journal of Climate,* **19**, (17), pp. 4154-4166.
Scaife, A. A., Folland, C. K., Alexander, L. V., Moberg, A. and Knight, J. R. (2008) 'European climate extremes and the North Atlantic Oscillation', *J. Climate,* **21**, pp. 72-83.
Schertzer, D., Tchiguirinskaia, I., Lovejoy, S. and Hubert, P. (2010) 'No monsters, no miracles: in nonlinear sciences hydrology is not an outlier!', *Hydrological Sciences Journal,* **55**, (6), pp. 965-979.
Schwarz, G. (1978) 'Estimating the Dimension of a Model', *The Annals of Statistics,* **6**, (2), pp. 461-464.
Seierstad, I. A., Stephenson, D. B. and KvamstØ, N. G. (2007) 'How useful are teleconnection patterns for explaining variability in extratropical storminess?', *Tellus A,* **59**, (2), pp. 170-181.
Serinaldi, F. (2009) 'Assessing the applicability of fractional order statistics for computing confidence intervals for extreme quantiles', *Journal of Hydrology,* **376**, (3-4), pp. 528-541.
Serinaldi, F. (2010) 'Use and misuse of some Hurst parameter estimators applied to stationary and non-stationary financial time series', *Physica A: Statistical Mechanics and its Applications,* **389**, (14), pp. 2770-2781.
Shinohara, Y., Kume, T., Komatsu, H. and Otsuki, K. (2010) 'Spatial and temporal variations in summer precipitation in Japanese mountain areas', *Hydrological Processes,* **24**, (13), pp. 1844-1855.
Sibley, A. (2010) 'Analysis of extreme rainfall and flooding in Cumbria 18–20 November 2009', *Weather,* **65**, (11), pp. 287-292.
Smith, A. P. (2009) *A national scale rainfall analysis and event-based model of extremes for the UK.* thesis. Newcastle University.
Smith, C. A. and Sardshmukh, P. (2000) 'The Effect of ENSO on the Intraseasonal Variance of Surface Temperature in Winter', *International Journal of Climatology,* **20**, pp. 1543-1557.
Smith, R. L. (1986) 'Extreme value theory based on the r largest annual events', *Journal of Hydrology,* **86**, (1-2), pp. 27-43.
Smith, R. L. (1987) 'Estimating tails of probability distributions', *Annals of Statistics,* **15**, pp. 1174-1207.
Smith, R. L. and Weissman, I. (1985) 'Maximum Likelihood Estimation of the Lower Tail of a Probability Distribution', *Journal of the Royal Statistical Society. Series B (Methodological),* **47**, (2), pp. 285-298.
Solanki, S. K., Usoskin, I. G., Kromer, B., Schussler, M. and Beer, J. (2004) 'Unusual activity of the Sun during recent decades compared to the previous 11,000 years', *Nature,* **431**, (7012), pp. 1084-1087.
Sornette, D. (2009) 'Dragon-Kings, Black Swans and the Prediction of Crises', *Swiss Finance Institute Research Paper,* **9**, (36).
Stahl, K., Hisdal, H., Hannaford, J., Tallaksen, L. M., van Lanen, H. A. J., Sauquet, E., Demuth, S., Fendekova, M. and Jódar, J. (2010) 'Streamflow trends in Europe: evidence from a dataset of near-natural catchments', *Hydrol. Earth Syst. Sci.,* **14**, (12), pp. 2367-2382.

Stedinger, J. R., Vogel, R. M. and Foufoula-Georgiou, E. (1993) 'Frequency analysis of extreme events', in *Handbook of Hydrology.* McGraw-Hill Companies.
Stenchikov, G., Robock, A., Ramaswamy, V., Schwarzkopf, M. D., Hamilton, K. and Ramachandran, S. (2002) 'Arctic Oscillation response to the 1991 Mount Pinatubo eruption: Effects of volcanic aerosols and ozone depletion', *J. Geophys. Res.,* **107**, (D24), pp. 4803.
Stephenson, A. (2002) 'evd: Extreme Value Distributions', *R News,* **2**, (2), pp. 31-32.
Stephenson, A. and Gilleland, E. (2006) 'Software for the analysis of extreme events: The current state and future directions', *Extremes,* **8**, (3), pp. 87-108.
Stephenson, D. B. (2008) 'Chapter 1: Definition, diagnosis, and origin of extreme weather and climate events', in *Climate Extremes and Society.* Cambridge University Press, Cambridge, UK, pp. 348.
Stern, N. H. (2007) *The Economics of Climate Change: The Stern Review.* Cambridge University Press.
Stewart, E. J., Reed, D. W., Faulkner, D. S. and Reynard, N. S. (1999) 'The FORGEX method of rainfall growth estimation I: Review of requirement', *Hydrol. Earth Syst. Sci.,* **3**, pp. 187-195.
Stott, P. A. and Trenberth, K. (2009) 'Linking Extreme Weather to Climate Variabiltiy and Change', *Eos Transactions, American Geophysical Union,* **90**, (21).
Suppiah, R. and Hennessy, K. J. (1998) 'Trends in total rainfall, heavy rain events and number of dry days in Australia, 1910–1990', *International Journal of Climatology,* **18**, (10), pp. 1141-1164.
Svensson, C. and Jones, D. A. (2010) 'Review of rainfall frequency estimation methods', *Journal of Flood Risk Management,* **3**, (4), pp. 296-313.
Taleb, N. N. (2011) *The Black Swan: The Impact of the Highly Improbable.* Random House Trade Paperbacks.
Taqqu, M. S., Teverovsky, V. and Willinger, W. (1995) 'Estimators for Long-range dependence: an empirical study', *Fractals,* **3**, pp. 785-798.
Tebaldi, C., Hayhoe, K., Arblaster, J. and Meehl, G. (2006) 'Going to the Extremes', *Climatic Change,* **79**, (3), pp. 185-211.
Thom, H. C. S. (1958) 'A note on the Gamma distribution', *Mon. Weather Rev.*, (86), pp. 117-121.
Thompson, D. W. J. and Wallace, J. M. (1998) 'The Arctic oscillation signature in the wintertime geopotential height and temperature fields', *Geophys. Res. Lett.,* **25**, (9), pp. 1297-1300.
Thompson, D. W. J. and Wallace, J. M. (2000) 'Annular Modes in the Extratropical Circulation. Part I: Month-to-Month Variability', *Journal of Climate,* **13**, (5), pp. 1000-1016.
Thompson, D. W. J., Wallace, J. M. and Hegerl, G. C. (2000) 'Annular Modes in the Extratropical Circulation. Part II: Trends', *Journal of Climate,* **13**, (5), pp. 1018-1036.
TORRO. (2009) http://www.torro.org.uk/TORRO/severeweather/tornadofaqs.php (Accessed: 18/03/2009)
Tramblay, Y., Neppel, L. and Carreau, J. (2011) 'Brief communication "Climatic covariates for the frequency analysis of heavy rainfall in the Mediterranean region"', *Nat. Hazards Earth Syst. Sci.,* **11**, (9), pp. 2463-2468.
Trapletti, A. and Hornik, K. (2011) *tseries: Time Series Analysis and Computational Finance* (0.10-27) [R package].

Trenberth, K. (2005a) 'Uncertainty in Hurricanes and Global Warming', *Science,* **308**, (5729), pp. 1753-1754.
Trenberth, K. E. (1976) 'Spatial and temporal variations of the Southern Oscillation', *Quarterly Journal of the Royal Meteorological Society,* **102**, (433), pp. 639-653.
Trenberth, K. E. (1997) 'The Definition of El Nino', *Bulletin of the American Meteorological Society,* **78**, (12), pp. 2771-2777.
Trenberth, K. E. (1998) 'Atmospheric Moisture Residence Times and Cycling: Implications for Rainfall Rates and Climate Change', *Climatic Change,* **39**, (4), pp. 667-694.
Trenberth, K. E. (2005b) '*The impact of climate change and variability on heavy precipitation, floods and droughts*', in M. G. Anderson(ed), *Encyclopedia of Hydrological Sciences* John Wiley & Sons,pp 11.
Trenberth, K. E. (2011) 'Changes in precipitation with climate change', *Climate Research,* **47**, pp. 123-138.
Trenberth, K. E., Caron, J. M., Stepaniak, D. P. and Worley, S. (2002) 'Evolution of El Niño - Southern Oscillation and global atmospheric surface temperatures', *J. Geophys. Res.,* **107**, (D8), pp. 4065.
Trenberth, K. E., Dai, A., Rasmussen, R. M. and Parsons, D. B. (2003) 'The changing character of precipitation', *Bulletin of the American Meteorological Society,* **84**, pp. 1205-1217.
Trenberth, K. E., Jones, P. D., Ambenje, P., Bojariu, R., Easterling, D., Klein Tank, A., Parker, D., Rahimzadeh, F., Renwick, J. A., Rusticucci, M., B., S. and Zhai, P. (2007) 'Observations: Surface and Atmospheric Climate Change', in *Climate Change 2007: The Physical Science Basis. Contribution of Working Group I to the Fourth Assessment Report of the Intergovernmental Panel on Climate Change 2007.* Cambridge University Press, Cambridge, United Kingdom and New York, NY, USA.
Trenberth, K. E. and Shea, D. J. (2005) 'Relationships between precipitation and surface temperature', *Geophys. Res. Lett.,* **32**.
Troup, A. J. (1965) 'The 'southern oscillation'', *Quarterly Journal of the Royal Meteorological Society,* **91**, (390), pp. 490-506.
Tukey, J. W. (1962) 'The Future of Data Analysis', *The Annals of Mathematical Statistics,* **33**, (1), pp. 1-67.
Ulbrich, U., Leckebusch, G. and Pinto, J. (2009) 'Extra-tropical cyclones in the present and future climate: a review', *Theoretical and Applied Climatology,* **96**, (1), pp. 117-131.
Underwood, F. M. (2009) 'Describing long-term trends in precipitation using generalized additive models', *Journal of Hydrology,* **364**, (3-4), pp. 285-297.
Upton, G. J. G. (2002) 'A correlation–regression method for tracking rainstorms using rain-gauge data', *Journal of Hydrology,* **261**, (1-4), pp. 60-73.
Upton, G. J. G. and Rahimi, A. R. (2003) 'On-line detection of errors in tipping-bucket raingauges', *Journal of Hydrology,* **278**, (1-4), pp. 197-212.
Usoskin, I. G., Schuessler, M., Solanki, S. K. and Mursula, K. (2004) 'Solar Activity over the last 1150 years: Does it correlate with climate?', *Proc. 13th Cool Stars Workshop*, pp. 19-22.
Van Oldenborgh, G. J., Burgers, G. and Tank, A. K. (2000) 'On the El Niño teleconnection to spring precipitation in Europe', *International Journal of Climatology,* **20**, (5), pp. 565-574.
Viglione, A. (2011) *Non-supervised Regional Frequency Analysis* (0.7-2)
Viglione, A., Laio, F. and Claps, P. (2007) 'A comparison of homogeneity tests for regional frequency analysis', *Water Resour. Res.,* **29**, (6), pp. 1745-1752.

Villarini, G. and Serinaldi, F. (2011) 'Development of statistical models for at-site probabilistic seasonal rainfall forecast', *International Journal of Climatology*.

Villarini, G., Serinaldi, F., Smith, J. A. and Krajewski, W. F. (2009) 'On the stationarity of annual flood peaks in the continental United States during the 20th century', *Water Resour. Res.,* **45**, (8), pp. W08417.

Villarini, G., Smith, J. A., Baeck, M. L., Vitolo, R., Stephenson, D. B. and Krajewski, W. F. (2011a) 'On the frequency of heavy rainfall for the Midwest of the United States', *Journal of Hydrology,* **400**, (1-2), pp. 103-120.

Villarini, G., Smith, J. A. and Napolitano, F. (2010) 'Nonstationary modeling of a long record of rainfall and temperature over Rome', *Advances in Water Resources,* **33**, (10), pp. 1256-1267.

Villarini, G., Smith, J. A., Ntelekos, A. A. and Schwarz, U. (2011b) 'Annual maximum and peaks-over-threshold analyses of daily rainfall accumulations for Austria', *J. Geophys. Res.,* **116**, (D5), pp. D05103.

Villarini, G., Smith, J. A., Serinaldi, F. and Ntelekos, A. A. (2011c) 'Analyses of seasonal and annual maximum daily discharge records for central Europe', *Journal of Hydrology,* **399**, (3-4), pp. 299-312.

Villarini, G., Smith, J. A., Vitolo, R. and Stephenson, D. B. (2012) 'On the temporal clustering of US floods and its relationship to climate teleconnection patterns', *International Journal of Climatology*.

Vincent, L. A., Aguilar, E., Saindou, M., Hassane, A. F., Jumaux, G., Roy, D., Booneeady, P., Virasami, R., Randriamarolaza, L. Y. A., Faniriantsoa, F. R., Amelie, V., Seeward, H. and Montfraix, B. (2011) 'Observed trends in indices of daily and extreme temperature and precipitation for the countries of the western Indian Ocean, 1961-2008', *J. Geophys. Res.,* **116**, (D10), pp. D10108.

Vitolo, R., Stephenson, D. B., Cook, I. M. and Mitchell-Wallace, K. (2009) 'Serial clustering of intense European storms', *Meteorologische Zeitschrift,* **18**, pp. 411-424.

The Oxford English Dictionary, Volume XI Ow - Poisant. (1989) Second edition. Ed. J. A. Simpson and E. S. C. Weiner Clarendon Press.

von Storch, H. and Zwiers, F. W. (1999) *Statistical Analysis in Climate Research.* 2nd ed Cambridge University Press.

Wald, A. and Wolfowitz, J. (1940) 'On a Test Whether Two Samples are from the Same Population', *The Annals of Mathematical Statistics,* **11**, (2), pp. 147-162.

Wallace, J. M. and Gutzler, D. S. (1981) 'Teleconnections in the Geopotential Height Field during the Northern Hemisphere Winter', *Monthly Weather Review,* **109**, (4), pp. 784-812.

Wang, C. and Dong, S. (2010) 'Is the basin-wide warming in the North Atlantic Ocean related to atmospheric carbon dioxide and global warming?', *Geophys. Res. Lett.,* **37**.

Wang, W., Chen, X., Shi, P. and Van Gelder, P. H. A. J. M. (2008) 'Detecting changes in extreme precipitation and extreme streamflow in the Dongjiang River Basin in southern China', *Hydrol. Earth Syst. Sci.*

Weather Log. (2010) 'UK annual weather summary - 2009', *Royal Meteorological Society Publication,* **65**, (43).

Wendy Lou, W. Y. (1996) 'On Runs and Longest Run Tests: A Method of Finite Markov Chain Imbedding', *Journal of the American Statistical Association,* **91**, (436), pp. 1595-1601.

Wentz, F. J., Ricciardulli, L., Hilburn, K. and Mears, C. (2007) 'How Much More Rain Will Global Warming Bring?', *Science,* **317**, (5835), pp. 233-235.

Westra, S. and Sisson, S. A. (2011) 'Detection of non-stationarity in precipitation extremes using a max-stable process model', *Journal of Hydrology,* **406**, (1–2), pp. 119-128.
White, E. P., Enquist, B. J. and Green, J. L. (2008) 'On estimating the exponent of power-law frequency distributions', *Ecology,* **89**, (4), pp. 905-912.
Wigley, T. M. L. and Jones, P. D. (1987) 'England and Wales precipitation: A discussion of recent changes in ariability and an update to 1985', *International Journal of Climatology,* **7**, (3), pp. 231-246.
Wigley, T. M. L., Lough, J. M. and Jones, P. D. (1984) 'Spatial patterns of precipitation in England and Wales and a revised, homogeneous England and Wales precipitation series', *International Journal of Climatology,* **4**, (1), pp. 1-25.
Wilby, R. L., Beven, K. J. and Reynard, N. S. (2008) 'Climate change and fluvial flood risk in the UK: more of the same?', *Hydrological Processes,* **22**, (14), pp. 2511-2523.
Wilby, R. L., Conway, D. and Jones, P. D. (2002) 'Prospects for downscaling seasonal precipitation variability using conditioned weather generator parameters', *Hydrological Processes,* **16**, (6), pp. 1215-1234.
Wilby, R. L. and Dessai, S. (2010) 'Robust adaptation to climate change', *Weather,* **65**, (7), pp. 180-185.
Wilby, R. L., Wedgbrow, C. S. and Fox, H. R. (2004) 'Seasonal predictability of the summer hydrometeorology of the River Thames, UK', *Journal of Hydrology,* **295**, (1-4), pp. 1-16.
Wilby, R. L. and Wigley, T. M. L. (2002) 'Future changes in the distribution of daily precipitation totals across North America', *Geophys. Res. Lett.,* **29**, (7), pp. 1135.
Wilde, O. (1997) *The critic as artist.* Green Integer.
Wilks, D. S. (1990) 'Maximum Likelihood Estimation for the Gamma Distribution Using Data Containing Zeros', *Journal of Climate,* **3**, (12), pp. 1495-1501.
Wilks, D. S. (1999) 'Interannual variability and extreme-value characteristics of several stochastic daily precipitation models', *Agricultural and Forest Meteorology,* **93**, (3), pp. 153-169.
Wilks, D. S. (2005) *Statistical methods in the atmospheric sciences : an introduction.* 2nd ed Oxford Academic.
Wilson, P. S. and Toumi, R. (2005) 'A fundamental probability distribution for heavy rainfall', *Geophys. Res. Lett.,* **32**, (14), pp. L14812.
Wolter, K. and Timlin, M. S. (2011) 'El Niño/Southern Oscillation behaviour since 1871 as diagnosed in an extended multivariate ENSO index (MEI.ext)', *International Journal of Climatology,* **31**, (7), pp. 1074-1087.
Wood, S. N. (2000) 'Modelling and smoothing parameter estimation with multiple quadratic penalties', *Journal of the Royal Statistical Society: Series B (Statistical Methodology),* **62**, (2), pp. 413.
Wood, S. N. (2006) *Generalized additive models: an introduction with R.* Chapman & Hall/CRC.
Wood, S. N. and Augustin, N. H. (2002) 'GAMs with integrated model selection using penalized regression splines and applications to environmental modelling', *Ecological Modelling,* **157**, (2-3), pp. 157-177.
Woods-Ballard, B., Kellagher, R., Martin, P., Jefferies, C., Bray, R. and Shaffer, P. (2007) *The SUDS manual.* CIRIA.
World Meteorological Organization. (2009) *Guidelines on Analysis of Extremes in a Changing Climate in Support of Informed Decisions for Adaptation.* World Meteorological Organization,Geneva, Switzerland.

World Meteorological Organization. (2011) http://www.wmo.int/pages/mediacentre/press_releases/pr_916_en.html (Accessed: 20/07/11)
Wuertz, D., Paxson, V., Beran, J., Taqqu, M. S., Fraley, C. and Nason, G. (2009) *fArma: ARMA Time Series Modelling* (2100.76) [R package].
Yadav, R. R., Park, W.-K., Singh, J. and Dubey, B. (2004) 'Do the western Himalayas defy global warming?', *Geophys. Res. Lett.,* **31**, (17), pp. L17201.
Yates, H. (2008) 'Climate Change At Home', *World@Risk*, p.22-24.
Yee, T. (2011) *VGAM: Vector Generalized Linear and Additive Models* (0.8-4)
Yee, T. and Stephenson, A. (2007) 'Vector generalized linear and additive extreme value models', *Extremes,* **10**, (1), pp. 1-19.
Yee, T. and Wild, C. J. (1996) 'Vector Generalized Additive Models', *J. R. Statist. Soc. B,* **58**, (3), pp. 481-493.
Yee, T. W. (2010) 'VGLMs and VGAMs: An overview for applications in fisheries research', *Fisheries Research,* **101**, (1–2), pp. 116-126.
Yue, S. and Pilon, P. (2004) 'A comparison of the power of the *t* test, Mann-Kendall and bootstrap tests for trend detection', *Hydrological Sciences Journal,* **49**, (1), pp. 1 - 37.
Yue, S., Pilon, P. and Cavadias, G. (2002) 'Power of the Mann-Kendall and Spearman's rho tests for detecting monotonic trends in hydrological series', *Journal of Hydrology,* **259**, (1-4), pp. 254-271.
Zaitchik, B. F., Macalady, A. K., Bonneau, L. R. and Smith, R. B. (2006) 'Europe's 2003 heat wave: a satellite view of impacts and land-atmosphere feedbacks', *International Journal of Climatology,* **26**, (6), pp. 743-769.
Zanchettin, D., Franks, S. W., Traverso, P. and Tomasino, M. (2008) 'On ENSO impacts on European wintertime rainfalls and their modulation by the NAO and the Pacific multi-decadal variability described through the PDO index', *International Journal of Climatology,* **28**, (8), pp. 995-1006.
Zhang, X., Alexander, L., Hegerl, G. C., Jones, P., Tank, A. K., Peterson, T. C., Trewin, B. and Zwiers, F. W. (2011) 'Indices for monitoring changes in extremes based on daily temperature and precipitation data', *Wiley Interdisciplinary Reviews: Climate Change,* **2**, (6), pp. 851-870.
Zhang, X., Hegerl, G., Zwiers, F. W. and Kenyon, J. (2005) 'Avoiding Inhomogeneity in Percentile-Based Indices of Temperature Extremes', *Journal of Climate,* **18**, (11), pp. 1641-1651.
Zhang, X., Zwiers, F. W. and Li, G. (2004) 'Monte Carlo Experiments on the Detection of Trends in Extreme Values', *Journal of Climate,* **17**, (10), pp. 1945-1952.
Zhou, L., Dai, A., Dai, Y., Vose, R., Zou, C.-Z., Tian, Y. and Chen, H. (2009) 'Spatial dependence of diurnal temperature range trends on precipitation from 1950 to 2004', *Climate Dynamics,* **32**, (2), pp. 429-440.
Zhou, X. N., Yang, G. J., Yang, K., Wang, X. H., Hong, Q. B., Sun, L. P., Malone, J. B., Kristensen, T. K., Berqquist, N. R. and Utzinger, J. (2008) 'Potential impact of climate change on schistosomiasis transmission in China', *Am. J. Trop. Med. Hyg.,* **78**, (2), pp. 188-194.
Zolina, O., Simmer, C., Gulev, S. K. and Kollet, S. (2010) 'Changing structure of European precipitation: Longer wet periods leading to more abundant rainfalls', *Geophys. Res. Lett.,* **37**, (6), pp. L06704.

Zwiers, F., W. and von Storch, H. (2004) 'On the role of statistics in climate research', *International Journal of Climatology,* **24**, (6), pp. 665-680.